Nr. 111

DOKTORSAVHANDLINGAR
VID
CHALMERS TEKNISKA HÖGSKOLA
Nr 111

INSTITUTE OF PHYSICS

CHALMERS TEKNISKA HÖGSKOLA — GÖTEBORGS UNIVERSITET

GÖTEBORG — SWEDEN

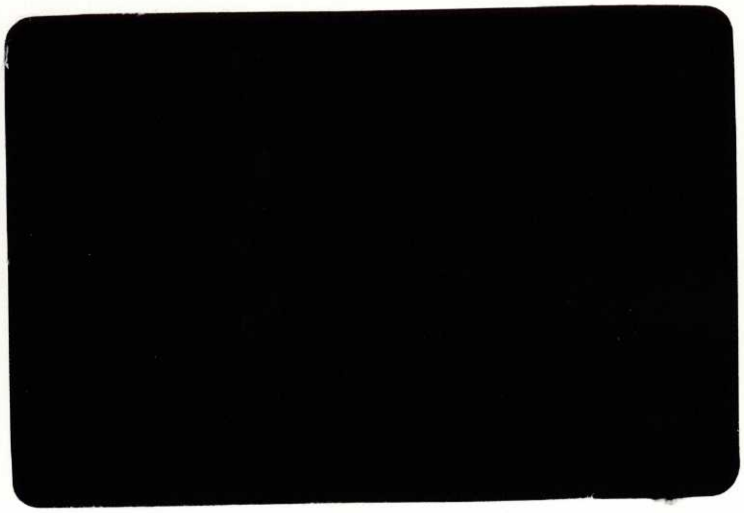

STUDIES OF PROMPT GAMMA RADIATION

FROM FISSION FRAGMENTS

HARRY ALBINSSON

DOKTORSAVHANDLINGAR
VID
CHALMERS TEKNISKA HÖGSKOLA

STUDIES OF PROMPT GAMMA RADIATION FROM FISSION FRAGMENTS

BY

H. ALBINSSON

GÖTEBORG 1971

STUDIES OF PROMPT GAMMA RADIATION FROM FISSION FRAGMENTS

BY

H. ALBINSSON

AKADEMISK AVHANDLING

SOM MED TILLSTÅND AV SEKTIONEN FÖR TEKNISK FYSIK VID CHALMERS TEKNISKA HÖGSKOLA, FRAMLÄGGES TILL OFFENTLIG GRANSKNING FÖR VINNANDE AV TEKNISK DOKTORSGRAD FREDAGEN DEN 28 MAJ 1971 KL. 10.00 Å HÖRSAL A, INSTITUTIONSBYGGNADEN FÖR FYSIK VID CHALMERS TEKNISKA HÖGSKOLA, GIBRALTARGATAN 5 B, GÖTEBORG.

GÖTEBORG
ELANDERS BOKTRYCKERI AKTIEBOLAG
1971

DOKTORSAVHANDLINGAR
VID
CHALMERS TEKNISKA HÖGSKOLA

STUDIES OF PROMPT GAMMA RADIATION FROM FISSION FRAGMENTS

BY

H. ALBINSSON

GÖTEBORG
ELANDERS BOKTRYCKERI AKTIEBOLAG
1971

This thesis consists of the following papers:

I. Studies of Prompt Gamma Radiation from Fission Fragments.

II. H. Albinsson and L. Lindow,
Prompt Gamma Radiation from Fragments in the Thermal Fission of ^{235}U. AE-398, AB Atomenergi, 1970.

III. H. Albinsson,
Energies and Yields of Prompt Gamma Rays from Fragments in Slow-Neutron Induced Fission of ^{235}U. AE-420, AB Atomenergi, 1971.

IV. H. Albinsson,
Yield of Prompt Gamma Radiation in Slow-Neutron Induced Fission of ^{235}U as a Function of the Total Fragment Kinetic Energy. AE-417, AB Atomenergi, 1971.

V. H. Albinsson,
Decay Curves and Half-Lives of Gamma-Emitting States from a Study of Prompt Fission Gamma Radiation. AE-421, AB Atomenergi, 1971.

SUMMARY

A growing interest in prompt gamma radiation from fission fragments has developed during the last five to seven years. This research field can be penetrated more efficiently since the advent of the solid state detectors of the surface barrier type, which facilitate several fission experiments. Moreover, different kinds of radiation from the fragments can now be recorded with improved accuracy in the associated mass determination. Data recording systems have become more effective and the decay of the fragments can be studied in several parameters simultaneously.

The expression "prompt" here signifies gamma radiation with half-lives shorter than 10^{-9} s and emitted from the fragments following the prompt neutron emission. Most studies have been performed on the spontaneous fission of ^{252}Cf and to a lesser extent on the slow neutron induced fission of ^{235}U. Measurements of the californium fission are easy to perform, mainly because the background problem is not so serious as in a reactor experiment. The light mass groups differ in the two fission processes and therefore a close examination of the uranium fission is worthwhile to give complementary data.

In the present work the gamma radiation was studied, whereas in some other experiments the decay of the fragments has also been studied through measurements of associated processes such as those of conversion electrons and K X-rays. The emission of prompt neutrons, and especially those neutrons which are emitted from the fragments, can yield information for the interpretation of the prompt fission gamma radiation. The prompt neutrons also include the so-called scission or central neutrons which are emitted at the

instant of scission, but these yield very little information about the deexcitation of the fragments.

The experimental set-up used to perform work on prompt fission gamma radiation at the R2 reactor, Studsvik, is described in detail in the present paper. A short survey is also given of the work done at other laboratories since 1965, at which time two reviews of earlier work were published. Finally, a few suggestions for future researchs are also given.

Two of the main features of the present experimental set-up, which were used throughout the project, are the gamma collimator and the time-of-flight technique. The gamma collimator was used to select different time intervals after the fission event. Such a technique has previously been used in a few other experiments. Time discrimination between the fission gamma radiation and the prompt neutrons released in the fission process was employed to reduce the background.

The main problems encountered when carrying out these experiments are described in paper II together with some general studies. The experimental set-up during the first two years of operation was slightly different from the one used during the later measurements. Data recording was initially often done with a one- or two-parameter standard analyzer, whereas later a small computer, PDP-8/S, was used. For the recording of mass spectra a logarithmic amplifier was first used. It was subsequently replaced by a linear divider circuit, which is more convenient when relative yields of photons as functions of mass are to be studied.

Paper III describes measurements of gamma-ray energy spectra as functions of mass and time after fission. The data are analyzed on the basis of a model in which the rigidity of the fragments plays an important role. This model assumes that fragments with nucleon numbers in the vicinity of the magic ones are more resistant to deformation than other fragments. It is now generally assumed that the initial excitation energy of the fragments is taken up by deformation, and the extent to which this deformation occurs will thus be of great importance for the estimation of the amount of initial excitation energy and the ensuing decay of the fragments.

A few studies have dealt with the yield of photons as a function of the total kinetic energy of the fragments. They are discussed in paper IV and their object is to provide a better understanding of the energy balance in fission. As the total kinetic energy increases, the photon yield seems to decrease in a regular manner as would be expected, but there are also certain results which indicate variations arising from spin effects.

Paper V, finally, presents a short account of the work dealing with the intensity distributions of the prompt fission gamma radiation as a function of time after fission which has permitted the derivation of decay curves and values of half-lives. The fission gamma radiation is emitted from a multitude of states and an integral gamma-ray energy spectrum does not reveal any structure. It is noteable, however, that proper use of the gamma collimator permits distinct half-lives in the decay curves to be obtained. As shown in paper III, the gamma-ray energy spectra associated with these half-lives are very different. There is good reason for believing that this particular field of nuclear spectroscopy, associated with the prompt gamma radiation from fission fragments, will yield much more information in the near future. It may then increase understanding both of fission process and more generally, the nuclear structure.

1. INTRODUCTION

Since Hahn and Strassmann reported the discovery of nuclear fission (1) in 1938, innumerable papers have been published in this field. Scientists have learnt to apply the fission process for purposes both good and bad, and the effort and the amount of money spent on research and on the application of nuclear fission are very great. It is remarkable, however, that, during more than thirty years of intense activity, there has not yet emerged any complete interpretation of fission, and our understanding of it is less than that of most other nuclear reactions. In fission every nucleon in the heavy nucleus is involved in a highly complicated process and, even if many-body theory and other similar ideas can be applied with considerable success it is still improbable that a full theoretical description of fission will be available for a considerable time to come.

Fission can be induced in heavy nuclei at relatively low excitation energies. These energies can be supplied through the capture of radiation of low energy. The amount of energy needed depends on the height of the potential barrier against fission, which, for the actinides, is seldom more than a few MeV. The cross sections for fission after capture of thermal neutrons in $^{233,235}U$ and ^{239}Pu are very high and even heavier nuclei fission spontaneously with increasing probability.

As regards the prompt gamma radiation from fission fragments the processes most studied have been those from the spontaneous fission of ^{252}Cf and the thermal neutron induced fission of ^{235}U. Both of these fission sources are easily accessible nowadays. ^{252}Cf fission is a suitable source as far as background conditions are concerned, whereas ^{235}U fission has to be performed at a reactor a requirement introducing background problems.

Unless otherwise stated, the binary fission process will be dealt with in this work. This is the most common type of fission, occuring on the average about a few hundred times more often than the most common type of ternary fission.

After breakup the fragments are accelerated in their mutual Coulomb fields, and acquire a total kinetic energy of about 170 MeV in the case of the thermal-neutron induced fission of ^{235}U. The primary fragments initially acquire a large amount of deformation energy from the scission act in addition to other forms of energy. It is assumed that the fragments collapse to their equilibrium shapes in a very short time. The deformation energy will then be available in other forms of excitation, and the fragments will consequently emit neutrons and photons.

The total excitation energy of the fragments is

$$E_{exc} = \nu(E_b + E_n) + E_\gamma$$

where ν is the number of prompt neutrons, E_b and E_n are their binding and kinetic energies and E_γ is the total gamma-ray energy. Neutron emission is presumed to take place within 10^{-15} s and most of the gamma-ray emission within about 10^{-11} s (2). Quite a few of the fragments emit isomeric gamma radiation after 10^{-11} s. The fragments are formed by the fission of nuclei of which the N/Z ratio exceeds that of the corresponding stable nuclei with the same mass numbers as the fragments. They are accordingly neutron rich, and so beta emission will occur. This latter process is much slower than the prompt processes of neutron and gamma emission. Sometimes these beta decays lead to states above the neutron threshold, resulting in the so-called delayed neutron radiation. The half-lives of the delayed neutron radiation correspond to the beta decays of the parent nuclei.

The prompt gamma radiation from fission fragments has many and often unusual features. It originates from a large number of fragments which, since they cover a considerable part of the isotope chart, differ greatly in shape; deformed and spherical and all intermediate cases are represented. Furthermore, all these fragments emerge in a single experiment, thus giving rise to complex radiation spectra which are difficult to resolve.

It has been found that the total energy of the gamma radiation is higher than might at first be expected. The number of gamma rays is also extraordinarily high, and it is current belief that these unusual features are attributable to high spin states (2-7).

Not until the last five years has fission gamma radiation received any great attention. The advent of the solid state detectors of the surface barrier type opened up a new era, facilitating the study of radiation as a function of fragment mass. More recently it has also been possible to determine both uniquely and easily, the K X-ray yield from specific fragments using Si(Li)-detectors (8-15). Ge(Li)-detectors are now mostly in use for study of the gamma radiation, especially in the energy range up to about 1 MeV (13,15,16). For higher energies the NaI-scintillator is still competitive because of its higher efficiency compared to that of the Ge(Li)-detector. This higher efficiency achieves greater significance at energies above roughly 1.5 MeV, where the yield of the prompt fission gamma radiation is very low.

Extensive studies have been made of conversion electrons and K X-rays, and they have yielded valuable information on the multipolarity of gamma radiation (10,12,13,15,17-27).

The life-time of the gamma radiation has been studied in a few experiments during the last few years, mostly by the so-called Doppler shift method (13,15,28). Gamma rays emitted by fragments moving towards the gamma-ray counter increase their energies compared to the same gamma rays emitted from fragments with zero velocity, whereas gamma rays from fragments moving away from the counter decrease their energies.

In the present work a different method has been adopted for determining the life-time of the gamma radiation, namely that of using a lead collimator which is moved along the path of the fragments. A decay curve is thus obtained from which half-lives can be determined (2,29-31).

2. SHORT REVIEW OF FISSION-FRAGMENT GAMMA-RAY WORK

2.1. General

A growing interest in the gamma radiation from fission fragments has developed during the last decade and results have been summarized in reviews by Johansson-Kleinheinz (32) and Maier-Leibnitz et al (33), and also in sections of more general reviews on the fission process (34-37). The most comprehensive reviews on gamma radiation appeared in the mid-60's (32,33).

The heading of this section refers to fission fragments. This implies that the gamma rays under discussion have been emitted from primary fragments, i.e. before the onset of beta decay. They are emitted, however, after the prompt neutrons, since the gamma decay is normally a slower process than neutron emission. Most of the experiments made so far have covered a time region of up to about 10^{-6} s after the fission event, and therefore only fragments and not products have been studied. According to Johansson (2), the radiation can be divided into two parts; a prompt and a delayed component, the limit between them lying at a half-life of about 10^{-9} s. The present experiment covered a time region in which only the prompt component was investigated.

Since the reviews by Johansson-Kleinheinz (32) and Maier-Leibnitz et al. (33) appeared in 1965, no similar summary of the work from 1965-70 has been published. The Proceedings of the Second Symposium on the Physics and Chemistry of Fission held by IAEA in Vienna, 28 July - 1 August, 1969, gives a very short summary of the situation up to that date (38). It may therefore be of some value to discuss briefly the work published on fission gamma radiation since 1965.

Most investigations have been performed on gamma rays from fragments formed in the spontaneous fission of ^{252}Cf (8-13,15,17-21, 30,39). These measurements are easier to perform than those of uranium fission (14,16,22-26,28,29,31,40,41) because there are no background problems of the kind encountered in reactor studies. The investigations have not only been concerned with gamma decays from the fragments but also with associated processes such as conversion electrons and K X-rays. Although the fission process may result in a large number of competing decays the most systematically studied of these has been binary fission, and consequently gamma radiation has been studied almost entirely in association with binary fission. The yield of binary fission events is much larger than that of any other fission, which is, of course, the main reason for its study. Another reason is to be found, however, in the geometry of fission chamber construction in addition to which the whole set-up directly favours studies of prompt gamma radiation from binary fission. The only exceptions so far studied deal with the prompt gamma-ray energy spectrum and K X-ray yield in the particular case of ternary fission, where the two fragments are accompanied by an alpha particle (42-47).

2.2 Gamma-ray energy spectra

The advent of new measuring tools, such as solid state detectors of the surface barrier type, Ge(Li)-detectors, Si(Li)-detectors, and more effective data acquisition systems, have been of very great value for fission gamma-ray studies. Some excellent set-ups have been used recently in the USA and Germany and the experiments have reached the stage at which gamma rays from individual fragments can sometimes be studied. For this purpose the experiments are performed by recording gamma-ray energy spectra in association with the fragment mass spectrum. If the gamma detector can see both fragments simultaneously, it cannot be stated with certainty which of the two fragments emitted a recorded photon. The gamma detector can therefore be located behind or in a direction close to a line adjoining the two fragment detectors, and then set to study the gamma radiation. Through an analysis making use of the Doppler shift method it is possible to state which of the two fragments in a fission event has emitted certain photons resulting in a line in the gamma-ray energy spectrum. This technique has been acopted very efficiently by, for instance, the Karlsruhe (16) and the Berkeley (10) groups and has resulted in a long table of energies of photons originating from specific fragments. The energy range is mostly up to a little over 1 MeV, a region in which the main bulk of photons is to be found. The Berkeley group has also provided supplementary data from studies of conversion electrons and K X-rays.

The Karlsruhe group has studied the thermal fission of ^{235}U and found a large number of gamma lines with energies similar to those of photons from fragments in ^{252}Cf fission and with the same fragment masses. The indication is that the fission process is so general that independent of the fission process in which a specific fragment is formed, it gives roughly the same gamma lines. As a very general statement this is probably true only to a certain extent. A detailed study of the same fragment in each of two fission processes will reveal that there are differences in the respective gamma decays. These arises from the excitation due to the influence of the partner fragment which differs from one fissioning nucleus to another. Depending on the fissioning nucleus the initial excitation following prompt neutron emission may differ, resulting in different gamma rays. The lower levels excited in each process, however, are the same. As a comment it may be mentioned that several of these gamma rays have energies of about a few hundred keV and life-times of the order of nano-seconds. They probably originate from the decay processes of the low-lying members of certain rotational and possibly also vibrational cascades. As such they should be equal in the same fragment whether it is produced in the fission of for instance uranium or californium.

The two projects described may be considered good examples of how experiments are now performed on fission gamma radiation. The other investigations referred to above are by no means unimportant or less interesting, but in some respects they have used techniques similar to those of the Karlsruhe and Berkeley groups. Detailed information has, for instance, been obtained by the

Livermore group (48) regarding isomeric transitions, the interpretation of which possesses many features in common with that of prompt radiation.

2.3 The time distribution

The adoption of a collimator to select different prompt intervals after the fission event has not been used widely so far. In addition to the present study there appears to be only two ^{252}Cf experiments (2,30) and two ^{235}U experiments (31,49). As regards delayed gamma rays some more experiments have been performed with a collimator, namely those involving "shadowing" the foil and the first part of the fragment's flight path to the gamma detector. Examples of such studies have been reported in refs. 30 and 48.

The time distribution of the prompt gamma radiation has been studied in very few experiments. In ^{252}Cf a half-life of about 20 ps was found from one of the prompt components (2) as well as in the present experiment on an early occasion. A faster component of 7 ps was also reported from the present experiment, while 8.5 ps was obtained by Armbruster et al. (31), also in uranium fission. No such short half-life has yet been measured in ^{252}Cf fission. A 50 ps half-life has been found in the present investigations and it can be estimated in one of Johansson's figures in ref. 2. Several isomers have been found with half-lives ranging from a few nanoseconds to about one microsecond (30,48,50).

By blocking different parts of the flight path of the fragment it has also been possible to estimate the half-lives of some gamma lines in ^{252}Cf (10,19,48,50). In principle the same technique as used in the present experiment was adopted, though in the first two cases only two positions were used. This technique is expected to become common practice in the future. In addition to these types of experiment coincidences between gamma rays and K X-rays have also been measured in the attempt to find more than one member of specific cascades. Quite a large number of such coincidences have been found, which is a great achievement in view of the considerable experimental difficulties. The measurements gave most of their information in those mass regions of deformed nuclei where rotational cascades are expected to exist. This type of cascade imposes a natural limit on the possibility of performing these measurements, as the conversion factors increase with decreasing gamma-ray energies and consewuently the lowest and sometimes also the next lowest members of a cascade are the most easily detectable. A K X-ray originating from such a member will have a much longer half-life than the higher and more energetic members of the cascade. This problem will be reflected in the experimental difficulties as the coincidence rates will fall.

2.4 The spin distribution

Of particular interest when studying the excited states of the fission fragments is the spin. On rather general grounds the initial spin distribution of the fragments has been calculated (3.5-7) and compared, where possible, with known experimental data (4,31,51). The shapes of the gamma-ray energy spectra, and also the first unexpectedly large amount of gamma-ray energy released, have been the subject of many discussions. As far as the large energy is concerned, it is supposed to be attributable to high spins of the initial excited states of the fragments. Neutron emission can remove much of the excitation energy, but only a few units of angular momentum. Finally, neutron emission will be hindered since states of low energy and large angular momenta are not available in the residual nuclei. The gamma emission will then compete and, in a cascade, remove both the angular momenta and the energy. This process may start at energies well above the neutron threshold. Observed half-lives of the prompt gamma radiation and their relation to the average energies are other indications of collective quadrupole transitions (52). Experiments have been reported which have indicated that the initial fragment spin is about seven to eight units of angular momentum (4,31,51).

3. EXPERIMENTAL PROCEDURE

3.1. Apparatus

The principle of the set-up of these experiments is shown in fig. 1. A neutron beam from the Studsvik R2 reactor was collimated so that no part of the beam struck more than the target and its mounting frame inside a vacuum chamber. Two solid state detectors of the surface barrier type were placed in parallel and symmetrically around the foil to measure the energies of the fission

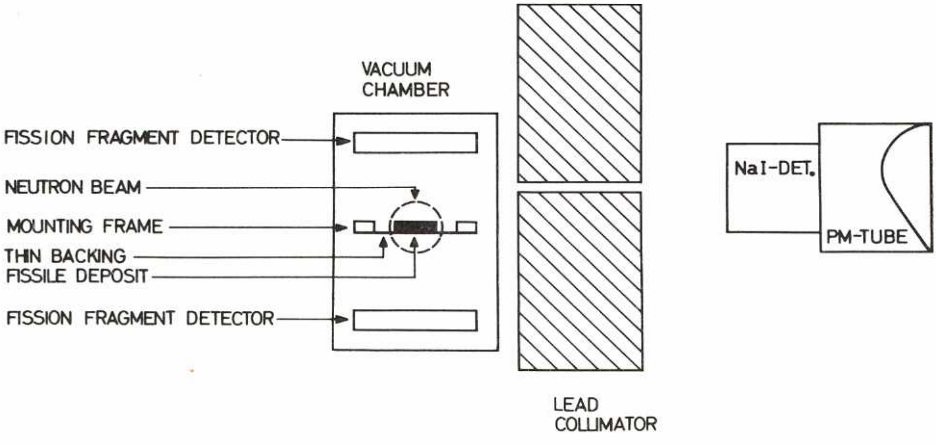

Fig. 1 Schematic diagram of the experimental arrangement.

fragments. The detectors[+] were about 4 cm^2 in area, fabricated from 400 ohmcm n-type silicon and operated at about 70 V bias. The distance between each detector and the fissile foil was 2 cm. The gamma detector was a NaI(TI) scintillator from Harshaw, 10.4 cm long and 13.0 cm in diameter, viewed by a Philips XP1040 photomultiplier tube. The associated electronics[x], consisting of a pulse-chaping unit and a discriminator, was coupled directly to the photomultiplier tube socket and gave a fast leading-edge time pulse and a linear pulse.

A lead collimator, movable in parallel with the direction of the detected fragments and also with a variable slit, was used to select gamma radiation in different time intervals after the fission event.

The fissile deposit was about 1 cm^2 in area and was prepared by electrodeposition on 100 $\mu g/cm^2$ nickel foils. In all runs employing mass selection the ^{235}U target was less than 100 $\mu g/cm^2$.

It is very important in this type of measurements that the uranium layer and the nickel foil are thin and uniform. The fragment energy loss has not been measured, but may be estimated to be not more than 3 MeV (54-56). As will be discussed below. the fragment energy spectra were used to derive mass spectra, and it was found that an upper practical limit of less than about 100 $\mu g/cm^2$ was enough to get energy spectra of good quality. In some measurements, however, when mass selection was either unnecessary, or for some reason impossible. thicker layers, of up to about 400 $\mu g/cm^2$, were allowed.

[+] Type C7904 Heavy Ion Detectors supplied by ORTEC, Oak Ridge, Tenn., USA.

[x] Designed and built at the Research Institute of National Defence, Stockholm (53).

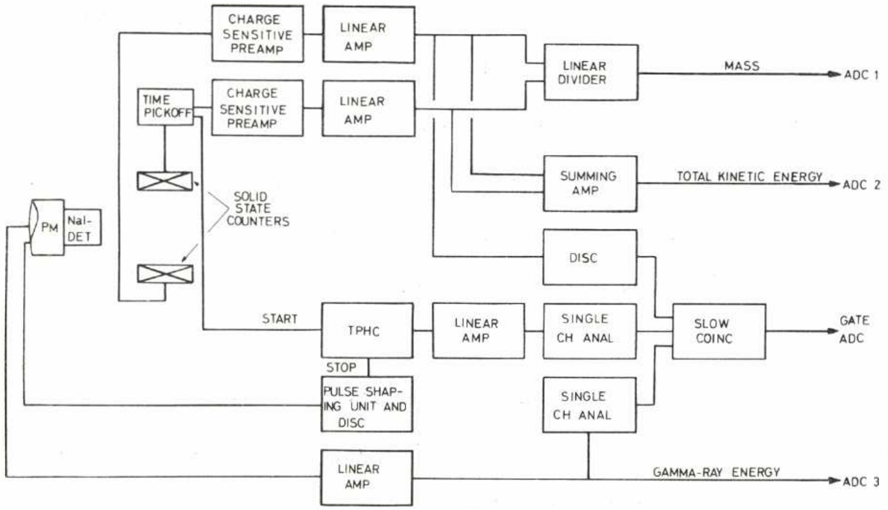

Fig. 2 Block schematic of the electronic equipment.

A block schematic of the electronics is shown in fig. 2. Pulses from the solid state detectors were amplified in charge-sensitive preamplifiers followed by linear amplifiers. The amplified pulses were then fed into a linear divider circuit+ which performed the operation of dividing one pulse by the sum of both. By disregarding prompt neutron evaporation and energy losses in the target material, it can easily be shown that the ratio of the energies of the two fragments is inversely proportional to the mass ratio. Consequently, if E_1 and E_2 are the kinetic energies of the respective fragments, and M_1 and M_2 are the associated mass numbers, one readily gets

$$\frac{E_1}{E_1 + E_2} = \frac{M_2}{M_1 + M_2} \propto M_2$$

i.e. the spectrum from the output of the divider circuit is simply the mass spectrum.

+ Designed and built at the Physics Department, University of Lund, Lund, after an idea by Gere and Miller (57).

During the first two years of the experiment a logarithmic amplifier was used instead of the linear divider circuit. The output pulse heights from that circuit were proportional to the logarithm of the incoming pulse heights (55,58). When this circuit was used one of the incoming amplified pulses was delayed and both of them stretched, after which they were added to give rise to a two-step function. After differentiating the output waveforms the first pulse from the step function was proportional to log E_1 and the second was then proportional to $\log (E_1 + E_2) - \log E_1 = \log (E_1 + E_2)/E_1 = \text{constant} - \log M_2$.

Fig. 2 includes more apparatus than can be used in one measurement when a two-parameter analyzer is available. When gamma-ray energies as functions of fragment mass were studied, the summing amplifier was not used; and when gamma-ray energies as functions of the total kinetic energy of the fragments were studied, the linear divider instead was not used.

A time-to-pulse-height converter (TPHC) was started on time pickoff pulses from one of the fragment detectors and stopped on timing pulses from the gamma detector. By incorporating a discriminator (DISC) with its level set to allow the fragment energy spectrum to pass from the detector which had no time pickoff unit, and by running this discriminator in slow coincidence with the time spectrum, it was insured that the recording system did not start unless both fragments from a fission event had been detected. Whenever necessary, use was made of a single channel analyzer (SCA) with its window set over the region of gamma-ray energy of interest. Also run in slow coincidence with the timing circuit this served to keep track of background pulses.

After amplification the timing pulses were passed into a single channel analyzer (SCA) with its window set over the gamma peak in the time-of-flight spectrum. The output pulse of the SCA were then passed to the slow coincidence circuit.

Data were stored in a two-parameter analyzer the memory of which was that of a small computer, PDP-8/S. It should be noted that the PDP-8/S was not working as a normal on-line computer, because no data analysis was done during the measurements but only recording of events. Data analysis was done with separate programs after the measurements were completed (59,60).

The interfacing unit between the computer and the nuclear physics electronics consisted of two ADC's and their associated registers. Each ADC had 400 channels and the computer memory consisted of 4 K words, i.e. 4096 positions or channels. When an analyzing signal had passed its ADC (or in a two-parameter mode two signals had passed their respective ADC's) it was stored momentarily in its register, from which the computer transferred the information into the memory. Of the 4096 channels in the computer memory 3200 channels could be used for data storage. The rest of the memory was used for programs performing operations such as transfer of data into the memory from the nuclear physics electronics, for display on a CRT, and for readout on a typewriter and/or a punch. The 3200 channels could then be divided into matrices of the following forms when measuring with two parameters: 8×400, 16×200, 32×100, or 64×50. In a one-parameter mode any of the above-mentioned single configurations was available.

The NaI detector was placed about 70 cm from the fission foil and in a direction perpendicular to the direction of the detected fragments (fig. 1). The main reason for using the time-of-flight technique was to discriminate between the prompt neutrons and the fission gamma radiation, but in this geometry it was possible to benefit by the form of the angular distribution of the prompt neutrons. As is well known, it is peaked in the direction of the fragments.

It is noteworthy that changing the distance between the fission foil and the gamma detector did not change the solid angle for gamma detection according to the inverse square law, as would be expected, but instead almost linearly. This is due to the generally narrow slit setting of the gamma collimator, the change in solid angle with distance being almost completely dependent upon the length of the collimator. Solid angles of the order of 10^{-5} - 10^{-4} sr are normal in these measurements. As is discussed elsewhere (61), however, this small solid angle is primarily dependent on the collimator setting rather than on the distance between the foil and the gamma detector.

3.2. Performance

3.2.1. The mass circuit

A typical mass spectrum from the thermal fission of ^{235}U recorded with the logarithmic amplifier is shown in fig. 3. The relative yield of fragments in a particular mass region is, of course, not the same as that obtained when the mass spectrum is on a linear scale. This is a drawback when comparisons are to be made between various relative yields as functions of fragment mass some of which are expressed on a linear scale. While direct quantitative comparisons cannot be made, it is possible to calculate a new yield curve as a function of mass on a linear scale. The variation in the energy of the prompt photons with fragment mass is, however, a

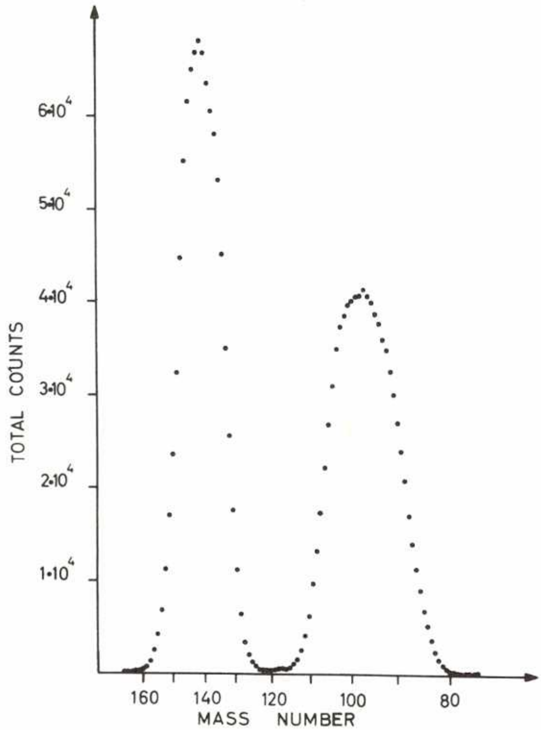

Fig. 3 Pulse spectrum from the logarithmic amplifier.

very slow function. Part of the drawback will therefore be less important in this experiment since these photon yields may be considered as functions of mass regions instead of individual masses (2). In any case qualitative comparisons can be made.

Mass spectra recorded with the linear divider circuit were acceptable in shape for performing this type of measurement and need no further discussion.

3.2.2. The time-of-flight system

Some typical time-of-flight spectra are shown in fig. 4 and 5. Fig. 4 shows a spectrum of the uncollimated gamma radiation with no gamma-ray-energy discrimination. The gamma detector "viewed" the whole region between and including the two fragment detectors.

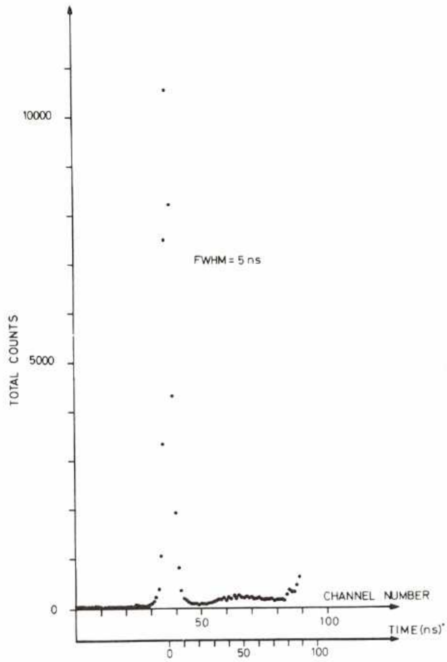

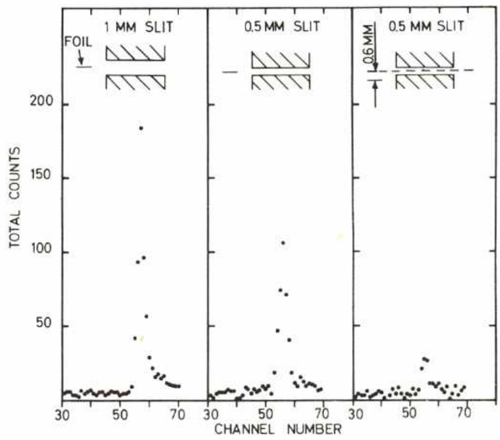

Fig. 4 Time-of-flight spectrum for the uncollimated fission gamma radiation.

Fig. 5 Time-of-flight spectra for the collimated fission gamma radiation with three different collimator settings.

The general background which has no correlation with the fission events is the level to the left of the gamma peak. The broad distribution just to the right of this peak is the prompt neutron yield. The time separation at the NaI detector between the fission gamma radiation and the prompt neutrons of largest yield is about 30 ns, which is achieved for a time-of-flight distance of about 70 cm. Fig. 5 represents plots of time-of-flight spectra with the lead collimator placed in three different positions; only small parts of the fragment paths are "visible" to the gamma detector.

As indicated in fig. 4 the full width at half maximum (FWHM) value of the gamma peak is 5 ns. This is due to three basic causes: 1) time walk due to amplitude variations in the detector signal, 2) different velocities of the fragments which produces a spread

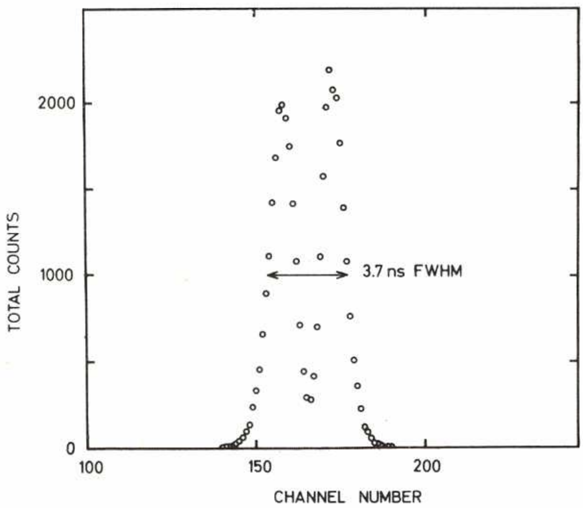

Fig. 6   Time spectrum from coincident fission fragments.

in the arrival time at the detector, and 3) the resolution of the gamma timing circuit. Time spectra were measured for coincident fission fragments by causing the TPHC to be started by the signal from one fragment detector and stopped by the signal from the other. The result is a two-peaked curve of the type shown in fig. 6, having a FWHM value of 3.7 ns. The FWHM value for each detector can thus be estimated to be a little less than 2 ns. The time spread in the gamma timing circuit is about 4 ns (53).

3.2.3. The gamma collimator

With the help of the collimator for selection of gamma radiation from different time intervals after the fission event, time-of-flight spectra were recorded with the collimator in different positions. The average velocity of the fragments is known to be about 1 cm/ns. Estimation of the intensity of the gamma peak gave the intensity variation with the collimator setting i.e. the variation with time after fission.

Three main decay components have been found so far, having tentative half-lives of 7, 20, and 50 ps. Measuring the fastest radiation was rather a mechanical than any other problem. The collimator had to be narrow - slit widths down to 0.15 mm were used - and well aligned with the plane of the foil. The foil had to be plane and its surface free from shrinkles. The adjustment of the foil in its holder was done in a darkroom with light falling through the collimator slit, and by moving the foil "towards" the collimator it was possible to see when and how the light "touched" the foil. Every little speck of dust and shrinkle on the foil first came into the light and reflected it from points and small areas. If the foil was smooth, clean and well aligned the reflection of the light came gradually from the whole surface.

This tedious and circumstantial procedure was carried out only once for every series of measurements, namely at its start. The decay curve was then obtained from the time-of-flight spectra, which in turn were recorded for consecutive collimator settings controlled by a micrometer screw. The accuracy of the screw is 0.01 mm. The settings of the collimator were performed in one direction, thus making it possible to benefit from the precision of the micrometer screw. The relative accuracy of the settings is thus of the order of 0.01 mm.

The gamma collimator was placed in the vacuum chamber and very close to the fission foil in order to minimize the solid angle subtended by the gamma detector (in reality by the collimator) and ensure the best possible time resolution. The distance between the nearest edge of the foil frame and the collimator was about 1 mm. The frame was about 5 mm between the inner and the outer radii. The setting of the foil was almost always performed with the micrometer screw, particularly when the shortest half-lives were studied. In those cases the gamma radiation of interest came from the fragments, when they were within two mm from the foil. These various settings resulted in small changes in the solid angle from the foil subtended by the fission detectors, but they could be considered as negligible in comparison with the foil - detector distance of two cm.

The measurements were initiated with a series of studies performed with a thick uranium foil in order to achieve a high counting rate. The data were stored in the two-parameter analyzer the time-of-flight spectra being registered on one axis and the gamma-ray energy spectra on the other. From these measurements it was easy to sum time-of-flight spectra in different portions of gamma-ray energy to obtain an estimate of the half-lives of different gamma rays. When, in addition, mass selection was employed thinner uranium layers were used in order to avoid recording deteriorated fragment-energy spectra.

Measurement of these time-of-flight spectra in the two-parameter mode has the particular advantage that besides the energy spectra themselves a direct estimate is obtained of the background in different regions of gamma-ray energy. This information is useful when counting rates are low, since background measurement becomes an increasingly time-consuming operation. Background is namely practically always best estimated from time-of-flight spectra. These background data were then employed in the analysis of the gamma-ray spectra measured as functions of mass, where low counting rates prevailed.

3.2.4. Considerations for the choice of a NaI-scintillator for gamma detection

The present experimental set-up has been very simple. As mentioned earlier there are some experiments now running, mainly in the USA and Germany, in which very sophisticated equipments and techniques are used. The present work has been directed towards a particular study of the fragment gamma radiation with regard to its time variation with energy. In none of the US or German experiments has a gamma collimator of the present type been used, simultaneously with the photons detected in Ge(Li)-counters. When studying such small time intervals as are relevant to the present work the gamma intensity diminishes to very low levels and the low efficiency of a Ge(Li)-detector rapidly becomes a disadvantage as compared with the efficiency of a NaI-scintillator. As mentioned earlier higher fission rates and as a consequence higher triple coincidence rates are possible. There remains, however, the practical limit set by the fission detectors and their rather fast deterioration when bombarded with fragment radiation. Thus in order to use the Ge(Li)-detector efficiently, it is necessary to place it fairly close (within roughly 10 cm) to the fission foil. This raises a serious difficulty, namely that of exposing the detector to different kinds of heavy radiation, which may lead to its rapid destruction. This argument indicates that the role of the NaI-scintillator in fission gamma-ray studies is not yet exhausted, and that certain important applications still remain. It is to be expected, however, that in the conceivable future some of the above-mentioned problems with the Ge(Li)-detector will be overcome, rendering it more acceptable for use in this type of experiment.

The immediate requirement for the use of Ge(Li)-detectors is effective data acquisition systems such as computers with large memory areas. Ancillary demands on the electronics system are for the inclusion in the set-up of pulse circuits for control purposes and stabilizing circuits to control the energy spectra from the fission counters and the gamma detector. The value of a big computer cannot, of course, be overestimated. since several parallel experiments can be performed, when the fission detectors and gamma detector are working. For each event the computer can calculate the mass and the total fragment kinetic energy. Use can then be made of different energy portions from the gamma detector. This is of particular value when a NaI detector is employed, since it is essential to make use of its different resolution in the different energy regions. It is not unreasonable to run the gamma spectrum in at least two portions simultaneously such as 50-800 keV and 0.5 - 5 MeV. This serves to reduce the measuring time by a factor of two.

3.2.5. Counting rates and circuit stability

The experimental equipment has been placed in tandem in the reactor channel behind a neutron crystal spectrometer. The neutrons falling on the uranium layer have therefore been those transmitted through the monochromator crystal. A monochromator held steady in any position offered no problems, but this was unfortunately seldom the case. When the crystal was turned, the distance through which the transmitted neutrons had to pass within the crystal, was altered, and the fission rate changed be a factor of 2-3 as a result of this operation.

This is not necessarily bad in itself as most studies are of the type in which yields are expressed as functions of fission events, and the total number of such events was monitored by a scaler. Unfortunately the background also changed by a similar factor and during long measurement periods such as were used here, the background could fluctuate seriously. These fluctuations were produced by the monochromator crystal which acted as a filter for all kinds of radiation. Thus while the thermal neutron flux and hence the fission rate were in process of varying, the fast neutrons and the gamma radiation also varied, thus giving rise to changes in the relative background level as counted by the NaI-scintillator.

When the R2 power was increased in the autumn of 1969, the number of thermal neutrons in the channel increased by a factor of two, thus enabling the neutron spectroscopists to run experiments over wider ranges of monochromator angles. At the same time the overall background level from the reactor increased, so that the background fluctuations in the present experiment frequently became unacceptable.

In the experimental set-up which was in use until December 1969 the reactor background from fast neutrons and gammas was reduced efficiently by means of a cooled quartz filter placed in the reactor channel. This filter worked well and gave an acceptable background level in the gamma detector particularly in the period up to the summer of 1969. when the reactor power was increased from 30 to 50 MW. After this the filter was still operative, but the transmitted background radiation increased to a level which unfortunately reduced the possibility of performing some experiments which had previously been possible.

When the neutron crystal spectrometer in the same reactor channel was rebuilt, the quartz filter was removed; this led to a very marked increase in the background. It became impossible to use the present set-up, because the counting rates in the gamma detector went up by a factor of ten, and the NaI-scintillator started to become activated.

Some figures are included here which give an idea of the various counting rates. They are given in ranges owing to the variations in monochromator settings of the neutron crystal spectrometer, which in turn caused variations in the intensities of the beams both of the thermal neutrons and the background. The fission experiment has suffered from these variations because the background level as sensed by the gamma detector has been changed. On many occasions these variations have been unimportant, since the gamma peak in the time-of-flight spectrum was superimposed on the background, and with acceptable statistics the number of fission gamma rays could still be estimated. When measuring gamma-ray energy spectra, however, the problems were many, since the background spectrum exhibited a tendency to change in shape slightly from time to time, depending on the amount of material in the monochromator crystal acting as a filter.

Total number of counts in the gamma detector	2000-5000 cps
Counting rates on the fission counters	140-380 cps
Coincidence fission counting rates (mass spectrum)	75-200 cps
Triple coincidence counting rates (uncollimated fission gamma radiation)	0.3-1.0 cps

When the gamma collimator was included the triple coincidence counting rate fell to different values depending on the type of radiation studied, i.e. which half-life was enhanced. For the slowest radiation studied here it decreased to roughly 0.5-1.0 counts per minute.

A knowledge of the drift in the electronic component is extremely important. Many of the results given in this report take the form of a relative yield per fragment mass. In order that comparisons can be made between photon yields from all the fragment masses, the photon yield from a given mass is divided by the yield of that particular mass. Accordingly two functions are used, namely the photon yield as a function of mass and the mass yield curve, the first function being divided by the second, point by point. The two functions, and especially the mass yield function, are steep for symmetric and very assymetric fissions. It is very important therefore that the change in position of the respective curves should be as small as possible during a measurement period. For this reason frequent checks of the mass yield curve were made during the measurements. The drift in the mass channel was found to be less than 1 % during a period of two weeks.

3.2.6. Miscellaneous

All measurements have been made in the coincidence mode, including accumulation of single spectra such as calibrations of fragment mass and gamma-ray energies. The reason for this is twofold. First, the data recording system needed a coincidence (opening) signal for each pulse to be analyzed. This coincidence pulse was obtained from the timing circuit. With the TPHC+ used in this experiment an output pulse is generated on the arrival of a start pulse (fission pulse). If no stop pulse has arrived within the range of time set on the converter, the output pulse is derived from the automatic reset of the TPHC. The second, and often more important, reason for using the coincidence technique is the fre-

+ Type 263, purchased from ORTEC, Oak Ridge, Tenn., USA.

quent need for making comparisons between coincidence (gated) and single spectra. In order to avoid uncertainties in the pulse heights brought about by the use of these different measuring modes, all spectra were therefore recorded in the coincidence mode. As described earlier comparison is made between yields as a function of fragment mass, and yield functions were also divided by one another. Thus by conducting all the experiments in the same way one possible source of error should be avoided.

As noted, the results are given as functions of fragment groups and not of individual masses. This is acceptable for physical reasons since, as was discussed by Johansson (2) several properties of the prompt gamma radiation varies slowly with mass number. This is fortunate in view of the impossibility of studying individual fragments with the present type of apparatus. Even if it were possible to select a single mass, the need to account for the charge dispersion remains. The best mass resolution which can be achieved in an experiment of this kind corresponds to a FWHM value of about 5 mass units, depending mainly on prompt neutron emission, the mass defect of the solid state detectors and the energy losses in the fissile foil and its backing (2,10). No thorough investigation of mass resolution has been made in the present experiment, but results from earlier studies of this kind have been published elsewhere together with a detailed description of the experimental equipment used (55,56).

4. COMMENTS AND SUGGESTIONS FOR FUTURE EXPERIMENTS

4.1 Improvements in experimental procedure

Counting rates present a crucial problem in many fission experiments. With uranium layers of thicknesses less than 100 $\mu g/cm^2$

it is possible to have acceptable fission rates with a slow-neutron beam whose intensity is about 10^8 n/cm^2 s. Such an intensity is by no means unusual from reactor channels today. A problem arises, however, in the form of the strong background radiation emanating from the reactor core, and reduction of this is generally sought by inserting appropriate filters into the channel. Unfortunately such a measure will affect the flux of the thermal neutron, although not to the same extent as that of the gamma radiation and the fast neutrons.

The main problem involved in experiments aimed at studying the fission gamma radiation is therefore seen to be one of obtaining a sufficiently low general background rather than obtaining a high flux. In an experiment of the type described in the present report the general background is easily estimated from the time-of-flight spectra and if interest is attached to a study of the prompt gamma radiation alone it becomes essential to maximize the signal/background ratio. For studies of delayed radiation, say in time intervals from 1-100 nanoseconds, the problem becomes even more serious.

The use of appropriate filters represents one widely adopted method, as for example the use of cooled filters of materials such as bismuth or quartz. Another, more effective, technique which is discussed more frequently nowadays, is the use of curved neutron guide tubes (62); the thermal flux is not decreased in this instance, but may even be increased. The main advantage behind the use of the guide tube lies, however, in the quite marked decrease produced in the fast neutron and gamma background.

It is not difficult to obtain thermal neutron fluxes of 10^8 -10^9 n cm^2 · s. It should be pointed out, however, that due to experimental difficulties it is unnecessary to increase the neutron intensity, and as a consequence the fission rate, beyond this level. The fission counters, which are mostly silicon detectors of the surface barrier type, have rather limited life times, owing to the destructive effect of the fragments. Normally, the detectors deteriorate to such a degree that after an accumulated dose of about 10^9 fragments/cm^2 the energy spectra are unacceptable for data analysis. The course of this deterioration can be periodically followed by measuring the leakage current through the detectors. The life of the detectors can be increased by keeping them constantly cooled. The temperature should then be of the order of -30^o C. If the fission rate is very high the fragment detectors will deteriorate more rapidly, which implies a rapid loss in the quality of their energy spectra. This in turn means that the studied mass spectra are destroyed. While this phenomenon must be checked frequently it is in fact unnecessary to have higher counting rates than can be easily followed by the leakage current. When running the experiment overnight the mass spectrum can easily be completely spoiled by using fluxes of more than 10^9 n/$cm^2 \cdot$s.

It may be asked whether any improvements can be achieved in the FWHM value of the gamma peak of the time-of-flight spectra, figs. 4 and 5. The significance of this question lies in the width of the gamma peak which, as it becomes narrower, leads to an improvment in the signal to background condition in the gamma-energy spectra. One approach would be to locate the "time detector" as close as possible to the fission foil which would afford a reduction in the time interval for the arrival of the fragments. The TPHC would, however, be triggered more often and consequently let through more background pulses. This problem can be avoided by means of an extra coincidence requirement, namely that of letting the time signal arrive in coincidence with a pulse from the other fission detector. A new problem now arises in the form of reduced time resolution of the gamma collimator, the analysis being performed on gamma radiation from fragments in a larger solid angle than used in the present geometry.

If it is considered essential to have the "time detector" very close to the fission foil, the other detector could be placed further away from the foil and then the geometry would be about the same as at present. In both instances, however, the "time detector" must be located very close to the foil, and therefore partly in the neutron beam. Such a location is unacceptable since additional material capable of increasing the background should not be permitted in the vicinity of the foil, where the fission gamma radiation is mostly studied. It is moreover, preferable for the detector itself to be clear of the neutron beam in order to minimize radiation damage.

In a future version of this set-up it should be possible to improve the time resolution, as for example by the use of anti-walk circuits (63). An improvement by a factor of two or more may be attainable. These improvements were not regarded as being vital to the experiment at this stage, however, and no attempt at their introduction has been made.

4.2. Suggestions for future research

It may be of interest to discuss briefly some of the measurements that can be performed in a continuous series of studies. As mentioned earlier, several investigations are in progress in which Ge(Li)-detectors are used. So far practically all of these studies have been made on the integrated prompt gamma radiation, but with no time separation as for instance with gamma-collimator technique. Several experiments have demonstrated that there are different time components even in the bulk of the radiation within 1 nanosecond after the fission event. It must be worthwhile therefore to try to eliminate a great part of the prompt gamma radiation in order to be able to select one time component after the other. As was observed in the present studies, the gamma-ray energy spectra, with the enhanced radiation of half-lives 7 and 50 ps respectively, are very different, and an investigation of their Ge(Li)-spectra would seem to be of considerable value. It is obvious from the present work that the spectra recorded with the NaI-scintillator from fragments with mass numbers of roughly 110 and 150 have very pronounced peaks for gamma-ray energies about 250 keV, while in each case the background is very low over the whole region from 70 keV and upwards. In this region the Ge(Li)-detector could be used efficiently, and even with low counting rates, the peaks can be expected to stand out clearly.

Another investigation which was tried, but did not lead to any successful result was that of studying the $(n,\gamma f)$-process. This process has received little attention, even though it is important to the investigations of the fission process. Some earlier authors, (64,65) pursuing theoretical arguments, came to different conclusions as far as the occurrence of this process is concerned. Soon after their results were published a (d,p)-reaction study was performed on ^{238}Pu (66), though with results having uncertain interpretations (67). Since then the shape isomers have come into the picture more and more, and at present there is an interest in trying to record the gamma radiation from the decay within the second potential minimum. It is perhaps here that effort should be concentrated in the future.

As regards the gross structure of the prompt gamma radiation from fission fragments the shape of the spectrum should be of great value for nuclear spectroscopists studying (n,γ)-reactions in ^{235}U. When studying the capture reactions from thermal neutrons a heavy background from fission gamma radiation is to be expected. A number of mass-dependent lines in the gamma-ray energy spectra are probably "burried" in the integrated fission gamma-ray energy spectrum. It is also possible, however, that some of these lines will be strong enough to emerge above the integrated spectrum. Knowledge of these lines will clearly be of some value when considering background in the capture gamma-ray spectra.

Prompt fission gamma radiation is most easily studied in the spontaneous fission of ^{252}Cf, where the background is low and considerably less than that in the vicinity of a reactor. There are, however, reasons for investigating gamma components from the thermal fission of ^{235}U other than those mentioned above, one being that the light mass group is different and the uranium fission will therefore yield complementary data to californium fission. As mentioned earlier, the background in the reactor channel should be reduced for this purpose to as low a level as possible and for the near future, with the new research reactors going into operation, one can have great expectations in this respect.

It should not be forgotten, however, that the study of prompt fission gamma radiation should not be regarded as an end in itself, but as a part of the investigation of the fission process, in which it is an important component in the total energy decay. Studied as a function of the fragment mass, it can therefore give valuable informations concerning the fission process.

There is one type of study of fission gamma radiation which is of significance to an understanding of the fission process in general, namely the study of the yield of the gamma rays in association with the total kinetic energy of the fragments. Some investigations were begun in these laboratories and reported earlier (68). The purpose of this study was to gain some knowledge of the gamma-ray yield as a function of the spin distribution. The part played by the spin distribution of the fragments has been discussed by several authors and a summary is given in section 2 of this paper. These studies concern the fundamental aspects of nuclear physics and are therefore of significance in a wider sense than is covered by the fission process alone. Many interesting results are to be expected from this field of study in the near future.

ACKNOWLEDGEMENT

It is a great pleasure to be able to thank Professor N. Ryde for his deep interest in, and his encouragement and continued support of the present work.

Professor S. Johansson was responsible for defining the scientific basis of the work and his ideas and suggestions on various occasions have been of great value. For this the author wishes to express his sincere gratitude.

The investigations presented in this thesis were carried out at the Research Establishment of AB Atomenergi, Studsvik, and special thanks go to Professor G. Holte, Dr. R. Pauli and Dr. T. Wiedling for supplying all the equipment needed and for their encouraging interest.

Thanks are also due to Dr. N. Starfelt for his active and continued support when, as former Head of the Neutron Physics Section, he made the experiment possible.

Dr. N. Bärring and his group made the excellent uranium foils for which the author is duly grateful.

The assistance from Dr. J. Higbie and Mr. L. Lindow cannot be too highly esteemed.

I also wish to extend my thanks to the employees and other members of the Neutron Physics Section of AB Atomenergi, who have been of assistance in the work and who created a pleasant personal atmosphere.

The Library and Secretarial Department of AB Atomenergi have been unfailing and excellent in their help.

The English text of this manuscript was kindly revised by Mrs. Ann Brown, M.A.

Financial support for this work from Statens Råd för Atomforskning is gratefully acknowledged.

Department of Physics

Chalmers University of Technology, Göteborg

March, 1971 Harry Albinsson

REFERENCES

1. O. Hahn and F. Strassmann,
Naturwissenschaften 27 (1939) 11.

2. S.A.E. Johansson,
Nucl. Phys. 60 (1964) 378.

3. V.M. Strutinskii,
JETP (Soviet Physics) 10 (1960) 613.

4. M.M. Hoffman,
Phys. Rev. 133 (1964) B714.

5. J.R. Grover and J. Gilat,
Phys. Rev. 157 (1967) 814.

6. T.D. Thomas and J.R. Grover,
Phys. Rev. 159 (1967) 980.

7. J.O. Rasmussen, W. Nörenberg, and H.J. Mang,
Nucl. Phys. A136 (1969) 465.

8. S.S. Kapoor, H.R. Bowman, and S.G. Thompson
Phys. Rev. 140 (1965) B1310.

9. R.L. Watson, H.R. Bowman, and S.G. Thompson,
Phys. Rev. 162 (1967) 1169.

10. R.L. Watson, J.B. Wilhelmy, R.C. Jared, C. Rugge, H.R. Bowman,
S.G. Thompson, and J.O. Rasmussen,
Nucl. Phys. A141 (1970) 449.

11. D.R. Ruegsegger, Jr., and R.R. Roy,
Phys. Rev. C 1 (1970) 631.

12. R.L. Watson, R.C. Jared, and S.G. Thompson,
Phys. Rev. C 1 (1970) 1866.

13. E. Cheifetz, R.C. Jared, S.G. Thompson, and J.B. Wilhelmy,
Phys. Rev. Lett. 25 (1970) 38.

14. S.K. Kataria, S.S. Kapoor, S.R.S.Murthy, and P.N. Rama Rao,
Nucl. Phys. A154 (1970) 458.

15. J.B. Wilhelmy, S.G. Thompson, R.C. Jared, and E. Cheifetz,
Phys. Rev. Lett. 25 (1970) 1122.

16. F. Horsch and W. Michaelis,
in Physics and chemistry of fission. 2.
Vienna, 28 Jul - 1 Aug 1968. Proc. symp. IAEA, Vienna (1969)
527.

17. R.L. Watson,
Ph. D. thesis, University of California. Berkeley, Cal.
UCRL-16798 (1966)

18. L.E. Glendenin and J.P. Unik,
Phys. Rev. 140 (1965) B1301.

19. R.A. Atneosen, T.D. Thomas, W.M. Gibson, and M.L. Perlman,
Phys. Rev. 148 (1966) 1206.

20. S.R. Dolce, W.M. Gibson, and T.D. Thomas,
Phys. Rev. 180 (1969) 1177.

21. A.B. Long, B.W. Wehring, and M.E. Wyman,
Phys. Rev. 188 (1969) 1948.

22. L. Bridwell, M.E. Wyman, and B.W. Wehring,
Phys. Rev. 145 (1966) 963.

23. B.W. Wehring and M.E. Wyman,
Phys. Rev. 157 (1967) 1083.

24. V.P. Eismont and V.A. Yurgenson,
Soviet J. Nucl. Phys. 5 (1967) 852.

25. S.S. Kapoor, V.S. Ramamurthy, and R. Zaghloul,
Phys. Rev. 177 (1969) 1776.

26. E.M. Bohn, B.W. Wehring, and M.E. Wyman,
Phys. Rev. 188 (1969) 1909.

27. Yu. P. Davydov, S.M. Solov'ev, and V.P. Eismont,
Soviet J. Nucl. Phys. 9 (1969) 18.

28. H. Maier-Leibnitz, H.W. Schmitt, and P. Armbruster,
in Physics and chemistry of fission.
Salzburg, 22 - 26 Mar 1965. Proc. symp. Vol. 2. IAEA, Vienna (1965) 143.

29. S. Dési, A. Lajtai, and L. Nagy,
Acta Phys. Hung. 15 (1962) 185.

30. K. Skarsvåg,
Nucl. Phys. A153 (1970) 82.

31. P. Armbruster, F. Hossfeld, H. Labus, and K. Reichelt,
in Physics and chemistry of fission. 2.
Vienna, 28 Jul - 1 Aug 1969. Proc. symp. IAEA, Vienna (1969) 545, and to be published

32. S.A.E. Johansson and P. Kleinheinz,
in Alpha-, beta-, and gamma-ray spectroscopy, ed. by K. Siegbahn, (North-Holland, Amsterdam, 1965) Vol. I, 805.

33. H. Maier-Leibnitz, P. Armbruster, and H.J. Specht,
in Physics and chemistry of fission.
Salzburg, 22 - 26 Mar 1965. Proc. symp. Vol. 2. IAEA, Vienna (1965) 113.

34. Yu. S. Zamyatnin,
in Physics of nuclear fission, ed. by N.A. Perfilov and V.P. Eismont (Israel progr. for sci. transl., Jerusalem, 1964, distr. Oldbourne Press, London 1964) 84. Transl. from Russian.

35. E.K. Hyde,
The nuclear properties of the heavy elements, III, Fission phenomena (Prentice-Hall, New Jersey, 1964) 279.

36. J.S. Fraser and J.C.D. Milton,
in Ann. rev. nucl. sci., ed. by E. Segrè, G. Friedlander, and H.P. Noyes. 16 (Annual Reviews, Palo Alto, Calif. 1966) 379.

37. J.E. Gindler and J.R. Huizenga,
in Nuclear chemistry, ed. by L. Yaffe. (Academic Press, New York, 1968) Vol. 2, 1.

38. Physics and chemistry of fission (Proc. Symp. Vienna, 28 July - 1 Aug 1969). IAEA, Vienna (1969) session F and H 477 and 669.

39. G.V. Val'skii, B.M. Aleksandrov, I.A. Baranov, A.S. Krivokhatskii, G.A. Petrov, and Yu. S. Pleva,
Soviet J. Nucl. Phys. 10 (1969) 137

40. G.V. Val'skii, G.A. Petrov, and Yu. S. Pleva,
Soviet J. Nucl. Phys. 5 (1967) 521.

41. G.V. Val'skii, G.A. Petrov, and Yu. S. Pleva,
Soviet J. Nucl. Phys. 8 (1969) 171.

42. V.M. Adamov, L.V. Drapchinskii, S.S. Kovalenko, K.A. Petrzhak, and I.I. Tyutyugin,
Sov. J. Nucl. Phys. 5 (1967) 655.

43. N.N. Ajitanand,
Nucl. Phys. A133 (1969) 625.

44. S.S. Kapoor, V.S. Ramamurthy, and P.N. Rama Rao,
Phys. Rev. 166 (1968) 1190.

45. R.L. Watson,
Phys. Rev. 179 (1969) 1109.

46. N. Feather,
Phys. Rev. C 1 (1970) 747.

47. V.M. Adamov, L.V. Drapchinskii, S.S. Kovalenko, K.A. Petrzhak, and I.I. Tyutyugin,
Soviet J. Nucl. Phys. 11 (1970) 557.

48. W. John, F.W. Guy, and J.J. Wesolowski,
Phys. Rev. C 2 (1970) 1451

(48A) F.W. Guy,
Ph. D. thesis, University of California, Livermore, Cal. UCRL-50810 (1970).

49. G.V. Val'skii, D.M. Kaminker, G.A. Petrov, and L.A. Popeko, Soviet At. Energy 18 (1965) 279.

50. S.A.E. Johansson, Nucl. Phys. 64 (1965) 147.

51. D.G. Sarantites, G.E. Gordon, and C.D. Coryell, Phys. Rev. 138 (1965) B353.

52. H. Albinsson, AE-420 (1971).

53. L. Beckman, J. Hansén, and R. Jansson, Nucl. Instr. Methods 52 (1967) 157.

54. H.R. Bowman, S.G. Thompson, J.C.D. Milton, and W.J. Swiatecki, Phys. Rev. 126 (1962) 2120.

55. J. Higbie, AE-367 (1969).

56. J. Higbie, Nucl. Instr. Methods 82 (1970) 253.

57. E.A. Gere and G.L. Miller, IEEE Trans. Nucl. Sci. NS-11 (1964) 382.

58. G.R Hogg and K.H. Lokan, Nucl. Instr. Methods 33 (1965) 319.

59. P.G. Sjölin, K. Granström and J. Björkman, AB Atomenergi, Sweden (Internal rep. AE-SSI-229) (1968).

60. L. Lindow and H. Albinsson, AB Atomenergi, Sweden (Internal rep. AE-TPM-FFN-100) (1969).

61. H. Albinsson, AE-421 (1971).

62. H. Maier-Leibnitz and T. Springer, in Ann. rev. nucl. sci., ed. by E. Segrè, G. Friedlander, and H.P. Noyes. 16 (Annual Reviews, Palo Alto, Calif., 1966) 207.

(62A) H. Maier-Leibnitz, in Neutron capture gamma-ray spectroscopy. Studsvik, 11 - 15 Aug 1969. Proc. symp. IAEA, Vienna (1969) 93.

63. F. Shiraishi and M. Hosoe, Nucl. Instr. Methods 66 (1968)130.

64. V. Stavinsky and M.O. Shaker, Nucl. Phys. 62 (1965) 667.

65. J.E. Lynn,
Phys. Lett. 18 (1965) 31.

66. C.D. Bowman, G.F. Auchampaugh, W.F. Stubbins, T.E. Young,
F.B. Simpson, and M.S. Moore,
Phys. Rev. Lett. 18 (1967) 15.

67. J.E. Lynn,
The theory of neutron resonance reactions (Clarendon Press,
Oxford, 1968) 432.

68. H. Albinsson,
AE-417 (1971).

GÖTEBORG 1971
ELANDERS BOKTRYCKERI AKTIEBOLAG

AE-398

UDC 539.166.08
539.122.164
539.173.4.162.2

AE-398

Prompt Gamma Radiation from Fragments in the Thermal Fission of ^{235}U

H. Albinsson and L. Lindow

This report is intended for publication in a perodical. References may not be published prior to such publication without the consent of the author.

AKTIEBOLAGET ATOMENERGI

STUDSVIK, NYKÖPING, SWEDEN 1970

PROMPT GAMMA RADIATION FROM FRAGMENTS IN THE THERMAL FISSION OF ^{235}U

H Albinsson* and L Lindow

ABSTRACT

Measurements were made on the gamma radiation emitted from fission fragments in slow neutron induced fission of ^{235}U. The fragments were detected with solid state detectors of the surface barrier type and the gamma radiation with a NaI(TI) scintillator. Mass selection was used so that the gamma radiation could be measured as a function of fragment mass. Time discrimination between the fission gammas and the prompt neutrons released in the fission process was employed to reduce the background. The gamma radiation emitted during different time intervals after the fission event was studied with the help of a collimator, the position of which was changed along the path of the fission fragments. In this way a decay curve was obtained from which the life-time of one of the gamma-emitting states could be estimated. The relative yield of the gamma-rays was determined as a function of mass for different gamma-ray energy portions and two specific time intervals after the fission events.

Comparisons were made with data obtained from ^{252}Cf fission. Attention is drawn to some features which seem to be the same in ^{235}U and ^{252}Cf fission.

* Chalmers University of Technology, Gothenburg

Printed and distributed in June 1970

LIST OF CONTENTS

1. INTRODUCTION

During recent years much interest has been devoted to the study of the gamma radiation emitted in the de-excitation of fission fragments [1 - 18]. Most of these studies have concerned the K X-ray and conversion electron yields [6 - 9, 12 - 15] in different time intervals within about 100 nanoseconds after the fission event. The main bulk of data have come from experiments with ^{252}Cf spontaneous fission and to a less extent from studies of slow neutron induced fission of ^{235}U [5, 10, 11, 17]. Measurements of the latter fission process are rather difficult to perform because of the severe background always present in reactor experiments. The light mass groups are different in the two fission processes and therefore a close examination of the uranium fission is worthwhile, even if the californium fission may be easier to investigate.

In most fission measurements nowadays mass selection is used and the yields of photons and electrons are studied in coincidence with the fragment masses.

The prompt neutrons which are also released during the fission events cause a background in the gamma detector. In very few cases has the time-of-flight technique been adopted for discrimination between the prompt neutrons and the fission gamma radiation [18 - 22]. At any rate no extensive study with this method has been made so far. To be effective, distances of about 50 cm or more between the fission foil and the gamma detector must be used, giving very small solid angles of the gamma detector and thus also low counting rates.

Of great interest are the life-times of the gamma-emitting states of the fragments. They can be studied by a collimator technique in the following way. The gamma radiation is emitted from fragments in flight and, by changing the position of a collimator along the path of the moving fragments, one can select different time intervals during which fission gamma radiation is allowed to reach the gamma detector. Such a technique has been used in few experiments up till now: in ^{252}Cf fission [1, 21] and in ^{235}U fission [10, 19]. As the average velocity of a fragment is about 1 cm/ns, a collimator with a slit width of 1 mm will let a fragment be exposed to the gamma detector for a time interval of about 10^{-10}s.

In the present investigation the so-called prompt gamma radiation from fragments in slow-neutron induced fission of ^{235}U was studied. The expression "prompt gamma radiation" used here was coined by Johansson[1]. In his studies of californium fission it was found that the radiation could be divided into two parts: a "prompt" component with a half-life shorter than 10^{-9}s and a "delayed" component. This division is, of course, somewhat arbitrary, but Johansson found a distinct difference in the characteristics of the radiation in the two cases.

2. EXPERIMENTAL PROCEDURE

2.1. Apparatus

The principle of the set-up of this experiment is shown in fig. 1. A neutron beam from the Studsvik R2 reactor was collimated, so that no part of the beam struck more than the target and its mounting frame inside a vacuum chamber. Two solid state detectors of the surface barrier type were placed in parallel and symmetrically around the foil to measure the energies of the fission fragments. The detectors+ were about 4 cm^2 in area, fabricated from 400 ohmcm n-type silicon and operated at about 70 V bias. The distance between each detector and

---

+ Type C7904 Heavy Ion Detectors supplied by ORTEC, Oak Ridge, Tenn., USA the fissile foil was 2 cm. The gamma detector was a NaI(TI) scintillator from Harshaw, 10.4 cm long and 13.0 cm in diameter, viewed by a Philips XP1040 photomultiplier tube. The associated electronics[+], consisting of a pulse-shaping unit and a discriminator, was coupled directly to the photomultiplier tube socket and gave a fast leading-edge time pulse and a linear pulse.

In this series of investigations a NaI scintillator was used for gamma radiation detection due to its high efficiency. As the counting rates are very low it was found to be more important to detect as many events as possible than to get high resolution but low efficiency as with a Ge(Li) detector.

A lead collimator, movable in parallel with the direction of the detected fragments and also with a variable slit, was used to select gamma radiation in different time intervals after the fission event.

The fissile deposit was about 1 cm^2 in area and prepared by electrodeposition on 100 $\mu g/cm^2$ nickel foils. In all runs when mass selection was used the ^{235}U target was less than 100 $\mu g/cm^2$.

It is very important in this type of measurements that the uranium layer and the nickel foil are thin and uniform. The fragment energy loss has not been measured but may be estimated to be $\leq$ 3 MeV [23, 24]. As will be discussed below, the fragment energy spectra were used to get mass spectra, and it was found that an upper practical limit of less than about 100 $\mu g/cm^2$ was enough to get energy spectra of good quality. In some measurements, however, when mass selection was not necessary, or for some reason not possible, thicker layers, of up to about 400 $\mu g/cm^2$, were allowed.

[+] Designed and built at the Research Institute of National Defence, Stockholm [25].

A block diagram of the electronics is shown in fig. 2. Pulses from the solid state detectors were amplified in charge-sensitive preamplifiers followed by linear amplifiers. After delaying one of the pulses and stretching both of them, they were added and fed into a logarithmic amplifier, the output pulse heights of which were proportional to the logarithm of the incoming pulse heights [24, 26]. By disregarding prompt neutron evaporation and energy losses in the target material, it can easily be shown that the ratio of the energies of the two fragments is inversely proportional to the mass ratio.

At an early stage of the experiment a fast coincidence circuit was used, triggering on time pickoff pulses from both fragment detectors, to start the time-to-pulse-height converter (TPHC), so that no timing signal passed unless both fragments from a fission event were registered [24]. Later the fast coincidence circuit was removed and the TPHC was started with pulses from one fission detector. In case only one fragment was detected, i. e. the other fragment missed its detector no mass pulse was recorded. The only problem with this latter arrangement was that for every run the number of measured fission pulses counted on the "timing" fission detector had to be checked and related to the recorded number of mass pulses (when both fragments of an event were detected). With this geometry there is a factor of 1.5 - 2 between these two numbers due to the different solid angles of the fragment detectors.

After amplification the timing pulses were sent into a single channel analyzer (SCA) with its window set over the gamma peak in the time-of-flight spectrum. The output of the SCA then served as the coincidence pulse for the multichannel analyzer.

Data were stored in a two-parameter analyzer the memory of which was that of a small computer, PDP-8/S. It should be noted that the PDP-8/S was not working as a normal on-line computer, because no data analysis was done during the measurements, but only recording of events. Data analysis was done with separate programs after the measurements were completed [27, 28].

The interfacing unit between the computer and the nuclear physics electronics consisted of two ADC's and their associate registers. Each ADC had 400 channels and the computer memory consisted of 4 K words, i. e. 4096 positions or channels. When an analysing signal had passed its ADC,(or in a two-parameter mode two signals had passed their respective ADC's) it was stored momentarily in its respective register, from where the computer transferred the information into the memory. Of the 4096 channels in the computer memory 3200 channels could be used for data storage. The rest of the memory was used for programs performing operations such as transfer of data into the memory from the nuclear physics electronics, for display on a CRT, and for readout on a typewriter and/or a punch. The 3200 channels could then be divided into matrices of the following forms when measuring with two parameters: 8 x 400, 16 x 200, 32 x 100, or 64 x 50. In a one-parameter mode any of the above-mentioned single configurations was available.

The NaI detector was placed about 70 cm from the fission foil and in a direction perpendicular to the direction of the detected fragments (fig. 1). The main reason for using the time-of-flight technique was to discriminate the prompt neutrons from the fission gamma radiation, but in this geometry it was possible to benefit by the form of the angular distribution of the prompt neutrons. As is well known,it is peaked in the direction of the fragments.

It might be mentioned at this point that a change of distance between the fission foil and the gamma detector did not change the solid angle for gamma detection according to the inverse square law, as would be expected, but instead almost linearly. This is due to the fact that the gamma collimator is mostly set with a narrow slit and the change in solid angle with distance is almost completely dependent on the length of the collimator. Solid angles of the order of 10^{-4} - 10^{-3} sr are normal in these measurements, but, as will be discussed in a coming report [29], this small solid angle is primarily dependent on the collimator setting and not so much on the distance between the foil and the gamma detector.

2.2. Performance

A typical mass spectrum from the thermal fission of ^{235}U recorded with the logarithmic amplifier is shown in fig. 3. The relative yield of fragments in a particular mass region is, of course, not the same as it is when the mass spectrum is on a linear scale. This is a drawback when comparisons are to be made with various relative yields as functions of fragment mass and the other results have been obtained with the fragment mass on a linear scale. Direct quantitative comparisons cannot be made, though it is possible to calculate a new yield curve as a function of mass on a linear scale. The variation in the energy of the prompt photons with fragment mass is, however, a very slow function, and so part of the drawback will be less important in this experiment as one is allowed to consider these photon yields as functions of mass regions instead of individual masses [1]. In any case qualitative comparisons can be made.

Some typical time-of-flight spectra are shown in fig. 4 and 5. Fig. 4 shows a spectrum of the uncollimated gamma radiation with no gamma-ray energy discrimination. The gamma detector was "viewing" the whole region between and including the two fragment detectors. The general background which has no correlation to the fission events is the level to the left of the gamma peak, and the broad distribution just to the right is the prompt neutron yield. The time separation at the NaI detector between the fission gamma radiation and the prompt neutrons of largest yield is about 30 ns, which is achieved for a time-of-flight distance of about 70 cm. In fig. 5 are plotted time-of-flight spectra with the lead collimator in three different positions, which means that only small parts of the fragments´ paths are "seen" by the gamma detector.

As indicated in fig. 4 the full width at half maximum (FWHM) value of the gamma peak is 5 ns. This is due to three basic causes: 1) time walk due to amplitude variations in the detector signal, 2) different velocities of the fragments giving a spread in the arrival time at the detector, and 3) the resolution of the gamma timing circuit. Time spectra were measured for coincident fission fragments by causing the TPHC to be started by the signal from one fragment detector and stopped by the signal from the other, resulting in two-peaked curves of the type shown in fig. 6, having a FWHM value of 3.7 ns. The FWHM value for each detector can thus be estimated to be a little less than 2 ns. The time spread in the gamma timing circuit is about 4 ns [25].

The question is whether any improvements can be achieved or not in the FWHM value of the gamma peak in the time-of-flight spectra. This is important to know, because a "narrower" gamma peak is an improvement on the signal to background condition in the gamma energy spectra. One approach would be to put the "time detector" as close as possible to the fission foil. That would give a reduction of the interval of the time of arrival of the fragments. But the TPHC would start more often and consequently let through more background pulses. This can be circumvented by means of an extra coincidence requirement, e.g. by letting the time signal arrive in coincidence with a pulse from the other fission detector. The drawback is, however, that the time resolution of the gamma collimator will be worse, because gamma radiation from fragments in a larger solid angle than with the present geometry will be analyzed.

If, for any reason, it is considered to be important to have the "time detector" very close to the fission foil, the other detector could be put further away from the foil and then about the same geometry as now would be used. But in both these cases the "time detector" must be put very close to the foil, which would mean that the detector would be partly in the neutron beam. This is not acceptable, because in the vicinity of the foil, where the fission gamma radiation is mostly studied, there should not be any extra material to give rise to more background. Besides, it is better for the detector itself to be clear of the neutron beam to reduce radiation damage to it.

In a future version of this set-up there are possible improvements to be made in the time resolution, e.g. by use of anti-walk circuits [30]. A factor of two or more may be possible. These improvements were not found to be very important at this stage of the experiment, and so they were not tried.

With the help of the collimator, to select gamma radiation from different time intervals after the fission event, time-of-flight spectra were recorded with the collimator in different positions. The average velocity of the fragments is known to be about 1 cm/ns. By estimating the intensity of the gamma peak the intensity variation with the collimator setting was obtained, i. e. the variation with time after fission.

Of extreme importance is the knowledge of the drift in the electronics. Many of the results given in this report are of the kind: relative yield per fragment mass. To be able to make comparisons between photon yields from all fragment masses, the photon yield from a certain mass is divided by the yield of that particular mass. Accordingly two functions are used, the photon yield as a function of mass and the mass yield curve, and the first function is divided by the second, point by point. The two functions, especially the mass yield function, are steep for very asymmetric and symmetric fissions. Consequently it is very important that the change in position of the respective curves should be as small as possible during a measurement period. Frequent checks of the mass yield curve were made during the measurements. The drift in the mass channel was found to be less than 1 % during a period of two weeks.

All measurements have been made in the coincidence mode, even accumulation of single spectra such as calibrations of fragment mass and gamma-ray energies. The reason for this is twofold. First, the data recording system needed a coincidence (opening) signal for each pulse to be analyzed. This coincidence pulse was obtained from the timing circuit. With the TPHC+ used in this experiment there is always an output pulse as soon as a start pulse (fission pulse) has arrived. In case no stop pulse has arrived within the range of time set on the converter, the output pulse is derived from the automatic reset of the TPHC. The second reason for using the coincidence technique, which is often more

---

+ Type 263, purchased from ORTEC, Oak Ridge, Tenn., USA.

important than the first one, was that quite often comparisons had to be made between coincidence (gated) and single spectra. In order to avoid uncertainties in the pulse heights brought about by different measuring modes, all spectra were recorded in the coincidence mode. As discussed above, yields as functions of fragment mass were compared, and yield functions were also divided by one another, and by making all experiments in the same way one possible source of error was avoided.

As noted, the results are given as functions of fragment groups and not of individual masses. For physical reasons this is acceptable, because, as was discussed by Johansson [1], the character of the prompt gamma radiation varies slowly with mass number. This is fortunate because one cannot study individual fragments with the present type of apparatus. Even if it were possible to select a single mass, one still has to account for charge dispersion. The best mass resolution which can be achieved in an experiment of this kind is a FWHM value of about 5 mass units, which mainly depends on prompt neutron emission, the mass defect of the solid state detectors and the energy losses in the fissile foil and its backing [1, 7]. No thorough investigation of the mass resolution has been made in this experiment, but results from earlier studies of that kind have been published elsewhere together with a detailed description of the experimental equipment [24].

3. RESULTS

3.1. General

The main object of the work presented in this report was to examine the number of prompt photons of different gamma energy portions as functions of fragment mass. All the investigations have been performed in a time interval of about 10^{-11} - 10^{-9}s. In an integral measurement, the result of which forms the basis for most of the discussion in the following section, a mass spectrum was accumulated in coincidence with fission gamma-rays, by taking the coincidence signal from the "timing" SCA as mentioned in section 2.1. The resulting mass spectrum was in coincidence with all fission gammas irrespective of their energies. Another, more or less preliminary investigation was a two-parameter measurement in which mass was one parameter and gamma-ray energy the other. For each mass it was possible to add the number of pulses in parts of the respective gamma-ray energy spectra, giving the total number of gamma-rays emitted, but now in different energy portions.

3.2. Mass-dependent yield of prompt photons of all energies

The above-mentioned integral measurement started with the accumulation of a direct mass spectrum and after division of the gated mass spectrum by this direct spectrum, the relative number of photons per fragment mass was obtained, and the result in the form of a gamma-ray yield curve is shown in fig. 7. The time interval analyzed here is about 10^{-11} - 10^{-10}s, corresponding to the gamma decays at practically the first mm of a fragment's flight path. The first striking feature of the curve in fig. 7 is the similarity with the so-called saw-tooth curve which is obtained in the study of the prompt neutron yield per fragment mass. Such curves have also been found in earlier fission gamma radiation studies of ^{252}Cf [1] and ^{235}U [11]. In the uranium experiment [11] the errors were rather large, due to difficulties in determining the exact number of fission gamma pulses over background. A more recent result [19] also showed the saw-tooth character even though the mass resolution was of poorer quality. The general background in the present experiment as estimated from its level in the time-of-flight spectrum (section 2.2) was less then 10 % of the intensity under the gamma peak.

One notices two kinds of deviations from the general appearance of the saw-tooth curve. The first is characterized by the dips at mass numbers 88 and 102. The second is the relatively low yield for both the very lightest and the very heaviest fragments, if they also were to give yields according to a curve of the saw-tooth type, like most of the other fragments do. The curve also seems to have a plateau around mass number 145, i.e. in the so-called transition region.

In some mass regions this yield curve is difficult to compare with the other similar curves [1, 11], e.g. in the regions of closed nucleon shells around mass numbers 132 and 82. The main difficulty in making comparisons with other experiments lies in the fact that these mass spectra are on a logarithmic scale[+]. The fragment mass of 82 is hardly seen in ^{252}Cf fission, but on the other hand there is a relatively high yield of fragments up to a mass number of about 115 in the light mass group, and these fragments have very low yields in uranium fission.

[+] In the course of preparing this report a linear divider circuit has become available for the experiment, so now it is possible to make direct comparisons between results from these studies and those of other fission laboratories. Furthermore it has also become possible in these studies to compare yields in terms of numbers from different fragment mass regions of particular interest, such as mass numbers 132 and 82.

3.3. Mass-dependent yield of prompt photons of specific energies

As mentioned above measurements have also started with the aim of looking at the gamma radiation for different energy portions. These studies will continue and only one preliminary result will be given here. The measurements were made with full use of all circuits shown in the block diagram in fig. 2. As soon as there was a gamma pulse in the time-of-flight spectrum, the "timing" SCA opened the ADC's of the two-parameter multichannel analyzer, to let in for analysis the linear pulses from the mass circuit and the gamma-ray energy amplifier. The data were then stored in a matrix, of the kind described in section 2.1, in the computer memory and were thus available in the form of two-parameter spectra, e.g. gamma-ray energy spectra as functions of fragment mass. In each gamma spectrum it was possible to add up the number of pulses in different gamma-ray energy portions, and by doing so for the various gamma spectra, i.e. for the spectra obtained by the different fragment mass groups, the yield of gammas of a particular energy portion was obtained for the respective mass groups. Dividing these yields by the yields of the mass groups, the latter given by a direct measurement of the mass distribution, resulted in a relative gamma-ray yield as a function of fragment mass. Two examples of such yield distributions are shown in fig. 8, which also indicates the respective gamma-ray energy portions for which these functions have been calculated. The lower part of the figure presents the relative gamma-ray yield as a function of mass for photons of energies less than 0.33 MeV, and the shape of the curve is roughly of the saw-tooth type. When photons of energies above 0.33 MeV but less than 1.35 MeV are studied, the yield function is not at all of the saw-tooth type. The time range studied here is from about 0.4 to 1 ns.

3.4. Time distribution

The half-life of one fission gamma component has been estimated by recording time-of-flight spectra with the lead collimator in different positions. The intensity variation of the gamma peak with the collimator setting gave the same variation with time after fission and in a decay curve of the same shape as shown in ref. 1 the half-life was estimated to be about 20 ps. The studies of the time distribution of the gamma radiation have been continued with a more sophisticated collimator system than was used in the present experiment, and those results will be published elsewhere [29].

3.5. Gamma-ray energy spectrum

In fig. 9 is shown a gamma-ray energy spectrum of all prompt fission gammas. It was recorded in coincidence with the gammas of a time-of-flight spectrum of the same type as shown in fig. 4. The overall background is very low, namely less than 1 %. No corrections have been made for the response function of the detector. The shape of the spectrum is the same as those recorded earlier by, e.g., Maienschein [31].

4. DISCUSSION

4.1. General

The observed fine structure of the relative gamma-ray yield as a function of fragment mass can be described in terms of the collimator definition, i.e. it is caused by geometrical effects of the collimator, which for each setting selects photons from a certain time interval and in which the gamma decay rates differ from one fragment mass region to another. Fragments which are slow gamma emitters compared to the time associated with the collimator setting and fragment velocity will give rise to dips, as will also fragments which are fast emitters. The former fragments have emitted few gamma quantas when they have just passed the collimator opening and the latter fragments have emitted a larger number even before they pass the collimator. A certain half-life will be dominant at a particular collimator setting and other half-lives will be suppressed. This feature of fast and slow gamma emitters is, of course, directly related to the properties of the fragment masses and their excitations. Deformed nuclei seem to be slow fission gamma emitters [2, 29], e.g. in a time interval after scission, when a 50 ps half-life is selected, there is a large intensity of low energy photons, with energies of about 200 keV, emitted by fragments with mass numbers around 110 and above 150.

A complete analysis of the gamma-ray yield curve in fig. 7 must include the following properties and their interrelations: the distributions of time of the fission gamma radiation, of the photon energy, and of the fragment mass. The yield curve in fig. 7, however, reflects, the integrated number of photons in a specific time region after fission as a function of mass. The reason for showing just this curve is its association with a time region which is very interesting as far as the prompt gamma radiation is concerned. As was discussed in ref. 1, during the first 25 ps or so the fragments emit photons of rather equal energy. This is an important consideration because, if it were not so, to mention the number of photons would have no meaning at all. The number of photons times their energy corresponds to the total amount of energy released by the gamma decay, and that is the quantity which is of ultimate interest in this fission study. As will be discussed later [29] the yield of photons of different gamma-ray energy varies with time after fission and thus the collimator setting is a parameter of great importance.

The number of photons and their energies is worth some extra attention before discussing the details of the yield curves in fig. 7 and 8. As was pointed out in section 3, the yield curve in fig. 7 looks similar to the well-known curve of the saw-tooth type representing the yield of prompt neutrons as a function of fragment mass. The gross appearance of the curve is about the same for both cases. In many respects the present discussion will run along the same lines as that when studying the yield of prompt neutrons per fragment mass. The prompt neutron yield curve does not show up so many details as this gamma-ray yield curve. The absence of this structure in the neutron yield curve as compared with the gamma-ray yield curve is probably due to the fact that the neutron yield concerns all neutrons, while the gamma yield concerns the number of photons emitted in a relatively short time interval. Consequently it can be expected that most of the "unusual" effects discussed here will disappear if the relative number of photons as a function of fragment mass is studied in a time interval which is longer than that for which fig. 7 is valid, namely 10^{-11} - 10^{-10} s.

So far very little attention has been paid to the mass-dependent structure of the gamma-ray yield function and its association with time after fission. Short mention of it was made by Johansson [1, 2], but to our knowledge only brief investigations have been made [32 - 35].

4.2. Mass-dependent yield of prompt photons of all energies

The discussion will now deal with the yield of the prompt gamma-rays as a function of fragment mass (fig. 7) from the point of view of nuclear structure, and specifically in terms of spherical and non-spherical nuclei.

One of the assumptions in fission theory is that most of the original excitation energy of the fragments, directly after the scission act, is taken up by deformation [36]. In this respect every fission mode must be considered by studying the joint contribution from the fragment pair. The shape of the nuclei as described by the shell theory or the collective model, whenever any of them fits into the description, can be applied in the following way. A spherical nucleus, with one or both nucleon shells almost closed, is resistant to deformation, and its excitation energy directly after fission should not be so high as in a nucleus which can easily be deformed, i. e. one or both of its nucleon numbers are far from magic. If the excitation energy of certain fragments is high, due to the fact that they are easily deformable (soft fragments), they are able to emit more neutrons and photons than fragments which are not easily deformable (stiff fragments), because in the latter one or both nucleon shells are closed or almost closed. A full discussion of this problem has been given by Vandenbosch and Terrell [37, 38]. The saw-tooth curve reflecting the yield of the prompt neutrons as a function of fragment mass is well described by this picture. Take one example, e. g. the binary fission of ^{236}U into the fragment pair with mass numbers 110 and 126. The light fragment will probably have the proton number $Z = 44$ and the neutron number $N = 66$, and the heavy partner will then have the respective nucleon numbers $Z = 48$ and $N = 78$. The heavy fragment is rather stiff, while the light fragment is more soft. The prompt neutron yield for fragments in the mass region around 110 is much larger than around 126. The whole prompt neutron yield curve can then be discussed in the same way as in this particular example. Further support for this model is given by the application of a so-called "universal" yield curve [36]. The absolute number of prompt neutrons from a particular fragment is about the same, no matter in which fission process it was formed. A "universal" saw-tooth type curve is the result of prompt neutron yields known so far in low-energy fission, from fissile nuclei with mass numbers all the way from thermal neutron induced fission of ^{233}U to spontaneous fission of ^{252}Cf.

The description given here of the excitation of the fission fragments and their consequences on the prompt neutron decay can be borrowed to discuss the prompt gamma decay following neutron emission. In principle the discussion is the same, but, as was pointed out above, one must never forget that the photon energy should be included. The fission gamma radiation of shortest half-life, which can be selected with the available collimator without making it too narrow for intensity reasons [29], seems to have about the same energy for all fragments. The yield curve looks similar to the prompt neutron yield curve, because the fragments are still highly excited after the neutron emission, the excitations being higher the higher the original excitations have been. As has been pointed out by Johansson [1], one might expect that at the first moment the fragments emit a similar type of radiation, and the basic reason for this is that all fragments are probably deformed in a similar manner, giving rise to neutron emission because the excitations are high enough, and then prompt gamma emission of similar type over the whole mass spectrum.

On the basis of the above-mentioned model, in which the rigidity of the fragments is an important quantity, the discussion will now turn to a direct application of that model. In order to see things more clearly, a figure is drawn to explain the locations of the fission fragments on an isotope chart. Fig. 10 shows the part of the chart of particular interest in this investigation. The line of beta stability is drawn as a solid curve and the light fragment group in uranium fission is represented by the dashed line. The mass regions for which low gamma-ray yields have been observed, as presented in fig. 7, are shaded in fig. 10. One such portion is around mass number 82 where the neutron number is expected to be about 50, another around 88 where the two nucleon shells may start to be deformed and a third portion is around 102 where the proton number is about 40.

When the mass number increases from 82 and upwards one would anticipate effects in the yield curve in fig. 7 which may be due to the deformation of those nuclei. Such effects would set in at mass numbers around 88, and then last through the rest of the light part of the mass curve as, according to the shell theory, there is no other closed nucleon shell than N = 50 in the mass region where the light mass group is located. A change of yield takes place, however, around the mass number 96, and the gamma-ray yield curve has there come up to values corresponding to an average saw-tooth type curve drawn through most of the values plotted in the figure. The presence of the two dips at mass numbers 88 and 102 may indicate the existence of variations in the deformation of nuclei in these mass regions. Z = 40 should be the proton number for fragments of mass number around 102. The relevant neutron number for A = 102 is N = 62. The proton shell is almost spherical, but the neutron shell with 12 neutrons outside the closed shell of N = 50 might be easily deformable.

Under the condition that the fragments with mass numbers around

102 have nucleon shells, $Z \approx 40$ and $N \approx 62$, it may be interesting to study available data on level schemes from nuclei in their vicinity on the nuclide chart. Take, for instance, the fragments with mass numbers around 102. The proton number is expected to be about 40, and the neutron number to be about 62. This neutron-rich mass region is not easily accessible with today's accelerator technique. The line of beta-stability (fig. 10) goes through $Z = 40$ and $N = 50$. These stable nuclei have few excited levels at low energies, which is explained by the shell theory as being due to the resistivity of closed shells to excitation of one or two nucleons. The neutron number is 50 and magic, but the proton number of 40 can, according to the shell theory, be called a semi-magic number. The presence of this semi-magic number may indicate the difficulties which will be encountered when one tries to extrapolate the energies of certain types of excited states of nuclei at the beta-stability line into the regions where these fragments have been formed. Another example is the fragment mass region around $A = 88$ with $Z = 34$ and $N = 54$. If one tries to extrapolate the energies of certain types of levels in different isotopes of selenium, one soon approaches $N = 50$ where the energies of the excited levels go up due to the fact that one approaches a closed neutron shell. Instead the extrapolation can start with fixed neutron number, say $N = 54$. Very soon one sees effects setting in close to $Z = 40$, and then there are few data available when Z is less than 40 and N still 54. Of particular interest is the fact that the sister fragment to 102 is 134, which is close to being double-magic ($Z \approx 51$, $N \approx 83$). Without being able to give any exact numbers for comparison, the relative yield, as seen in fig. 7, is larger from the fragment with mass num-

ber 102 than it is from 134. This particular fission mode consists of a spherical nucleus, A = 134, which is thus stiff. As regards the partner fragment with A = 102 its yield of both prompt neutrons and prompt gamma radiation is larger than that from the fragment with A = 134.

The mass region around A = 110 deserves some extra attention, because the fission gamma studies in ^{252}Cf fission have given rather strong evidence that this mass region may have stable deformation [2, 39]. In the ^{252}Cf gamma-ray yield curve there is a dip in this mass region with about the same collimator setting as was used in the present experiment. Unfortunately the fragment yield in the mass region around 110 is very low in ^{235}U fission, while in ^{252}Cf fission the same mass region is almost where the fragment yield is the largest in the light mass group. Even though it may be difficult to make any detailed comparisons between the two yield curves in this mass region, some interesting and differing features occur. In the ^{235}U fission there is an anomalously high gamma-ray yield, contrary to the case in ^{252}Cf fission. This difference can probably be explained by studying the two fission modes in ^{235}U and ^{252}Cf fission resulting in a light fragment with mass number around 110. The sister fragment in ^{235}U fission has a mass number of 126, which means that it must be almost spherical (Z = 48, N = 78), while in ^{252}Cf fission the number is 142 which probably corresponds to a nucleus which is slightly more susceptible to deformation. This is because this mass region is close to the so-called transition region. Under the condition that quantities like energy and linear momentum are conserved in the fission process, it is very instructive to study the respective combinations of fragments in binary fission under these cirumstances. If a certain fission mode results in one spherical (stiff) fragment and one fragment with both nucleon numbers somewhere between the magic numbers 50 and 82 (soft fragment), the soft fragment will be able to tie up more deformation energy than the stiff fragment. ^{252}Cf symmetric fission results in the two stiff fragments with A = 126, while in ^{235}U fission, resulting in fragments with A = 126 and 110, most of the deformation energy is imparted to the fragment with A = 110. In ^{235}U fission one must expect to have relatively more excitation energy in the fragment with mass number 110 than the same fragment would have if it was formed in ^{252}Cf fission.

When the gamma-ray yield from the fragment mass region of 102 was discussed, it was seen in fig. 7, that the partner fragment with mass number 134 had a lower yield than 102. The heavy fragment emits a smaller number of photons and from this reasoning one can only conclude that the light partner is relatively soft compared to the heavy one. So-called deformation parameters characterizing the resistivity of the fragments to deformation have been calculated [38] and they have their largest values for N = 50, Z = 50, and N = 82, but there is a slightly larger value for Z = 40 than would be expected if Z = 40 was not a semi-magic number. It must be mentioned that these deformation parameters were calculated directly from fission data, and not through the use of extrapolations.

Now it is easy to complete the discussion of the appearance of the gamma-ray yield curve in fig. 7 with the fragment structure in mind. With increasing mass number the prompt neutron yield curve falls off sharply when the region of symmetric fission is reached. The gamma-ray yield curve in fig. 7 does the same, which is in agreement with the discussion above.

The relatively low yield in the mass region around A = 132 has already been discussed in relation to the partner fragments. The plateau around mass number 145, which is where the transition region is reached, is difficult to explain. It is a bit too low in mass number to be the partner fragment of 88, where another of the dips in fig. 7 occurred, and which could be due to some susceptibility to deformation. The probability that the dip at A = 88 and the plateau at A = 145 are due to a specific fragment combination cannot be completely ruled out at this stage, because if the mass calibration is changed by one unit downwards around A = 88 and A = 145, one is close to the fragment combination which would fit into this picture. The prompt neutron release may also contribute to give the proper mass around A = 145. The plateau at A = 145 can consequently be due to the fact that the light partner fragment is slightly soft and therefore able to pick up some extra deformation energy which will be obtained at the expense of the excitation of the heavy partner.

Finally the decrease of the prompt gamma-ray yield as a function of fragment mass in fig. 7 when the mass exceeds 148 should be mentioned. This is probably most obvious on the basis of the models used so far in this paper. The fragments with mass numbers above 148 are deformed and belong to the same mass region where many other deformed nuclei have been found.

4.3. Comparisons between prompt photon yields in ^{235}U and ^{252}Cf fission

In order to try further to illuminate the situation regarding the fission-fragment gamma-decay in ^{235}U fission, it is interesting to make comparisons with some of the known data from prompt gamma radiation in ^{252}Cf fission. The yields of the K X-rays and the conversion electrons as functions of fragment mass are both strongly increasing functions in the heavy mass region [4, 6-9, 12, 14, 16], until mass numbers around 148 are reached, when the yields suddenly drop. There have been discussions in the literature about this effect, and even though most authors seem to believe that it is a physical one, arguments have been put forward as to its origin. Whatever the reason is for this drop of yield, in some measurements it was found to be less drastic when the studied time region after fission was longer. This maybe due to the fact that many of the converted transitions come from rather long-lived states with life-times of the order of some tens of ns. Comparisons between the K X-ray and conversion electron yield curves as functions of fragment mass with that of the delayed gamma radiation in ^{252}Cf fission [2] may support this assumption. Around the mass number A = 155 a large yield of photons was found. This fits well into the description given at the beginning of this section, according to which it is expected that most of the "unusual" effects showing up in fig. 7 will disappear when longer time intervals are studied. This statement was made in connection with the prompt neutron yield discussion and has now found further support.

Some arguments have been advanced [8, 9, 12, 41] concerning the relatively low K X-ray and conversion electron yield in the heaviest fragment mass region. The energies of the first excited states of these fragments are believed to be so low that a proportionally small number of electrons are converted [41]. This is a plausible result, which cannot be tested further for the time being owing to the absence of this type of information from fission fragments or similar nuclei.

As was mentioned above, when the relatively low yield of prompt photons from fragments with mass numbers above 148 was discussed (fig. 7), comparisons made with delayed gamma radiation in ^{252}Cf fission [2] favoured the argument that, both in ^{235}U and ^{252}Cf fission, the heaviest fragments are slow gamma emitters. The mass region around A = 110 is interesting from this point of view. In ^{252}Cf fission [2] a large yield of delayed gamma radiation was found there too. On the assumption that deformable fragments are slow emitters, the dip in the relative gamma-ray yield curve as a function of fragment mass for prompt gamma radiation in ^{252}Cf fission corresponds to the increased yield in the same mass region for delayed radiation. The question is how can this increased yield correspond to the same fragments having a large yield of prompt photons in ^{235}U fission. As mentioned earlier, it is probably an effect associated with the particular fission mode in uranium, where the fragment with mass number 110 has a partner with mass number 126, the latter being very stiff, and thus most of the excitation energy, in the form of deformation just after scission, is imparted to the lighter fragment. In californium fission the heavy partner of the fragment with mass number 110 is 142, which is probably more deformable than 126.

The other mass regions in ^{252}Cf fission giving large yields of delayed gamma radiation are 92, 96 and 132 [2]. The delayed radiation emitted by fragments of mass numbers around 132 was thought to be caused by vibrations in the double-magic nuclei, in which the gamma transitions from the third to the second, and from the second to the first excited state in a beta-vibration cascade have energies in the range of 100 - 300 keV, and are thus rather slow. The ground-state transition energy is expected to be something between 1 and 1.5 MeV. Indications of all these transitions showed up in the gamma-ray energy spectra for the delayed gamma transitions in ^{252}Cf fission. The large yield of delayed gamma radiation in ^{252}Cf fission in the fragment mass regions around 92 and 96 seems to have no correspondence in the present ^{235}U data. Nor need it have, as the two fission processes result in unequal modes. Both fragments are in a region about five units or more from the magic numbers, A = 92 corresponds to Z = 36, N = 56 and A = = 96 corresponds to Z = 38 and N = 58. In ^{252}Cf fission both fragments have partners in the deformed mass region, as the partner of 92 is 160 and of 96 is 156. The respective partners in ^{235}U fission are 144 and 140. On the same basis as before, that in a particular fission mode the softest fragment ties up most of the available deformation energy, it can only be concluded that the light fragments are less excited in ^{252}Cf fission than in ^{235}U fission.

Unfortunately there is no result of the delayed gamma-ray yield in ^{235}U fission of similar accuracy to that in ^{252}Cf fission [2] to make a detailed comparison between the yield curves. A direct comparison is, however, very difficult between yields of prompt and delayed photons. The first part of the prompt gamma decay seems to take place in a similar way in the case of all fragments as far as the energy is concerned, and the number of photons can help to get a rough estimate of the original excitation of the fragments. As discussed in ref. 1, this is probably due to the fact that the fragments, as they are formed in a scission act, are probably all of them deformed in a similar way. The soft fragments can take a relatively long time to come down to their ground states. They have more deformation energy than the stiff nuclei if a pair of these two types of fragments have been formed in a scission act. The spherical nuclei may also be slow gamma emitters, as discussed above. Their deformations, however, are normally less than those of soft fragments, causing less excitation energy. It is here, after the first decays, that one must start to consider the energy of the photons, when direct comparisons between the gamma-ray yield curves become more or less irrelevant, at least if one tries to compare numbers. One example will show this. The gamma-ray energy spectra [29] show a very large yield of photons of energies around 200 keV in the mass regions around 110 and above 148. The half-life of the integral gamma radiation is about 50 ps. The low yield for fragments with mass numbers above 148 will increase if the yield curves from a prompt and a slow gamma decay are added. In the same time region in which the gamma radiation with the 50 ps half-life was enhanced, there was an increased yield of photons of energies around 1.2 MeV and 250 keV from fragments in the mass region around 132. It does not make sense to add up numbers of photons of such different energies and then compare with numbers obtained from other kind of spectra. The crucial quantity from the beginning of the gamma decay is the total excitation energy which is obtained through the fission act, even though in this experiment it is studied after the prompt neutrons have been released.

4.4. Mass-dependent yield of prompt photons of specific energies

The gamma-ray yield curves in fig. 8 have not been discussed explicitly so far, but an analysis indicates that the prominent features of those two curves have more or less been considered while discussing fig. 7. The time region studied goes from $4 \times 10^{-10} - 10^{-9}$s and the above-mentioned half-life of 50 ps is enhanced. The lower yield curve shows a large relative yield of photons of energies less than 0.33 MeV from the heaviest fragments in both the light and the heavy mass group. As was mentioned above a later but not yet fully analyzed experiment indicates that both these types of fragments have very large yields of photons of energies around 200 keV. The mass number is on a logarithmic scale, so the yields above the mass numbers 148 will increase relative to the 110 yield if the data are taken with the mass number on a linear scale. The newer data have given yields of 200 keV photons which are about equal in these two mass regions for a certain collimator setting enhancing the gamma radiation of 50 ps half-life. As far as the higher energies are concerned the yield of photons of energies between 0.33 and 1.35 MeV is somewhat larger in some particular mass regions, such as A = 90 and A = 135. In later experiments the division of gamma-ray energy intervals, and also the energy spectra, has shown that there is a relatively large yield of 1.2 MeV photons from fargments with mass numbers around 132, and then also from the very lightest fragments.

5. CONCLUSIONS

In this report a presentation has been given of one way of studying prompt gamma decays from fission fragments. One of the basic ideas behind the experimental set-up, namely that of using a collimator for the separation of the radiation from the two fragments of a fission event, has been applied earlier [1, 2], but the technique has here been developed by the incorporation of time discrimination between the prompt fission gamma radiation and the prompt neutrons. Recently a similar set-up was reported to the IAEA Fission Symposium in Vienna, 1969 [19].

The experiment performed with it was, however, different in most respects from that presented in this report. One of the most important points in the present measurement is the collimator definition and the associated time resolution. It has shown that it is possible to get acceptable signal to background ratios even with rather narrow slits and in a reactor surrounding, where the background is very high.

Fission gamma radiation as such can most successfully be studied in ^{252}Cf fission due to the low background, but complementary data from ^{235}U fission is of great value for several reasons:

1) the light mass group is different in the two types of fission,
2) one wants to know as much as possible about the total energy release of the fragments,
3) details of the fission gamma energy-spectra can be of help in the analysis of the neutron capture gamma-ray spectra to determine background,
4) as a by-product one may be able to study the (n, γf) process, which is of great importance for the knowledge of the fission process.

Some of the difficulties encountered in fission-gamma data analysis have been discussed, and particularly those concerning the extrapolation of energies of certain types of excited states in nuclei at the line of beta-stability when going out to mass regions involving the light fragment group. A fruitful way will be opened in the near future when more and more data have come out of the experiments now in progress at the on-line isotope separators, such as ISOLDE, TRISTAN, OSIRIS and others [42]. A completely new kind of spectroscopy has started, as one now studies neutron-rich nuclei far off the stability line.

Investigations with the present technique have continued and data analysis is in progress. Special emphasis has been laid upon the study of gamma-ray energy spectra as functions of mass, time after fission, and the total kinetic energy of the fragments.

ACKNOWLEDGEMENT

It is a pleasure to thank Prof. S. Johansson and Dr. N. Starfelt for their deep interest, the former for his ideas and patient handling of many of our problems, and the latter for his active and continued support when, as former Head of the Neutron Physics Section of AB Atomenergi, he made this experiment possible. Thanks are also due to Prof. N. Ryde and Dr. T. Wiedling for their interest, the latter in his character of Head of the Neutron Physics Section, and also for his critical review of the manuscript. The authors are grateful to Dr. J. Higbie for his assistance and trouble in getting the electronics to work. One of us (H. A.) is indebted to "Statens råd för atomforskning" for financial support.

REFERENCES

1. JOHANSSON S. A. E.,
Gamma de-excitation of fission fragments.
(I). Prompt radiation.
Nucl. Phys. 60 (1964) p. 378.

2. JOHANSSON S. A. E.,
Gamma de-excitation of fission fragments.
(II). Delayed radiation.
Nucl. Phys. 64 (1965) p. 147.

3. JOHANSSON S. A. E. and KLEINHEINZ P.,
Gamma-radiation from fission.
Alpha-, beta- and gamma-ray spectroscopy.
Ed. by K. Siegbahn. North Holland Publ. Co.
Amsterdam 1965. Vol. 1, p. 805.

4. Physics and chemistry of fission.
Proc. of a symp. Salzburg, 22-26 March 1965.
(IAEA) Vienna, 1965. Vol. 1 and 2. Sess. IV and VII.

5. KAPOOR S. S. and RAMANNA R.,
Emission of prompt gamma rays in the thermal-neutron fission of U^{235}.
Phys. Rev. 133B (1964) p. 598.

6. KAPOOR S. S., BOWMAN H. R. and THOMPSON S. G.,
Emission of K X rays and division of nuclear charge in the spontaneous fission of ^{252}Cf.
Phys. Rev. 140B (1965) p. 1310.

7. WATSON R. L.,
A study of the internal conversion electrons emitted within three nanoseconds after the spontaneous fission of ^{252}Cf. Thesis. 1966.
(UCRL-16798)

8. GLENDENIN L. E. and UNIK J. P.,
Division of nuclear charge deduced from X-ray measurements in the spontaneous fission of ^{252}Cf.
Phys. Rev. 140B (1965) p. 1301.

9. ATNEOSEN R. A. et al.,
X rays and electrons emitted in coincidence with the fission of ^{252}Cf.
Phys. Rev. 148 (1966) p. 1206.

10. VAL´SKII G. V. et al.,
Gamma-ray emission times in fission.
Soviet At. Energy 18 (1965) 279.

11. MAIER-LEIBNITZ H., SCHMITT H. W. and ARMBRUSTER P.,
Average number and energy of gamma-rays emitted as a function of fragment mass in U^{235} thermal-neutron-induced fission.
Physics and chemistry of fission.
Proc. of a symp. Salzburg, 22-26 March 1965.
(IAEA) Vienna, 1965. Vol. 2, p. 143.

12. WATSON R. L., BOWMAN H. R. and THOMPSON S. G.,
K X-ray yields of primary ^{252}Cf fission products.
Phys. Rev. 162 (1967) p. 1169.

13. BRIDWELL, WYMAN E. and WEHRING W.,
Half-lives and yields of X rays from thermal fission of U^{235} and Pu^{239}.
Phys. Rev. 145 (1966) p. 963.

14. DOLCE R., GIBSON W. M. and THOMAS T. D.,
Emission times and yields of K X rays coincident with ^{252}Cf spontaneous fission.
Phys. Rev. 180 (1969) p. 1177.

15. KAPOOR S. S., RAMAMURTHY V. S. and ZAGHLOUL R.,
Yield of K X rays emitted from U^{236} fragments.
Phys. Rev. 177 (1969) p. 1776.

16. Physics and chemistry of fission.
Proc. of a symp. Vienna, 28 July - 1 August 1969.
(IAEA) Vienna, 1969. Sess. F and H.

17. POPEKO L. A. et al.,
Delayed gamma rays from U^{235} fission.
Soviet At. Energy 19 (1965) p. 1082.

18. BLINOV M. V. et al.,
Angular anisotropy of the gamma quanta accompanying U^{235} fission.
Soviet Phys. JETP 16 (1963) p. 1159.

19. ARMBRUSTER P. et al.,
Mass dependence of anisotropy and yield of prompt γ-rays in ^{235}U thermal fission.
Physics and chemistry of fission.
Proc. of a symp. Vienna, 28 July - 1 August 1969.
(IAEA) Vienna, 1969, p. 545.

20. GRAFF G., LAJTAI A. and NAGY L.,
The angular distribution of gamma-rays from the fission of U^{235}.
Physics and chemistry of fission.
Proc. of a symp. Salzburg, 22-26 March 1965.
(IAEA) Vienna, 1965. Vol. 2, p. 163.

21. SKARSVÅG K.,
Delayed gamma-rays from spontaneous fission of ^{252}Cf. (Abstract.)
Physics and chemistry of fission.
Proc. of a symp. Vienna, 28 July - 1 August 1969.
(IAEA) Vienna, 1969, p. 927.

22. VERBINSKI V. V., WEBER H. and SUND R. E.,
Prompt gamma-rays from $^{235}U(n, f)$, $^{239}Pu(n, f)$ and ^{252}Cf(spontaneous fission). (Abstract.)
Physics and chemistry of fission.
Proc. of a symp. Vienna, 28 July - 1 August 1969.
(IAEA) Vienna, 1969, p. 929.

23. BOWMAN H.R. et al.,
Velocity and angular distributions of prompt neutrons from spontaneous fission of Cf^{252}.
Phys. Rev. 126 (1962) p. 2120.

24. HIGBIE J.,
Gamma radiation from fission fragments.
Experimental apparatus - mass spectrum resolution.
AB Atomenergi, Sweden, 1969
(AE-367)

25. BECKMAN L., HANSÉN J. and JANSSON R.,
A fast time-of-flight spectrometer.
Nucl. Instr. Methods 52 (1967) p. 157.

26. HOGG G.R. and LOKAN K.H.,
An analogue ratio circuit for fission fragment mass determination.
Nucl. Instr. Methods 33 (1965) p. 319.

27. SJÖLIN P.G., GRANSTRÖM K. and BJÖRKMAN J.,
A two-parameter analyser based on a small computer.
1968, AB Atomenergi, Studsvik, Sweden.
(Internal report AE-SSI-229.)

28. LINDOW L. and ALBINSSON H.,
A program package for a small computer.
1969, AB Atomenergi, Studsvik, Sweden.
(Internal report TPM-FFN-100.)

29. ALBINSSON H. and LINDOW L.,
to be published.

30. SHIRAISHI F. and HOSOE M.,
Energy and time-of-flight correlation experiments with solid-state detectors for mass distribution measurement of ^{235}U fission fragments.
Nucl. Instr. Methods 66 (1968) p. 130.

31. MAIENSCHEIN F.C. et al.,
Gamma-rays associated with fission.
U.N. intern. conf. on peaceful uses of atomic energy.
2. Geneva 1958. Proc. Vol. 15, p. 366.
(UN) Geneva, 1958.

32. ALBINSSON H., HIGBIE J. and LINDOW L.,
The prompt gamma radiation from fission fragments.
Nuclear structure: Dubna symp. 1968.
Dubna, 4-11 July, 1968.
(JINR, Dubna publication D-3893)

33. ALBINSSON H. and LINDOW L.,
Gamma radiation from fission products.
In Neutron physics laboratory. Annual progress report.
Ed. by T. Wiedling, October 1, 1967 - September 30, 1968.
AB Atomenergi, Sweden, 1969.
(AE-354) p. 17.

34. ALBINSSON H. and LINDOW L.,
Prompt gamma-rays from thermal neutron-induced fission of ^{235}U.
(Abstract.)
Physics and chemistry of fission.
Proc. of a symp. Vienna, 28 July - 1 August 1969.
(IAEA) Vienna, 1969, p. 930.

35. JOHN W., WESOLOWSKI J. J. and GUY F.,
Mass-dependent structure in the fission γ-ray yields from ^{252}Cf.
Phys. Lett. 30 B (1969) p. 340.

36. TERRELL J.,
Neutron yields from individual fission fragments.
Phys. Rev. 127 (1962) p. 880.

37. VANDENBOSCH R.,
Dependence of fission fragment kinetic energies and neutron yields on nuclear structure.
Nucl. Phys. 46 (1963) p. 129.

38. TERRELL J.,
Prompt neutrons from fission.
Physics and chemistry of fission.
Proc. of a symp. Salzburg, 22-26 March 1965.
(IAEA) Vienna, 1965, Vol. 2, p. 3.

39. JOHANSSON S. A. E.,
New regions of deformed nuclei
Why and how should we investigate nuclides far off the stability line.
Proc. of the international symp. Lysekil, August 21-27, 1966.
Arkiv Fysik 36 (1967) p. 599.

40. GLENDENIN L. E. et al.,
High-resolution studies of K X-ray emission and the distribution of mass and nuclear charge in the thermal-neutron-induced fission of ^{233}U, ^{235}U and ^{239}Pu.
Physics and chemistry of fission.
Proc. of a symp. Vienna, 28 July - 1 August 1969.
(IAEA) Vienna, 1969, p. 781.

41. VANDENBOSCH R.,
Discussion in Physics and chemistry of fission.
Proc. of a symp. Salzburg, 22-26 March 1965.
(IAEA) Vienna, 1965. Vol. 1, p. 399.

42. Why and how should we investigate nuclides far off the stability line.
Proc. of the international symp. Lysekil, August 21-27, 1966.
Arkiv Fysik 36 (1967).

FIGURE CAPTIONS

Fig. 1. Schematic diagram of the experimental arrangement.

Fig. 2. Block diagram of the instrumentation for the measurement of fission gamma radiation.

Fig. 3. Pulse spectrum from the logarithmic amplifier.

Fig. 4. Time-of-flight spectrum for the uncollimated fission gamma radiation.

Fig. 5. Time-of-flight spectra for the collimated fission gamma radiation with three different collimator settings.

Fig. 6. Time spectrum from coincident fission fragments.

Fig. 7. The relative gamma-ray yield as a function of fragment mass.

Fig. 8. The relative gamma-ray yield of two different energy portions as a function of fragment mass for a collimator setting not so close to the fission foil as was the case shown in fig. 7.

Fig. 9. The energy spectrum of the uncollimated gamma-rays emitted within 5×10^{-9}s after the fission event.

Fig. 10. The nuclide chart showing the line of beta stability (full curve) and the area of the light fission fragments (dashed curve). The locations of the dips in fig. 7 are indicated by shaded areas.

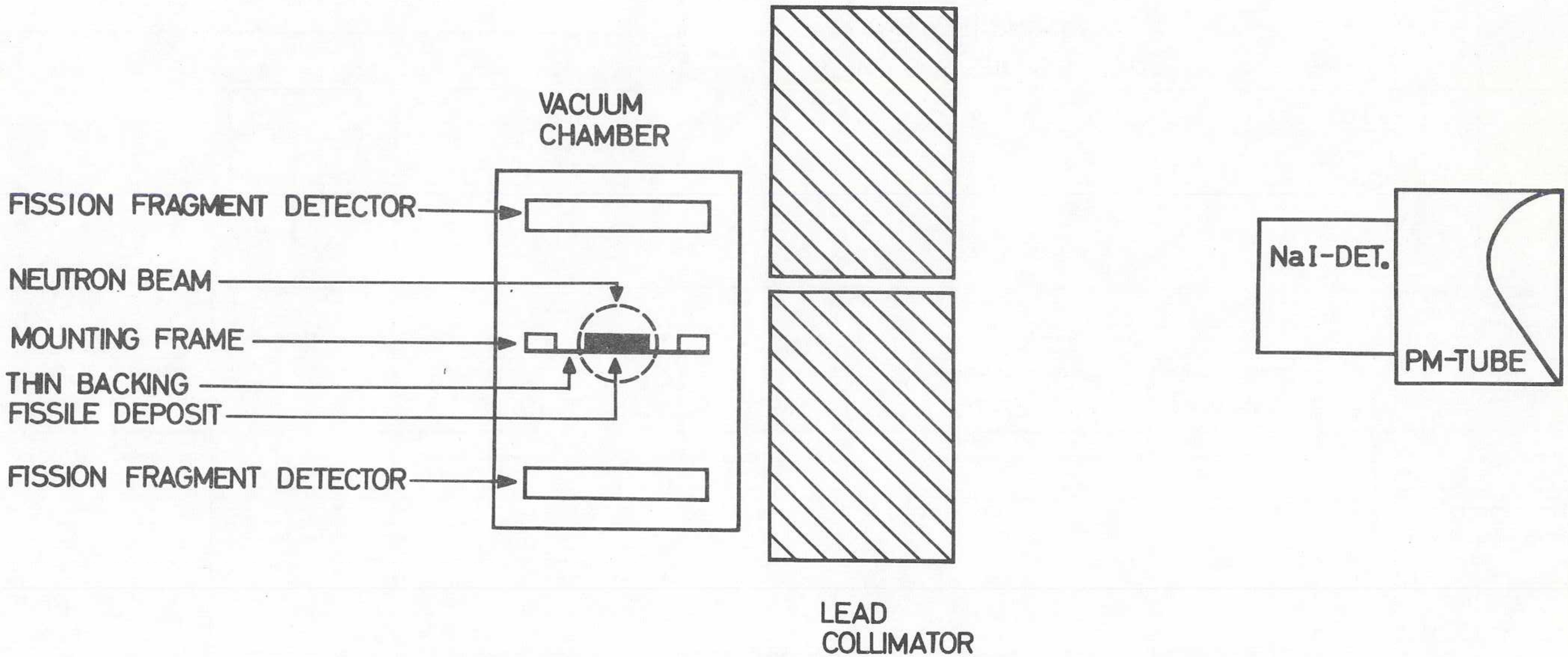
VACUUM
CHAMBER
FISSION FRAGMENT DETECTOR
NEUTRON BEAM
MOUNTING FRAME
THIN BACKING
FISSILE DEPOSIT
FISSION FRAGMENT DETECTOR
LEAD
COLLIMATOR
NaI-DET.
PM-TUBE

Fig. 1

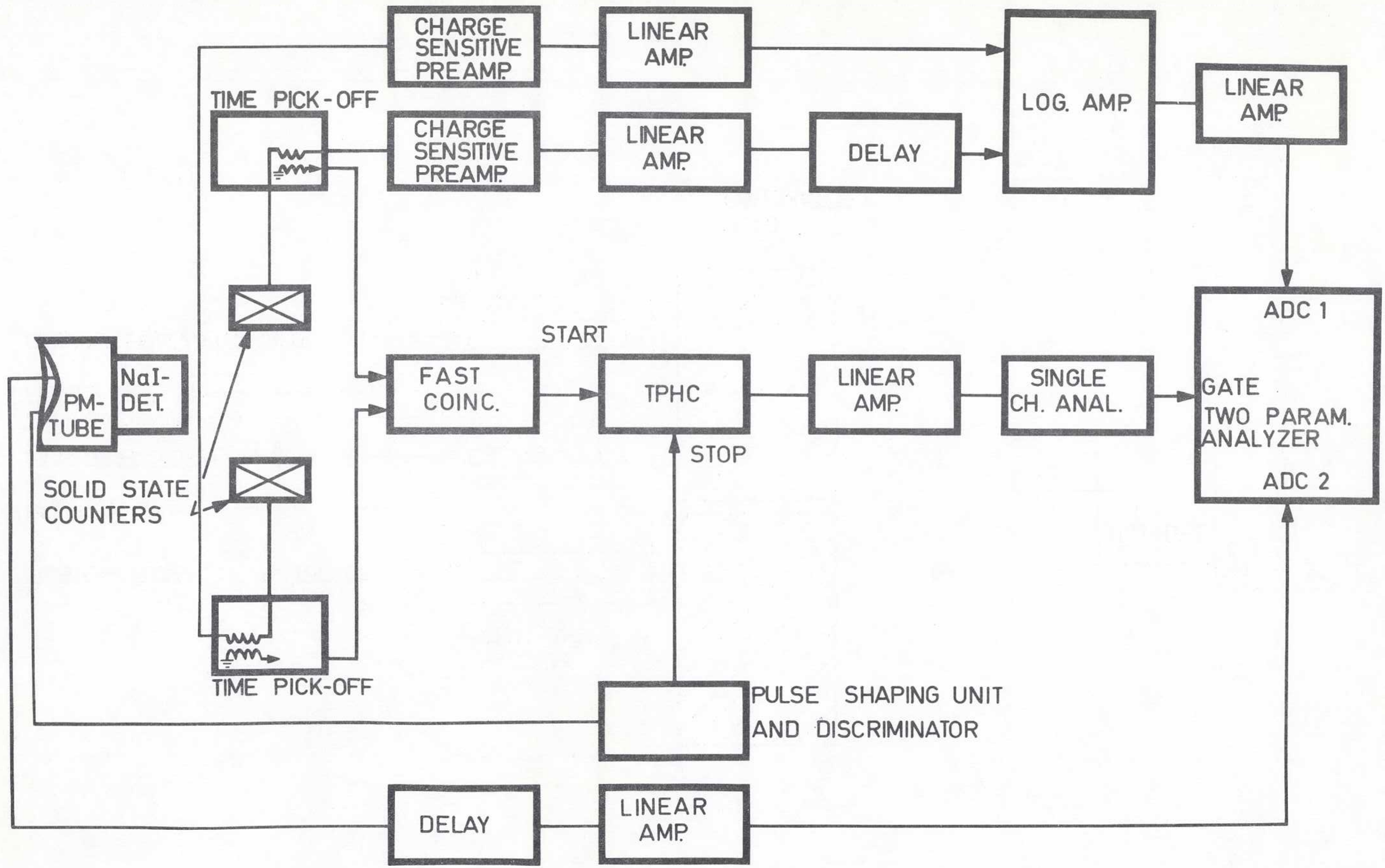
CHARGE SENSITIVE PREAMP.
LINEAR AMP.
LOG. AMP.
LINEAR AMP.
TIME PICK-OFF
CHARGE SENSITIVE PREAMP.
LINEAR AMP.
DELAY
ADC 1
START
FAST COINC.
TPHC
LINEAR AMP.
SINGLE CH. ANAL.
GATE
TWO PARAM. ANALYZER
ADC 2
PM-TUBE
NaI-DET.
STOP
SOLID STATE COUNTERS
TIME PICK-OFF
PULSE SHAPING UNIT AND DISCRIMINATOR
DELAY
LINEAR AMP.

Fig. 2

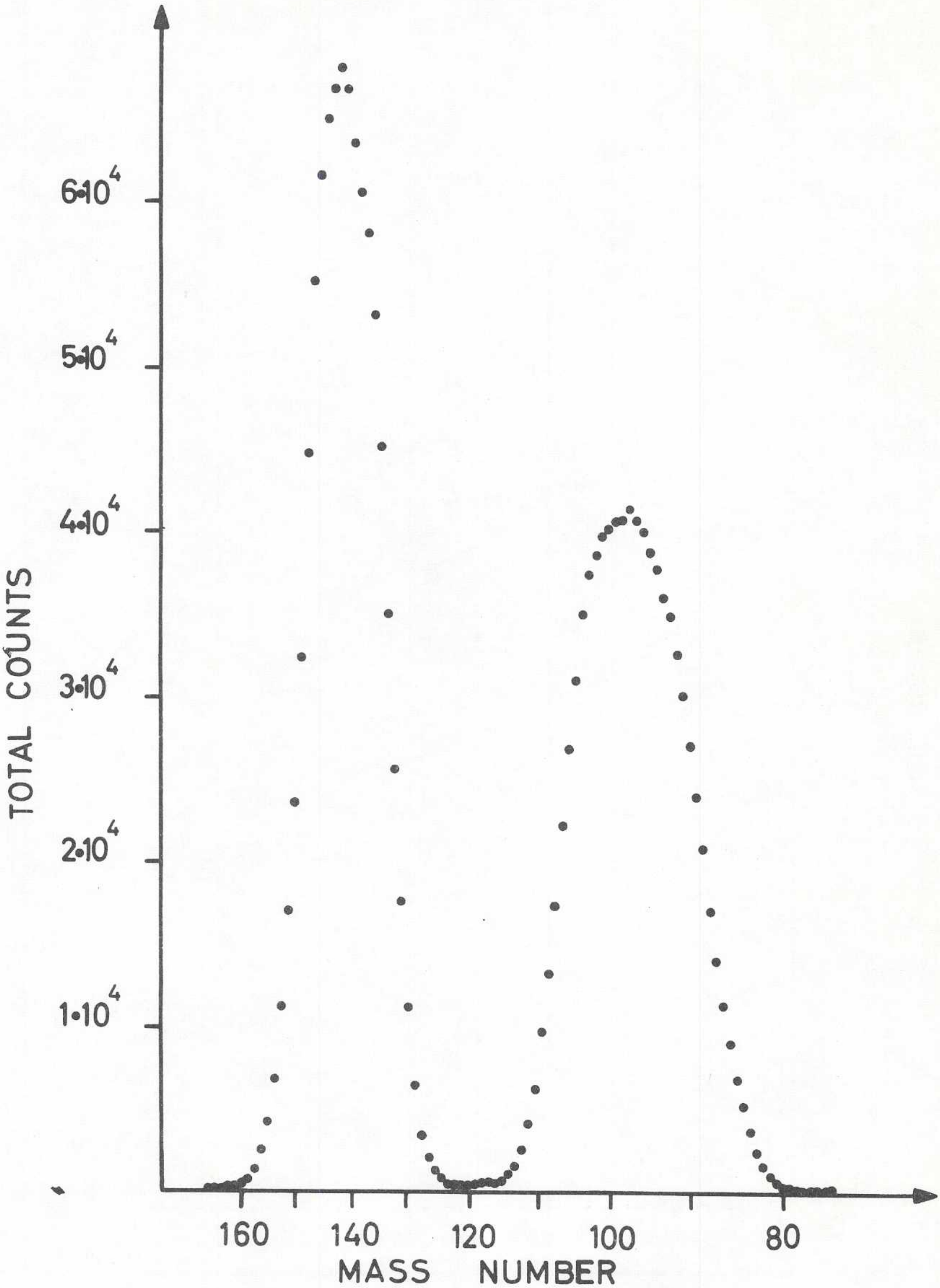
TOTAL COUNTS
6·10^4
5·10^4
4·10^4
3·10^4
2·10^4
1·10^4
160
140
120
100
80
MASS NUMBER

Fig. 3

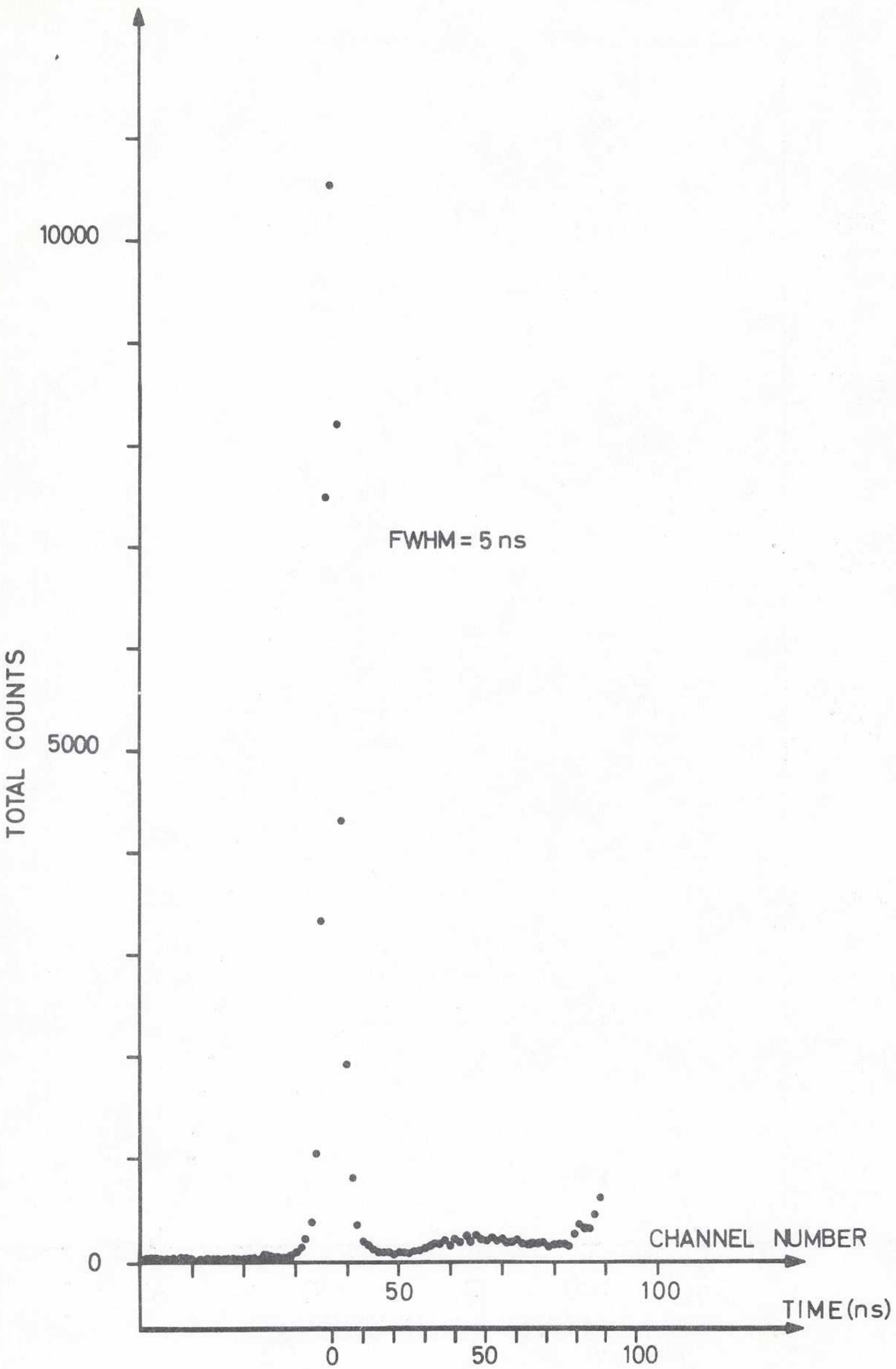
TOTAL COUNTS
10000
5000
0
FWHM = 5 ns
CHANNEL NUMBER
50
100
TIME (ns)
0
50
100

Fig. 4

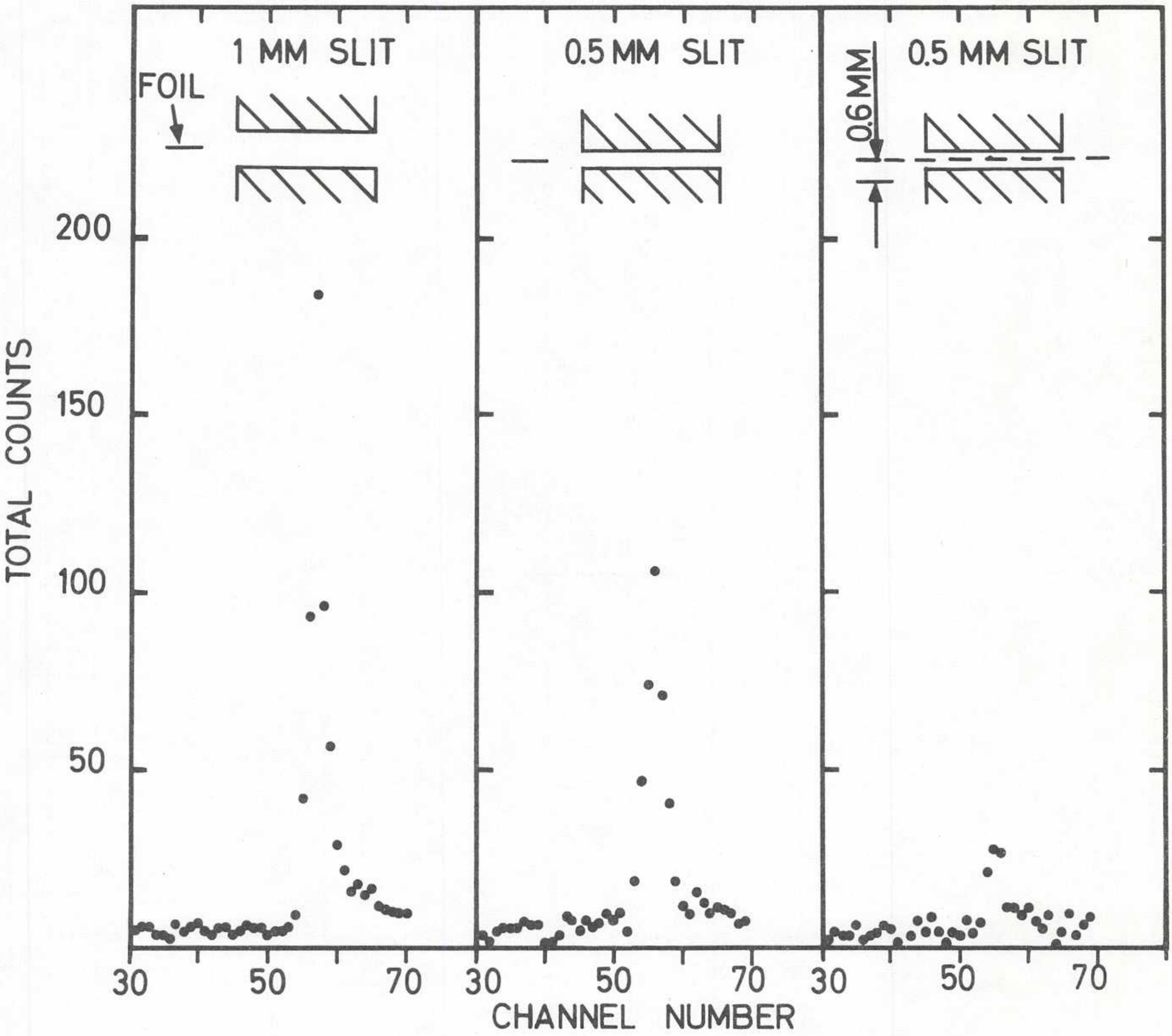
1 MM SLIT
FOIL
0.5 MM SLIT
0.5 MM SLIT
0.6 MM
TOTAL COUNTS
200
150
100
50
30
50
70
30
50
70
30
50
70
CHANNEL NUMBER

Fig. 5

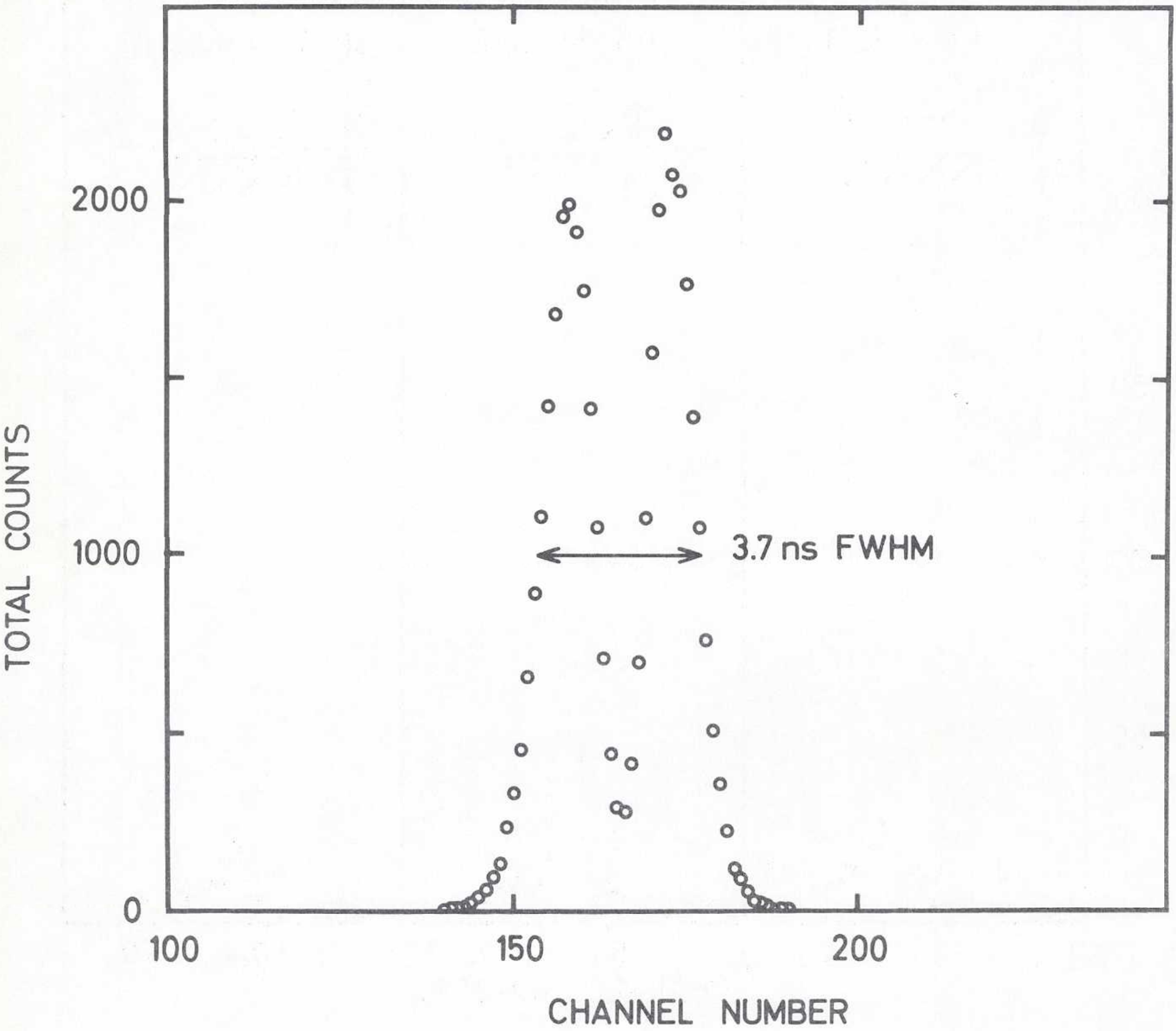

2000
1000
0
100
150
200
TOTAL COUNTS
CHANNEL NUMBER
3.7 ns FWHM

Fig. 6

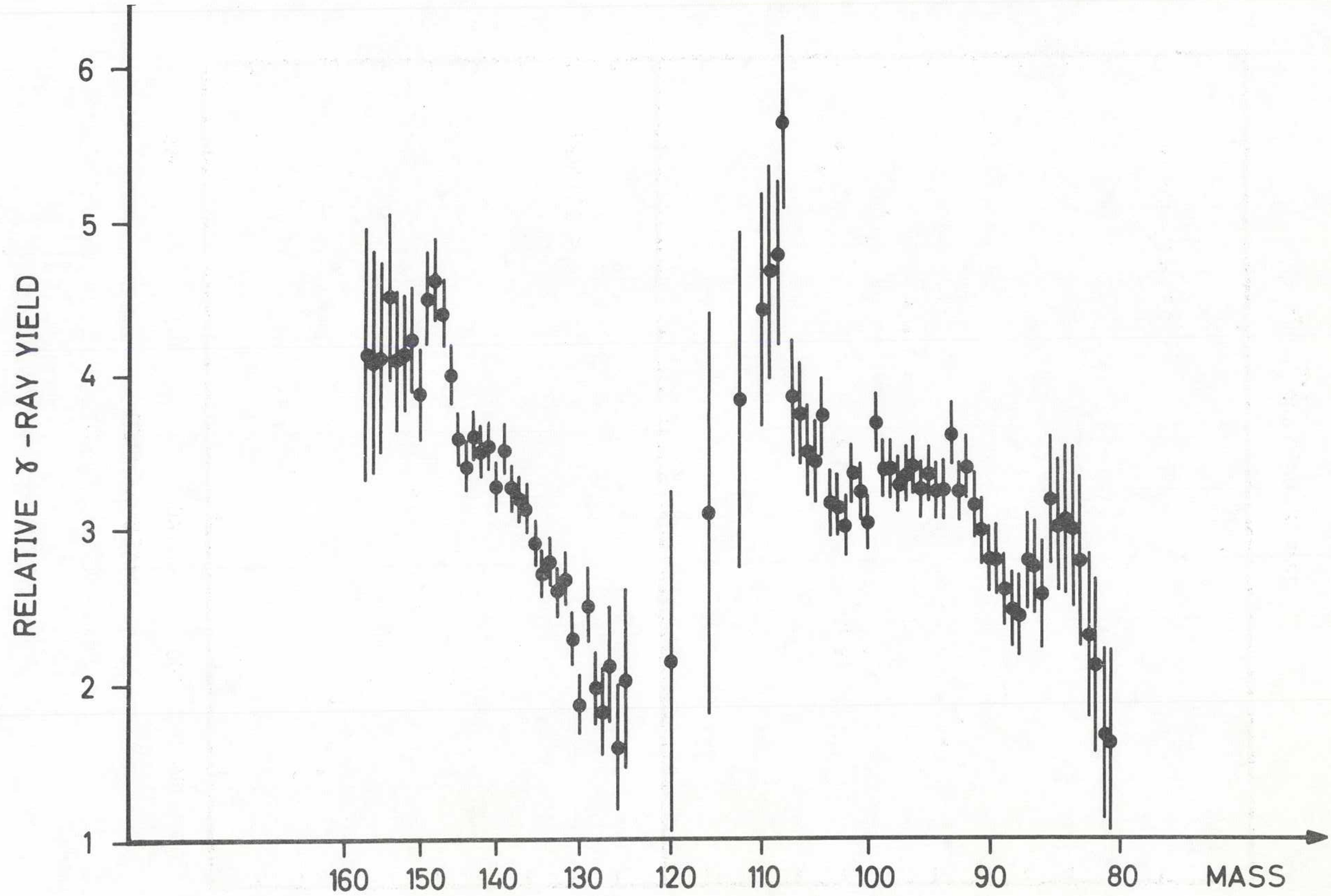
RELATIVE γ -RAY YIELD
6
5
4
3
2
1
160
150
140
130
120
110
100
90
80
MASS

Fig. 7

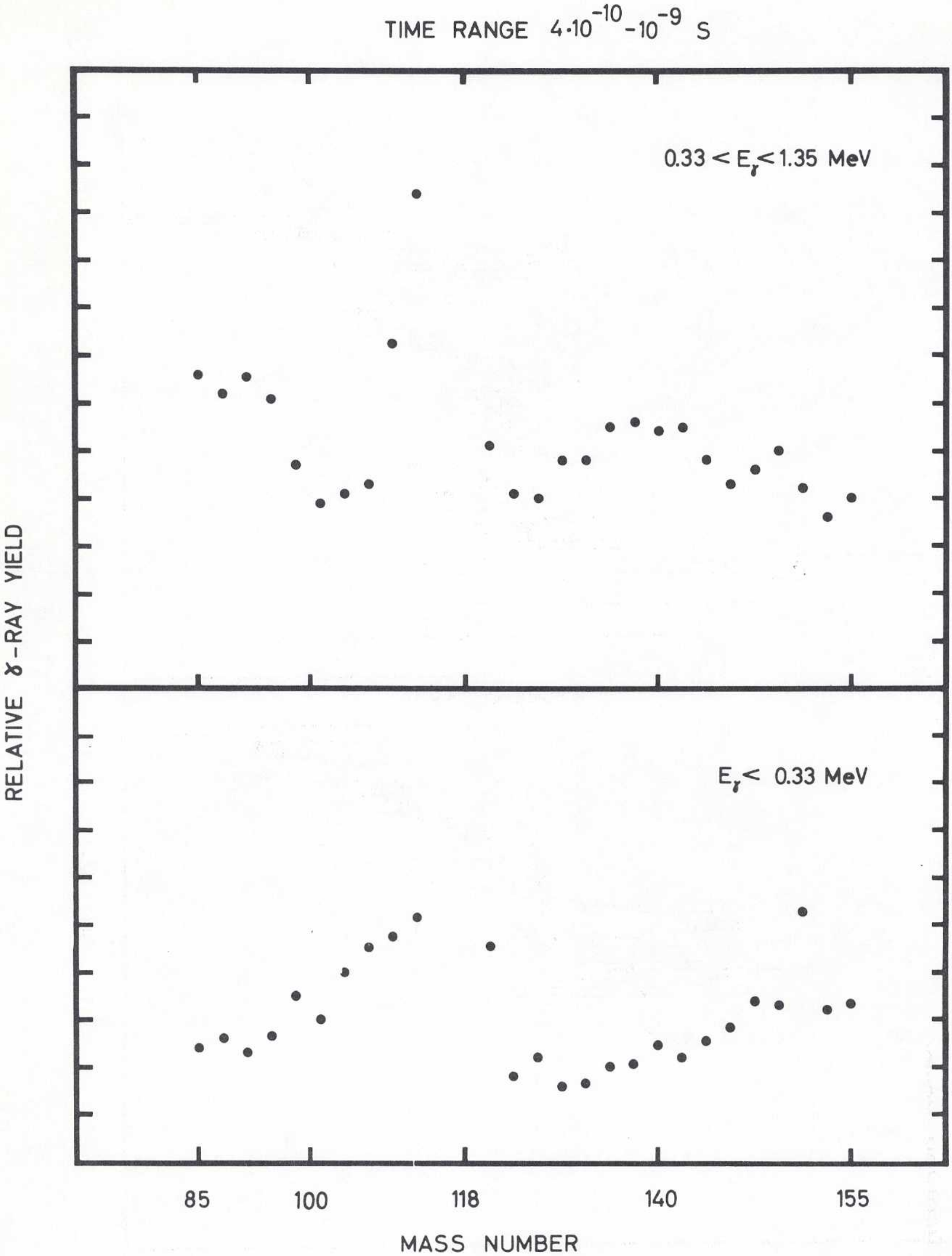

TIME RANGE 4·10^-10 - 10^-9 S
0.33 < Eγ < 1.35 MeV
Eγ < 0.33 MeV
RELATIVE γ-RAY YIELD
85
100
118
140
155
MASS NUMBER

Fig. 8

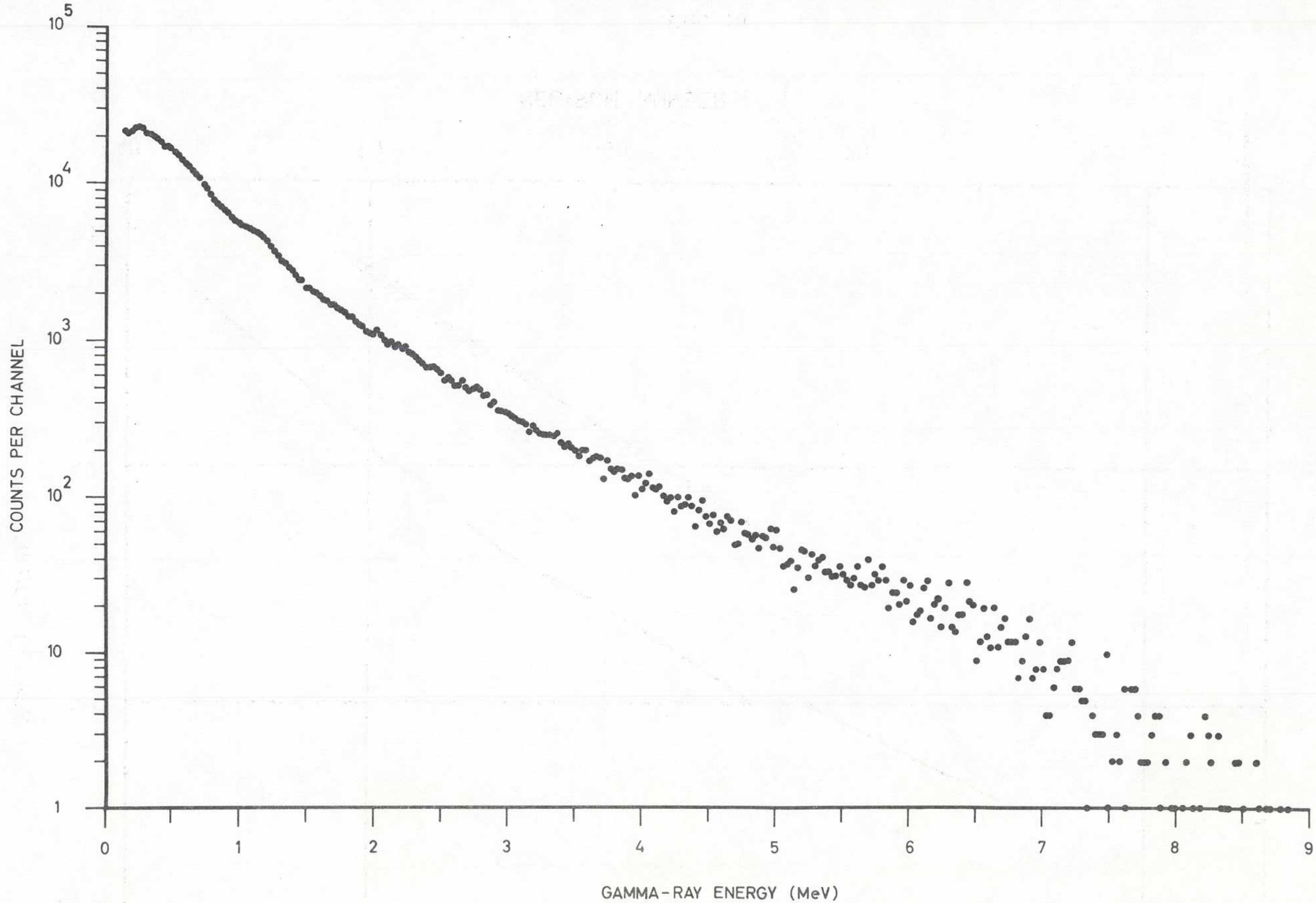
10^5
10^4
10^3
10^2
10
1
COUNTS PER CHANNEL
0
1
2
3
4
5
6
7
8
9
GAMMA-RAY ENERGY (MeV)

Fig. 9

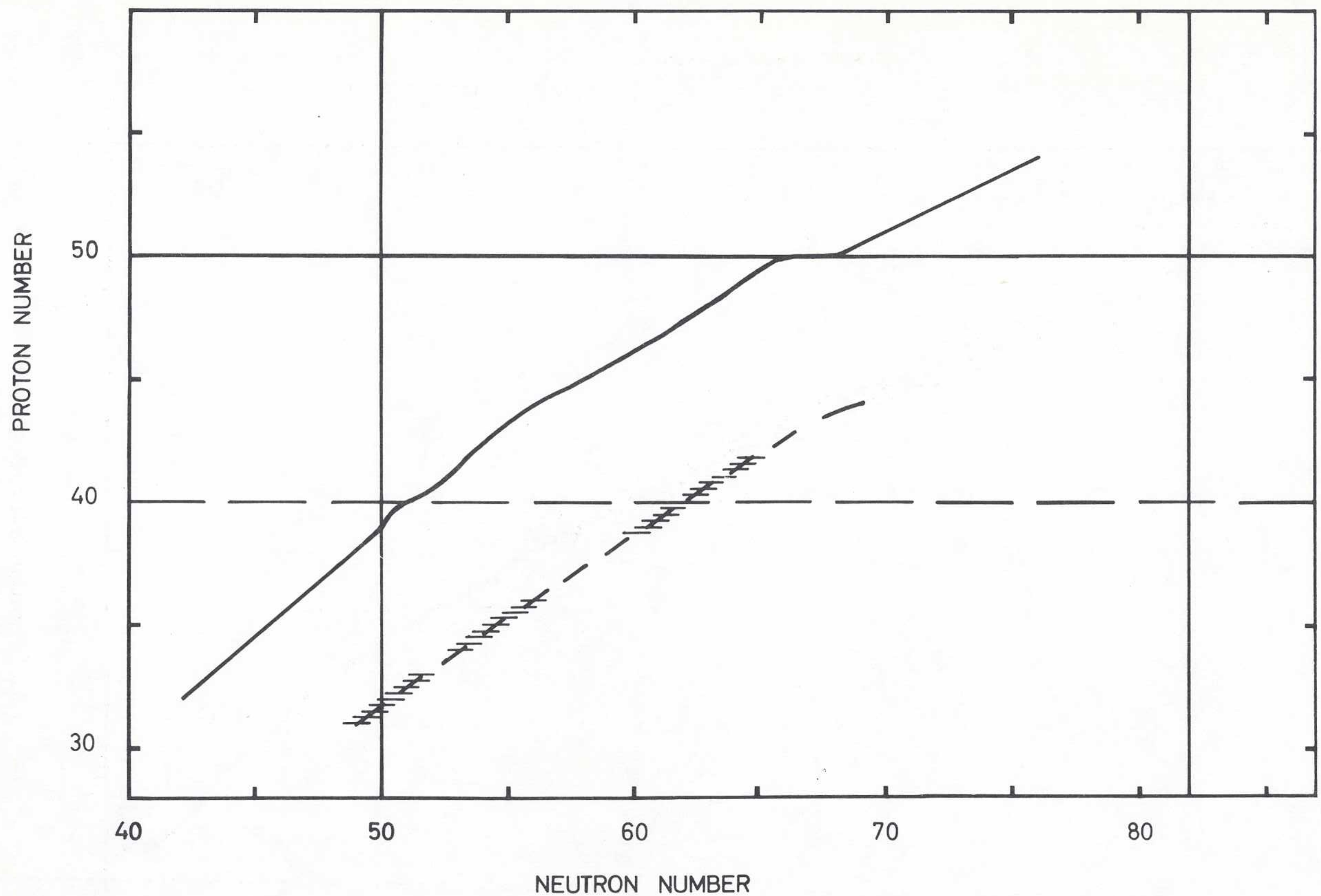

Fig. 10

LIST OF PUBLISHED AE-REPORTS

1–320 (See back cover earlier reports.)

321 Stability of a steam cooled fast power reactor, its transients due to moderate perturbations and accidents. By H. Vollmer. 1968. 36 p. Sw. cr. 10:–.

322. Progress report 1967. Nuclear chemistry. 1968. 30 p. Sw. cr. 10:–.

323 Noise in the measurement of light with photomultipliers. By F. Robben. 1968. 74 p. Sw. cr. 10:–.

324. Theoretical investigation of an electrogasdynamic generator. By S. Palmgren. 1968 36 p. Sw. cr. 10:–.

325 Some comparisons of measured and predicted primary radiation levels in the Ågesta power plant. By E. Aalto, R Sandlin and Å. Krell. 1968. 44 p. Sw. cr. 10:–.

326. An investigation of an irradiated fuel pin by measurement of the production of fast neutrons in a thermal column and by pile oscillation technique. By Veine Gustavsson. 1968 24 p. Sw. cr. 10:–.

327. Phytoplankton from Tvären, a bay of the Baltic, 1961–1963. By Torbjörn Willén. 1968 76 p Sw. 10:–.

328. Electronic contributions to the phonon damping in metals. By Rune Jonson. 1968. 38 p. Sw cr 10:–.

329. Calculation of resonance interaction effects using a rational approximation to the symmetric resonance line shape function. By H. Häggblom. 1968. 48 p. Sw. cr 10:–.

330. Studies of the effect of heavy water in the fast reactor FR0. By L. I. Tirén. R. Håkansson and B. Karmhag. 1968. 26 p. Sw. cr. 10:–.

331. A comparison of theoretical and experimental values of the activation Doppler effect in some fast reactor spectra By H. Häggblom and L. I. Tirén. 1968. 28 p. Sw. cr. 10:–.

332. Aspects of low temperature irradiation in neutron activation analysis. By D Brune. 1968. 12 p. Sw. cr. 10.–.

333. Application of a betatron in photonuclear activation analysis. By D. Brune, S. Mattsson and K. Lidén. 1968. 13 p. Sw. cr. 10:–.

334. Computation of resonance-screened cross section by the Dorix-Speng system. By H Häggblom. 1968. 34 p. Sw. cr. 10:–.

335. Solution of large systems of linear equations in the presence of errors A constructive criticism of the least squares method. By K. Nygaard. 1968 28 p. Sw. cr 10:–.

336 Calculation of void volume fraction in the subcooled and quality boiling regions. By S. Z. Rouhani and E. Axelsson. 1968. 26 p. Sw. cr. 10:–.

337. Neutron elastic scattering cross sections of iron and zinc in the energy region 2.5 to 8.1 MeV. By B. Holmqvist, S. G. Johansson, A. Kiss, G. Lodin and T. Wiedling. 1968. 30 p. Sw. cr. 10:–.

338. Calibration experiments with a DISA hot-wire anemometer. By B. Kjellström and S. Hedberg. 1968. 112 p. Sw. cr. 10:–.

339 Silicon diode dosimeter for fast neutrons. By L. Svansson, P. Swedberg, C-O. Widell and M. Wik. 1968. 42 p. Sw. cr. 10:–.

340 Phase diagrams of some sodium and potassium salts in light and heavy water. By K. E. Holmberg. 1968 48 p. Sw. cr. 10:–.

341. Nonlinear dynamic model of power plants with single-phase coolant reactors. By H. Vollmer. 1968. 26 p. Sw. cr. 10:–.

342. Report on the personnel dosimetry at AB Atomenergi during 1967. By J Carlsson and T. Wahlberg. 1968. 10 p. Sw. cr. 10:–.

343. Friction factors in rough rod bundles estimated from experiments in partially rough annuli – effects of dissimilarities in the shear stress and turbulence distributions. By B. Kjellström. 1968. 22 p. Sw cr. 10:–.

344. A study of the resonance interaction effect between ^{238}U and ^{239}Pu in the lower energy region. By H. Häggblom. 1968. 48 p Sw. cr. 10:–.

345 Application of the microwave discharge modification of the Wilzbach technique for the tritium labelling of some organics of biological interest By T. Gosztonyi. 1968. 12 p. Sw. cr. 10:–.

346 A comparison between effective cross section calculations using the intermediate resonance approximation and more exact methods. By H. Häggblom. 1969. 64 p. Sw. cr. 10:–.

347. A parameter study of large fast reactor nuclear explosion accidents. By J. R. Wiesel. 1969. 34 p. Sw. cr. 10·–.

348. Computer program for inelastic neutron scattering by an anharmonic crystal. By L. Bohlin, I. Ebbsjö and T. Högberg. 1969. 52 p. Sw. cr. 10:–.

349. On low energy levels in ^{185}W. By S G. Malmskog, M. Höjeberg and V. Berg. 1969. 18 p. Sw. cr. 10:–.

350. Formation of negative metal ions in a field-free plasma. By E. Larsson. 1969. 32 p. Sw. cr 10:–.

351. A determination of the 2 200 m/s absorption cross section and resonance integral of arsenic by pile oscillator technique. By E. K. Sokolowski and R. Bladh. 1969. 14 p. Sw. cr. 10:–.

352. The decay of ^{191}Os. By S. G Malmskog and A. Bäcklin. 1969. 24 p. Sw cr 10:–.

353 Diffusion from a ground level point source experiment with thermoluminescence dosimeters and Kr 85 as tracer substance. By Ch. Gyllander, S Hollman and U Widemo. 1969. 23 p. Sw. cr. 10:–

354 Progress report, FFN, october 1, 1967 – september 30, 1968. By T. Wiedling. 1969. 35 p. Sw. cr. 10:–.

355. Thermodynamic analysis of a supercritical mercury power cycle. By A. S Roberts, Jr., 1969. 25 p. Sw. cr. 10:–.

356. On the theory of compensation in lithium drifted semiconductor detectors By A. Lauber. 1969. 45 p. Sw cr 10:–.

357 Half-life measurements of levels in ^{75}As. By M. Höjeberg and S. G Malmskog. 1969. 14 p. Sw. cr. 10:–.

358. A non-linear digital computer model requiring short computation time for studies concerning the hydrodynamics of the BWR. By F. Reisch and G Vayssier. 1969. 38 p. Sw. cr. 10: –

359. Vanadium beta emission detectors for reactor in-core neutron monitoring. I. Ö. Andersson and B. Söderlund. 1969. 26 p. Sw. cr. 10:–.

360. Progress report 1968 nuclear chemistry. 1969. 38 p. Sw. cr. 10:–.

361. A half-life measurement of the 343.4 keV level in ^{175}Lu. By M. Höjeberg and S. G Malmskog. 1969. 10 p. Sw. cr. 10:–.

362. The application of thermoluminescence dosimeters to studies of released activity distributions. By B-I. Rudén. 1969. 36 p. Sw cr. 10:–.

363 Transition rates in ^{161}Dy. By V Berg and S. G. Malmskog. 1969. 32 p Sw. cr 10:–.

364. Control rod reactivity measurements in the Ågesta reactor with the pulsed neutron method. By K. Björeus 1969 44 p. Sw. cr. 10:–.

365. On phonons in simple metals II. Calculated dispersion curves in aluminium. By R. Johnson and A. Westin. 1969. 124 p. Sw. cr. 10:–.

366. Neutron elastic scattering cross sections. Experimental data and optical model cross section calculations A compilation of neutron data from the Studsvik neutron physics laboratory. By B. Holmqvist and T. Wiedling. 1969. 212 p. Sw. cr 10:–.

367 Gamma radiation from fission fragments. Experimental apparatus – mass spectrum resolution. By J. Higbie. 1969. 50 p. Sw. cr. 10:–.

368. Scandinavian radiation chemistry meeting Studsvik and Stockholm, september 17–19, 1969. By H. Christensen. 1969. 34 p. Sw cr. 10:–.

369. Report on the personnel dosimetry at AB Atomenergi during 1968. By J Carlsson and T Wahlberg. 1969. 10 p. Sw. cr 10:–.

370. Absolute transition rates in ^{188}Ir. By S G. Malmskog and V. Berg. 1969. 16 p. Sw. cr. 10:–.

371. Transition probabilities in the 1/2+(631) Band in ^{235}U. By M. Höjeberg and S. G Malmskog. 1969. 18 p. Sw. cr. 10:–.

372. E2 and M1 transition probabilities in odd mass Hg nuclei. By V. Berg, A. Bäcklin, B. Fogelberg and S. G Malmskog. 1969. 19 p. Sw. cr. 10:–.

373. An experimental study of the accuracy of compensation in lithium drifted germanium detectors. By A. Lauber and B. Malmsten. 1969. 25 p. Sw. cr. 10:–.

374. Gamma radiation from fission fragments. By J. Higbie. 1969. 22 p. Sw. cr. 10:–.

375 Fast Neutron Elastic and Inelastic Scattering of Vanadium. By B. Holmqvist, S. G. Johansson, G. Lodin and T. Wiedling. 1969. 48 p. Sw. cr. 10:–.

376. Experimental and Theoretical Dynamic Study of the Ågesta Nuclear Power Station. By P.-Å. Bliselius, H. Vollmer and F. Åkerhielm. 1969. 39 p. Sw. cr. 10: –

377. Studies of Redox Equilibria at Elevated Temperatures 1. The Estimation of Equilibrium Constants and Standard Potentials for Aqueous Systems up to 374°C. By Derek Lewis. Sw. cr. 10:-

378. The Whole Body Monitor HUGO II at Studsvik. Design and Operation. By L. Devell, I. Nilsson and L. Venner. 1970. 26 p. Sw. cr. 10:-.

379. ATOMSPHERIC DIFFUSION Investigations at Studsvik and Ågesta 1960–1963. By L-E Hæggblom, Ch Gyllander and U Widemo. 1969. 91 p. Sw. cr. 10: –

380. An expansion method to unfold proton recoil spectra. By J. Kockum. 1970. 20 p. Sw. cr. 10: –.

381. The 93. 54 keV level in ^{91}Sr, and evidence for 3-neutron states above N=50. By S. G. Malmskog and J. Mc Donald. 1970. 24 p. Sw. cr. 10:-.

382. The low energy level structure of ^{191}Ir. By S. G. Malmskog, V. Berg, A. Bäcklin and G. Hedin. 1970. 24 p. Sw. cr. 10:–.

383. The drinking rate of fish in the Skagerack and the Baltic. J. E. Larsson. 16 p. Sw. cr. 10: –.

384. Lattice dynamics of NaCl, KCl, RbCl and RbF. G. Raunio and S. Rolandson 26 p. Sw. cr. 10: –.

385 A neutron elastic scattering study of chromium, iron and nickel in the energy region 1.77 to 2.76 MeV. 26 p. By B. Holmqvist, S .G Johansson, G. Lodin, M. Salama and T. Wiedling. 1970. Sw. cr. 10: –

386. The decay of bound isobaric analogue states in ^{28}Si and ^{32}S using (d. nγ) reactions. By L. Nilsson, A. Nilsson and I. Bergqvist. 1970. 34 p. Sw. cr. 10:–.

387. Transition probabilities in ^{189}Os. By S. G. Malmskog, V. Berg and A. Bäcklin. 1970. 40 p. Sw. cr. 10: –.

388. Cross sections for high-energy gamma transitions from MeV neutron capture in ^{206}Pb. By I. Bergqvist, B. Lundberg and L. Nilsson. 1970. 16 p. Sw. cr. 10: –.

389 High-speed, automatic radiochemical separations for activation analysis in the biological and medical research laboratory. By K. Samsahl. 1970. 18 p. Sw. cr. 10: –.

390. Use of fission product Ru-106 gamma activity as a method for estimating the relative number of fission events in U-235 and Pu-239 in low-enriched fuel elements. By R. S. Forsyth and W. H. Blackadder. 1970. 26 p. Sw. cr. 10: –.

391. Half-life measurements in ^{134}I. By V. Berg and Å. Höglund. 1970. 16 p. Sw. cr. 10: –.

392. Measurement of the neutron spectra in FR0 cores 5, 9 and PuB-5 using resonance sandwich detectors. By T. L. Andersson and M. N. Qazi. 1970. 30 p. Sw. cr. 10: –.

393. A gamma scanner using a Ge(Li) semi-conductor detector with the possibility of operation in anti-coincidence mode. By R. S. Forsyth and W. H. Blackadder. 1970. 22 p. Sw. cr. 10: –.

394. A study of the 190 keV transition in ^{141}La. By V. Berg, Å. Höglund and B. Fogelberg. 1970. 22 p. Sw. cr. 10:–.

395. Magnetoacoustic waves and instabilities in a Hall-effect-dominated plasma. By S. Palmgren. 1970. 20 p. Sw. cr. 10:–.

396. A new boron analysis method By J.Weitman, N.Dåverhög and S. Farvolden 26 p. Sw. cr. 10:-.

397. Progress report 1969. Nuclear chemistry. 39 p. Sw. cr. 10:–.

398. Prompt gamma radiation from fragments in the thermal fission of ^{235}U. By H Albinsson and L Lindow. 1970. 48 p. Sw. cr. 10:–.

List of published AES-reports (In Swedish)

1. Analysis be means of gamma spectrometry. By D. Brune. 1961. 10 p. Sw. cr. 6:–.
2. Irradiation changes and neutron atmosphere in reactor pressure vessels-some points of view. By M. Grounes. 1962. 33 p. Sw cr. 6:–.
3. Study of the elongation limit in mild steel. By G. Östberg and R. Attermo 1963 17 p Sw. cr. 6:–.
4. Technical purchasing in the reactor field. By Erik Jonson. 1963. 64 p. Sw. cr. 8:–.
5. Ågesta nuclear power station. Summary of technical data, descriptions, etc. for the reactor. By B Lilliehöök. 1964. 336 p. Sw cr. 15:–.
6. Atom Day 1965. Summary of lectures and discussions. By S. Sandström. 1966. 321 p. Sw. cr. 15:–.
7. Building materials containing radium considered from the radiation protection point of view. By Stig O W. Bergström and Tor Wahlberg. 1967. 26 p. Sw. cr 10:–.

Additional copies available from the library of AB Atomenergi, Fack, S-611 01 Nyköping, Sweden.

EOS-tryckerierna, Stockholm 1970

AE-420

UDC 539.166
539.122.16:
539.173.4.162.2

AE-420

Energies and Yields of Prompt Gamma Rays from Fragments in Slow-Neutron Induced Fission of ^{235}U

H. Albinsson

This report is intended for publication in a periodical. References may not be published prior to such publication without the consent of the author.

AKTIEBOLAGET ATOMENERGI

STUDSVIK, NYKÖPING, SWEDEN 1971

ENERGIES AND YIELDS OF PROMPT GAMMA RAYS FROM FRAGMENTS IN SLOW-NEUTRON INDUCED FISSION OF ^{235}U

H. Albinsson*

ABSTRACT

Measurements were made on the gamma radiation emitted from fission fragments in slow-neutron induced fission of ^{235}U. The fragments were detected with solid state detectors of the surface barrier type and the gamma radiation with a NaI(Tl) scintillator. Mass selection was used so that the gamma radiation could be measured as a function of fragment mass. Time discrimination between the fission gammas and the prompt neutrons released in the fission process was employed to reduce the background. The gamma radiation emitted during different time intervals after the fission event was studied with the help of a collimator, the position of which was changed along the path of the fission fragments. In this way it was possible to select various collimator settings and let gamma radiation of different half-lives be enhanced. Gamma-ray energy spectra from these time components were then recorded as function of mass. The spectrum shape differed greatly depending on the half-life of the radiation and the fragment from which it was emitted.

The results of the present measurements were discussed in the light of existing fission models, and comparisons were made with prompt gamma-ray and neutron data from other fission experiments.

* Chalmers University of Technology, Gothenburg

Printed and distributed in April 1971.

LIST OF CONTENTS

1. INTRODUCTION

Prompt gamma radiation from fission fragments is of interest to study for two reasons. First, a knowledge of this radiation should be of value for any detailed theory of the fission process, and second, it can provide information for designing shielding around a reactor.

The gamma-ray energy spectra are very complicated owing to the many nuclei (fragments) which emit this radiation. Furthermore these nuclei can start emitting their radiation from states in a rather wide energy range, depending on the way in which the fragments were formed. Studies of gamma rays from fragments formed in a fission process induced by neutrons from a reactor often involve experimental difficulties, because the background at a reactor is mostly very heavy. All these problems have probably hindered a faster progress of the knowledge of prompt fission gamma radiation from the thermal-neutron induced fission of ^{235}U, and so far most studies have concerned gamma rays from fragments formed in the spontaneous fission of ^{252}Cf.

Measurements of the prompt gamma radiation have been made recently with Ge(Li) detectors on ^{252}Cf fission [1, 2], and also on ^{235}U fission [3]. The experimental technique has been improved considerably during the last five to seven years, for instance by the introduction of Si(Li) detectors, with which K X-ray energy spectra from the fragments can be recorded in a simple way [1, 2, 4-9]. These X-rays are formed through conversion of the prompt gamma rays, and studies of them can therefore yield complementary data to the knowledge of the prompt gamma radiation. Recently experiments have also been performed with X-rays and gamma rays in coincidence [1, 2, 7], and so it is now possible to determine a few of the lower gamma-ray cascades in some mass regions.

The main difference between the present experiment and most others reported so far is the use of a collimator to select different time intervals after the fission event. This technique has been used in few experiments up till now [10-13]. The present study follows in basic principle the ideas outlined by Johansson [10]. With the collimator it is possible to study the time distribution of the gamma radiation, such as decay curves of the integral radiation from all fragments or from certain fragments, and also to record gamma-ray energy spectra from certain fragments during different time intervals after the fission event. This means that gamma radiation of different half-lives as a function of fragment mass can be studied.

Another interesting parameter in these investigations is the total fragment kinetic energy. This will be reported separately [14]. The data acquisition system was a two-parameter analyzer, so that there is simply no possibility to add more parameters to the two whose interrelations were studied: gamma-ray energy and fragment mass.

It is sometimes possible to use more than one existing model in nuclear physics for the interpretation of fission data. One often used model is the collective model, the reason being of course that the fission process is really a collective, many-particle process. Some extra problems arise, however, as the fragments, just after their formation, are very neutron-rich, and it may be difficult to compare results of fission gamma-ray studies with those of other nuclear reactions. Of great interest for purposes of comparison are the data from prompt neutron emission studies, and quite a lot of the discussion from these studies can be adopted for the interpretation of prompt fission gamma radiation. Unfortunately the situation surrounding prompt neutron emission is far from clear, and it seems as if more effort will have to be put into the studies of the prompt decays of the fragments.

The gamma radiation studied in the present work is the part which is characterized as prompt. Somewhat arbitrarily the radiation is usually divided into two parts, namely a prompt part whose components have half-lives shorter than 1 ns, and a delayed part with longer half-lives. This division is further justified by the fact that the experimental techniques for study of the two parts differ and that the properties of the radiation in the two cases show a distinct difference [10].

In the present experiment a special technique was adopted, namely that of using time-of-flight discrimination between the prompt neutrons and the fission gamma radiation. This was done by placing the gamma detector about 70 cm from the fission foil. This technique has not been used extensively so far, probably because of the small solid angles involved and, as a consequence, the low counting rates in the gamma detector [12, 13, 15-17].

2. EXPERIMENTAL PROCEDURE

2.1. Apparatus

Fig. 1 shows a block diagram of the electronics used in this experiment. The details of the design and the system performance have been discussed recently [18], and it will suffice to describe briefly some of the specific features of this set-up.

The fissile deposit was 1 cm^2 in area and prepared by electrodeposition on 100 $\mu g/cm^2$ nickel foils. The thickness of the uranium layer was about 100 $\mu g/cm^2$ in order to allow measurements of mass spectra with acceptable resolution. Two solid state detectors of the surface barrier type were placed in parallel and symmetrically around the foil to measure the energies of the fission fragments. The detectors* were about 4 cm^2 in area, fabricated from 400 ohmcm n-type silicon and operated at about 70 V bias. The distance between each detector and the fissile foil was 2 cm. The gamma detector was a NaI(Tl) scintillator, 10.4 cm long and 13.0 cm in diameter, viewed by a Philips XP 1040 photomultiplier tube. The associated electronics**, consisting of a pulse-shaping unit and a discriminator, was coupled directly to the photomultiplier tube socket and gave a fast leading-edge time pulse and a linear pulse.

Pulses from the solid state detectors were amplified in charge-sensitive preamplifiers followed by linear amplifiers.

The amplified pulses were then fed into a linear divider circuit which performed the operation of dividing one pulse by the sum of both. By disregarding prompt neutron evaporation and energy losses in the target material, it can easily be shown that the ratio of the energies of the two fragments is inversely proportional to the mass ratio. Consequently, if E_1 and E_2 are the kinetic energies of the respective fragments and M_1 and M_2 are the associated mass numbers, one readily gets

$$\frac{E_1}{E_1 + E_2} = \frac{M_2}{M_1 + M_2} \propto M_2$$

i.e. the spectrum from the output of the divider circuit is simply the mass spectrum. As distinguished from an earlier divider circuit [18], which was mainly a logarithmic amplifier, the present divider circuit was linear***.

---

* Type C7904 Heavy Ion Detectors supplied by ORTEC, Oak Ridge, Tenn., USA.

** Designed and built at the Research Institute of National Defence, Stockholm [19].

*** Designed and built at the Physics Department, University of Lund, Lund, after an idea presented by Gere and Miller [20].

In all these measurements a NaI scintillator was used for gamma radiation detection due to its high efficiency. As the counting rates are very low, it was found to be more important to detect as many events as possible than to get high resolution but low efficiency, as with a Ge(Li) detector.

A lead collimator, movable in parallel with the direction of the detected fragments and also with a variable slit, was used to select gamma radiation in different time intervals after the fission event.

The data recording system was the same as in ref. [18], namely a two-parameter analyzer, the memory of which was that of a small computer, PDP-8/S.

2.2. Performance

As will be demonstrated in some figures in the following section, the resolution of the gamma peaks is in general very poor. The reason for this is that a NaI scintillator has been used for gamma detection instead of a Ge(Li) detector, and furthermore that the gamma radiation has been accumulated as function of mass groups rather than single masses. The reason for measuring in this way was discussed briefly in an earlier paper [18], and some additional arguments will now be presented which are pertinent mainly to the gamma-ray energy spectra which are the subject of the present study.

That the resolution of the gamma-ray spectra is poor need not necessarily be a serious drawback in the present studies, as one can obtain a lot of information about the excitation of the fragments without doing any "normal" nuclear spectroscopy. As has been discussed by Johansson [10], the fragments de-excite mainly through vibrational cascades just after the prompt neutron emission, and these transitions seem to be similar for all fragments. Instead of presenting level schemes for individual fragments, one can calculate and show yields of photons in specific energy regions as function of fragment mass and thus study gamma-energy variations over the mass spectrum. These yield functions have been calculated by summing up the number of recorded photons in specific gamma-ray energy portions and then dividing these functions by the yield of the mass spectrum.

There are many ways of making the summation, depending on the gamma-ray energy regions of interest, and the interest usually arises gradually when studying the behaviour of the gamma-ray energy spectra. Several of these yield functions will appear in the following section.

3. RESULTS

3.1. General

The gamma-ray energy spectra of all prompt fission gammas is presented in fig. 2. It was recorded in coincidence with the gammas of the time-of-flight spectrum and no lead collimator was used. The over-all background is less than 1 %. No corrections have been made for the response function of the detector, because the only intention in presenting it here is to demonstrate its general appearance and the similarity to the same spectrum recorded earlier, for instance by Mainschein [21]. The latter reference contains a review of these types of spectra together with theoretical comparisons. The shape of the spectra has often been fitted to analytical expressions, and the spectrum in fig. 2 fits well into those expressions. But the analytical equations have no significance from the fission physics aspect other than that they might be used in reactor shielding calculations [21].

As mentioned above, the gamma-ray energy spectrum in fig. 2 is very complex, but some details can be obtained through certain procedures. One procedure is to record the gamma spectra in coincidence with the mass spectrum in a two-parameter analyzer, and another, which can also be used together with the first one, is to select certain time regions after the fission event by use of a lead collimator. The collimator will then enhance gamma radiation with a certain half-life, and figs. 3 and 4 show examples of such gamma-ray energy spectra. The enhanced radiation has a half-life of about 50 ps and the spectra are integrated over the whole mass spectrum. The only difference between figs. 3 and 4, as seen, is the gamma-ray energy range. Comparison of the figures of these two spectra with the spectrum in fig. 2 shows very clearly that the structure of the "whole" spectrum in fig. 2 can be revealed by proper use of a collimator. For the respective half-lives the different fragments, in turn, can give very different spectra. It might be mentioned at this point that mass separation is not fully effective without the collimator, because the mass spectrum is obtained by dividing the fragment energy pulse heights electronically. In a certain fission event, however, the gamma detector can never tell which of the two fragments emitted a recorded photon, unless one of the fragments has been shadowed by a collimator.

3.2. Gamma rays associated with half-lives of about 50 ps

One series of measurements, consisting of the accumulation of gamma-ray energy spectra as function of mass, were recorded for a time interval after fission corresponding to a fragment flight path of 2 to 15 mm. The half-life of the radiation enhanced with this collimator setting was 50 ps and more. The average velocity of the fragments is about 1 cm/ns, and this collimator setting means that the time interval covered after fission is 0.2 - 1.5 ns on the average. The length of the collimator is about 13 cm and therefore there is about 1 mm more on both sides of the studied flight path which is seen by the gamma detector. Anyway, with this collimator setting the prompter half-lives of the gamma radiation have very low intensities, even if it may be said that the experiment might not have been optimized as far as the intensity is concerned. This collimator setting was chosen so as to reduce the background in the recorded gamma-ray spectra, due to faster radiations, to a very low level, namely less than 5 %. The main contribution to the background was the general reactor background and amounted to less than 20 %.

The measurement was performed in two steps covering the gamma-ray energy ranges of 0 - 4.2 MeV and 0 - 0.8 MeV respectively. The integrated gamma spectra with no mass selection are those shown in figs. 3 and 4, and examples of mass-sorted spectra are presented in fig. 5. The division of the gamma-ray energy portions was performed somewhat arbitrarily, but with the aim, if possible, of resolving gamma lines in the two regions in the most effective way with regard to the resolution of the detector and the number of channels available in the data recording system. In the spectrum covering energies up to 4.2 MeV it is impossible, even theoretically, to resolve lines of gamma rays of energies less than about 0.5 MeV. On the other hand it should be possible to resolve peaks in the energy region 0.5 to 2 MeV, while peaks in regions of higher energies should appear as broad bumps, unless they are very intense.

The spectra in fig. 5 are from the raw data, and the absolute intensities of each curve have not been corrected for the mass distribution.

The 1.2 MeV bump is present in several gamma-ray spectra and will therefore be presented under a separate heading in this chapter.

Gamma rays of energies around 200 keV have been found in a considerable proportion in some mass regions. The relative yield of such photons as a function of fragment mass is shown in fig. 6. This function is seen to be strongly mass-dependent and has a sawtooth type appearance.

The relative number of gamma rays of energies in the region of about 400 to 800 keV is also mass-dependent, as can be seen from fig. 7. The shape of this curve will be considered in detail in the discussion, but it is noticeable that it looks similar to the corresponding yield of photons of energies around 1200 keV (fig. 8).

The selection of energy region is a very important task, and one must be very careful in drawing conclusions from the above-mentioned results. To illustrate the problem a little, fig. 9 has been included. To obtain the yield presented there, namely the relative yield of photons with energies less than about 400 keV, a summation of the number of counts was made for the first ten gamma-ray energy channels in the spectra of gamma-ray energies between 0 and 4.2 MeV as function of fragment mass. The relative yield covered goes from about 1 to 4 in this figure, while in fig. 6 it goes from about 1 to about 2.5. It might seem self-explanatory that the yield ranges should be different, because the energy regions covered are not the same; but when starting the analysis one may be tempted to overlook this significance, as the recorded spectra do not differ too much except as regards the yield of the 200 keV photons. These yield curves, however, clearly show that there is more difference in the spectra than just the photons of lowest energy.

One reason for choosing such a wide gamma-ray energy range as up to 4.2 MeV was to look for possible octupole transitions. With this collimator setting, which enhances radiation with a half-life of about 50 ps and more, one can estimate that the corresponding collective octupole radiation has an energy of about 2 - 3 MeV. There are reasons to believe that these radiations should exist as a result of the breakup of the fissioning nucleus. Besides quadrupole-shaped, pear-shaped fragments might be formed and the asymmetric part of the latter nuclei would be sloshing back and forth. Unfortunately no clear evidence of such radiations was found, for the main part probably because of intensity reasons. The recorded number of counts per channel was low in these gamma-ray energy portions.

3.3. Gamma rays associated with half-lives of about 20 ps

One series of measurements was performed with a 1 mm wide collimator slit placed so close to the fission foil that radiation with half-lives around 20 ps was enhanced. The gamma-ray energy spectra do not differ very much as a function of the fragment mass investigated, even though a small difference does in fact exist, as can be found from a closer analysis (fig. 10). Differences can be observed, however, by studying the yields of photons of certain energies as function of fragment mass. One study covered the energy region from about 0.2 to 2.0 MeV. The yield curve of all those photons is shown in fig. 11 together with yield curves for specific gamma-ray energy portions.

In all gamma-ray energy spectra a broad distribution of photons has been found, with energies from about 200 to 1800 keV and, especially in mass regions around 105 and 145, an abundance of 400 keV photons superposed over the broad distribution.

Two measurements were performed with this collimator position, but with different gamma-ray energy ranges. One was the above-mentioned study covering 0.2 to 2.0 MeV and the other covered 70 to 700 keV. Where the two measurements overlap in gamma-ray energy, the relative yield curves of the number of photons are identical within the error limits.

The general background in the time-of-flight spectra was about 15 %. The signal-to-background ratio was normally an increasing function with gamma-ray energy in the present set-up [22] and for energies above about 400 keV the background was about 10 % or less.

One may argue that the collimator slit width in this measurement was too wide, and even if gamma radiation with a half-life of 20 ps was mainly enhanced, there could be a considerable contribution of slower radiation as well. However, by studying the shapes of the gamma-ray spectra and also the yield curves of the number of photons as function of fragment mass, one is readily convinced that the contribution of slower radiation, i.e. mainly with $T_{1/2}$ = 50 ps, must be quite small. The adjustment of the collimator for the enhancement of the $T_{1/2}$ = 50 ps radiation is very easily done, and consequently the shapes of those gamma-ray energy spectra are well known.

The distribution around 200 keV from the heaviest fragments in each mass group are probably coming from the above-mentioned 50 ps component. The intensity of those bumps in fig. 5 are roughly equal to what can be estimated from the intensity distribution of each of these two components [22].

3.4. Gamma rays associated with half-lives of about 7 ps

Measurements of gamma radiation with a half-life of about 7 ps are very difficult to perform mechanically. Some of the difficulties have been described briefly in ref. [22]. One measurement was done with a gamma-ray energy window covering about 0.2 to 2.0 MeV. The integrated gamma-ray energy spectrum is shown in fig. 12. There it can be seen that the recorded spectrum is a broad distribution centered around 1 MeV. Examples of mass-sorted spectra are shown in fig. 13. There is not much difference between them; there is a slight shift in medium energy, so that the average gamma-ray energy is slightly larger over the heavy mass peak than over the light one.

The relative yield of photons within the whole gamma-ray energy range is typically of the sawtooth type as demonstrated in fig. 14. More limited gamma-ray energy portions show in general the same behaviour, even though the yield curves differ in details.

3.5. The uncollimated gamma radiation

One short measurement has been devoted to the study of gamma-ray energy spectra as function of the fragment mass ratio. The gamma-ray spectra appear in two groups, but one spectrum in one group should have a correspondence in the other group. The two groups, of course, resemble the mass spectrum. It should therefore be possible to add the two corresponding spectra to one spectrum in order to improve the statistics. This has been done in a few cases. Of particular interest has been that the 1200 keV photons are enhanced for the mass combinations around 104 + 132, and this bump stands out very clearly for mass combinations around these mass numbers (fig. 15). The 1200 keV photons will be treated under a separate heading.

3.6. The 1200 keV distribution

In the integrated gamma-ray spectrum (fig. 2) one notices the presence of a small bump around 1200 keV. This bump has not received any particular attention earlier, even though it can be seen in the first fission gamma-ray spectra presented, for instance, by Maienschein. The reason for the lack of its discussion is probably that it is not very pronounced and that spectra covering energy ranges of more than 1 MeV have seldom been recorded earlier as function of mass. As the 1200 keV gamma rays show up both in spectra in which the 7 ps and in which the 50 ps half-life is enhanced, the bump deserves some special attention.

First one must be convinced that these gamma rays come from fission fragments and not from background. This is, of course, not at all clear from the integrated gamma-ray spectrum (fig. 2). The relative yield of 1200 keV photons, however, has been found to be a function of fragment mass (fig. 8), and so one has a firm ground on which to base the assumption that the 1200 keV gamma rays come from the energy release of particular fragments. The largest yield was found for the lightest mass in the heavy and light mass groups, respectively, but a broad bump also appears around mass number 95. There is a tendency to an increase in yield for mass numbers above 145, but the number of recorded photons was very low and therefore the yield value contains a large error in that mass region. The structure between mass numbers 80 and 95 is noteworthy and will be dealt with in the discussion. The yield, especially from the radiation with the 50 ps half-life, and its mass dependence, will be discussed in greater detail later on.

As has been discussed earlier [18], with the present technique there is no possibility of resolving individual lines in the gamma-ray spectra, as the mass dispersion is too poor. On the other hand this limitation need not be too much of a drawback. Instead one can take advantage of the high efficiency of this type of gamma detector as compared to the low efficiency but high resolution of, for example, a Ge(Li) detector.

4. ANALYSIS OF THE DATA

4.1. Comparisons with prompt neutron data

It has been pointed out earlier that the prompt fission gamma radiation exhibits features which in many respects are unusual compared to those of the radiation in other reactions. On the assumption that the gamma emission can occur only after the prompt neutron emission is energetically impossible, a total energy release in the form of gamma emission may be calculated at about 5 MeV [23]. The total energy is, in fact, about double this figure and the discrepancy is nowadays explained as being due to decays from high-spin states [10, 24].

In the interpretation of the results of the present measurements it is plausible to introduce arguments given when discussing the yield of prompt neutrons from fission fragments, as the gamma radiation follows the neutrons. There are several reasons, however, to be very careful in making such comparisons. Studies of prompt neutrons are beset with considerable experimental difficulties, as the neutrons can only be assumed to be emitted from moving fragments with a certain amount of probability. Several experiments have shown that, depending on the fissioning nucleus, a considerable fraction of the prompt neutrons is also emitted at the instant of scission. Nowadays one makes a clear distinction between the two types of neutrons. The term fragment neutrons is used to describe the neutrons emitted from the fragments, whereas scission neutrons or central neutrons describe the neutrons appearing at scission. It has been concluded that, on average, 85 - 90 %

of the neutrons in uranium fission are emitted from moving fragments [25, 26]. In a detailed description of the de-excitation of the fragments this fact must be taken into account. It has recently been estimated that in an event in the thermal fission of ^{235}U, resulting in a total kinetic energy of about 190 MeV, about one half of the total number of the emitted neutrons are scission neutrons [27]. This has given rise to some interesting discussions about the excitation energies of the fragments.

As is well known, the yield of prompt neutrons decreases as the fragment total kinetic energies increase. When the total kinetic energy has its maximum, it is also known that it is associated with a nearly asymmetric fission event. According to Maslin et al. [28] the average number of prompt neutrons emitted is then about 1.2 and so, according to Blinov et al. [27], there would be no more than about 0.6 fragment neutrons emitted per fission event. The average number of prompt neutrons in all uranium fission events is about 2.4. As mentioned above, several experimentalists have reported that about 85 - 90 % of these are fragment neutrons, which means that about 0.3 neutrons per fission event are scission neutrons. It cannot be stated that the number of scission neutrons should increase, as it seems here, from 0.3 to 0.6 when the total kinetic energy increases. One can only assume that a fission event resulting in the highest kinetic energies may arise from a more than "normally" violent process. In general it is believed that the scission neutrons are emitted at the time of scission because of disturbance associated with the breaking of the neck and the consecutive retraction of the stumps into the fragments [29, 30]. The high total kinetic energy may result in a lower than expected average number of fragment neutrons. Another possibility, however, is that the high total kinetic energy is associated with a higher than average initial spin value of the fragments, which may constitute a hindrance factor, and instead the gamma decay will be enhanced. Problems associated with the total kinetic energy have been discussed in detail elsewhere [14].

A complete discussion of the fission gamma decay can therefore hardly be based on the fragments emitting all the prompt neutrons and the consecutive decay coming in the form of gamma emission. These two decays are, of course, linked together, neutron decay being the faster, followed by the gamma decay. As mentioned earlier, the initial spin distribution of the fragments will then be one of the "means" through which the fragments select their decay modes.

Some of the features of the yield curves in figs. 6 - 9, 11, 14 showing the relative number of photons as a function of fragment mass for the different half-lives can be interpreted on the same basis as discussed in an earlier work [18]. The important physical idea behind this interpretation is that the fragments are more or less susceptible to deformation, depending on whether they consist of closed nucleon shells or not. This idea was put forward by Vandenbosch and Terrell [31, 32] and has been very successful in interpreting data on de-excitation of fission fragments. Most of the excitation energy of the fragments is, according to this idea, taken up by deformation directly after the scission act. A spherical nucleus, with one or both nucleon shells closed or almost closed, is resistant to deformation and its initial excitation energy should not be so high as in a nucleus which can easily be deformed, i.e. with one or both of its nucleon numbers far from being magic. The sawtooth curve reflecting the yield of prompt neutrons and also the yield of prompt photons as a function of fragment mass is well described by this model.

As far as the prompt gamma radiation is concerned, it is well interpreted according to this model. It has often been assumed that the prompt neutron is the result of an evaporation, and in a first simple approximation one often describes the prompt neutron emission in terms of a Maxwellian spectrum. It is known, however, that the prompt gamma emission can compete with the prompt neutron emission at excitation energies well above the binding energy of the neutron in the fragments, and this effect seems to be the result of the spin distribution.

4.2. Fragment spin and gamma-ray energy yield

The spin distribution of the fragments has not been measured in this work. As the spin plays an important role in the de-excitation of the nuclei, some of the spectra will be discussed on the basis of what is known today about it.

One of the latest papers on the initial spin distribution of the fission fragments is that by Armbruster et al. [33]. An average value of seven units of angular momentum was obtained, which increased strongly within each fission mass group from values of about 5 - 10 units of angular momentum. Another interesting conclusion drawn by Armbruster et al. was that the de-excitation mechanism of the fission fragments is not governed by the level density following from a statistical model, but that the fragments mainly de-excite by emission of quadrupole radiation from stretched collective cascades. This idea has also been put forward earlier [10, 24].

It is interesting to study the relationship between the average energies of the main groups of the gamma rays in the three spectra and their associated half-lives. Such a study may yield information which can form a basis for interpretation of the type of gamma radiation involved. It was found that the time component with a half-life of about 7 ps was associated with a broad bump in the gamma-ray energy spectrum around 1100 keV, whereas for the 20 ps component there was an abundance of photons around 800 keV, and for the 50 ps component the photon yield was very large around 200 keV. In a plot of the logarithm of the half-life as a function of the gamma-ray energy in the three cases mentioned above, namely (200 keV, 50 ps), (800 keV, 20 ps) and (1200 keV, 7 ps), these three points will fall in a region having values taken from data sheets for the energy of the lowest excited 2^+ levels and their corresponding half-lives for gamma decay in even-even nuclei. This could be a strong indication that collective quadrupole radiation constitutes a very great part of the prompt fission gamma radiation, i.e. the same conclusion as arrived at by, for instance, Armbruster et al. [33] in their measurements, and also suggested by Johansson [10].

As mentioned in the previous section and also discussed above, a considerable difference seems to exist in the shapes of the gamma-ray energy spectra, depending on whether the 7, 20 or 50 ps half-lives were enhanced. The paper by Armbruster et al. [33] presents a figure showing that the gamma-ray energy spectrum for the uncollimated beam is practically the same, as far as the shape is concerned, as the one with the collimator selecting photons in the time region 10 - 100 ps after scission. This collimator setting means that the 20 ps half-life component is enhanced, which can be easily checked by studying fig. 6 in Johansson's work [10], which concerns ^{252}Cf fission. The present work on ^{235}U fission gives a similar intensity distribution leading to a half-life of about 20 ps. Johansson presented gamma-ray energy spectra with the collimator set to enhance radiation in practically the same time interval, 10 - 70 ps. In Armbruster's work the corresponding time interval was 10 - 100 ps, which should not give any significant difference in the energy spectra because the intensity distribution is a strongly decreasing function with time after scission, and so the extra 30 ps from 70 to 100 ps should not make much difference. The energy spectra in the present work resemble those presented by Johansson [10] when this time component was enhanced, but the broad distribution of photons with energies around 800 keV seems to have no similarity to the spectra presented by Armbruster et al. [33]. The collimator setting used in the present work was practically the same as the one used by Armbruster et al. [33]. Moreover, the energy spectrum recorded without the collimator by Armbruster et al. does not look the same as the one presented in ref. [18], whereas the uncollimated spectrum from the present work does. Unfortunately Armbruster et al. did not comment on this matter in their paper, as the main object of their work was to study the primary spins of the ^{235}U fission fragments.

4.3. Comparisons with gamma-ray data from ^{252}Cf fission

A few recently published papers have given the half-lives of some gamma transitions in ^{252}Cf fission [1, 2, 6]. Several of these half-lives are of the order of nanoseconds and the associated energies are around 100 keV. Some of the measurements were performed in such a way that the energies of coincident internal conversion electrons and K X-rays were recorded. In one of the most recent reports giving data on the ground-state bands of nuclei in the mass region around 100, information is given which at first glance should be of great value for the interpretation of the present results. Differences exist, however, in the ways in which the present and the californium measurements have been performed. The californium work included studies of K X-rays, and therefore a certain selection of the transition type has been made. X-rays formed as a result of conversion are favoured for the lower gamma-ray energies. The californium work has resulted in a set of gamma-ray energy values and associated half-lives, especially in the mass region around 100, where predictions for ground-state rotational bands have been given with great confidence. Gamma-ray energies and half-lives were also given, however, for many other low-energy photons from fragments elsewhere along the mass distribution of the spontaneous fission of ^{252}Cf. A direct comparison cannot be made in all respects between the present data and those of the ^{252}Cf work. As far as the radiation of $T_{1/2} = 50$ ps and more is concerned, several of the gammas found around 200 keV in the present work are probably the same as those found in the californium experiments.

The Karlsruhe measurements [3] concern thermal-neutron induced fission of ^{235}U, and the results in the form of gamma lines show that there are several similarities between californium and uranium fission. The Karlsruhe as well as the Berkeley group used a Ge(Li) detector and therefore obtained a set of gamma lines of well defined energies, especially in the low energy portion. The energies found in the uranium work very often coincide with those of the californium studies, and therefore one may assume that several of those lines are the same as those of the present measurement. Most of these lines have been found in mass regions around the heaviest masses in each mass group, where fragments easily susceptible to deformation are expected to occur. They may then originate from the slowest time component.

4.4. Gamma rays of energies around 1200 keV

The 1200 keV photons deserve special attention in this analysis.

From the results of the present measurements it is clear that these gammas play a very important role in the de-excitation of the fragments, and in fig. 3 the broad distribution stands out very clearly. In the mass-sorted spectra the 1200 keV photons show up mostly in mass regions around 82, 94 and 130. Of particular interest is that the relative yield of gamma rays of energies in the region 400 - 800 keV is a similar function, except that the yield is low from the very lightest fragments. This yield curve was obtained with the same collimator setting as that for the 1200 keV photons. No specific conclusion should be drawn from this fact, even though it is tempting to venture the guess that these gamma rays form part of a cascade. With a slightly different collimator setting one would have seen a difference in the respective relative intensities of these gamma rays, and from this difference it would be possible to calculate whether and how these gamma rays are associated in a cascade. The difference in gamma-ray energy would be associated with a consecutive difference in half-life, the 1200 keV being the faster decay.

The gamma-ray energy spectra in the mass regions showing an abundance of the 1200 keV also show a slight shift towards higher energies in the average gamma-ray energy for the photon distribution in the energy portion of less than 400 keV (fig. 16). The 1200 keV gamma rays may therefore be associated with gamma rays of energies of around 300 keV. That the 1200 keV gamma rays are present in the spectra where the 50 ps half-life gamma component is enhanced is an extraordinary feature. On the assumption that the 1200 keV gamma rays are of the collective quadrupole type, one would assume a half-life of no more than 10 ps, and the 1200 keV photons would never be recorded with any measurable intensity with this collimator setting. There are therefore reasons to believe that the 300 keV photons precede the 1200 keV photons in a cascade, and that the collimator setting is suitable for detecting the low-energy photons, whereas the 1200 keV photons are delayed. A slightly different collimator setting would be of great help in indentifying this proposed cascade. As was suggested by Johansson [10], one may assume the possibility of a vibration of the beta type among the stiff fragments with mass numbers around 82 and 132, from which fragments the 300 and 1200 keV photons appear in greater abundance than elsewhere.

The 1100 keV gamma rays appearing in the spectra for which the 7 ps half-life is enhanced are probably of more normal vibrational type. The relative yield of these gamma rays is a typical sawtooth function and reflects directly the excitation energies of the fragments soon after the prompt neutrons have been emitted. They must be among the first members of the gamma cascades, and their relative yields from mass to mass depend on the relative excitation energies of the fragments. When the collimator is set to enhance gamma radiation with a half-life of about 20 ps, the 1200 keV gamma rays have low yields compared to the photons of energies of 800 keV and below. When the 50 ps half-life is enhanced, most of the yields of photons are of energies around 200 keV from the heaviest fragments in each mass group, whereas the 1200 keV photons have low yields compared to the 200 keV photons, but still of the same order as the associated 300 keV photons.

4.5. Average gamma-ray energies

The average energies of the gamma rays were estimated in some of the gamma-ray energy spectra. In the case when radiation of half-life $T_{1/2} = 7$ ps was enhanced, the variation of the average gamma-ray energy with fragment mass was within about 0.1 MeV, with the highest energies for the lightest fragments in each mass group and the lowest energies for the heaviest fragments (fig. 17). A similar calculation for the radiation of half-life $T_{1/2}$ = 20 ps showed a similar curve with the average energy around 0.85 MeV (fig. 18).

Maier-Leibnitz et al. [34] arrived at the conclusion that the uncollimated radiation showed no essential dependence on mass. The average energy in the mass region around 130, however, was appreciably higher than in other mass regions, namely around 4 MeV. The present measurement and that of Maier-Leibnitz et al. have been performed in different ways, and the average photon energies estimated in this study are smaller for masses around 130 than those obtained by Maier-Leibnitz et al. The aim of the present work has been to study the gamma-ray energies as function of mass and time after fission, and therefore gamma-ray energy portions have been selected bearing in mind previous knowledge obtained from the work of, for instance, Maier-Leibnitz et al. Figs. 17 and 18 only show where the bulk of the gammas in these energy spectra are centered, i.e. they tell which average energy is associated with most of the photons emitted when the radiations of $T_{1/2}$ = = 7 and 20 ps, respectively, are enhanced.

It is reasonable to assume that, if a gamma-ray energy portion of about 10 MeV had been studied, i.e. as in fig. 2, the average gamma-ray energy for the whole spectrum would vary more in fig. 17 and 18. Such a measurement should be performed, as it would result in a total gamma-ray energy release associated with the half-lives of 7 and 20 ps. In the present work this measurement was omitted because of lack of time. In principle such a measurement differs from the one performed only in the respect that the gamma-ray energy range of the data recording system should be differently chosen.

When an estimate of the average photon energy has been obtained, and also the relative yield of photons as a function of fragment mass, one can qualitatively get the variation of the energy release of the fragments in the form of gamma radiation in the respective time regions studied in the present work. As far as the 7 and 20 ps components are concerned, the respective average gamma-ray energies vary but little from one mass region to another, and the average energy release in the form of gamma radiation as a function of fragment mass will be a curve of the sawtooth type. A rough estimate of the total energy release within the first one-tenth of a nanosecond would give an average for the light and heavy mass groups of about 3 MeV, with a sawtooth variation in each mass group going from about 1 to 5 MeV. By studying the decay curve of the prompt fission gamma radiation one finds that at least 75% of the total energy has been released within this time region, and this value agrees rather well with the accumulated yields mentioned by earlier authors [10, 35].

4.6. Possible octupole vibrations

During recent years more and more attention has been paid to octupole vibrational states in deformed nuclei [36 - 39]. It is reasonable to expect these states to be formed also in fission fragments as, just after scission, there is a large probability that easily deformable fragments may assume shapes resembling pears. Recent calculations, which agree well with experimental results, give energies for the first 3^- states in the rare-earth region of about 1.5 MeV [39]. As far as the energies are concerned, the 1^- states could coincide with the 1.2 MeV photons, but the yield curve of those photons is in disagreement with this picture, as the 1.2 MeV photons are mainly released from nuclei containing closed or almost closed nucleon shells. On the other hand it is reasonable to expect the E3 transitions from the 3^- states to be of the order of 2 MeV. A calculated yield curve, however, covering the gamma-ray energy region of about 1.6 to 2.4 MeV, as a function of fragment mass showed practically no variation over the whole fragment mass distribution. Studies of other energy portions up to about 4 MeV showed very little variation with mass.

As far as the heaviest fragments are concerned, one may expect their lowest octupole states to have excitation energies of about 1.2 to 1.5 MeV, and the yield curve of the 1200 keV photons as a function of fragment mass (fig. 8) there is indeed the beginning of an increase in yield when the mass number goes from 145 and upwards. Unfortunately the number of counts is not very large and it is not possible to state, or even assume, anything indicative of the presence of this kind of radiation in that region.

The half-life of this radiation is expected to be larger than that of the quadrupole radiation, and in a future experiment, one should be able to select this radiation by using a narrower collimator slit. The collimator could first be positioned at the "beginning" of the time interval chosen in the experiment presented here. With the same narrower collimator, but placed further away from the foil, one can then get the slower radiation enhanced and very little contribution from the quadrupole radiation, and the variation in intensity between the two types of radiation would come out clearly.

5. DISCUSSION

One may remark that the yield curves presented do not show up so much structure as the one presented in an earlier work [18]. The collimator settings were, however, slightly different from the one used in ref. [18], as in the present work the settings were chosen carefully to allow enhancement of the two time components with half-lives of 7 and 20 ps. As mentioned in ref. [18], the selected time interval was $10^{-11} - 10^{-10}$ s, but it was found later that the 10^{-10} s limit was slightly higher, so that the intensity of the 20 ps component was decreased relatively more than that of the 50 ps time component. In the present work the gamma-ray energy ranges were limited to the first two MeV, which should have some, though a small, effect, whereas in the earlier work there was no limit on the gamma-ray energy portion selected.

As has been mentioned earlier [18], the resolution of the gamma detector is about 10 %. Since several fragments can contribute to one gamma-ray energy spectrum, it is impossible with this system to resolve single gamma lines in a spectrum. The mass resolution is about 4 - 5 amu [18] and it is no use trying to look for single lines which might belong to specific fragments. It may be remarked, for instance, that within the mass regions where the nuclei seem to have deformed shapes, the variation in mass number of 4 - 5 amu may change the energy of the first 2^+ levels in even-even nuclei by about 10 keV. Bearing this in mind it is easy to understand that the distributions around 200 keV in the gamma-ray spectra of figs. 4 and 5 probably come from decays of several fragments.

The inherent bad resolution of this system was of course known when the present studies started, but, as mentioned earlier [18], the aim of this work has been to study gamma-ray yields as function of fragment groups and time of fission. For physical reasons this can be acceptable, as the energy of the gamma radiation from rotational and vibrational cascades varies slowly with mass number in regions of deformed nuclei. Even though a unique determination of the fragment mass number could be made, the charge dispersion is not known very accurately.

6. CONCLUSIONS

Studies have been performed of the gamma radiation from fission fragments in slow-neutron induced fission of ^{235}U. Gamma-ray energy spectra were recorded as function of mass and time after fission. The main conclusions from the investigation may be summarized as follows:

1. The gamma-ray energy spectra vary in shape with time after fission.

2. The gamma-ray energy spectra vary in shape with mass within each time interval, the variation being stronger the later the time interval studied.

3. When a time interval is selected in which half-lives of the radiation of 50 ps and more are enhanced, there is a strongly mass-dependent yield of 1200 keV photons, which might come late in a cascade of gammas.

4. There is a very strong dependence on mass of the yield of photons of a few hundred keV in the time interval in which half-lives of 50 ps and more are enhanced.

5. The relationship between the average gamma-ray energies and the associated half-lives gives a strong indication that the bulk of prompt photons from fission fragments are of the quadrupole type.

6. Yield curves of the photons as function of mass can be interpreted on the basis of a model including the property of the varying resistance to deformation of the nuclei, depending on whether they contain nucleons of magic numbers or not.

Investigations in this field are in progress at various laboratories, which will add to the information on excited states in nuclei far from the line of beta stability. It is hoped that, with some luck, it will also be possible to make some contributions to the understanding of the fission process.

ACKNOWLEDGEMENTS

It is a great pleasure to thank Professor S. Johansson for valuable discussions and Professor N. Ryde and Dr. T. Wiedling for their interest in this work. The assistance from Mr. L. Lindow is gratefully acknowledged. Many thanks are due to Mr. E. Karlsson for building the divider circuit.

REFERENCES

1. CHEIFETZ E. et al.,
Experimental information concerning deformation of neutron rich nuclei in the A $\sim$100 region.
Phys. Rev. Lett. 25 (1970) p. 38.

2. WILHELMY J.B. et al.,
Ground-state bands in neutron-rich even Te, Ba, Ce, Nd, and Sm isotopes produced in the fission of ^{252}Cf.
Phys. Rev. Lett. 25 (1970) p. 1122.

3. HORSCH F. and MICHAELIS W.,
Prompt gamma rays emitted from individual fragments in neutron-induced fission. Physics and chemistry of fission.
Proc. of a symp. Vienna, 28 July - 1 August 1969.
IAEA, Vienna, 1969, p. 527.

4. KAPOOR S.S., BOWMAN H.R., and THOMPSON S.G.,
Emission of K X-rays and division of nuclear charge in the spontaneous fission of ^{252}Cf.
Phys. Rev. 140 (1965) p. B 1310.

5. WATSON R.L., BOWMAN H.R., and THOMPSON S.G.,
K X-ray yields of primary ^{252}Cf fission products.
Phys. Rev. 162 (1967) p. 1169.

6. WATSON R.L. et al.,
A study of the low-energy transitions arising from the prompt de-excitation of fission fragments.
Nucl. Phys. A141 (1970) p. 449.

7. RUEGSEGGER, Jr., D.R. and ROY R.R.,
Gamma rays in coincidence with K X-rays from the La, Ce, and Pr fission fragments of Cf^{252}.
Phys. Rev. C 1 (1970) p. 631.

8. WATSON R.L., JARED R.C., and THOMPSON S.G.,
Distribution of K X-rays as a function of mass and atomic number in the spontaneous fission of ^{252}Cf.
Phys. Rev. C 1 (1970) p. 1866.

9. KATARIA S.K. et al.,
K X-ray yields in 0 - 1 μs from ^{236}U fragments.
Nucl. Phys. A154 (1970) p. 458.

10. JOHANSSON S.A.E.,
Gamma de-excitation of fission fragments. (I). Prompt radiation.
Nucl. Phys. 60 (1964) p. 378.

11. VAL'SKII G.V. et al.,
Concerning the emission times of γ-quanta as a result of fission.
Sov. At. Energy 18 (1965) p. 279.

12. SKARSVÅG K.,
Time distribution of γ-rays from spontaneous fission of ^{252}Cf.
Nucl. Phys. A153 (1970) p. 82.

13. ARMBRUSTER P. et al.,
Mass dependence of anisotropy and yield of prompt γ-rays in ^{235}U thermal fission.
Physics and chemistry of fission.
Proc. of a symp. Vienna, 28 July - 1 August, 1969.
IAEA, Vienna, 1969, p. 545.

14. ALBINSSON H.,
Yield of prompt gamma radiation in slow-neutron induced fission of ^{235}U as a function of the total fragment kinetic energy. 1971.
(AE-417).

15. BLINOV M.V. et al.,
Angular anisotropy of the gamma quanta accompanying U^{235} fission.
Sov. Phys. JETP 16 (1963) p. 1159.

16. GRAFF G., LAJTAI A., and NAGY L.,
The angular distribution of gamma-rays from the fission of U^{235}.
Physics and chemistry of fission.
Proc. of a symp. Salzburg, 22 - 26 March, 1965.
IAEA, Vienna, 1965. Vol. 2, p. 163.

17. VERBINSKI V.V., WEBER H., and SUND R.E.,
Prompt gamma-rays from ^{235}U (n, f), ^{239}Pu (n, f) and ^{252}Cf (spontaneous fission). (Abstract.)
Physics and chemistry of fission.
Proc. of a symp. Vienna, 28 July - 1 August, 1969.
IAEA, Vienna, 1969, p. 929.

18. ALBINSSON H. and LINDOW L.,
Prompt gamma radiation from fragments in the thermal fission of ^{235}U. 1970.
(AE-398).

19. BECKMAN L., HANSÉN J., and JANSSON R.,
A fast time-of-flight spectrometer.
Nucl. Instr. Methods. 52 (1967) p. 157.

20. GERE E.E. and MILLER G.L.,
A high speed analog pulse divider.
IEEE Trans. Nucl. Sci. NS-11 (1964):3 p. 382.

21. MAIENSCHEIN F.C. et al.,
Gamma-rays associated with fission.
U.N. intern. conf. on peaceful uses of atomic energy.
2. Geneva 1958. Proc. Vol. 15, p. 366.
U.N. Geneva, 1958.

21A. PEELLE R. W. and MAIENSCHEIN F. C.,
Spectrum of photons emitted in coincidence with fission of ^{235}U by thermal neutrons.
Phys. Rev. C. 3 (1971) p. 373.

22. ALBINSSON H.,
To be published.

23. TERRELL J.,
Fission neutron spectra and nuclear temperatures.
Phys. Rev. 113 (1959) p. 527.

24. JOHANSSON S. A. E. and KLEINHEINZ P.,
Gamma-radiation from fission. Alpha-, beta- and gamma-ray spectroscopy.
Ed. by K. Siegbahn. North Holland Publ. Co.
Amsterdam 1965, Vol. 1, p. 805.

25. KAPOOR S. S., RAMANNA R., and RAMA RAO P. N.,
Emission of prompt neutrons in the thermal neutron fission of U^{235}.
Phys. Rev. 131 (1963) p. 283.

26. SKARSVÅG K. and BERGHEIM K.,
Energy and angular distributions of prompt neutrons from slow neutron fission of U^{235}.
Nucl. Phys. 45 (1963) p. 72.

27. BLINOV M. V. et al.,
Dependence of the anisotropy of fission neutron emission on the total kinetic energy of the fragments.
Sov. J. Nucl. Phys. 12 (1971) p. 22.

28. MASLIN E. E., RODGERS A. L., and CORE W. G. F.,
Prompt neutron emission from U^{235} fission fragments.
Phys. Rev. 164 (1967) p. 1520.

29. STAVINSKII V. S.,
On the emission mechanism of prompt fission neutrons.
Sov. Phys. JETP 9 (1959) p. 437.

30. FULLER R. W.,
Dependence of neutron production in fission on rate of charge of nuclear potential.
Phys. Rev. 126 (1962) p. 684.

31. VANDENBOSCH R.,
Dependence of fission fragment kinetic energies and neutron yields on nuclear structure.
Nucl. Phys. 46 (1963) p. 129.

32. TERRELL J.,
Prompt neutrons from fission.
Physics and chemistry of fission.
Proc. of a symp. Salzburg, 22 - 26 March, 1965.
IAEA, Vienna, 1965, Vol. 2, p. 3.

33. ARMBRUSTER P., LABUS H., and REICHELT K.,
Investigation on the primary spins of the ^{235}U fission fragments.
To be published in Z. Naturforschung, March 1971.

34. MAIER-LEIBNITZ H., SCHMITT H. W., and ARMBRUSTER P.,
Average number and energy of gamma-rays emitted as a function of fragment mass in U^{235} thermal-neutron-induced fission.
Physics and chemistry of fission.
Proc. of a symp. Salzburg, 22 - 26 March 1965.
IAEA, Vienna, 1965. Vol. 2, p. 143.

35. MAIER-LEIBNITZ H., ARMBRUSTER P., and SPECHT H. J.,
Prompt and delayed gamma-rays from fission.
Physics and chemistry of fission.
Proc. of a symp. Salzburg, 22 - 26 March 1965.
IAEA, Vienna, 1965, Vol. 2, p. 113.

36. JOHANSSON S. A. E.,
Nuclear octupole deformation and the mechanism of fission.
Nucl. Phys. 22 (1961) p. 529.

37. DONNER W. and GREINER W.,
Octupole vibrations of deformed nuclei.
Z. Physik 197 (1966) p. 440.

38. KRAPPE H. J. and WILLE U.,
Collective model for pear-shaped nuclear.
Nucl. Phys. A124 (1969) p. 641.

39. NEERGÅRD K. and VOGEL P.,
Low-lying octupole states of the doubly even deformed nuclei with $152 \leq A \leq 190$.
Nucl. Phys. A145 (1970) p. 33.

FIGURE CAPTIONS

Fig. 1 Block schematic of the electronic equipment.

Fig. 2 The energy spectrum of the uncollimated gamma-rays emitted within 5×10^{-9} s after the fission event.

Fig. 3 The energy spectrum of the gamma radiation from all fragments associated with half-lives of 50 ps and more.

Fig. 4 The low energy part of the spectrum of the gamma radiation from all fragments associated with half-lives of 50 ps and more.

Fig. 5 Gamma-ray energy spectra of the same radiation as in fig. 3 for a number of different masses.

Fig. 6 The relative gamma-ray yield of the energy portion 100 - 230 keV as a function of fragment mass associated with the half-lives of 50 ps and more.

Fig. 7 The relative gamma-ray yield of the energy portion 0.4 - 0.8 MeV as a function of fragment mass associated with half-lives of 50 ps and more.

Fig. 8 The relative gamma-ray yield of the energy portion 1.0 - 1.4 MeV as a function of fragment mass associated with half-lives of 50 ps and more.

Fig. 9 The relative gamma-ray yield of the energy portion 50 - 400 keV as a function of fragment mass associated with half-lives of 50 ps and more.

Fig. 10 Gamma-ray energy spectra of the radiation with a half-life of about 20 ps for a number of different masses.

Fig. 11 Relative gamma-ray yields as function of fragment mass from the radiation shown in fig. 10 and for different energy portions: (a) 0.2 - 2.0 MeV, (b) 0.2 - 0.6 MeV, (c) 0.2 - 0.4 MeV, (d) 0.4 - 0.6 MeV, (e) 0.6 - 0.8 MeV, (f) 0.8 - 1.0 MeV.

Fig. 12 The energy spectrum of the gamma radiation from all fragments associated with half-lives shorther than 10 ps.

Fig. 13 Gamma-ray energy spectra of the radiation with half-lives shorter than 10 ps for some different masses.

Fig. 14 The relative gamma-ray yield of the energy range 0.2 - 2.0 MeV as a function of fragment mass associated with half-lives shorter than 10 ps.

Fig. 15 A portion of the gamma-ray energy spectrum of the uncollimated radiation from the fragment mass regions 104+132.

Fig. 16 The average quantum energy as a function of fragment mass for the energy distribution from 100 - 400 keV associated with half-lives of 50 ps and more.

Fig. 17 The average quantum energy as a function of fragment mass associated with half-lives shorter than 10 ps.

Fig. 18 The average quantum energy as a function of fragment mass associated with half-life of about 20 ps.

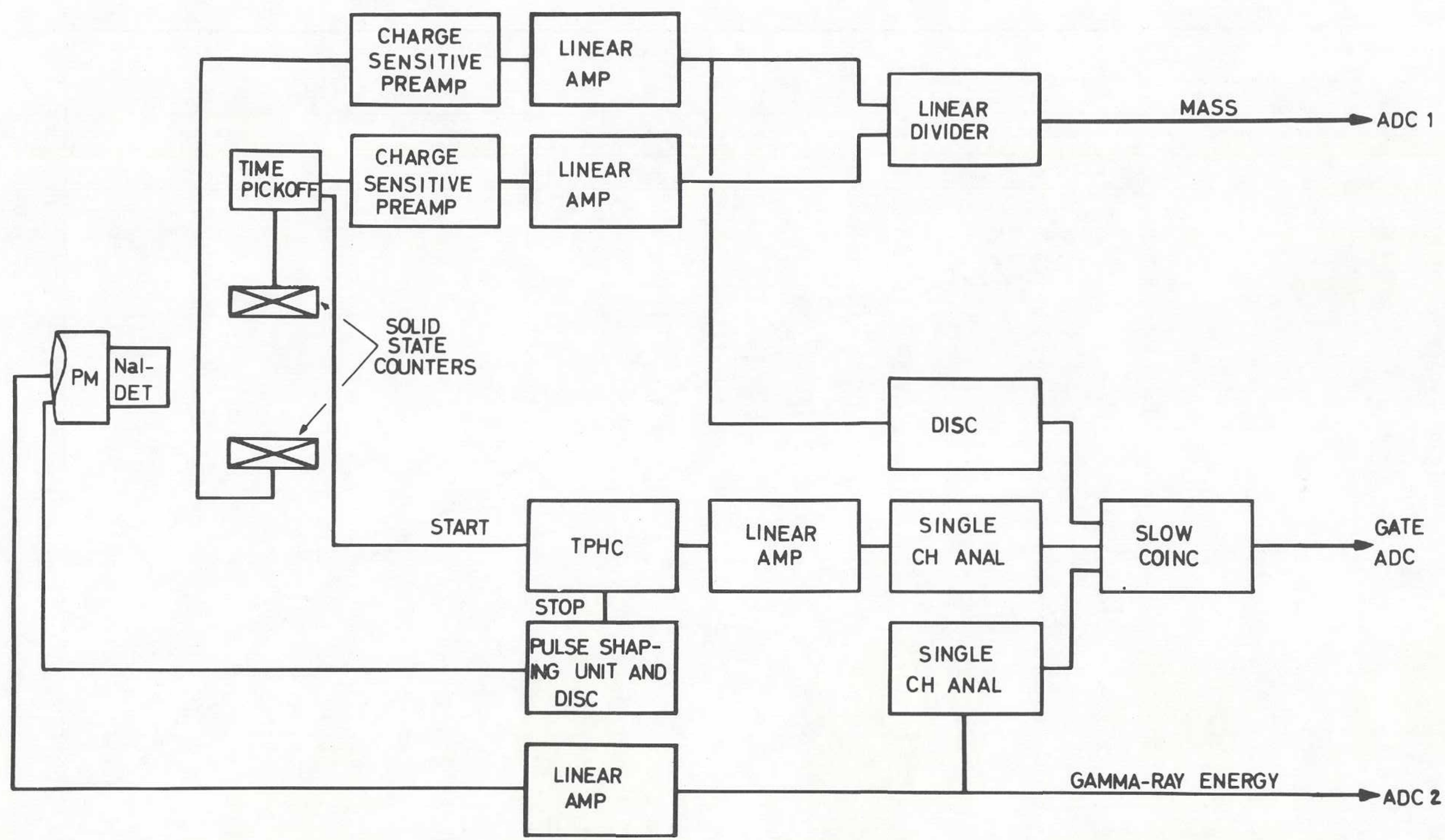
CHARGE SENSITIVE PREAMP
LINEAR AMP
LINEAR DIVIDER
MASS
ADC 1
TIME PICKOFF
CHARGE SENSITIVE PREAMP
LINEAR AMP
SOLID STATE COUNTERS
PM
NaI-DET
DISC
START
TPHC
LINEAR AMP
SINGLE CH ANAL
SLOW COINC
GATE ADC
STOP
PULSE SHAPING UNIT AND DISC
SINGLE CH ANAL
LINEAR AMP
GAMMA-RAY ENERGY
ADC 2

Fig 1

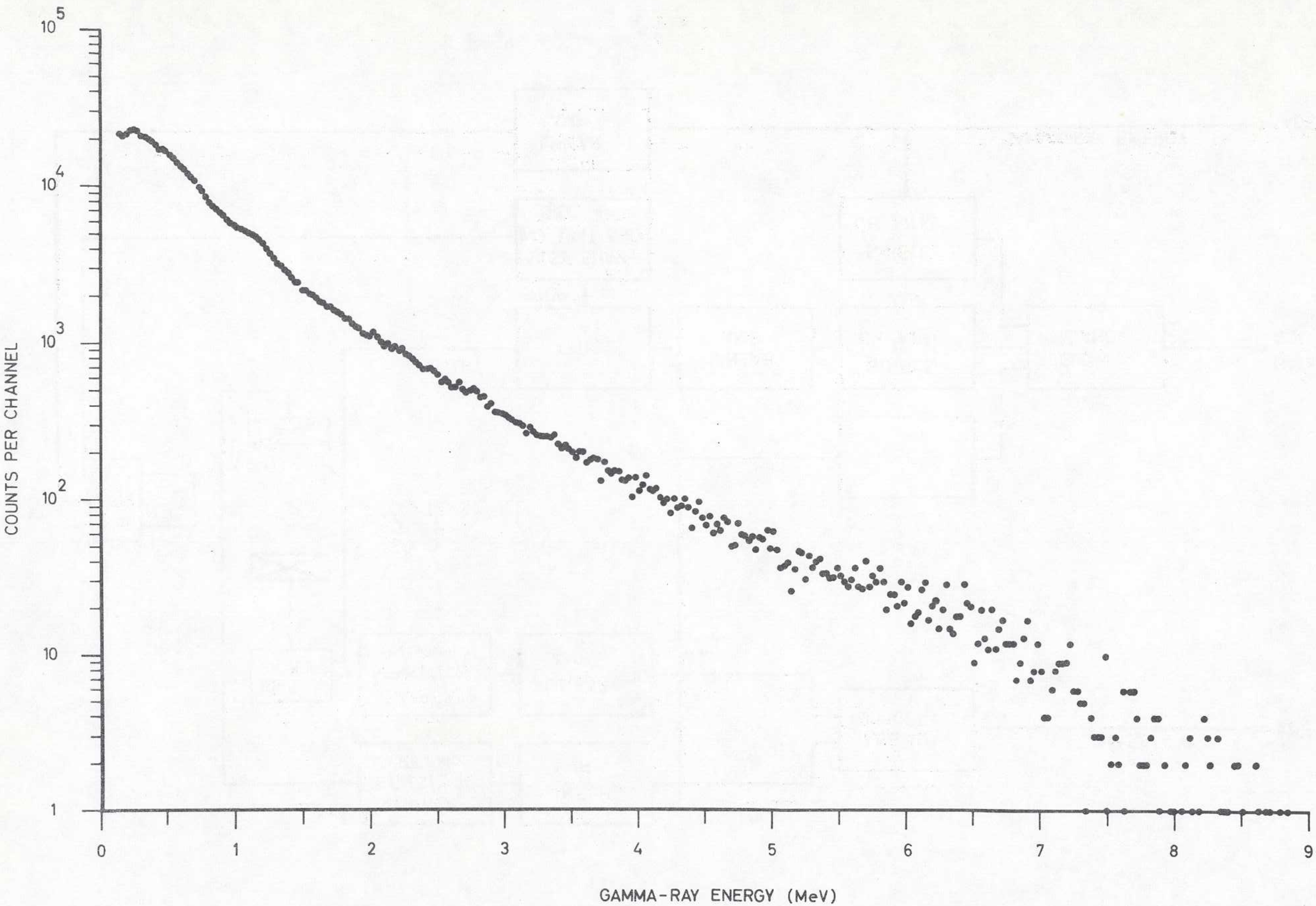
10^5
10^4
10^3
10^2
10
1
COUNTS PER CHANNEL
0
1
2
3
4
5
6
7
8
9
GAMMA-RAY ENERGY (MeV)

Fig 2

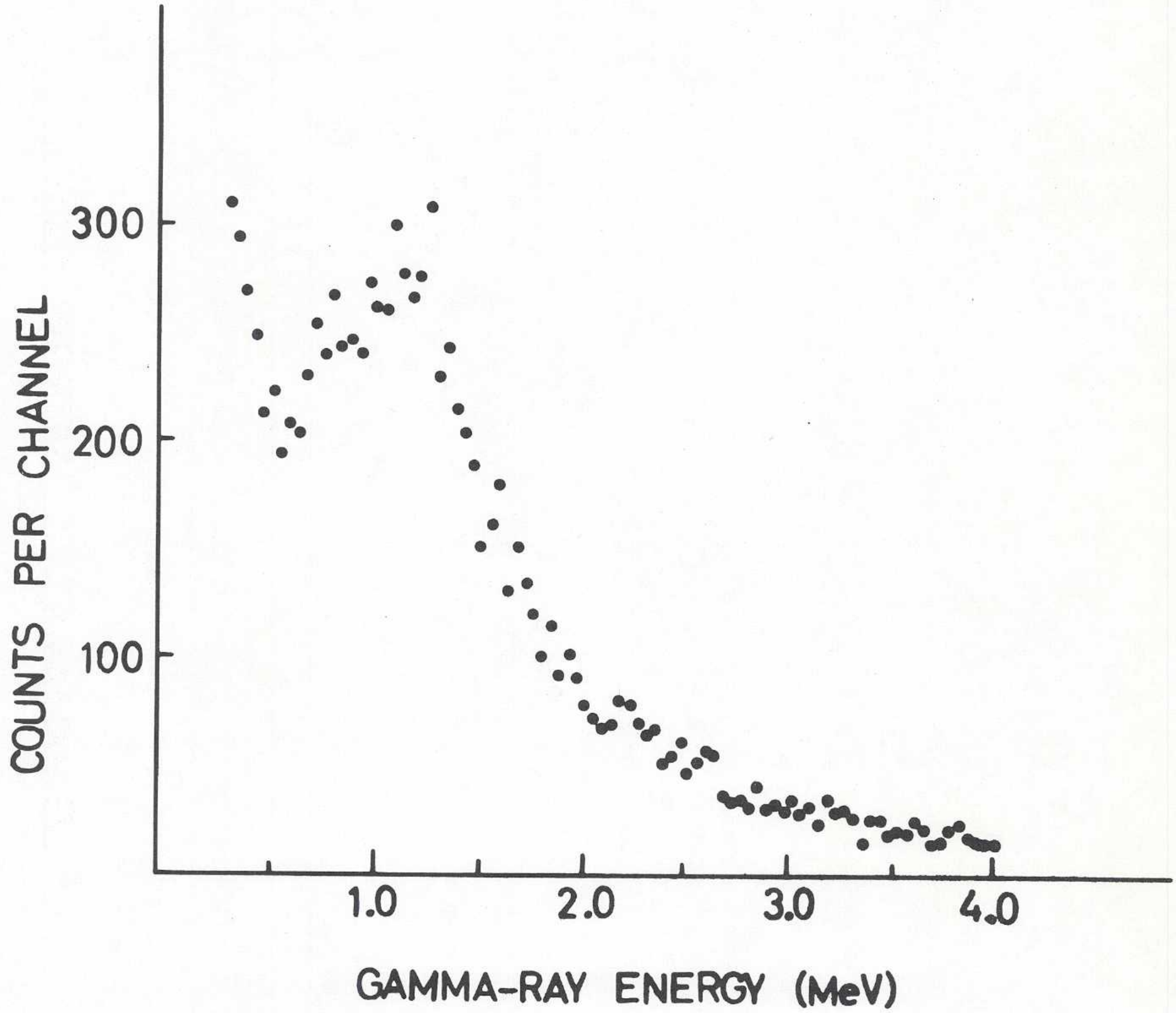

300
200
100
COUNTS PER CHANNEL
1.0
2.0
3.0
4.0
GAMMA-RAY ENERGY (MeV)

Fig 3

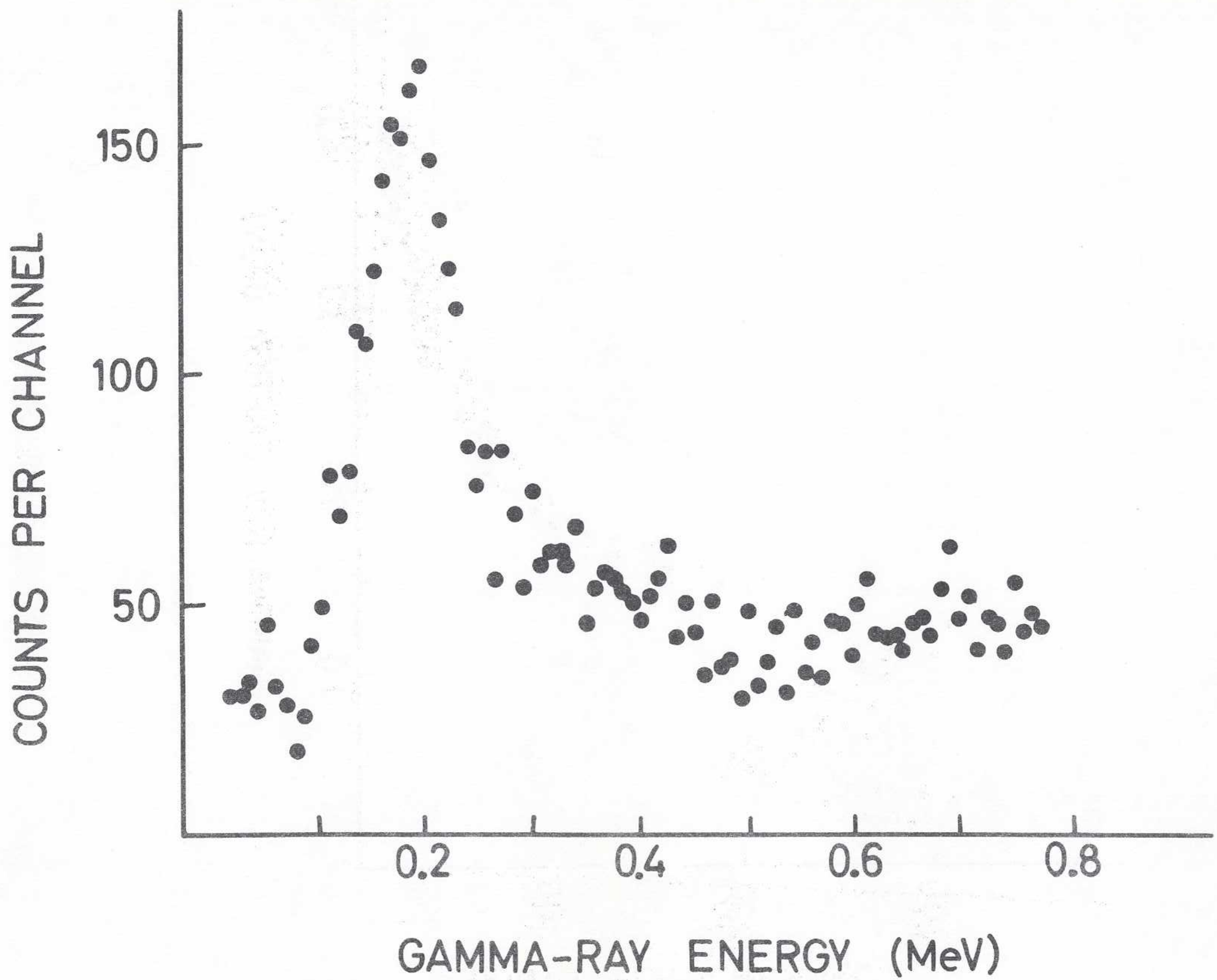

Fig 4

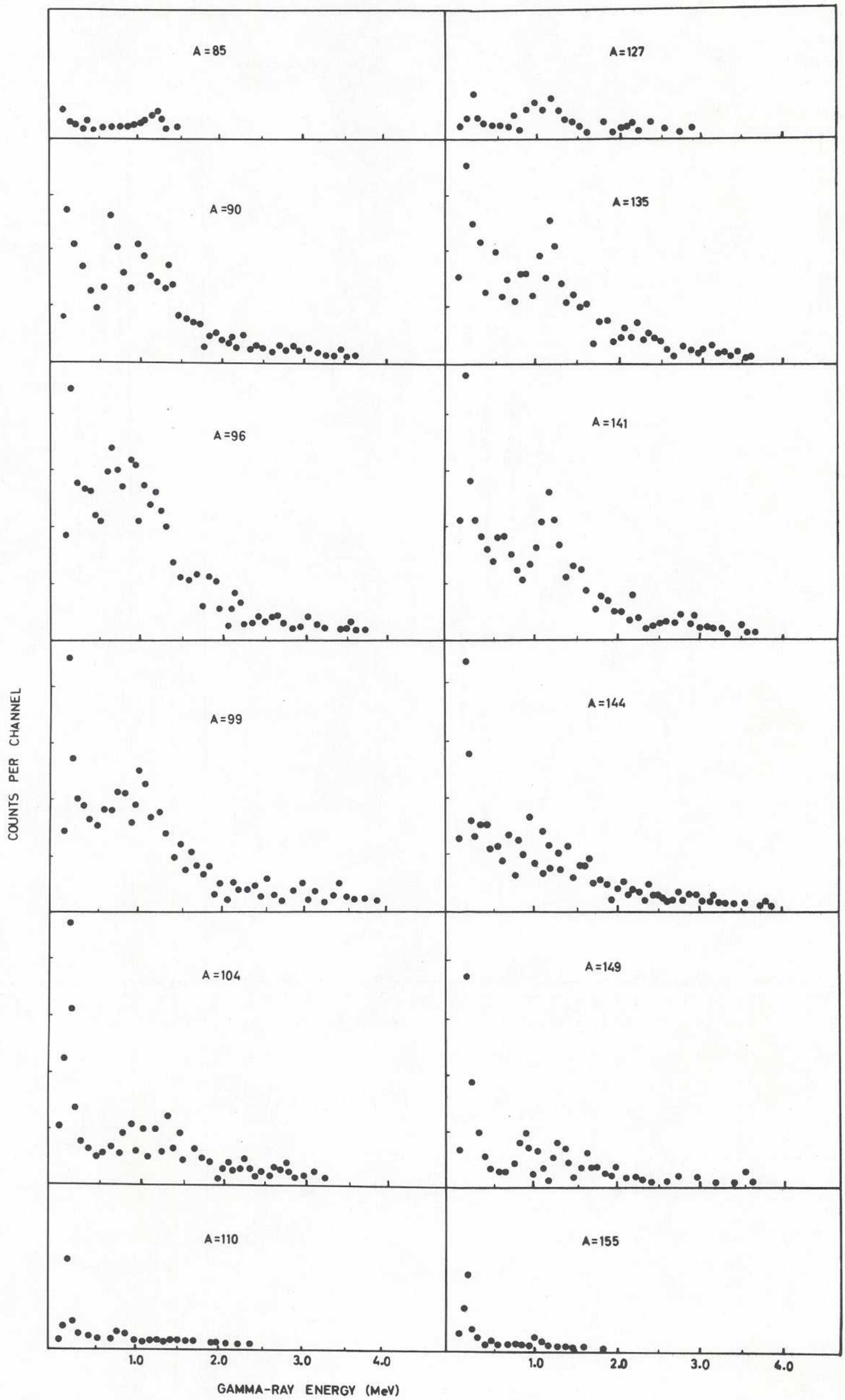
A=85
A=127
A=90
A=135
A=96
A=141
A=99
A=144
A=104
A=149
A=110
A=155
COUNTS PER CHANNEL
1.0
2.0
3.0
4.0
GAMMA-RAY ENERGY (MeV)

Fig 5

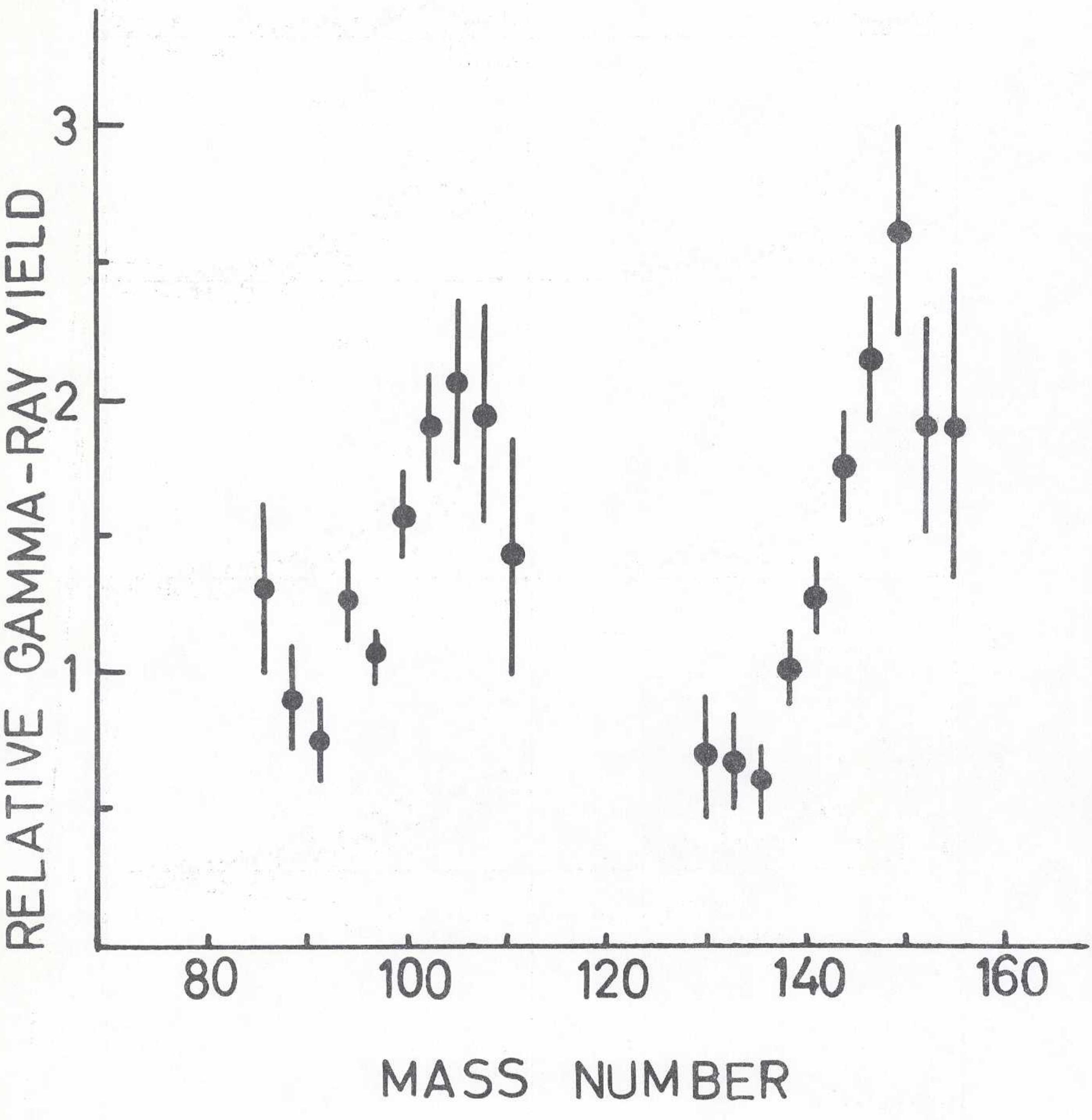

Fig 6

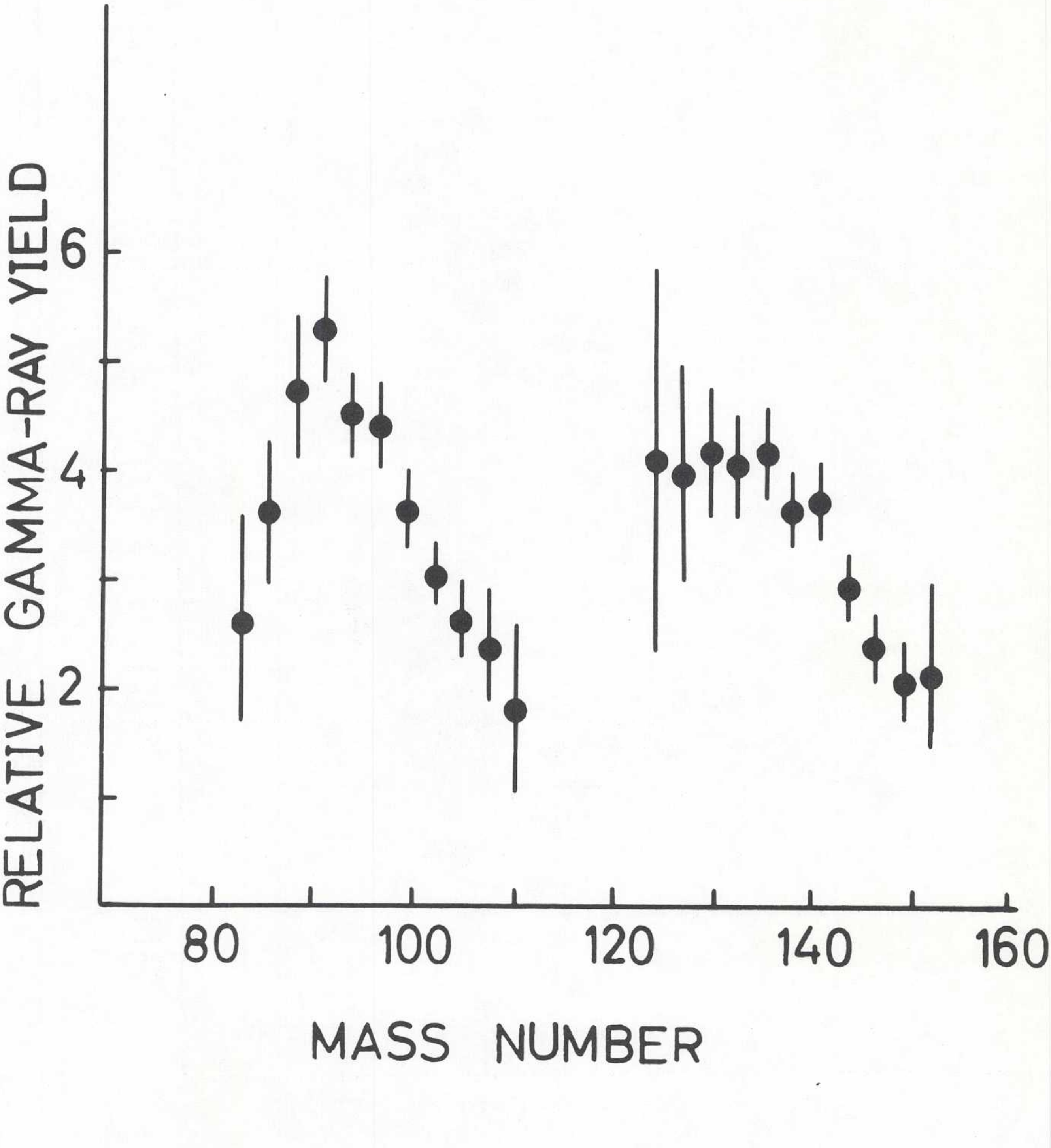

Fig 7

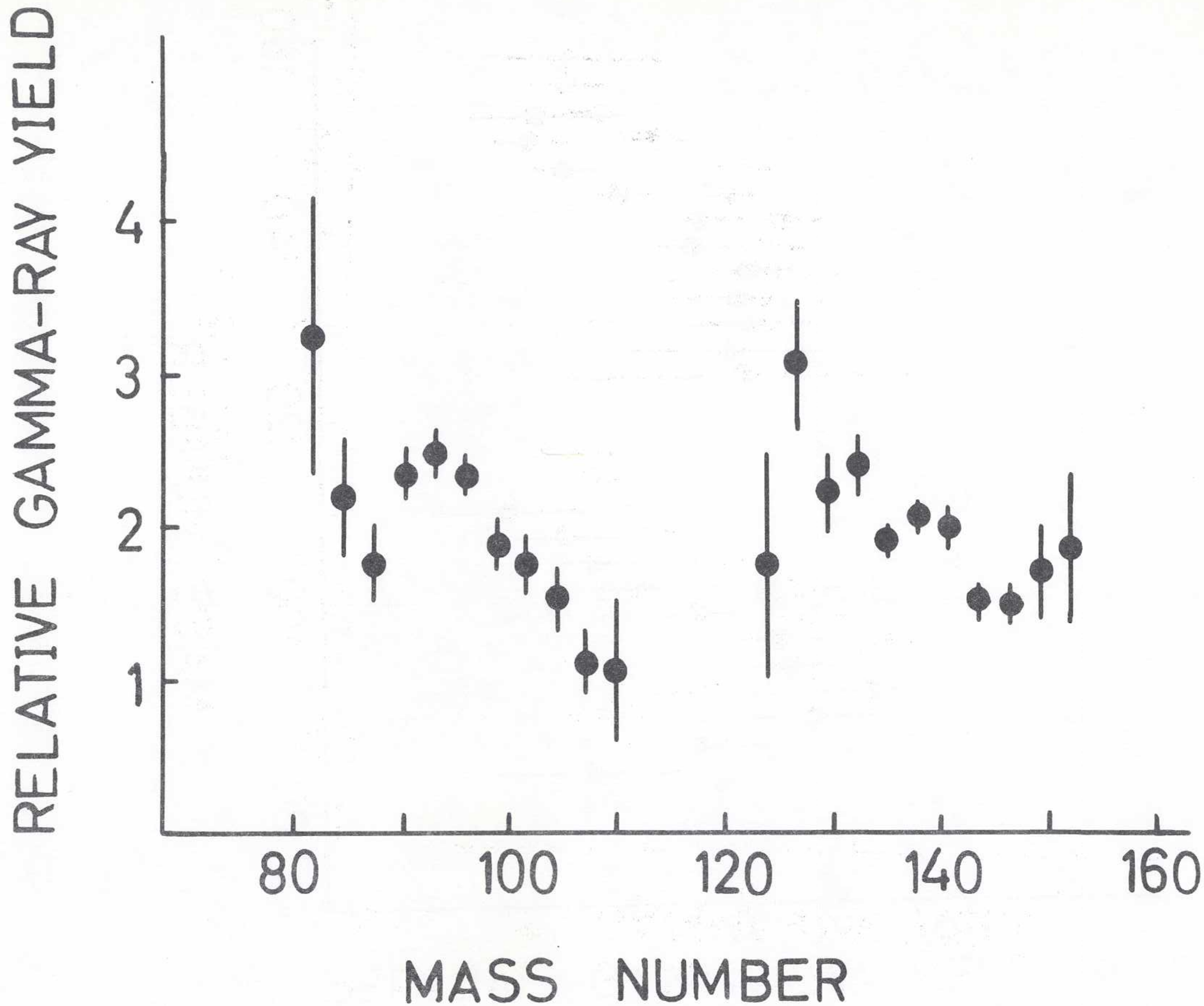

Fig 8

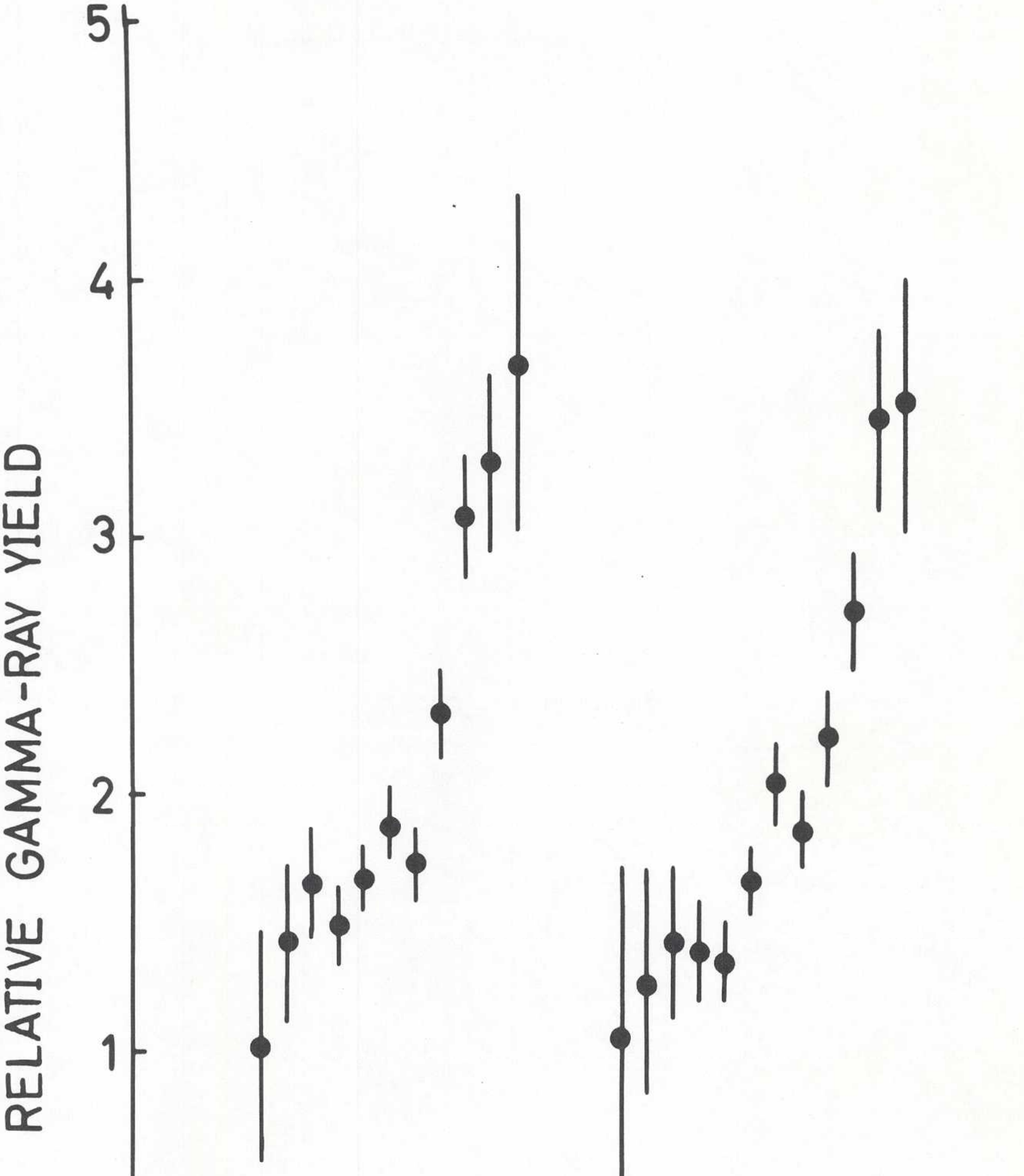
5
4
3
2
1
RELATIVE GAMMA-RAY YIELD
80
100
120
140
160
MASS NUMBER

Fig 9

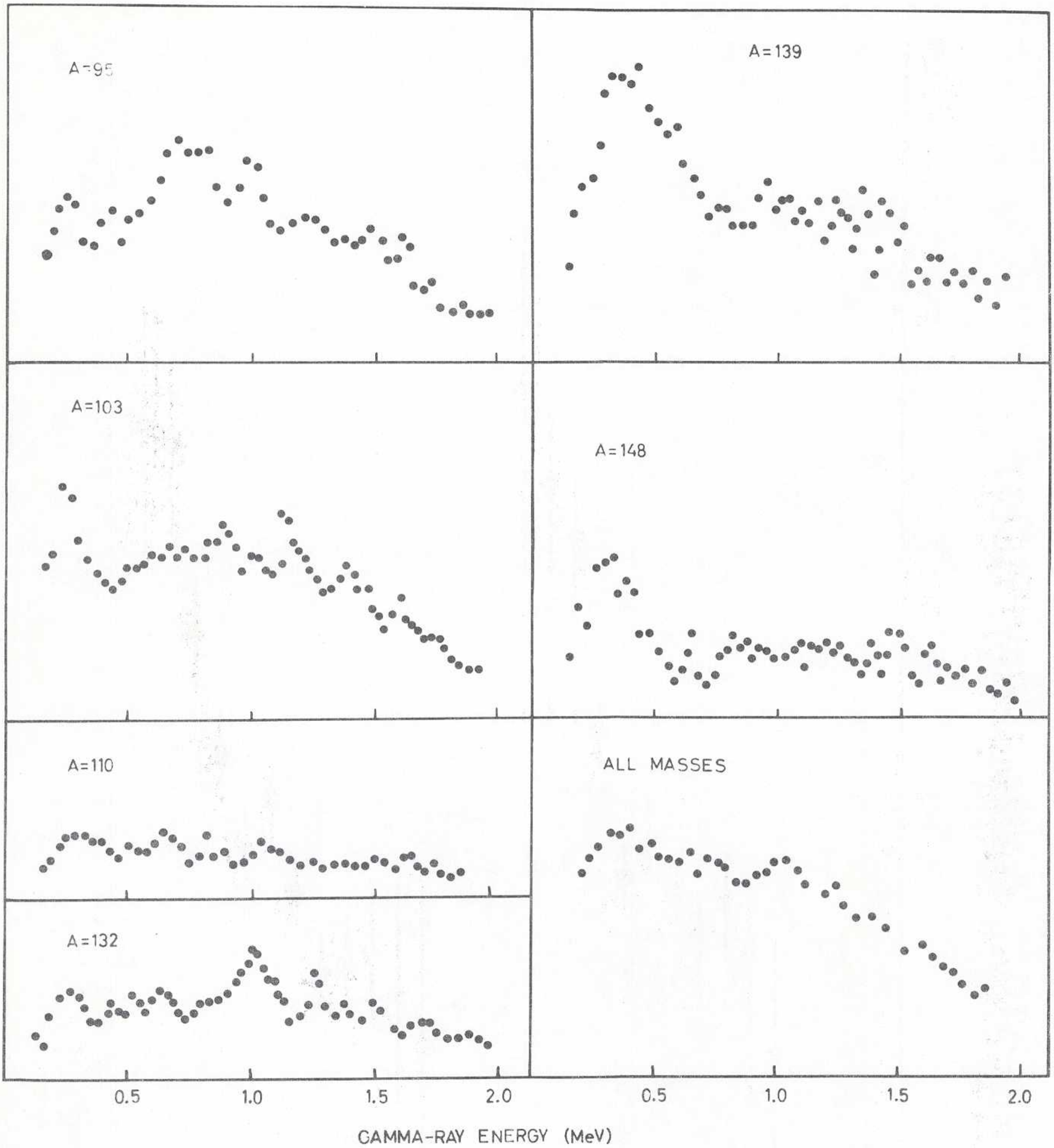
A=95
A=139
A=103
A=148
A=110
ALL MASSES
A=132
0.5
1.0
1.5
2.0
0.5
1.0
1.5
2.0
GAMMA-RAY ENERGY (MeV)

Fig 10

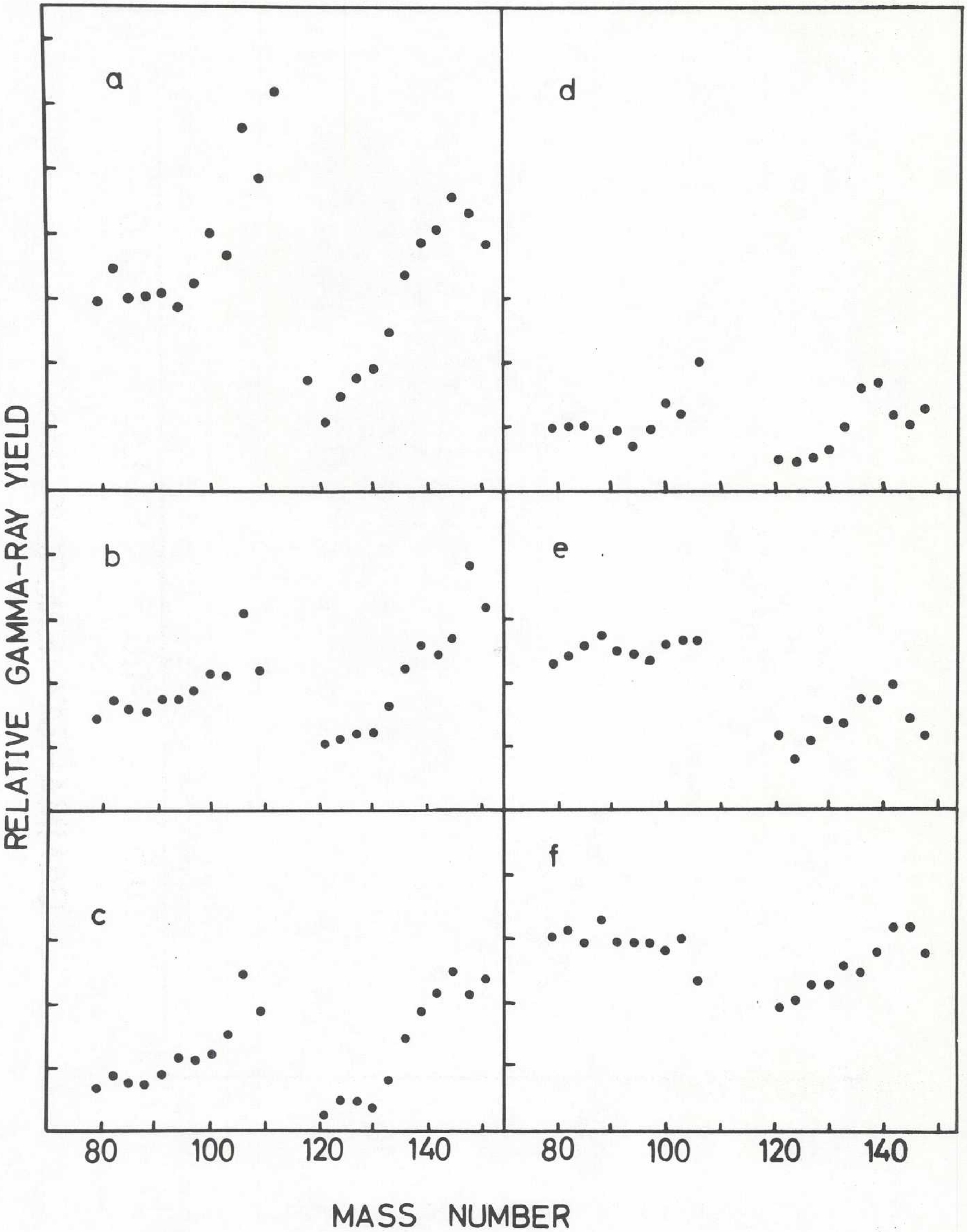
a
b
c
d
e
f
RELATIVE GAMMA-RAY YIELD
80
100
120
140
80
100
120
140
MASS NUMBER

Fig 11

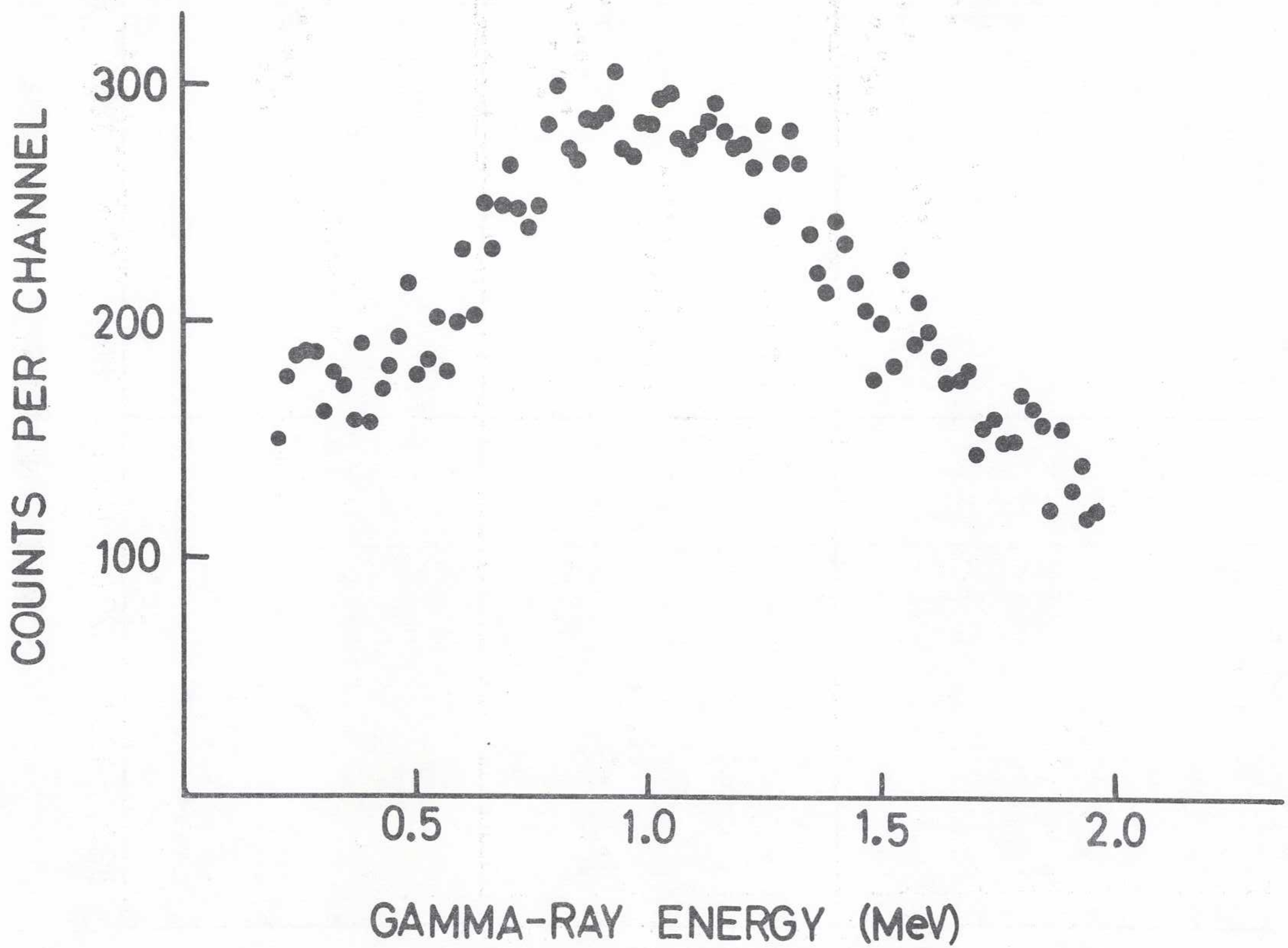
300
200
100
COUNTS PER CHANNEL
0.5
1.0
1.5
2.0
GAMMA-RAY ENERGY (MeV)

Fig 12

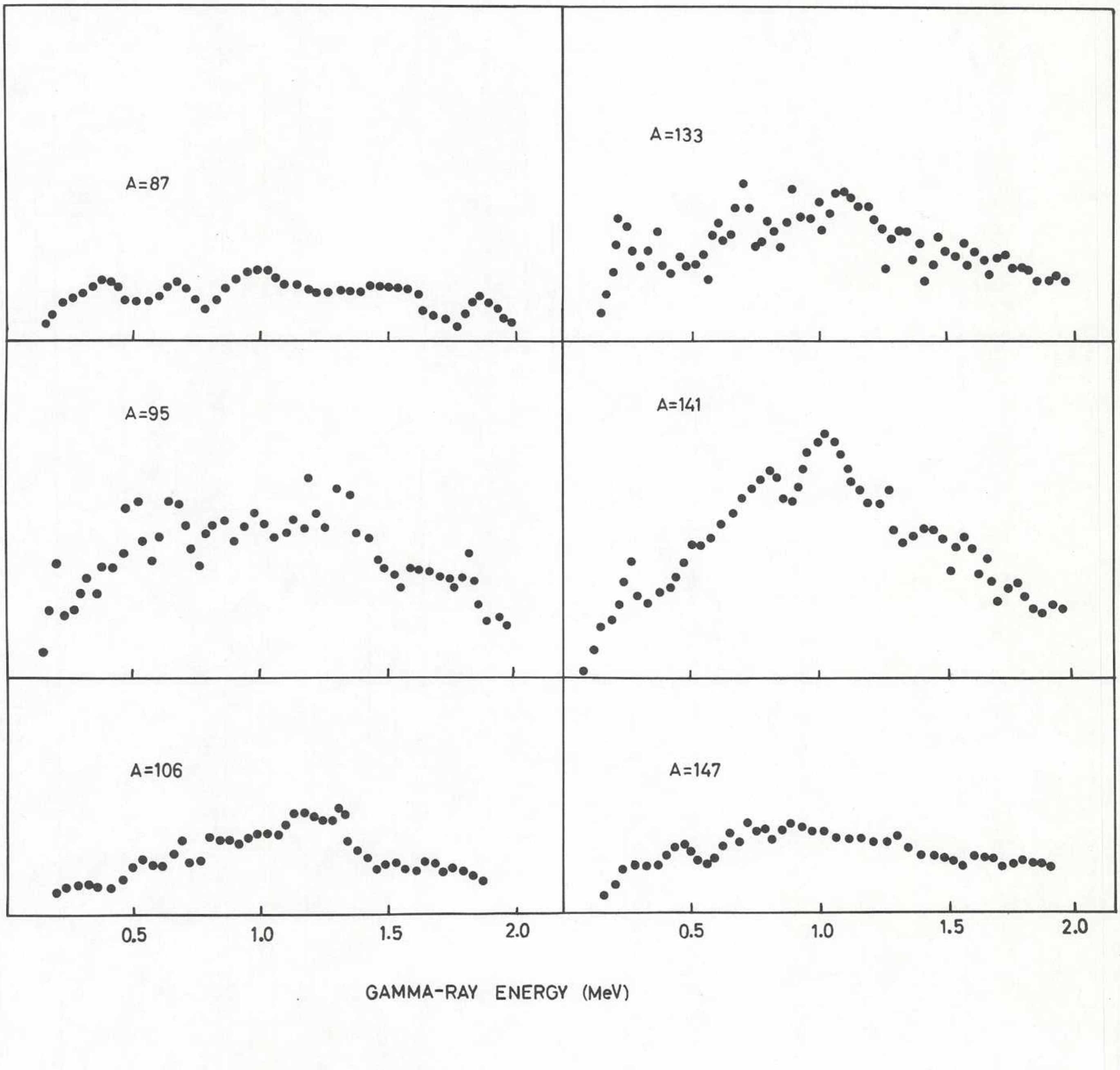
A=87
A=133
A=95
A=141
A=106
A=147
0.5
1.0
1.5
2.0
0.5
1.0
1.5
2.0
GAMMA-RAY ENERGY (MeV)

Fig 13

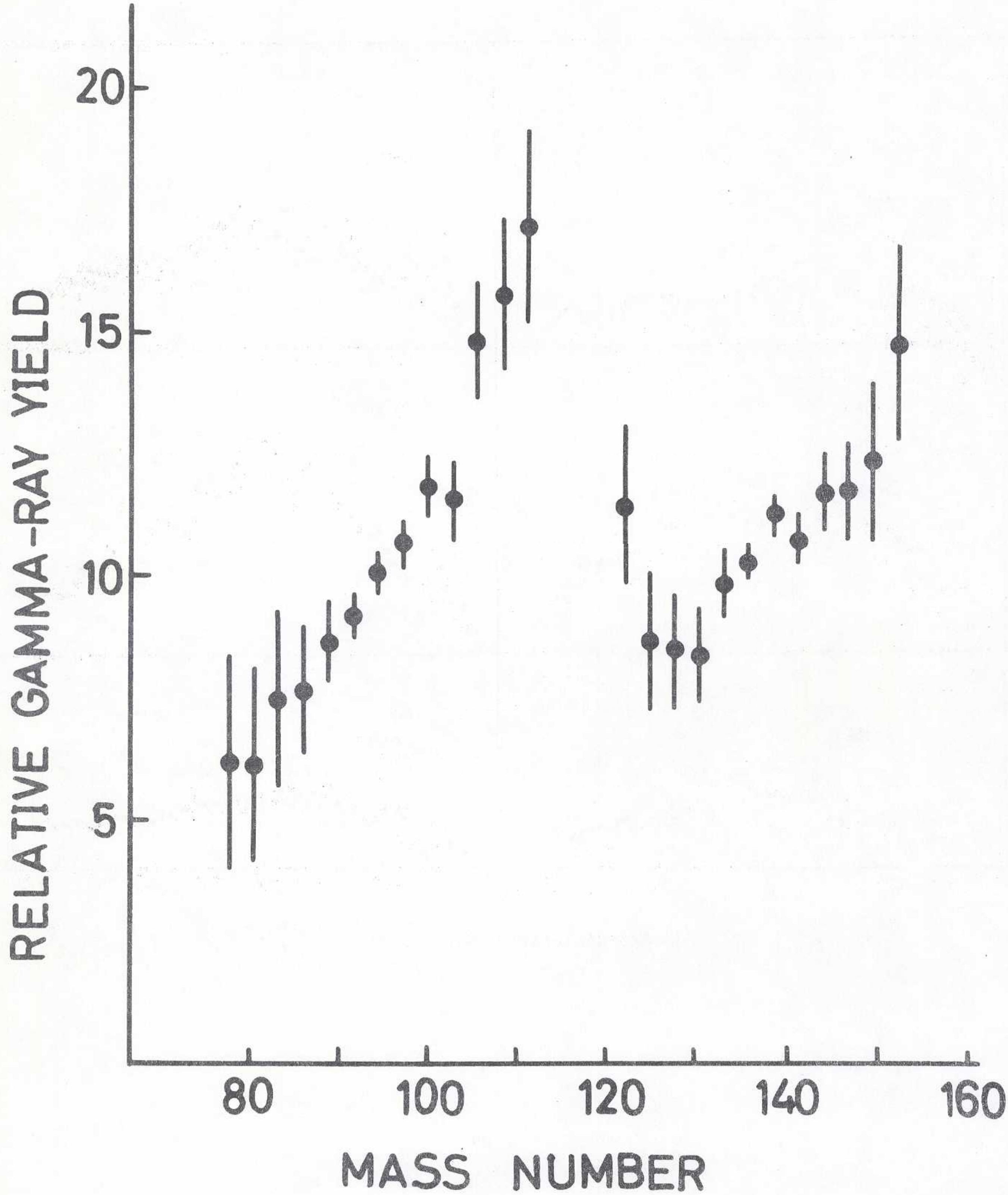
RELATIVE GAMMA-RAY YIELD
20
15
10
5
80
100
120
140
160
MASS NUMBER

Fig 14

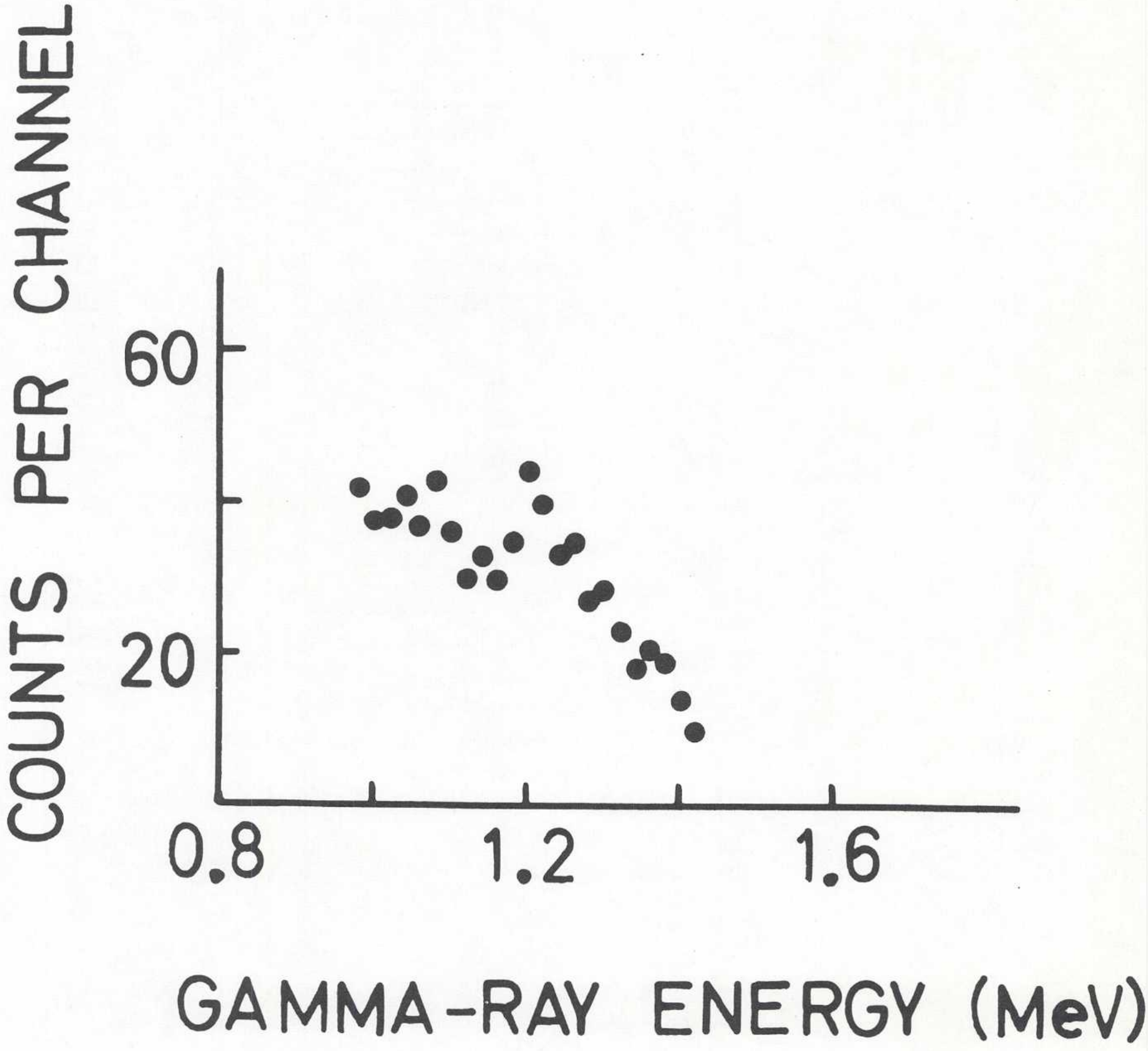

Fig 15

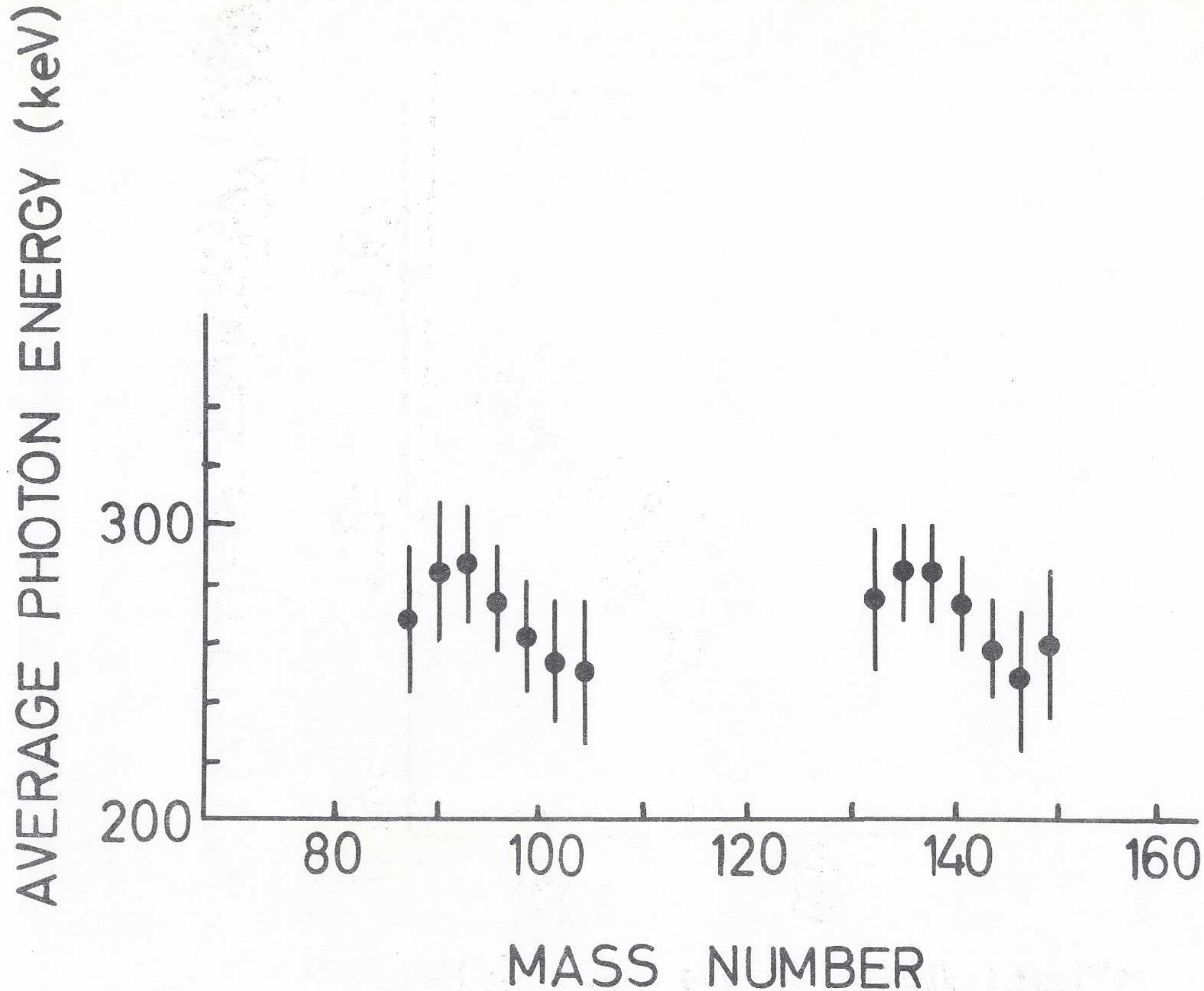
AVERAGE PHOTON ENERGY (keV)
300
200
80
100
120
140
160
MASS NUMBER

Fig 16

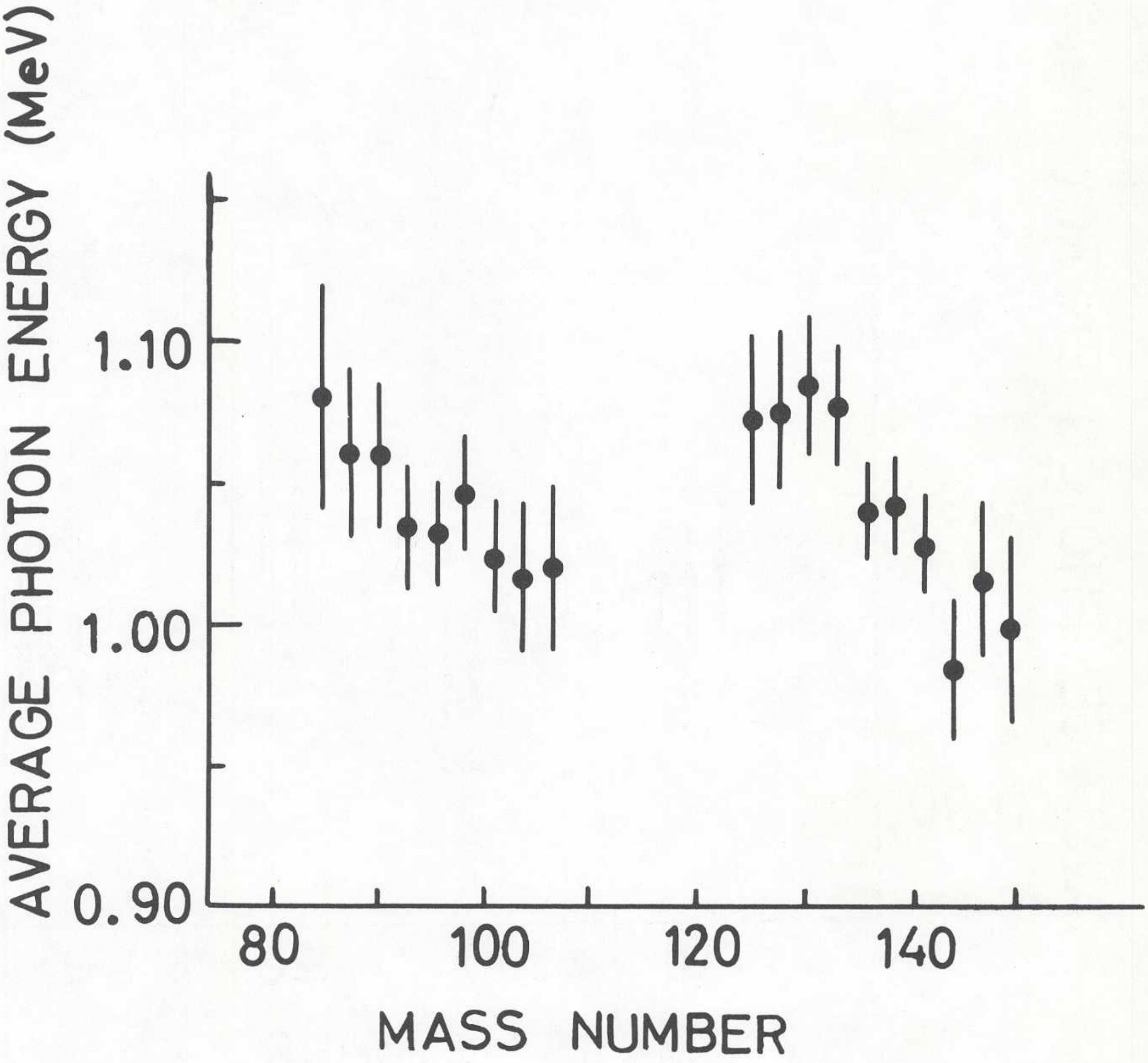

AVERAGE PHOTON ENERGY (MeV)
1.10
1.00
0.90
80
100
120
140
MASS NUMBER

Fig 17

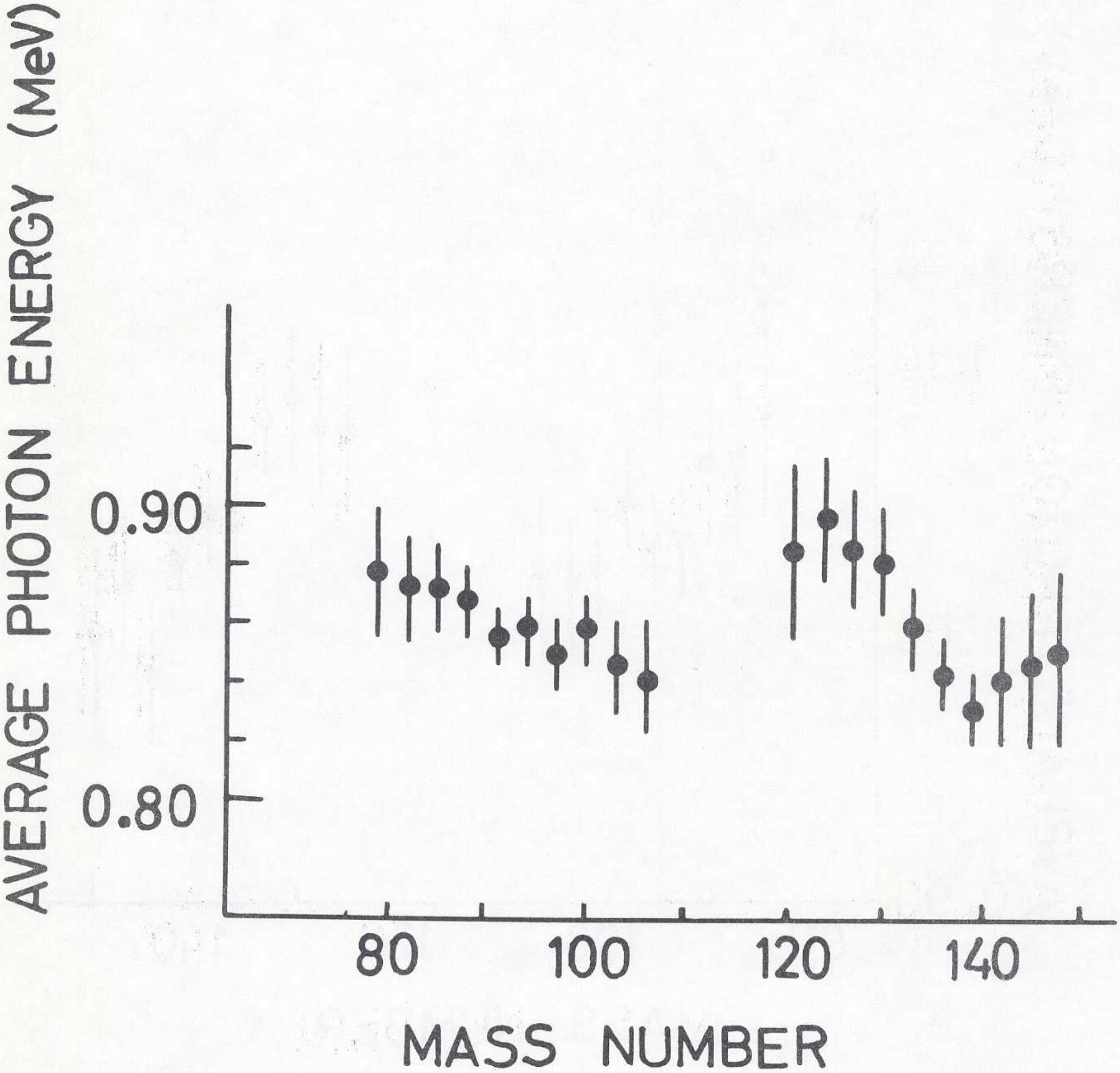

Fig 18

LIST OF PUBLISHED AE-REPORTS

1–350 (See back cover earlier repports.)

351. A determination of the 2 200 m/s absorption cross section and resonance integral of arsenic by pile oscillator technique. By E. K. Sokolowski and R. Bladh. 1969. 14 p. Sw. cr. 10:–.
352. The decay of ^{191}Os. By S. G. Malmskog and A. Bäcklin. 1969. 24 p. Sw. cr. 10:–.
353. Diffusion from a ground level point source experiment with thermoluminescence dosimeters and Kr 85 as tracer substance. By Ch. Gyllander, S. Hollman and U. Widemo. 1969. 23 p. Sw. cr. 10:–.
354. Progress report, FFN, October 1, – September 30, 1968. By T. Wiedling. 1969. 35 p. Sw. cr. 10:–.
355. Thermodynamic analysis of a supercritical mercury power cycle. By A S. Roberts, Jr. 1969. 25 p. Sw. cr. 10:–.
356. On the theory of compensation in lithium drifted semiconductor detectors By A. Lauber. 1969. 45 p. Sw. cr. 10:–.
357. Half-life measurements of levels in ^{75}As. By M. Höjeberg and S. G Malmskog. 1969. 14 p. Sw. cr. 10:–.
358. A non-linear digital computer model requiring short computation time for studies concerning the hydrodynamics of the BWR. By F. Reisch and G. Vayssier. 1969. 38 p. Sw. cr. 10:–.
359. Vanadium beta emission detectors for reactor in-core neutron monitoring. By I. Ö. Andersson and B. Söderlund. 1969. 26 p Sw. cr. 10:–
360. Progress report 1968. Nuclear chemistry. 1969. 38 p. Sw. cr. 10:–.
361. A half-life measurement of the 343.4 keV level in ^{175}Lu. By M. Höjeberg and S. G. Malmskog. 1969. 10 p. Sw. cr. 10:–.
362. The application of thermoluminescence dosimeters to studies of released activity distributions. By B-I. Rudén. 1969. 36 p. Sw. cr. 10:–.
363. Transition rates in ^{161}Dy. By V. Berg and S. G. Malmskog. 1969. 32 p Sw. cr. 10:–.
364. Control rod reactivity measurements in the Ågesta reactor with the pulsed neutron method. By K. Björeus. 1969. 44 p. Sw. cr. 10:–.
365. On phonons in simple metals II. Calculated dispersion curves in aluminium. By R. Johnson and A. Westin. 1969. 124 p. Sw. cr. 10:–.
366. Neutron elastic scattering cross sections. Experimental data and optical model cross section calculations. A compilation of neutron data from the Studsvik neutron physics laboratory. By B. Holmqvist and T. Wiedling. 1969. 212 p. Sw. cr. 10:–.
367. Gamma radiation from fission fragments. Experimental apparatus – mass spectrum resolution. By J. Higbie. 1969. 50 p. Sw. cr. 10:–.
368. Scandinavian radiation chemistry meeting, Studsvik and Stockholm, September 17–19, 1969. By H. Christensen. 1969. 34.p. Sw. cr. 10:–.
369. Report on the personnel dosimetry at AB Atomenergi during 1968. By J. Carlsson and T. Wahlberg. 1969 10 p. Sw. cr. 10:–.
370. Absolute transition rates in ^{188}Ir. By S. G. Malmskog and V. Berg. 1969. 16 p. Sw. cr. 10:–.
371. Transition probabilities in the 1/2+(631) Band in ^{235}U. By M. Höjeberg and S. G. Malmskog. 1969. 18 p. Sw. cr. 10:–.
372. E2 and M1 transition probabilities in odd mass Hg nuclei. By V. Berg, A Bäcklin, B. Fogelberg and S. G. Malmskog. 1969. 19 p. Sw. cr. 10:–.
373. An experimental study of the accuracy of compensation in lithium drifted germanium detectors. By A. Lauber and B. Malmsten. 1969. 25 p. Sw cr. 10:–.
374. Gamma radiation from fission fragments. By J. Higbie. 1969. 22 p. Sw. cr. 10:–.
375. Fast neutron elastic and inelastic scattering of vanadium. By B. Holmqvist, S. G. Johansson, G. Lodin and T. Wiedling. 1969. 48 p. Sw. cr. 10:–.
376. Experimental and theoretical dynamic study of the Ågesta nucler power station. By P. Å. Bliselius, H. Vollmer and F. Åkerhielm. 1969. 39 p Sw. cr. 10:–.
377. Studies of Redox equilibria at elevated temperatures 1. The estimation of equilibrium constants and standard potentials for aqueous systems up to 374°C. By D. Lewis. 1969. 47 p. Sw. cr. 10:–.
378. The whole body monitor HUGO II at Studsvik. Design and operation By L Devell, I. Nilsson and L. Venner. 1970. 26 p. Sw. cr. 10:–.
279. ATOMSPHERIC DIFFUSION. Investigations at Studsvik and Ågesta 1960–1963. By L-E. Hæggblom, Ch. Gyllander and U. Widemo. 1969. 91 p. Sw cr. 10:–.
380. An expansion method to unfold proton recoil spectra. By J. Kockum. 1970. 20 p. Sw. cr. 10:–.
381. The 93.54 keV lever ^{91}Sr, and evidence for 3-neutron states above N=50. By S. G. Malmskog and J. McDonald. 1970. 24 p. Sw. cr. 10:–.
382. The low energy level structure of ^{191}Ir. By S. G. Malmskog, V. Berg, A. Bäcklin and G Hedin. 1970. 24 p Sw cr. 10:–.
383. The drinking rate of fish in the Skagerack and the Baltic. By J. E. Larsson. 1970. 16 p. Sw. cr. 10:–.
384. Lattice dynamics of Nacl, KCl, RbCl and RbF. By G. Raunio and S. Rolandson. 1970. 26 p. Sw. cr. 10:–.
385. A neutron elastic scattering study of chromium, iron and nickel in the energy region 1.77 to 2.76 MeV. By B. Holmqvist, S. G. Johansson, G. Lodin, M Salama and T. Wiedling. 1970. 26 p. Sw. cr. 10:–.
386. The decay of bound isobaric analogue states in ^{28}Si and ^{32}Si using (d. nγ) reactions. By L. Nilsson, A Nilsson and I. Bergqvist. 1970. 34 p. Sw. cr. 10–.
387. Transition probabilities in ^{189}Os. By S. G. Malmskog, V. Berg and A. Bäcklin. 1970 40 p. Sw. cr. 10:–.
388. Cross sections for high-energy gamma transition from MeV neutron capture in ^{206}Pb. By I. Bergqvist, B. Lundberg and L. Nilsson. 1970. 16 p. Sw. cr. 10:–.
389. High-speed, automatic radiochemical separations for activation analysis in the biological and medical research laboratory. By K. Samsahl. 1970. 18 p. Sw. cr. 10:–.
390. Use of fission product Ru-106 gamma activity as a method for estimating the relative number of fission events in U-235 and Pu-239 in low-enriched fuel elements. By R. S. Forsyth and W. H. Blackadder. 1970. 26 p. Sw. cr. 10:–.
391. Half-life measurements in ^{134}I. By V. Berg and Å. Höglund. 1970. 16 p Sw. cr. 10:–.
392. Measurement of the neutron spectra in FRO cores 5, 9 and PuB-5 using resonance sandwich detectors. By T. L. Andersson and M. N. Qazi. 1970. 30 p. Sw. cr. 10:–.
393. A gamma scanner using a Ge(Li) semi-conductor detector with the possibility of operation in anti-coincidence mode. By R. S. Forsyth and W. H. Blackadder. 1970. 22 p. Sw. cr. 10:–.
394. A study of the 190 keV transition in ^{141}La. By B. Berg, Å. Höglund and B. Fogelberg. 1970 22 p. Sw cr. 10:–.
395. Magnetoacoustic waves and instabilities in a Hall-effect-dominiated plasma. By S. Palmgren 1970. 20 p Sw. cr. 10:–.
396. A new boron analysis method. By J. Weitman, N. Dåverhög and S. Farvolden. 1970 26 p. Sw. cr. 10:–.
397. Progress report 1969. Nuclear chemistry. 1970. 39 p. Sw. cr. 10:–.
398. Prompt gamma radiation from fragments in the thermal fission of ^{235}U. By H. Albinsson and L. Lindow. 1970. 48 p. Sw. cr. 10:–.
399. Analysis of pulsed source experiments performed in copper-reflected fast assemblies. By J. Kockum. 1970. 32 p. Sw. cr. 10:–.
400. Table of half-lives for excited nuclear levels. By S. G. Malmskog. 1970. 33 p. Sw. cr. 10:–.
401. Needle type solid state detectors for in vivo measurement of tracer activity. By A. Lauber, M. Wolgast. 1970. 43 p. Sw. cr. 10:–.
402. Application of pseudo-random signals to the Ågesta nuclear power station By P-Å. Bliselius. 1970. 30 p. Sw. cr. 10:–.
403. Studies of redox equilibria at elevated temperatures 2. An automatic divided-function autoclave and cell with flowing liquid junction for electrochemical measurements on aqueous systems. By. K. Johnsson, D Lewis and M. de Pourbaix. 1970. 38 p. Sw. cr. 10:–.
404. Reduction of noise in closed loop servo systems. By K. Nygaard. 1970. 23 p Sw. cr. 10:–
405. Spectral parameters in water-moderated lattices. A survey of experimental data with the aid of two-group formulae. By E. K. Sokolowski. 1970. 22 p. Sw. cr. 10:–.
406. The decay of optically thick helium plasmas, taking into account ionizing collisions between metastable atoms or molecules. By J. Stevefelt. 1970. 18 p. Sw. cr. 10:–.
407. Zooplankton from Lake Magelungen, Central Sweden 1960-63. By E. Almquist. 1970. 62 p. Sw. cr. 10:–.
408. A method for calculating the washout of elemental iodine by water sprays. By E Bachofner and R. Hesböl. 1970. 24 p. Sw. cr. 10:–.
409. X-ray powder diffraction with Guinier–Hägg focusing cameras. By A. Brown. 1970. 102 p. Sw. cr. 10:–.
410. General physic section Progress report. Fiscal year 1969/70. By J. Braun. 1970. 92 p. Sw. cr. 10:–.
411. In-pile determination of the thermal conductivity of UO_2 in the range 500–2 500 degrees centigrade. By J-Å Gyllander. 1971. 70 p. Sw. cr. 10:–.
412. A study of the ring test for determination of transverse ductility of fuel element canning. By G. Anevi and G. Östberg. 1971. 17 p. Sw. cr. 15:–.
413. Pulse radiolysis of Aqueous Solutions of aniline and substituted anilines. By H. C. Christensen. 1971. 40 p. Sw. cr. 15:–.
414. Radiolysis of aqueous toluene solutions. By H. C. Christensen and R. Gustafson. 1971. 20 p. Sw. cr. 15:–.
415. The influence of powder characteristics on process and product parameters in UO_2 pelletization. By U. Runfors. 1971. 32 p. Sw. cr. 15:–.
416. Quantitative assay of Pu239 and Pu240 by neutron transmission measurements. By E. Johansson. 1971. 26 p. Sw. cr 15:–.
417. Yield of prompt gamma radiation in slow-neutron induced fission of ^{235}U as a function of the total fragment kinetic energy. By H. Albinsson. 1971. 38 p. Sw. cr. 15:–.
418. Measurements of the spectral light emission from decaying high pressure helium plasmas. By J. Stevefelt and J. Johansson. 1971. 48 p. Sw. cr. 15:–.
419. Progress report 1970. Nuclear chemistry. 1971. 32 p. Sw. cr. 15:–.
420. Energies and yields of prompt gamma rays from fragments in slow-neutron induced fission of ^{235}U. By H. Albinsson. 1971. 56 p. Sw. cr. 15:–.

List of published AES-reports (In Swedish)

1. Analysis by means of gamma spectrometry. By D. Brune. 1961. 10 p. Sw. cr. 6:–.
2. Irradiation changes and neutron atmosphere in reactor pressure vessels-some points of view. By M. Grounes 1962. 33 p. Sw. cr. 6:–.
3. Study of the elongation limit in mild steel. By G. Östberg and R. Attermo. 1963. 17 p. Sw cr. 6:–.
4. Technical purchasing in the reactor field. By Erik Jonson. 1963. 64 p. Sw. cr. 8:–.
5. Ågesta nuclear power station. Summary of technical data, descriptions, etc for the reactor. By B. Lilliehöök. 1964. 336 p. Sw. cr. 15:–.
6. Atom Day 1965. Summary of lectures and discussions. By S. Sandström. 1966 321 p. Sw. cr. 15:–.
7. Building materials containing radium considered from the radiation protection point of view. By Stig O. W. Bergström and Tor Wahlberg. 1967. 26 p. Sw. cr. 10:–

Additional copies available from the Library of AB Atomenergi, Fack, S-611 01 Nyköping 1, Sweden.

EOS-tryckerierna, Stockholm 1971

AE-417

AE - 417

UDC 539.166.08
539.122.164
539.173.4.162.2

Yield of Prompt Gamma Radiation in Slow-Neutron Induced Fission of ^{235}U as a Function of the Total Fragment Kinetic Energy

H. Albinsson

AKTIEBOLAGET ATOMENERGI

STUDSVIK, NYKÖPING, SWEDEN 1971

YIELD OF PROMPT GAMMA RADIATION IN SLOW-NEUTRON INDUCED FISSION OF ^{235}U AS A FUNCTION OF THE TOTAL FRAGMENT KINETIC ENERGY

H Albinsson*

ABSTRACT

Fission gamma radiation yields as functions of the total fragment kinetic energy were obtained for ^{235}U thermal-neutron induced fission. The fragments were detected with silicon surface-barrier detectors and the gamma radiation with a NaI(Tl) scintillator. In some of the measurements mass selection was used so that the gamma radiation could also be measured as a function of fragment mass. Time discrimination between the fission gammas and the prompt neutrons released in the fission process was employed to reduce the background. The gamma radiation emitted during different time intervals after the fission event was studied with the help of a collimator, the position of which was changed along the path of the fission fragments.

Fission-neutron and gamma-ray data of previous experiments were used for comparisons of the yields, and estimates were made of the variation of the prompt gamma-ray energy with the total fragment kinetic energy.

*Chalmers University of Technology, Gothenburg

LIST OF CONTENTS

1. INTRODUCTION

Experiments on nuclear fission can give a variety of information on many aspects of nuclear structure. One of the main reasons for performing the present experiments on ^{235}U was to obtain a better understanding of the energy balance of this process. A fissioning nucleus contains a certain amount of energy, which will be shared between the kinetic and the excitation energies of the fragments. The release of the fission gamma radiation, like the release of the prompt neutrons, is a measure of part of the excitation energy in the fragments. A study of the prompt fission gamma radiation as a function of the total kinetic energies of the fragments can give information regarding the energy balance in the fission process. Very few experiments have so far been tried along this line (1 - 5).

A big computer is most suitable as a data recording system when simultaneously collecting information on the following three parameters: the kinetic energies of each of the two fragments in a binary fission event and the associated gamma-ray energy. The computer can be programmed to calculate the fragment masses and the total kinetic energy of this fission event. However, a three-parameter data recording system was not available in the present study, only a two-parameter analyzer; but by choosing the measured conditions in certain ways it was not necessary to suffer too much from the limitations of the data system.

The present report is a preliminary survey of one aspect of a larger project for study of prompt fission gamma radiation as a function of mass and time after fission. As few similar measurements (2 - 4) have previously been reported, one of which appeared recently and was not known to us before this investigation was undertaken, it was felt that this preliminary study would be of interest. All previous investigations suffer from the same weakness, namely that of using an incomplete mass separation. When fission gamma radiation is recorded in coincidence with the fragments, one can never with certainty state which of the two fragments has emitted the detected photon unless one can discriminate between the fragments, for instance by use of a collimator. Thus, a mass divider circuit arrangement can only be used with full efficiency in fission gamma radiation studies when a collimator is incorporated. Without using a collimator, the gamma radiation is studied as a function of the mass ratio; and even if it is possible to obtain information on certain gammas as a function of fragment mass, by use of an unfolding technique in the analysis, the results must be uncertain and contain considerable errors.

2. EXPERIMENTAL ARRANGEMENT

Fig. 1 shows a block schematic of the electronics used in this experiment. The details of the design and the system performance have been discussed previously (6), and so only some of the specific features of this set-up will be described briefly.

The fissile deposit was 1 cm^2 in area and was prepared by electrodeposition on 100 $\mu g/cm^2$ nickel foils. The thickness of the uranium layer was about 100 $\mu g/cm^2$ in order to allow measurements of mass spectra with acceptable resolution. Two solid state detectors of the surface barrier type were placed in parallel and symmetrically around the foil to measure the energies of the fission fragments. The detectors* were about 4 cm^2 in area, fabricated from 400 ohmcm n-type silicon and operated at about 70 V bias. The distance between each detector and the fissile foil

* Type C7904 Heavy Ion Detectors supplied by ORTEC, Oak Ridge, Tenn., USA

was 2 cm. The gamma detector was a NaI(Tl) scintillator, 10.4 cm long and 13.0 cm in diameter, viewed by a Philips XP 1040 photomultiplier tube. The associated electronics, consisting of a pulse-shaping unit and a discriminator, was coupled directly to the photomultiplier tube socket and gave a fast leading-edge time pulse and a linear pulse.

Pulses from the solid state detectors were amplified in charge sensitive preamplifiers followed by linear amplifiers. The amplified pulses were then fed into a summing amplifier. Depending on the type of experiment the pulses could also be fed into the divider circuit in order to record mass spectra.

Apart from the time interval which is fixed with each collimator setting, there are three basic parameters involved in these measurements, viz. fragments mass, total kinetic energy of the fragments, and the gamma-ray energy. Two types of measurements were performed: 1) gamma-ray energy spectra in coincidence with the total kinetic energy of the fragments, and 2) a two-parameter study of fragment mass and the total kinetic energy associated with gamma rays of energies above a certain threshold.

The data recording system was the same as in ref. 6, namely a two-parameter analyzer, the memory of which was that of a small computer, PDP-8/S.

3. RESULTS

The first measurement in the present work was done without the gamma collimator and in a gamma-ray energy range of 0 - 2 MeV. The yield of photons with energies less than about 2 MeV as a function of the total kinetic energy is a smooth function, decreasing slowly with total kinetic energy (fig. 2). The shape of the curve did not change noticeably for more limited gamma energy ranges.

The ensuing measurements dealt with practically all the prompt gamma radiation except that within about 10^{-11} s, after the fission event which is found to be of similar type for all fragments (7). As the fission gamma radiation intensity within this time interval is less than 30% of all the prompt gamma radiation (8), a considerable part of the radiation is thus studied. The radiation with half-lives of more than 10^{-11} s, on the other hand, varies greatly from mass to mass as regards the half-life, intensity and average photon energy. The measurement was performed with the gamma collimator placed so as just to "shadow" the foil. The yield of photons with energies less than about 2 MeV as a function of the total kinetic energy was very similar to that in the first case (fig. 3).

As there was no three-parameter data acquisition system available it was not possible to record simultaneously the energy of the prompt fission gamma radiation associated both with the fragment mass and with the sum of the fragment kinetic energy. One measurement, however, was made over a few days in which the total fragment kinetic energies were recorded as a function of the mass spectrum and in coincidence with the fission gamma radiation, but the variation with gamma-ray energy was not included. The yield of photons as a function of fragment mass and total kinetic energy is presented in the contour diagram in fig. 4. The statistics is not overwhelming, but a clear structure can be seen, similar to the one obtained when studying the yield of fragments as a function of the fragment mass and the total kinetic energy.

From the contour diagram relative yield curves of two types were obtained. They came out as cuts in the diagram parallel to the respective axes and they are 1) the relative yield of prompt photons as a function of fragment mass for a certain total kinetic energy interval, and 2) the relative yield of prompt photons as a function of the total kinetic energy with certain fragment-mass regions as parameters. The two sets of yield curves are shown in fig. 5 and 6. In fig. 7 and 8 are presented the integrated relative yield curves. The saw-tooth type curve in fig. 7 is not so well demonstrated as one would expect. The yield of the heaviest fragments in the light mass group is lower than would be expected from earlier fission gamma-ray studied (6, 9). In fig. 8 the yield curve seems to decrease less with increasing total kinetic energy than the yield curve in fig. 2.

In fig. 9 is shown a calibration curve of the total fragment kinetic energy as a function of fragment mass. The measurement was performed as a two-parameter recording of events where fragment mass was one parameter and the total kinetic energy the other. For each mass the location of the peak value in the total kinetic energy curve has been plotted and fig. 9 shows the distribution around the heavy fragment group only, as the distribution is of course symmetric around mass number 118. The difference in the average total kinetic energy, between symmetric fission and the fission in which the heavy fragment has a mass number around 130, is about 24 MeV. This value must be considered to be in good agreement with the latest data from other laboratories. A list of such values is given in Table 1. .

The signal-to-background ratio in the measurements presented in figs. 4 - 8, as determined in the time-of-flight spectra from the NaI scintillator, was less than 15%. This is the average value with no reference to the gamma-ray energy. The signal-to-background ratio improves with increasing gamma-ray energy, and as an example it may be mentioned that it improves by about a factor of two when the gamma-ray energy is changed from 0.4 to2.0 MeV (7). The signal-to-background ratio for the uncollimated gamma radiation (fig. 2) was less than 1 % (6).

4. DISCUSSION

4.1. General

The total kinetic energy of the fragments in uranium fission as a function of the heavy mass group has, as is well known, low values for symmetric and very asymmetric fission. The behaviour of this function can be understood on the basis of the model introduced by Vandenbosch (19) in which the rigidity of the fragments is an important parameter. This model has been fully described in Vandenbosch's paper and only some of the most important features of it will be mentioned here.

One of the assumptions in fission theory is that the excitation energy of the fragments just after scission is tied up in the form of deformation. A rigid fragment, i.e. a fragment having closed or almost closed nucleon shells, is not able to take up so much deformation energy as mid-shell fragments. If a certain fission event results in two rigid (spherical) fragments one assumes that after scission the acceleration in their mutual Coulomb field starts, as their centres are at a distance of about the sum of the two radii from each other. A fission event may result in both fragments being less rigid (more deformed) than in the previous case. After the break-up of the fissioning nucleus the fragments are probably elongated, and they will start their acceleration with their respective centres further away from each other than the spherical fragments will do. The spherical fragments will acquire more kinetic energy than the deformed ones, but on the other hand the deformed fragments will obtain more excitation energy in the form of deformation. As one studies all fragments along a fission mass spectrum, all possible energy combinations between these two extremes will appear. The model is presented here in a simplified form to give a physical outline of it, though a better description, of course, includes such sophisticated features as the acceleration of the fragments before the rupture of the neck between the fragments has taken place.

4.2. The total fragment kinetic energy distribution

The study of the properties of the prompt neutron and gamma emission as a function of the sum of the fragment kinetic energy may cast some light on the way in which the different forms of energy are distributed in fission, and thus be a way to test the Vandenbosch model. The discussion must, however, start on the basis of what is known about the distribution of the sum of the fragment kinetic energy as a function of fragment mass. This distribution has its lowest values for symmetric and very asymmetric uranium fission, while in californium fission the same distribution has decreasing values as the asymmetry increases. Symmetric fission in californium results in two rigid fragments ($A \approx 126$), while in uranium the two fragments are less rigid ($A \approx 118$). As the two distributions are "mirrored" around the respective symmetric fission, it is enough to study them around the heavy mass peak. The values for uranium fission increase as one approaches the mass number 132 ($Z \approx 51$, $N \approx 81$) and then decrease.

The dip in the average total kinetic energy curve in fig. 9, i.e. the difference in the total kinetic energy at maximum and at symmetric fission, is 24 MeV. This value is somewhat higher than 21.2 MeV reported by Signarbieux et al. (17), 21 MeV reported by Apalin et al. (14), but in good agreement with 24 MeV by Schmitt et al. (16). Apalin et al. and

Maslin et al. (18) discussed their respective results in some detail, and came to the conclusions that some of their "spurious" events for symmetric fission must be deleted, giving the respective results of 21 and 22 MeV. Signarbieux et al., on the other hand, used a different measuring method in which the velocities of the fragments were included as an additional parameter and which eliminated some of the difficulties introduced by false events in the symmetric fission.

It should be emphasized that even though a well established value of the energy dip is in itself a measure of the quality of the experiment, it is not very important when fission gamma radiation is studied. The measured intensity of the gamma radiation is often decreased by an order of magnitude or more when using than when not using a collimator, and consequently very few events are recorded for symmetric fission in the collimator case (6). The number of these events is in fact so few that it is very seldom possible to use them in the final analysis.

4.3. The prompt photon yield as a function of the total fragment kinetic energy

Measurements of the prompt gamma radiation as a function of the total fragment kinetic energy has not yet received much interest. Four reports have been made of studies of the thermal fission of ^{235}U (1 - 3, 5) and one of the spontaneous fission of ^{252}Cf (4). Papers 3 and 4 became known while the present paper was being prepared for publication. As far as the study of K X-rays associated with the total fragment kinetic energy is concerned (5), it gives some additional information about the type of gamma radiation mainly involved.

The fission gamma radiation studied earlier (1 - 4) has been recorded without the use of a gamma collimator and consequently all prompt gamma rays have been recorded. A yield function obtained in such a way may be expected to be very different from the one obtained for a specific time interval. This was also noticed when the relative number of prompt photons as a function of fragment mass was investigated. The same gamma radiation is involved in both cases, giving rise to a certain type of yield as a function of fragment mass, and this must also mean that there should exist a related yield as a function of the total kinetic energy, as the two quantities, mass and kinetic energy, are interrelated.

The yield function in fig. 2 resembles that of prompt neutrons as a function of the total fragment kinetic energy. This resemblance can be understood on the basis of the similarity between the prompt neutron and the prompt photon yields as functions of fragment mass, and if the underlying arguments are accepted (19). Fig. 2 shows the yield of the uncollimated radiation. No observable fine structure is present, but only a smooth variation with the total fragment kinetic energy. Fig. 3 looks the same as fig. 2 for the greater part of the studied kinetic energy region. This is remarkable in view of the fact that the radiation studied in fig. 3 concerns the part of the total prompt gamma radiation between 30 and 75 % in the accumulated yield curve (8) according to the collimator setting in section 3 of the present paper. However, if the mass-dependent photon yield curves are "folded" around the respective symmetric fission mass numbers, added up, and then plotted as a function of the heavy mass group, one may assume that the fine structure of the original functions would probably be smoothed out. This smoothing out would be due to the fact that the low yields in one of the mass groups would often be balanced by high yields from the partner fragment. A three-parameter study is therefore of very great value, viz. a study of mass, total kinetic energy of the fragments, and the associated gamma-ray energy.

In fig. 4 is plotted the variation of the prompt photon yield as a function both of total fragment kinetic energy and of fragment mass. As mentioned earlier one important parameter, the gamma-ray energy, is missing. Even though this parameter is essential when discussing the total energy release, in the form of gamma radiation from fragments, one can do without it in the first approximation if the studied time interval after fission is chosen as close as possible to the scission time. As discussed earlier (6, 21), the "first" photons are of similar energy for all fragments and their respective numbers are proportional to the energy release by gamma radiation.

The curves of the relative yields in fig. 5 and 6 look different from the yield curves of prompt photons as functions of fragment mass and total fragment kinetic energy, respectively, and therefore figs. 5 and 6 deserve some extra attention.

In order to test the over-all functioning of the experiment, the respective integrated yield curves were calculated, the results of which are presented in figs. 7 and 8. There is no drastic difference in these curves as compared to previous ones. One noticeable result in fig. 7 which differs from those of earlier measurements is that the yield from the heaviest light fragment may be unusually low. It must be pointed out, however, that the absolute yields in this mass region were low and consequently beset with large errors. Another feature which is not so well established in this curve, but has been found previously (6), is the decrease in yield for mass numbers above 150. This last point is, however, not so important, as the collimator slit width is wider than used in (6). So the general trend of the relative photon yield as a function of fragment mass is, on the whole, as would be expected from the earlier reported measurements.

As regards the relative yield of the prompt photons as a function of the total fragment kinetic energy (fig. 8), the only data available for comparison are those of figs. 2 and 3 of this work. They are the only measurements in which a gamma collimator has been used. Once again it may be said that no significant differences are observable.

The curves in fig. 5 are interesting from many points of view. First of all they show no similarity with the saw-tooth curve as does the relative yield of prompt photons as a function of fragment mass. Recently a study of the prompt neutron emission from ^{235}U fission fragments has been reported (18) which very clearly demonstrated the saw-tooth curve for the yield of all neutrons, and also the same characteristics when different total kinetic energy groups were considered. Very typical of all these curves was that the first half of the saw-tooth stood out clearly. One might then expect that a similar feature would appear in the yield curves from the present experiment, but it does not. This expectation, however, may be based on too far-reaching conclusions of the similarities in some of the properties of prompt neutrons and prompt photons.

Fig. 5 shows readily that the highest excitations are found in the asymmetric fission fragments, when the total fragment kinetic energy is low, and that the maximum of the relative yield of prompt photons comes from more symmetric fission fragments as the total kinetic energy increases. Unfortunately the statistics in the yield from light fragments with mass numbers above 108 is too low to give a fair detailed curve in this mass region, but it would be interesting to know whether those fragments contribute significantly when the total kinetic energy is below 160 MeV. In the lowest energy region, below 151 MeV, there is a very distinct difference between the yields from fragments formed in symmetric and very asymmetric fission. The fragment yield in this energy region is low, though it is easily measurable, but the coincident gamma rays in the present time interval are very few. The photon yield from fragments with mass numbers around 132 is very low, and when a fission event of this type takes place, viz. fragments with A = 132 and 104, these fragments are resistant to deformation, especially the heavy one, and so little excitation energy will be gained (19). It is interesting to notice that in the fission mode resulting in the fragment pair, $A \approx 80$ and $A \approx 156$, the heavy partner has released many more photons than the light one; and if the gamma-ray energies are not too different, this means that the heavy partner has gained far more excitation energy than the light one. It is known that the heavy fragment is easily deformable, and may even be deformed in its ground state. This directly reflects the same situation as was observed in the study of prompt neutron and prompt photon yields as functions of fragment mass.

Turning to the other extreme energy region, i.e. for the total kinetic energy above 192 MeV, fragments with mass numbers around 132 and their associate partners are studied. The prompt photon yield as a function of fragment mass demonstrates that only these fragments were excited, and once again it is clear that most of the energy has been imparted to the light fragment, which is in accordance with earlier observations of the prompt neutron and the prompt photon yields.

In general all the yield curves in fig. 5 fit into the above-mentioned description.

Fig. 6 needs no specific explanation, as it is in agreement with fig. 5 and the discussion relating to it. The two figures are, of course, interrelated, so there should not be any significant discrepancy between the underlying assumptions for their explanations.

4.4. Comparisons with earlier reported neutron and gamma yields in fission

Unfortunately there exist only few data of the prompt photon yield as a function of the total fragment kinetic energy. K X-rays in coincidence with the total kinetic energy from thermal fission of ^{235}U have been studied (5), but not in ^{252}Cf fission. K X-rays and conversion electrons from ^{252}Cf fission should be possible to study and would give new and interesting information about the decays of fission fragments.

The prompt neutron distribution as a function of the total fragment kinetic energy has been studied by some physicists (18, 22). All results are in agreement with one another and can be explained on the basis of the Vandenbosch model (19) outlined above.

Figs. 2, 3 and 8 do not show any significant increase in photon yield as the total kinetic energy decreases below 150 MeV. On the contrary fig. 2 shows a plateau around 150 - 169 MeV. This result is in contradiction to the one shown in fig. 1 of ref. (2). The reason for this discrepancy is not understood and more work is needed to clarify the situation.

For comparison, one can again study experimental results on the prompt neutron emission from fission fragments (18). It is hard to find any significant increase in the neutron yield when the total fragment kinetic energy decreases below 150 MeV. Instead, the neutron yield shows a decrease when the total kinetic energy decreases from about 150 to 135 MeV where a plateau is reached (18).

On the basis of energy considerations, a fission mode resulting in two fragments with their total kinetic energy as low as 150 MeV or less must signify very asymmetric fission. In the contour diagram in fig. 4 there are very few gamma events from symmetric fission in a total kinetic energy region below 150 MeV. From fig. 5 a it can be seen that the heavy fragment has carried most of the available excitation energy and the reason for this has already been discussed. The point is, however, that when the total fragment kinetic energy has values below about 155 MeV the fission is very asymmetric. The lightest fragments have very low excitation energies and thus low prompt neutron and prompt photon yields. The heaviest fragments, on the other hand, are highly excited, but in the studies of prompt photon yields one must take into account the effect of the gamma collimator. The heaviest fragments have been found to be slow gamma emitters and, by using a particular collimator setting, one may prevent a great deal of the gamma radiation from being detected. Maslin et al. (18) suspected the possibility of deletion of some of their recorded events from symmetric fission, on the grounds that they corresponded to energy degradation, although the cause of the degraded energy remained uncertain. The data of Schmitt et al. (16), however, support their idea.

Blinov et al. (23) have recently studied the dependence of the anisotropy of fission neutron emission on the total kinetic energy of the fragments in the fission of ^{235}U by thermal neutrons. They came to the conclusion that, as the total kinetic energy is made larger, an increased part of the emission of neutrons may take place at the instant of fission, and the number of "evaporated" neutrons from the fragments may amount to about only one half of the number of neutrons emitted at a total kinetic energy of 190 MeV. Maslin et al. (18) made no distinction in their work between "scission" and "fragment" neutrons. If their yields of neutrons, emitted by fragments in near-symmetric fisssion and at high total kinetic energies, were to be divided by two to get the actual number of "fragment" neutrons emitted, there would be no more than 0.2 - 0.3 neutron from each fragment. This is a very low number. From figs. 6c and 6d in the present work it can be roughly estimated that 1.5 - 2 photons are emitted at a total kinetic energy of about 190 MeV. The total gamma-ray energy released is therefore about 1 - 1.5 MeV. The slopes of curves 6c and 6d are opposite to those for neutron emission (18). The reason for this discrepancy may simply be that at these high total kinetic energies there is a small amount of excitation energy available. Moreover, the fragments in the mass region 119 - 132 are quite stiff and the total excitation energy may be around or even below the neutron threshold, and so gamma emission will compete favourably with neutron emission. As regards the light partner in this fission mode, it is more susceptible to deformation, but nevertheless it may have acquired a rather low excitation energy. Both more neutrons and more photons are emitted at a total kinetic energy of 190 MeV than from the heavy fragment, but the total excitation energy may still be so low that gamma emission is a strong competitor for neutron emission also from the light fragments.

In another recent work (24) Armbruster et al. have experimently verified that the initial spin distribution of the fragments depends on the mass value and strongly increases in both mass groups. In the case of near-symmetric fission the light fragment may have a value of ten units of angular momentum, whereas the heavy fragment has only five units. This fact will at least not be in contradiction but support the arguments about the neutron and photon yields in near-symmetric fission when the total kinetic energy is high. The light fragment is able to have more initial excitation energy and, even if it may be excited to an energy well above the neutron threshold, the initial spin value of the fragment may be a hindering factor for neutron emission.

To sum up the situation as regards the differences in the prompt photon yields for low total fragment kinetic energies as obtained in the present investigation and in that by Val'skii et al., some experimental results from prompt neutron yields are in support of ours, but further experiments are needed.

The available data from the K X-ray yield as a function of the total fragment kinetic energy in ^{235}U fission cannot be used to compare the results of this report, because even if the K X-ray yield function provides a test of the excitation energy of the fragments, the internal conversion must also be considered.

To clarify the situation involved in fission giving rise to low total kinetic energies, data from ^{233}U, ^{239}Pu, and ^{252}Cf fission are desirable to see whether any possible variation with mass and related total fragment kinetic energies can be found. The study of fragments in the mass region A = 115 - 135 is in itself very interesting, because depending on the fissile nuclei used, one may get certain fragments which derive from symmetric fission in one case and from asymmetric fission in another. The excitations of the fragments will differ according to whichever heavy (or light) partner fragment is involved.

4.5. Estimate of the variations of the prompt gamma-ray energy with the total fragment kinetic energy

Val'skii et al. (24) calculated the quantity

$$\frac{dE_{\gamma}}{dE_K} \cdot \frac{1}{E_{\gamma,tot}}$$

where E_{γ} is the average energy of the prompt gamma rays from fission, E_K is the total fragment kinetic energy and $E_{\gamma,tot}$ is the total energy release of prompt gamma rays. In the case of uranium fission they obtained a value of - 0.0097 MeV^{-1}, whereas the present investigation gives - 0.0084 MeV^{-1}, which is within the uncertainty reported by Val'skii et al. The corresponding value from the study of californium fission is - 0.0075 MeV^{-1}.

The quantity

$$\frac{dE_{\gamma}}{dE_K}$$

is equal to - 0.068 in the present experiment and is a measure of the rate of decrease in gamma-ray energy with the increase in total fragment kinetic energy. This last quantity is more correct to use in comparisons between data from fissile nuclei which differ in total number of prompt photons. Unfortunately this matter is not discussed by Val'skii et al. (2, 4).

$$\frac{dE_{\gamma}}{dE_K} \cdot \frac{1}{E_{\gamma,tot}}$$

on the other hand is a measure of the change in energy of the respective photons with change in total kinetic energy.

The total gamma-ray energy decrease when the total fragment kinetic energy is increased from 160 to 200 MeV is about 2.7 MeV. A rough calculation of the error of this value indicates that it should not exceed 0.4 MeV. A more precise determination of the error must wait till more data are available on the numbers and energies of the photons in the different fission modes. One may argue that the present experiment has not revealed any possible change or lack of change in the average energy per photon. It is known, however, that a fission event resulting in such large total kinetic energies has resulted in a fragment pair with mass numbers around 110 and 126. According to Maier-Leibnitz et al. (9) this fission mode does not have any particularly large values of the total gamma-ray energy, and the number of photons both from the light and the heavy fragment is not unusual either. So it is reasonable to think that there is an energy decrease per fission event in the form of gamma-rays of about 2.5 MeV when the total fragment kinetic energy has increased by 40 MeV.

Unfortunately there are no new data of this type from ^{252}Cf fission, except one by Milton and Fraser (11), which is - 0.0029 MeV^{-1}, in fair agreement with the calculated value of - 0.0042 MeV^{-1} by Leachman and Kazek (25). Both these values, however, seem to be doubtful, as they use $E_{\gamma, tot}$ = 4.0 MeV, which is much lower than the measured values of around 9 MeV (8).

5. CONCLUSIONS

When studying the literature covering prompt fission gamma radiation, it is a great surprise to find how little has been done so far to investigate the contributions to the energy balance of the fissioning nuclei. Preliminary measurements of these kinds are among the easiest that can be undertaken on fission gamma radiation and are as follows:

1. two-parameter recordings of the fragment mass and the total fragment kinetic energies in coincidence with the uncollimated fission gamma radiation and
2. two-parameter recordings of the total fragment kinetic energy and the gamma-ray energy spectrum in coincidence with the uncollimated fission gamma radiation.

These preliminary studies concern properties of the mass ratio, as the gamma radiation is not collimated and one cannot directly tell which of the two fragment in a fission event has emitted the recorded photon.

The energy release in the form of fission gamma radiation is a quantity of great interest in the study of the energy balance of the fissioning nuclei. In order to obtain a measure of the total energy, the assumption has often been made that the total gamma-ray energy of the fragment is one half of the binding energy of the first neutron not emitted after the prompt neutrons (16, 26, 27). This assumption may be reasonable, but it is not satisfactory that a direct measurement has not been tried. Even though a result of the total gamma-ray energy will be beset with large errors, it will nevertheless be less uncertain than the assumption mentioned above, and it will probably also show better how the energy varies with the mass ratio.

ACKNOWLEDGEMENTS

The author is greatly indebted to Professor S. Johansson for his support of the present work and the enlightening discussion of the results. It is also a pleasure to thank Professor N. Ryde and Dr. T. Wiedling for their great interest and continued support.

REFERENCES

1. VAL'SKII G V, PETROV G A and PLEVA Yu S,
Dependence of the γ radiation anisotropy at the thermal neutron fission of ^{235}U on the fragment mass ratio.
Soviet J. Nucl. Phys. 5 (1967) p. 521.

2. VAL'SKII G V, PETROV G A and PLEVA Yu S,
Anisotropy of γ radiation in slow-neutron fission of U^{235}, as a function of fragment combined kinetic energy and mass ratio.
Soviet J. Nucl. Phys. 8 (1969) p. 171.

3. IVANOV O I, KUSHNIR Yu A and SMIRENKIN G N,
Angular anisotropy of gamma quanta and kinetic energy of fission fragments.
JETP Lett. 6 (1967) p. 327.

4. VAL'SKII G V et al.,
Some characteristics of the γ radiation accompanying fission of Cf^{252}.
Soviet J. Nucl. Phys. 10 (1969) p. 137.

5. BOHN E M, WEHRING B W and WYMAN M E,
Prompt K X-rays as a function of fragment mass and total kinetic energy in the thermal fission of U^{235}.
Phys. Rev. 188 (1969) p. 1909.

6. ALBINSSON H and LINDOW L,
Prompt gamma radiation from fragments in the thermal fission of ^{235}U.
AB Atomenergi, Sweden, 1970.
(AE-398).

7. ALBINSSON H,
To be published.

8. MAIER-LEIBNITZ H, ARMBRUSTER P and SPECHT H J,
Prompt and delayed gamma-rays from fission.
Physics and chemistry of fission.
Proc. of a symp. Salzburg, 22 - 26 March 1965. (IAEA) Vienna, 1965. Vol. 2, p. 113.

9. MAIER-LEIBNITZ H, SCHMITT H W and ARMBRUSTER P,
Average number and energy of gamma-rays emitted as a function of fragment mass in U^{235} thermal-neutron-induced fission.
Physics and chemistry of fission.
Proc. of a symp. Salzburg, 22 - 26 March 1965. (IAEA) Vienna, 1965. Vol. 2, p. 143.

10. NIDAY J B,
Radiochemical study of the ranges in metallic uranium of the fragments from thermal neutron fission.
Phys. Rev. 121 (1961) p. 1471.

11. MILTON J C D and FRASER J S,
Time-of-flight fission studies on U^{233}, U^{235}, and Pu^{239}.
Canad. J. Phys. 40 (1962) p. 1626.

12. ALEXANDER J M et al.,
Kinetic energy release in 23-MeV deuteron fission of U^{238}.
Phys. Rev. 129 (1963) p. 2659.

13. ARAS N K, MENON M P and GORDON G E,
Ranges of fragments from fission of U^{235} with thermal neutrons and the kinetic energy deficit.
Nucl. Phys. 69 (1965) p. 337.

14. APALIN V F et al.,
Kinetic energy of fragments and energy balance in the fission of U^{235} by thermal neutrons.
Nucl. Phys. 71 (1965) p. 546.

15. THOMAS T D, GIBSON W M and SAFFORD G J,
Thermal-neutron-induced fission of U^{235}, U^{233}, and Pu^{239}.
Physics and chemistry of fission.
Proc. of a symp. Salzburg, 22 - 26 March 1965. (IAEA) Vienna, 1965. Vol. 1, p. 467.

16. SCHMITT H W, NEILER J H and WALTER F J,
Fragment energy correlation measurements for ^{252}Cf spontaneous fission and ^{235}U thermal-neutron fission.
Phys. Rev. 141 (1966) p. 1146.

17. SIGNARBIEUX C, RIBRAG M and NIFENECKER H,
Mesure précise, dans la région des masses symétriques, de l'énergie cinétique des fragments de la fission thermique de l'^{235}U.
Nucl. Phys. A99 (1967) p. 41.

18. MASLIN E E, RODGERS A L and CORE W G F,
Prompt neutron emission from U^{235} fission fragments.
Phys. Rev. 164 (1967) p. 1520.

19. VANDENBOSCH R,
Dependence of fission fragment kinetic energies and neutron yields on nuclear structure.
Nucl. Phys. 46 (1963) p. 129.

20. JOHN W, WESOLOWSKI J J and GUY F,
Mass-dependent structure in the fission γ-ray yields from ^{252}Cf.
Phys. Lett. 30B (1969) p. 340.

21. JOHANSSON S A E,
Gamma de-excitation of fission fragments.
(I). Prompt radiation.
Nucl. Phys. 60 (1964) p. 378.

22. BOWMAN H R et al.,
Further studies of the prompt neutrons from the spontaneous fission of Cf^{252}.
Phys. Rev. 129 (1963) p. 2133.

23. BLINOV M V et al.,
Dependence of the anisotropy of fission neutron emission on the total kinetic energy of the fragments.
Soviet J. Nucl. Phys. 12 (1971) p. 22.

24. ARMBRUSTER P et al.,
Mass dependence of anisotropy and yield of prompt γ-rays in ^{235}U thermal fission.
Physics and chemistry of fission.
Proc. of a symp. Vienna 28 July - 1 August 1969. (IAEA) Vienna, 1969, p. 545.
Also to be published in Z. Naturforschung, March 1971.

25. LEACHMAN R B and KAZEK Jr C S,
Neutron emission from fission modes.
Phys. Rev. 105 (1957) p. 1511.

26. KLUGE Gy and LAJTAI A,
Average number and energy of prompt neutrons from fission.
Phys. Lett. 27B (1968) p. 65.

27. SARKAR R and CHATTERJEE A,
Prompt gamma decay of fission fragments.
Phys. Lett. 33B (1970) p. 263.

TABLE I

The difference between the maximum average kinetic energy and that at symmetry.

Ref. no.	Energy "dip" MeV
(10)	27
(11)	36
(12)	23
(13)	21
(14)	21
(15)	32
(16)	24
(17)	21.2
(18)	(33) 22*
Present work	24

* value in parenthesis observed in experiment, whereas the other value obtained after a rather arbitrary deletion of the degraded events around symmetric fission

FIGURE CAPTIONS

Fig. 1 Block schematic of the electronic equipment.

Fig. 2 Relative yield of the uncollimated gamma radiation as a function of the total fragment kinetic energy for $E_\gamma < 2$ MeV.

Fig. 3 Relative yield curves of part of the collimated gamma radiation as a function of the total fragment kinetic energy. The gamma collimator was set to enhance radiation with half-lives of $10^{-12} < T_{1/2} < 5 \cdot 10^{-11}$ s. The gamma-ray spectra were divided into three consecutive pulse-height intervals in which the total number of counts were added. Pulse-height intervals are: (a) 100 - 600 keV, (b) 600 - 1200 keV, (c) 1200 - 2000 keV.

Fig. 4 Contour diagram representing the distribution of recorded gamma events as a function of the fragment mass and the total fragment kinetic energy. The mass spectrum was recorded on 64 channels and the total kinetic energies on 50 channels. The gamma collimator was set to enhance radiation with half-lives of $10^{-12} < T_{1/2} < 5 \cdot 10^{-11}$ s.

Fig. 5. Mass-dependent yield functions of gamma emission for different kinetic energy groups. Cuts in contour diagram fig. 4. Energy groups are: (a) < 151 MeV, (b) 152 - 159 MeV, (c) 160 - 167 MeV, (d) 168 - 175 MeV, (e) 176 - 183 MeV, (f) > 184 MeV.

Fig. 6 Gamma-ray yield curves as functions of total kinetic energy for different mass groups. Cuts in contour diagram fig. 4. Mass groups are: (a) < 89, (b) 90 - 103, (c) 104 - 117, (d) 119 - 132, (e) 133 - - 146, (f) > 147.

Fig. 7 The integrated gamma-ray yield from fig. 4 as a function of fragment mass. Yield on a relative scale.

Fig. 8 The integrated gamma-ray yield from fig. 4 as a function of the total kinetic energy. Yield on a relative scale.

Fig. 9 The total fragment kinetic energy as a function of mass of the heavy fragment.

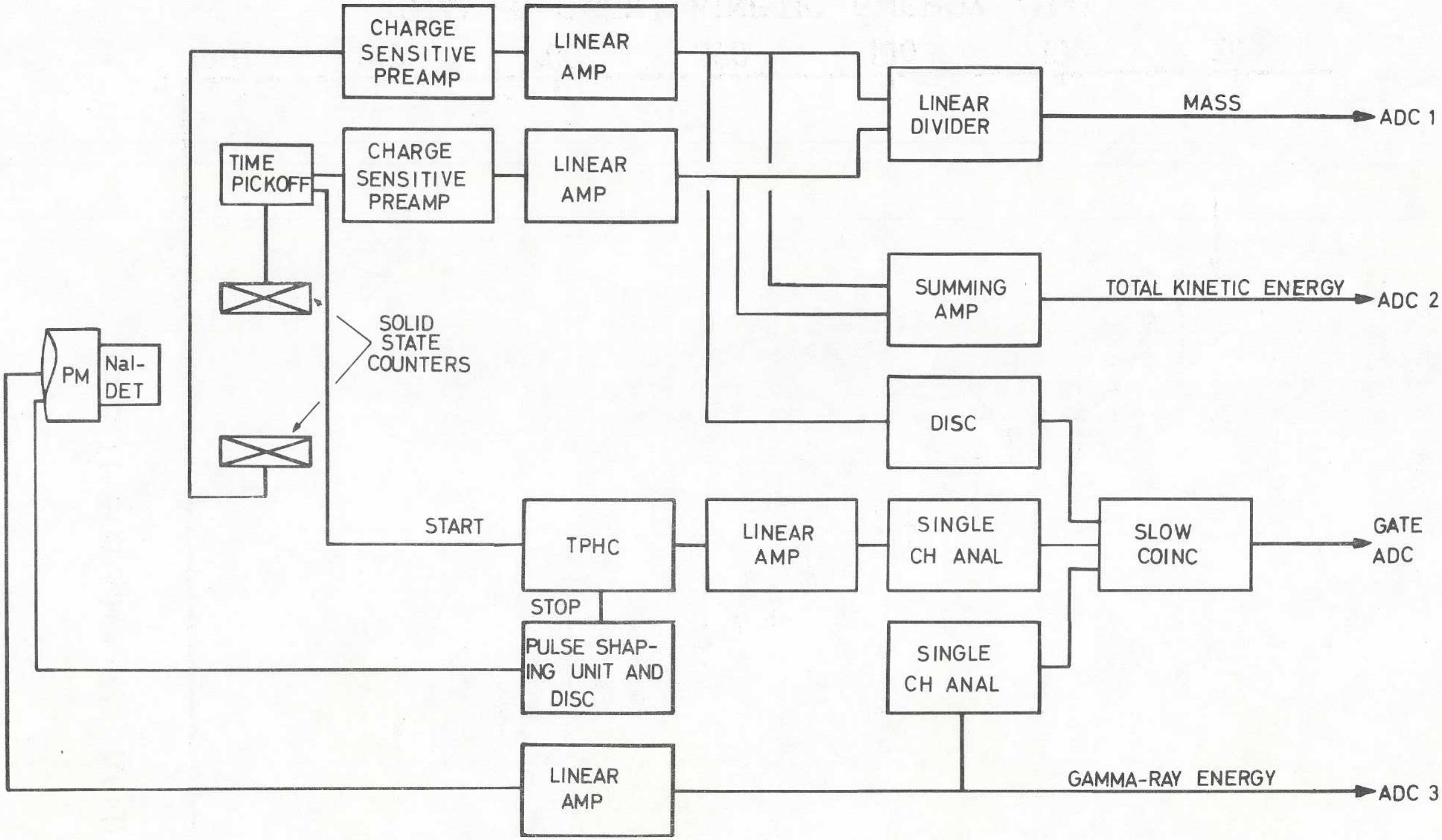
CHARGE SENSITIVE PREAMP
LINEAR AMP
TIME PICKOFF
CHARGE SENSITIVE PREAMP
LINEAR AMP
LINEAR DIVIDER
MASS
ADC 1
SUMMING AMP
TOTAL KINETIC ENERGY
ADC 2
SOLID STATE COUNTERS
PM
NaI-DET
DISC
START
TPHC
LINEAR AMP
SINGLE CH ANAL
SLOW COINC
GATE ADC
STOP
PULSE SHAPING UNIT AND DISC
SINGLE CH ANAL
LINEAR AMP
GAMMA-RAY ENERGY
ADC 3

Fig. 1

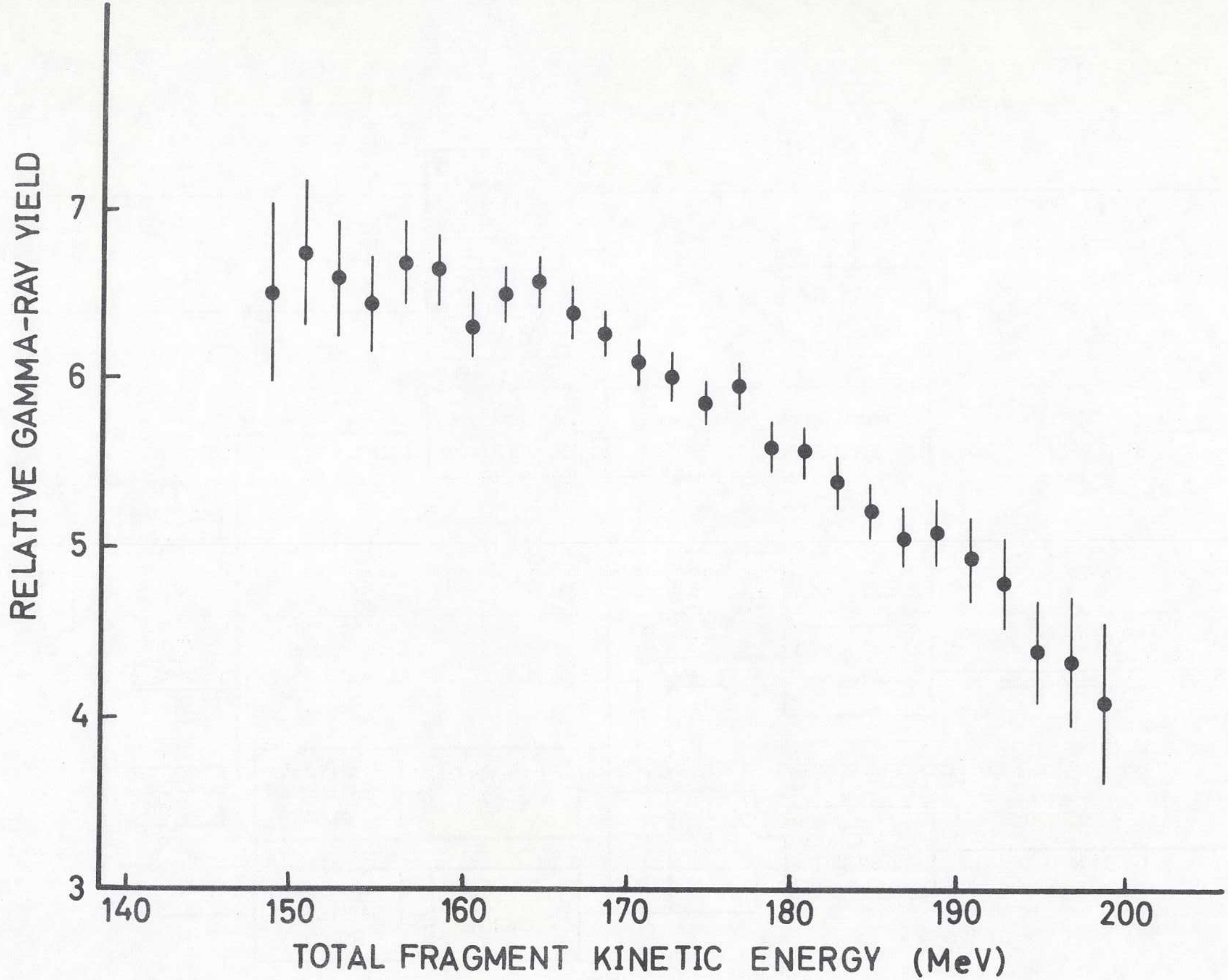
RELATIVE GAMMA-RAY YIELD
7
6
5
4
3
140
150
160
170
180
190
200
TOTAL FRAGMENT KINETIC ENERGY (MeV)

Fig.2

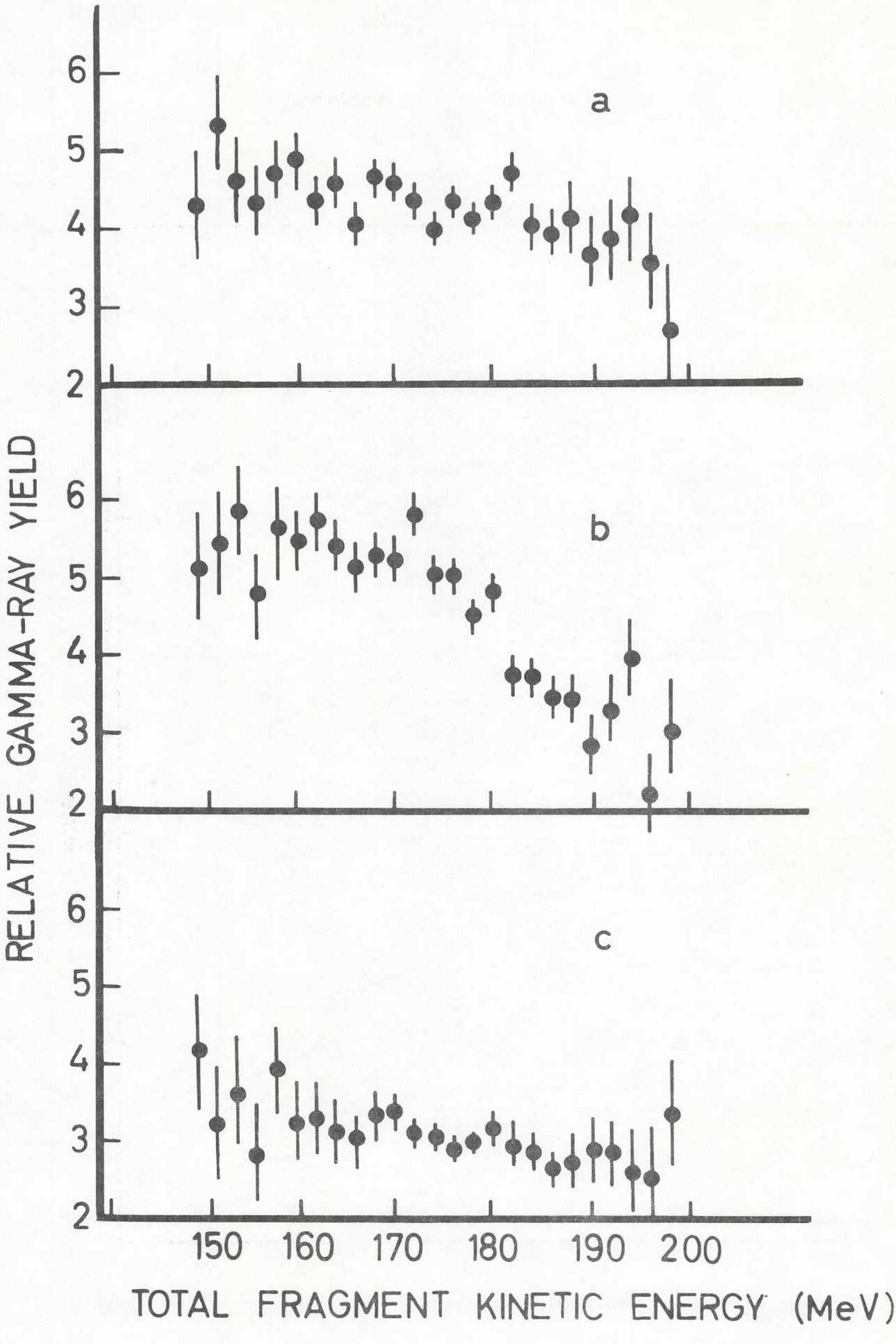

RELATIVE GAMMA-RAY YIELD
a
b
c
2
3
4
5
6
150
160
170
180
190
200
TOTAL FRAGMENT KINETIC ENERGY (MeV)

Fig. 3

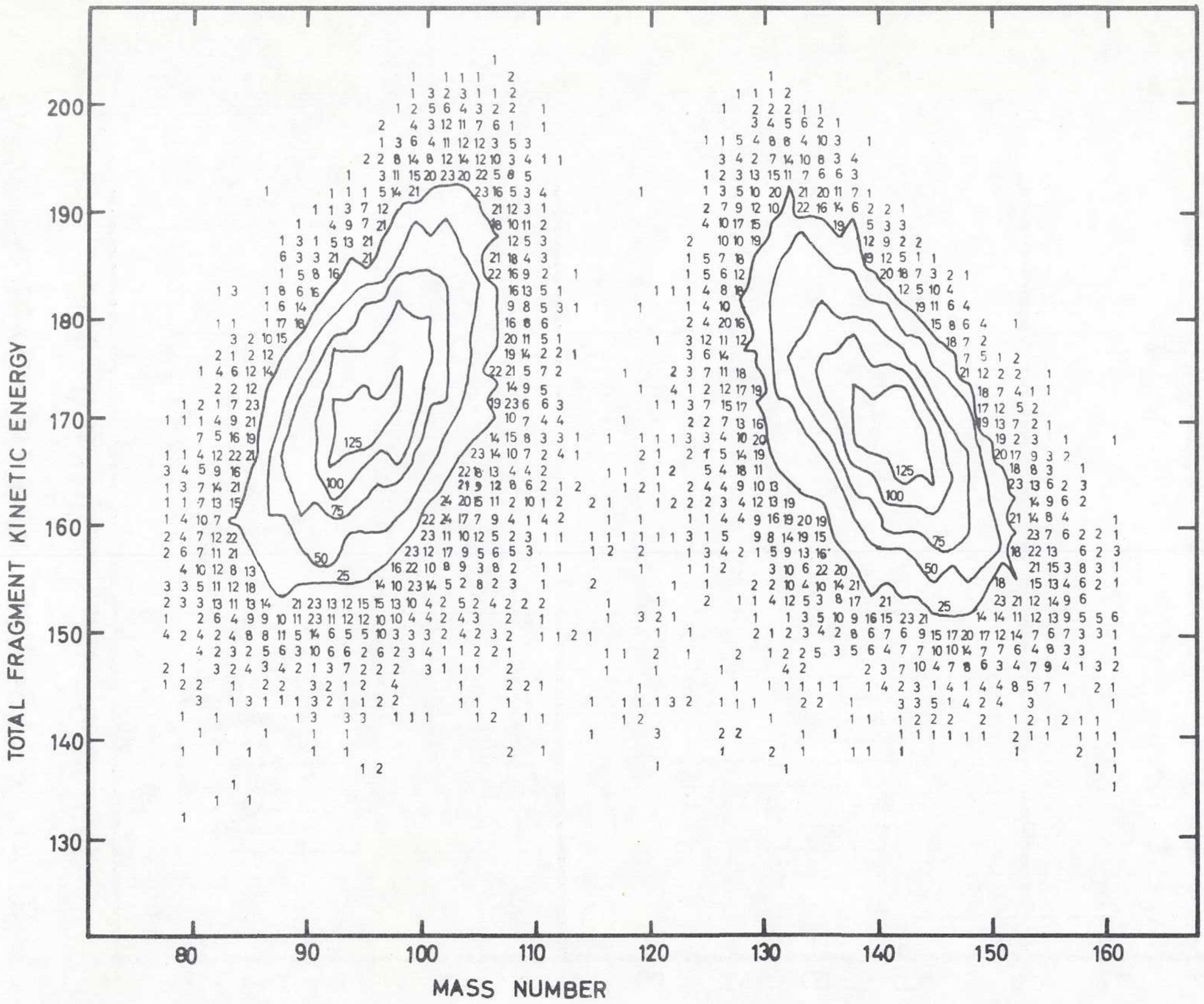

Fig. 4

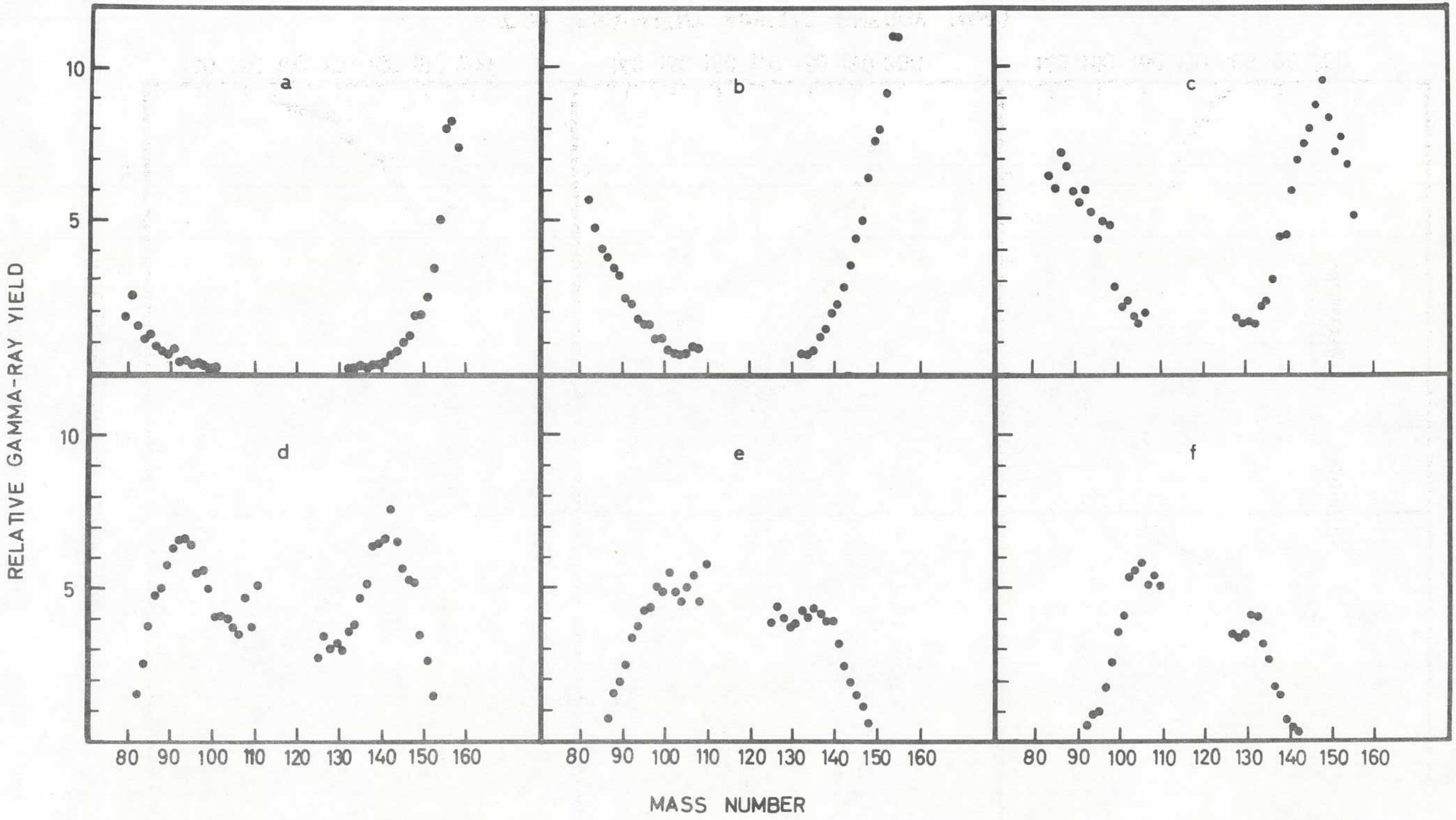
RELATIVE GAMMA-RAY YIELD
10
5
a
b
c
d
e
f
80 90 100 110 120 130 140 150 160
MASS NUMBER

Fig. 5

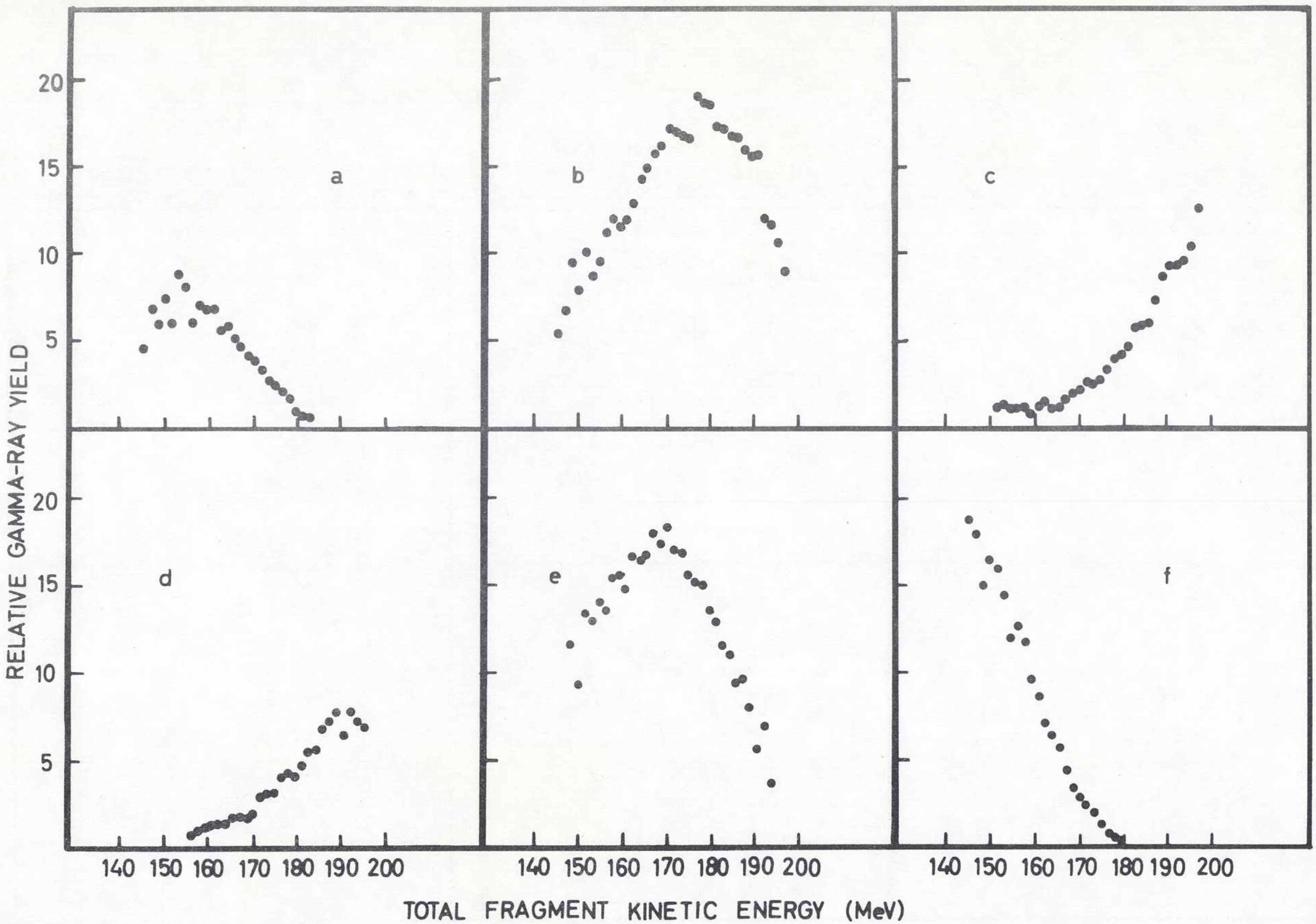
RELATIVE GAMMA-RAY YIELD
a
b
c
d
e
f
TOTAL FRAGMENT KINETIC ENERGY (MeV)

Fig. 6

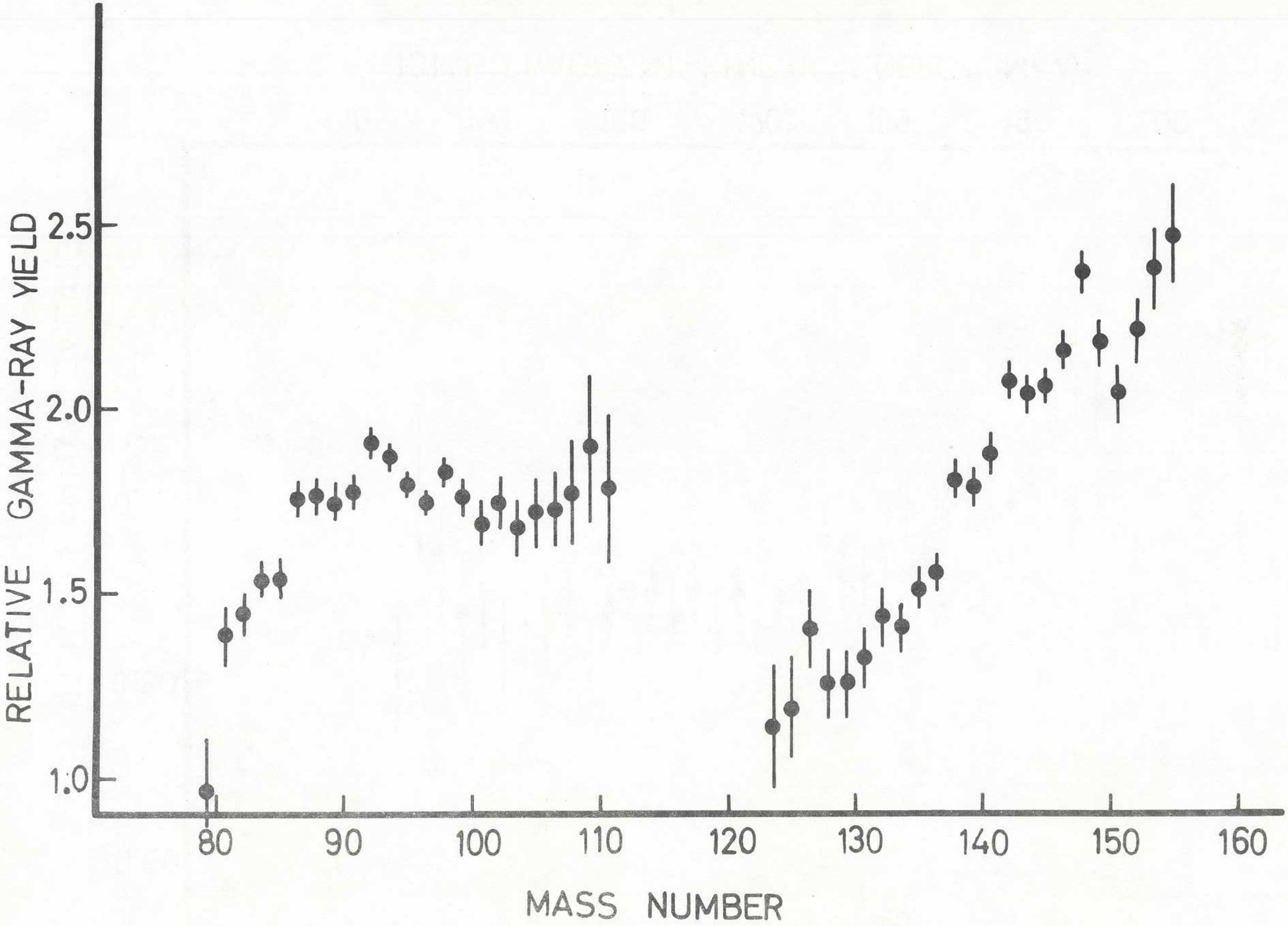
RELATIVE GAMMA-RAY YIELD
2.5
2.0
1.5
1.0
80
90
100
110
120
130
140
150
160
MASS NUMBER

Fig. 7

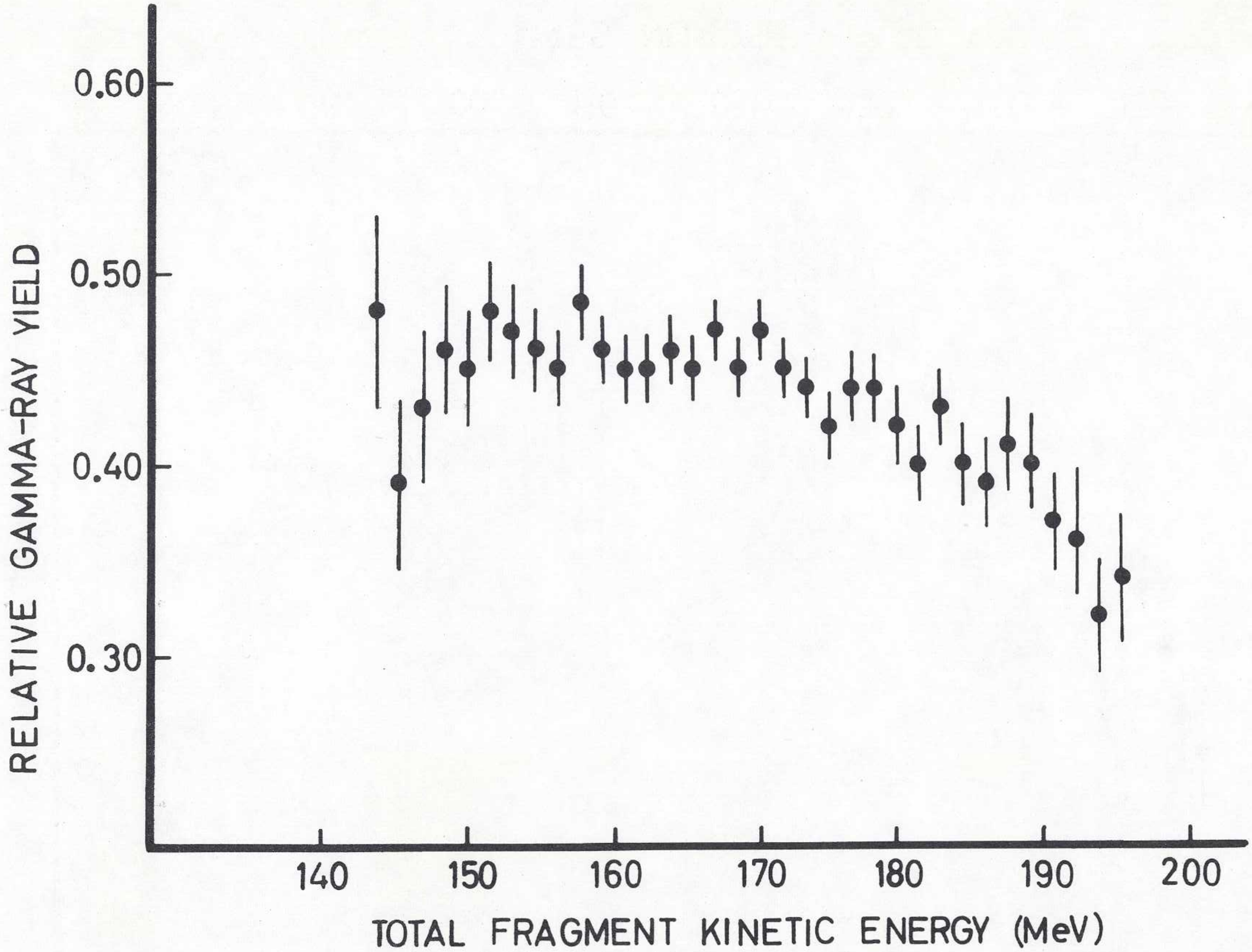
RELATIVE GAMMA-RAY YIELD
0.60
0.50
0.40
0.30
140
150
160
170
180
190
200
TOTAL FRAGMENT KINETIC ENERGY (MeV)

Fig. 8

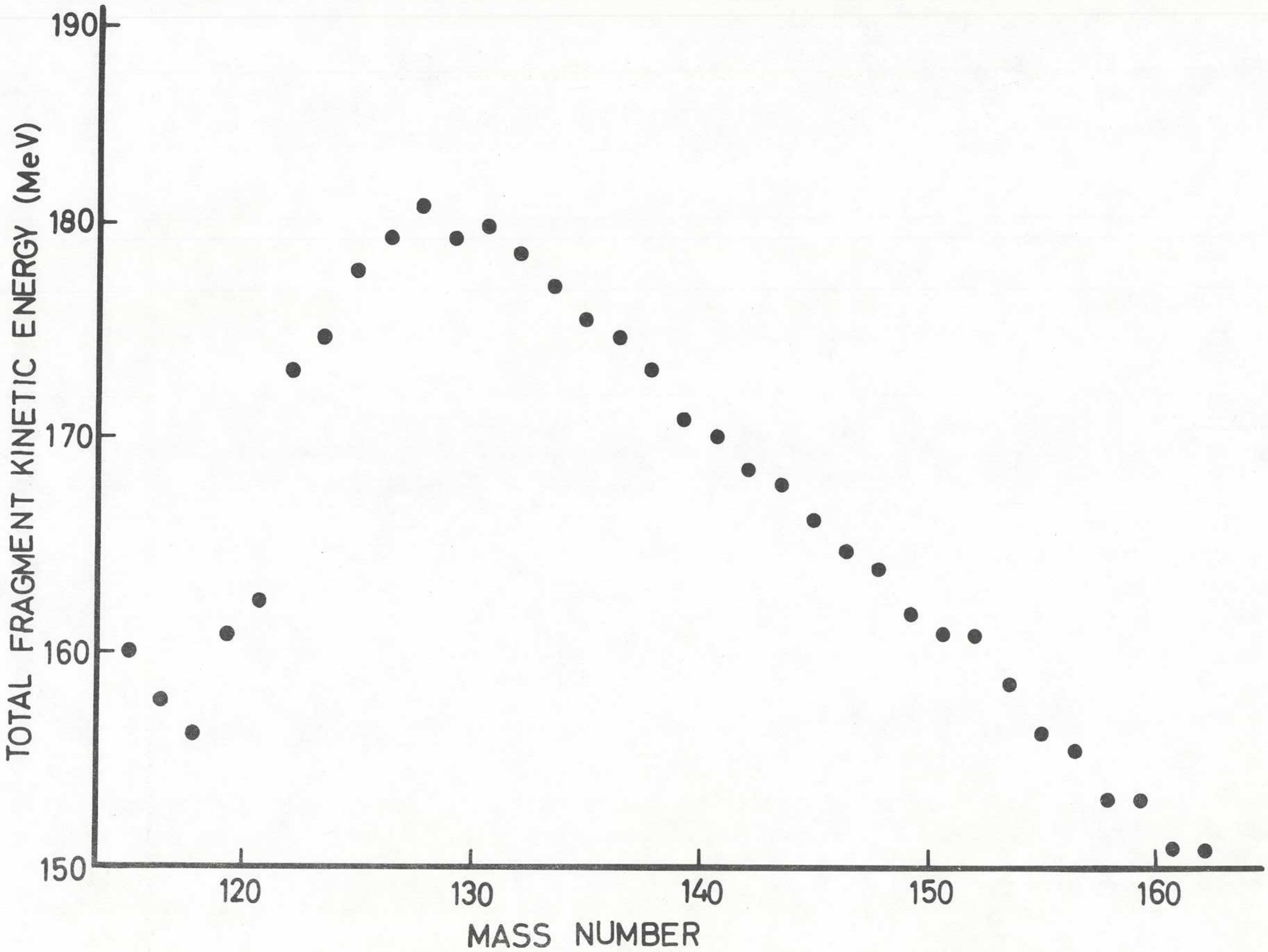
TOTAL FRAGMENT KINETIC ENERGY (MeV)
190
180
170
160
150
120
130
140
150
160
MASS NUMBER

Fig. 9

LIST OF PUBLISHED AE-REPORTS

1–350 (See back cover earlier repports.)

351. A determination of the 2 200 m/s absorption cross section and resonance integral of arsenic by pile oscillator technique. By E. K. Sokolowski and R. Bladh. 1969. 14 p. Sw. cr. 10:–.
352. The decay of ^{191}Os. By S. G. Malmskog and A. Bäcklin. 1969. 24 p. Sw. cr. 10:–.
353. Diffusion from a ground level point source experiment with thermoluminescence dosimeters and Kr 85 as tracer substance. By Ch. Gyllander, S Hollman and U. Widemo. 1969. 23 p. Sw. cr. 10:–.
354. Progress report, FFN, October 1, – September 30, 1968. By T. Wiedling. 1969. 35 p. Sw. cr. 10:–.
355. Thermodynamic analysis of a supercritical mercury power cycle. By A S. Roberts, Jr 1969. 25 p. Sw. cr. 10:–.
356. On the theory of compensation in lithium drifted semiconductor detectors By A. Lauber. 1969. 45 p. Sw. cr. 10:–.
357. Half-life measurements of levels in ^{75}As. By M. Höjeberg and S. G Malmskog. 1969. 14 p. Sw. cr. 10:–.
358. A non-linear digital computer model requiring short computation time for studies concerning the hydrodynamics of the BWR. By F. Reisch and G. Vayssier. 1969. 38 p. Sw. cr. 10:–.
359. Vanadium beta emission detectors for reactor in-core neutron monitoring By I. Ö. Andersson and B. Söderlund. 1969. 26 p Sw. cr. 10:–
360. Progress report 1968. Nuclear chemistry. 1969. 38 p. Sw. cr. 10:–.
361. A half-life measurement of the 343.4 keV level in ^{175}Lu. By M. Höjeberg and S. G. Malmskog. 1969. 10 p. Sw. cr. 10:–.
362. The application of thermoluminescence dosimeters to studies of released activity distributions. By B-I. Rudén. 1969. 36 p. Sw. cr. 10:–.
363 Transition rates in ^{161}Dy. By V. Berg and S. G. Malmskog. 1969 32 p Sw. cr. 10:–.
364. Control rod reactivity measurements in the Ågesta reactor with the pulsed neutron method. By K. Björeus. 1969. 44 p. Sw. cr. 10:–.
365. On phonons in simple metals II. Calculated dispersion curves in aluminium. By R. Johnson and A. Westin. 1969. 124 p. Sw. cr. 10:–.
366. Neutron elastic scattering cross sections. Experimental data and optical model cross section calculations. A compilation of neutron data from the Studsvik neutron physics laboratory. By B. Holmqvist and T. Wiedling 1969. 212 p. Sw. cr. 10:–.
367. Gamma radiation from fission fragments. Experimental apparatus – mass spectrum resolution. By J. Higbie. 1969. 50 p. Sw. cr. 10:–.
368. Scandinavian radiation chemistry meeting, Studsvik and Stockholm, September 17–19, 1969. By H. Christensen. 1969. 34.p. Sw. cr. 10:–.
369. Report on the personnel dosimetry at AB Atomenergi during 1968. By J. Carlsson and T. Wahlberg. 1969 10 p. Sw. cr. 10:–.
370. Absolute transition rates in ^{188}Ir. By S. G. Malmskog and V. Berg. 1969. 16 p. Sw. cr. 10:–.
371. Transition probabilities in the 1/2+(631) Band in ^{235}U. By M. Höjeberg and S. G. Malmskog 1969. 18 p. Sw. cr. 10:–.
372. E2 and M1 transition probabilities in odd mass Hg nuclei. By V. Berg, A Bäcklin, B Fogelberg and S. G. Malmskog. 1969. 19 p. Sw. cr. 10:–
373. An experimental study of the accuracy of compensation in lithium drifted germanium detectors. By A. Lauber and B. Malmsten. 1969. 25 p. Sw cr. 10:–.
374. Gamma radiation from fission fragments. By J. Higbie. 1969. 22 p. Sw. cr. 10:–.
375. Fast neutron elastic and inelastic scattering of vanadium. By B. Holmqvist, S. G. Johansson, G. Lodin and T. Wiedling. 1969. 48 p. Sw. cr. 10:–.
376. Experimental and theoretical dynamic study of the Ågesta nucler power station. By P. Å. Bliselius, H. Vollmer and F. Åkerhielm. 1969. 39 p Sw. cr. 10:–.
377. Studies of Redox equilibria at elevated temperatures 1. The estimation of equilibrium constants and standard potentials for aqueous systems up to 374°C. By D. Lewis. 1969. 47 p. Sw. cr. 10:–.
378. The whole body monitor HUGO II at Studsvik. Design and operation By L Devell, I. Nilsson and L. Venner. 1970. 26 p. Sw. cr. 10:–.
279. ATOMSPHERIC DIFFUSION. Investigations at Studsvik and Ågesta 1960–1963. By L-E. Hæggblom, Ch. Gyllander and U. Widemo. 1969. 91 p. Sw cr. 10:–.
380. An expansion method to unfold proton recoil spectra. By J. Kockum. 1970. 20 p. Sw. cr. 10:–.
381. The 93.54 keV lever ^{91}Sr, and evidence for 3-neutron states above N=50. By S. G. Malmskog and J. McDonald. 1970. 24 p. Sw. cr. 10:–.
382. The low energy level structure of ^{191}Ir. By S. G. Malmskog, V. Berg, A. Bäcklin and G Hedin. 1970. 24 p Sw cr. 10:–.
383. The drinking rate of fish in the Skagerack and the Baltic. By J. E. Larsson. 1970. 16 p. Sw. cr. 10:–.
384. Lattice dynamics of Nacl, KCl, RbCl and RbF. By G. Raunio and S. Rolandson. 1970. 26 p. Sw. cr. 10:–.
385. A neutron elastic scattering study of chromium, iron and nickel in the energy region 1.77 to 2.76 MeV. By B. Holmqvist, S. G. Johansson, G. Lodin, M Salama and T. Wiedling. 1970. 26 p. Sw. cr. 10:–.
386. The decay of bound isobaric analogue states in ^{28}Si and ^{32}Si using (d. nγ) reactions. By L. Nilsson, A Nilsson and I. Bergqvist. 1970. 34 p. Sw. cr. 10–.
387. Transition probabilities in ^{189}Os. By S. G. Malmskog, V. Berg and A. Bäcklin. 1970 40 p Sw. cr. 10:–.
388. Cross sections for high-energy gamma transition from MeV neutron capture in ^{206}Pb. By I. Bergqvist, B. Lundberg and L. Nilsson. 1970. 16 p. Sw. cr. 10:–.
389. High-speed, automatic radiochemical separations for activation analysis in the biological and medical research laboratory. By K. Samsahl. 1970. 18 p. Sw. cr. 10:–.
390. Use of fission product Ru-106 gamma activity as a method for estimating the relative number of fission events in U-235 and Pu-239 in low-enriched fuel elements. By R. S. Forsyth and W. H. Blackadder. 1970. 26 p. Sw. cr. 10:–.
391. Half-life measurements in ^{134}I. By V. Berg and Å. Höglund. 1970. 16 p Sw. cr. 10:–.
392. Measurement of the neutron spectra in FRO cores 5, 9 and PuB-5 using resonance sandwich detectors. By T. L. Andersson and M. N. Qazi. 1970. 30 p. Sw. cr. 10:–.
393. A gamma scanner using a Ge(Li) semi-conductor detector with the possibility of operation in anti-coincidence mode. By R. S. Forsyth and W. H. Blackadder. 1970. 22 p. Sw. cr. 10:–.
394. A study of the 190 keV transition in ^{141}La. By B. Berg, Å. Höglund and B. Fogelberg. 1970 22 p. Sw cr. 10:–.
395. Magnetoacoustic waves and instabilities in a Hall-effect-dominiated plasma. By S. Palmgren 1970. 20 p Sw. cr. 10:–.
396. A new boron analysis method. By J. Weitman, N. Dåverhög and S. Farvolden. 1970. 26 p. Sw. cr. 10:–.
397. Progress report 1969. Nuclear chemistry. 1970. 39 p. Sw. cr. 10:–.
398. Prompt gamma radiation from fragments in the thermal fission of ^{235}U. By H. Albinsson and L. Lindow. 1970. 48 p. Sw. cr. 10:–.
399. Analysis of pulsed source experiments performed in copper-reflected fast assemblies. By J. Kockum. 1970. 32 p. Sw. cr. 10:–.
400. Table of half-lives for excited nuclear levels. By S G. Malmskog. 1970 33 p. Sw. cr. 10:–.
401. Needle type solid state detectors for in vivo measurement of tracer activity. By A. Lauber, M. Wolgast. 1970. 43 p. Sw. cr. 10:–.
402. Application of pseudo-random signals to the Ågesta nuclear power station By P-Å. Bliselius. 1970. 30 p. Sw. cr. 10:–.
403. Studies of redox equilibria at elevated temperatures 2. An automatic divided-function autoclave and cell with flowing liquid junction for electrochemical measurements on aqueous systems. By. K. Johnsson, D. Lewis and M. de Pourbaix. 1970. 38 p. Sw. cr. 10:–.
404. Reduction of noise in closed loop servo systems. By K. Nygaard. 1970. 23 p. Sw. cr. 10:–
405. Spectral parameters in water-moderated lattices. A survey of experimental data with the aid of two-group formulae. By E. K. Sokolowski. 1970. 22 p. Sw. cr. 10:–.
406. The decay of optically thick helium plasmas, taking into account ionizing collisions between metastable atoms or molecules. By J. Stevefelt. 1970. 18 p. Sw. cr. 10:–.
407. Zooplankton from Lake Magelungen, Central Sweden 1960-63. By E. Almquist. 1970. 62 p. Sw. cr. 10:–.
408. A method for calculating the washout of elemental iodine by water sprays. By E. Bachofner and R. Hesböl. 1970. 24 p. Sw. cr. 10:–.
409. X-ray powder diffraction with Guinier–Hägg focusing cameras. By A. Brown. 1970. 102 p. Sw. cr. 10:–.
410. General physic section Progress report. Fiscal year 1969/70. By J. Braun. 1970. 92 p. Sw. cr. 10:–.
411. In-pile determination of the thermal conductivity of UO_2 in the range 500–2 500 degrees centigrade. By J-Å Gyllander. 1971. 70 p. Sw. cr. 10:–.
412. A study of the ring test for determination of transverse ductility of fuel element canning. By G. Anevi and G. Östberg. 1971. 17 p. Sw. cr. 15:–.
413. Pulse radiolysis of Aqueous Solutions of aniline and substituted anilines. By H. C. Christensen. 1971. 40 p. Sw. cr. 15:–.
414. Radiolysis of aqueous toluene solutions. By H. C. Christensen and R. Gustafson. 1971. 20 p. Sw. cr. 15:–.
415. The influence of powder characteristics on process and product parameters in UO_2 pelletization. By U. Runfors. 1971. 32 p. Sw. cr. 15:–.
416. Quantitative assay of Pu239 and Pu240 by neutron transmission measurements. By E. Johansson. 1971. 26 p. Sw. cr 15:–.
417. Yield of prompt gamma radiation in slow-neutron induced fission of ^{235}U as a function of the total fragment kinetic energy. By H. Albinsson. 1971. 38 p. Sw. cr. 15:–.

List of published AES-reports (In Swedish)

1. Analysis by means of gamma spectrometry. By D. Brune. 1961. 10 p. Sw. cr. 6:–.
2. Irradiation changes and neutron atmosphere in reactor pressure vessels-some points of view. By M. Grounes 1962. 33 p. Sw. cr. 6:–.
3. Study of the elongation limit in mild steel. By G. Östberg and R. Attermo. 1963. 17 p. Sw cr. 6:–.
4. Technical purchasing in the reactor field. By Erik Jonson. 1963. 64 p. Sw. cr. 8:–.
5. Ågesta nuclear power station. Summary of technical data, descriptions, etc for the reactor. By B. Lilliehöök. 1964. 336 p. Sw. cr. 15:–.
6. Atom Day 1965. Summary of lectures and discussions. By S. Sandström. 1966 321 p. Sw. cr. 15:–.
7. Building materials containing radium considered from the radiation protection point of view. By Stig O. W. Bergström and Tor Wahlberg. 1967. 26 p. Sw. cr. 10:–

Additional copies available from the Library of AB Atomenergi, Fack, S-611 01 Nyköping 1, Sweden.

EOS-tryckerierna, Stockholm 1971

AE-421

UDC 539.163:
539.166
539.122.16

AE-421

Decay Curves and Half-Lives of Gamma-Emitting States from a Study of Prompt Fission Gamma Radiation

H. Albinsson

AKTIEBOLAGET ATOMENERGI

STUDSVIK, NYKÖPING, SWEDEN 1971

DECAY CURVES AND HALF-LIVES OF GAMMA-EMITTING STATES FROM A STUDY OF PROMPT FISSION GAMMA RADIATION

H. Albinsson*

ABSTRACT

Measurements were made on the time distributions of the prompt gamma radiation emitted from fragments in the thermal-neutron induced fission of ^{235}U. The gamma radiation emitted during different time intervals after the fission event was studied with the help of a collimator, the position of which was changed along the path of the fragments. In this way decay curves were obtained from which half-lives could be estimated. Time components with half-lives of 7.5, 18 and 60 ps were found and their relative intensities were calculated. Half-lives and associated intensities are in good agreement with earlier data from uranium and californium fission.

Problems involved in this type of study are discussed. The collimator technique has proved to be effective for determination of half-lives down to less than 10 ps.

* Chalmers University of Technology, Gothenburg

Printed and distributed in April 1971.

LIST OF CONTENTS

1. INTRODUCTION

The time distribution of the gamma radiation from fission fragments has been studied in several experiments during the past fifteen years. Results of photon yields in different time intervals after the fission event have been obtained. It has been difficult, however, to fit these results into one time distribution covering the first microsecond of the life-time of the fragment. The disagreement might be due to experimental difficulties such as contributions to the photon yields from the prompt neutron emission and poor time resolution when measuring decays within the first 100 ps after the fission event. Another reason for the insufficient agreement between the earlier results could be that the gamma-ray energy ranges have been defined differently. This latter argument is seldom put forward in the discussion of the various results.

As far as the prompt gamma radiation is concerned about 75 % of it is emitted within 100 ps [1] according to estimates by Maienschein [2] and Johansson [3]. It has also been shown, however, that very few of these gamma-rays are emitted before 1 ps [4, 5]. The prompt radiation comes from a very large number of states and a first glance at the integrated gamma-ray energy spectrum, from all fragments and within 1 ns from the fission event, does not reveal any interesting structure. It is therefore notable that by use of collimator technique one can resolve the spectrum into different energy and associated time components. Johansson found radiation with a half-life of 20 ps in ^{252}Cf fission in the gross spectrum [3], whereas 8.5 ± 1.5 ps was found in a study of thermal neutron induced fission of ^{235}U [6]. Val'skii et al. stated that most of the gamma radiation in uranium fission is emitted within a time shorter than 50 ps [7] . Higbie reported a half-life of 150 ps within the first manosecond after fission [8] .

Spectra of the gamma radiation have been recorded in which, which simple blocking technique, half-lives of several gamma lines have been obtained [9, 10] . In an earlier reported work from this laboratory [11] gamma-ray energy spectra have been recorded in association with different half-lives, resulting in further support for the argument that the bulk of prompt gamma radiation consists of collective quadrupole radiation [3] . The present report will discuss the basis for selection of the different half-lives and how the actual measurements were performed. In the present studies the collimator technique has been used, and its significance for the time resolution and possible improvements will be discussed. The time range covered is from a few picoseconds to two nanoseconds, the higher limit being imposed by the average time it takes for a fragment to move from the fission foil to the fragment detector. Time-of-flight technique was adopted in order to discriminate the prompt neutrons from the prompt gamma radiation.

2. EXPERIMENTAL ARRANGEMENT

2.1. Apparatus

Fig. 1 shows a block diagram of the electronic system used in the present experiment. The details of the design and the system performance have been discussed previously [11] and therefore only some of the specific features of the set-up will be briefly described.

A solid state detector of the surface barrier type was placed with its active surface in front of the foil to measure the energies of the fission fragments. The detector* was about 4 cm^2 in area, fabricated from 400 ohmcm n-type silicon and operated at about 70 V bias. The distance between the detector and the fissile foil was 2 cm. The gamma detector was a NaI(Tl) scintillator from Harshaw, 10.4 cm long and 13.0 cm in diameter, viewed by a Philips XP 1040 photomultiplier tube. The associated electronics, consisting of a pulse-shaping unit and a discriminator, was coupled directly to the photomultiplier tube socket and gave a fast leading-edge time pulse and a linear pulse.

A lead collimator, movable in parallel with the direction of the detected fragments and also with a variable slit, was used to select gamma radiation in different time intervals after the fission event.

The fissile deposit was 1 cm^2 in area and prepared by electrodeposition on 100 $\mu g/cm^2$ nickel foils. The thickness of the uranium layer was about 100 $\mu g/cm^2$ in most runs.

It is very important in this type of measurements that the uranium layer and the nickel foil are thin and uniform. The fragment energy loss has not been measured, but may be estimated to be no more than 3 MeV [12, 13]. It was found that an upper practical limit of less than about 100 $\mu g/cm^2$ was enough to get energy spectra of good quality in which not too much of velocity degradation was introduced.

The recording of time-of-flight spectra was often done in association with the gamma-ray energy. It would have been of interest, however, to include simultaneous recording of mass spectra, but as the available multichannel analyzer could handle only two parameters at a time, the measurements had to be adapted accordingly.

---

* Type C7904 Heavy Ion Detectors supplied by ORTEC, Oak Ridge, Tenn., USA

The NaI detector was placed about 70 cm from the fission foil and in a direction perpendicular to the direction of the detected fragments (fig. 1). The main reason for using the time-of-flight technique was to discriminate the prompt neutrons from the fission gamma radiation, but in this geometry it was possible to benefit from the form of the angular distribution of the prompt neutrons. As is well known, it is peaked in the direction of the fragments.

The data recording system was the same as in ref. 11, namely a two-parameter analyzer, the memory of which was that of a small computer, PDP-8/S.

2.2. Performance

With the help of the collimator for selection of gamma radiation from different time intervals after the fission event, time-of-flight spectra were recorded with the collimator in different positions. The average velocity of the fragments is about 1.2 cm/ns. By estimating the intensity of the gamma peak the intensity variation with the collimator setting was obtained, i.e. the variation with time after fission.

Three main decay components have been found so far, having half-lives of 7.5, 18 and 60 ps. They will be discussed further in the following section. Measurement of the fastest radiation was rather a mechanical than any other problem. The technique used and its performance have been discussed in detail in an earlier report [11] and a few of the main features will be mentioned here.

A great part of the prompt gamma radiation is known to have an average half-life of less than 10 ps. As the fragments have velocities of a little more than 1 cm/ns the choice of collimator depends on which type of radiation is to be studied.

The foil had to be plane and its surface free from shrinkles. The adjustment of the foil in its holder was made in a darkroom with light falling through the collimator slit. The decay curve was obtained from the time-of-flight spectra, which were recorded for consecutive collimator settings controlled by a micrometer screw. The actual setting of the collimator was done by moving the foil holder, and the control by the micrometer screw was in fact done on this holder. The foil holder is a light device, whereas the collimator is heavy, weighing about 7 kg. Thus it is easier to perform the settings on the holder. The changes in the solid angle from the foil subtended by the fission detector through this operation may be regarded as negligible.

The response curve for the collimator slit width of 0.5 mm is shown in fig. 2. This curve has been calculated from the gamma detector solid angles with a gamma-emitting source in different positions. The curve was tested by using a source, and the results is shown in fig. 2a by the points which fall on the theoretical curve. This is an indication that the collimator worked as it should. The collimator response function for fission fragment radiation is shown in the same figure and clearly demonstrates that the fragments emit gamma radiation long after they have left the foil.

One problem when performing these studies is to move the foil "close" enough to the collimator without the gamma detector receiving radiation from both fragments. If the radiation is not well enough collimated, but radiation from both fragments can reach the detector, it is difficult with the present type of set-up to distinguish which of the two fragments actually emitted a recorded photon. By placing the gamma detector behind one of the fragment detectors or close to a line adjoining them, one can analyse the gamma-ray energy spectra by use of Doppler-shift technique and often say, with a great probability, which fragment has emitted a particular gamma line. The gamma detector must then be a Ge(Li) detector owing to its superior energy resolution compared to that of a NaI-detector. It is not possible, however, with Doppler-shift technique alone, to obtain the half-life of the recorded radiation.

It is essential in the analysis of the gamma-ray energy spectra to know the background distribution as a function of gamma-ray energy. The background is best estimated by recording time-of-flight spectra and from them estimating the background level [11] . A time-of-flight spectrum for the gross gamma-ray energy distribution gives an average value of the background. The spectra in the present experiment were often recorded with a bias set at about 70 keV, and all photons with energies above that level were recorded. By recording a time-of-flight spectrum as a function of gamma-ray energy portions, estimates can be obtained of the signal/background ratio for the prompt fission gamma radiation with a particular collimator setting. In the present work this variation could only come from average values in every gamma-ray energy portion. The present set-up was run in tandem with a neutron crystal spectrometer. The background level - taken over all gamma-ray energies above 70 keV - could vary by a factor of 2 - 3 because of the angular variation of the monochromator crystal, through which the reactor radiation (thermal and fast neutrons and gamma radiation) was transmitted.

The time definition obtained by the collimator depends on the velocity spread of the fragments, but also on the geometry of the collimator. Some relevant numbers may explain the situation, which is illustrated in fig. 3. The uranium sources used in the present work have had a circular shape of 1 cm in diameter. The length of the collimator (x) has always been more than 10 cm in order to obtain a good reduction of the intensity of the radiation which penetrated the shield. The gamma peak in the integrated time-of-flight spectrum was reduced to less than 5 % with a collimator of 10 cm and more. The average gamma-ray energy of the integrated prompt spectrum is about 0.9 MeV, and there are about 8 photons on the average per fission event [2]. It is therefore essential to have good shielding of the unwanted radiation. As will be readily understood, the time resolution of the collimator in terms of geometry is improved the longer the collimator. The length of 13.5 cm chosen in the present set-up is a compromise between acceptable shielding of the unwanted radiation and good time resolution. Table I gives some figures in connection with fig. 3.

The actual measurements of the various time components of the prompt fission gamma radiation are reported in the following section, together with the collimator settings chosen. The accuracy of the half-lives is about $\pm$ 25 %.

2.3. Analysis of data

In quite a few of the earlier reported measurements [3, 7, 8, 14] an analysis of the data was made on the basis of decay functions of the exponential form $\exp\left[-\frac{x}{v\tau}\right]$ where v is the average velocity of the fragments, x is the distance from the fission foil to the axis of the collimator, and τ is the lifetime of the radiation under study. The gross radiation is a sum of a number of decay functions, one function for every half-life. The present experimental data have been analysed with respect to one average velocity of the fragments namely 1.20 cm/ns. It is well known, however, that the average velocity varies by a factor of almost two over the mass distribution. As regards the determination of half-lives, they are obtained from the change in the intensity distributions with different collimator settings, and the average velocity distribution should be practically the same within the first 2 mm of the flight path of the fragments. Determination of absolute intensities for each collimator setting, however, requires a correction factor in which the velocity distribution is used. This correction was also considered when the absolute intensities of the different time components were calculated.

3. RESULTS

To measure life-times of the fission gamma radiation shorter than 10^{-10} s, the best method is to use the time-of-flight technique. A flight path of 1 cm corresponds to a time interval of about 1 ns, and a collimator slit width of 0.1 mm will therefore correspond to 10^{-11} s. By use of the accuracy of the micrometer screw it was possible to set the collimator consecutively with points as close as 0.01 mm, corresponding to a change of 10^{-12} s in the time interval. In principle it should therefore be possible to estimate half-lives of a few tenths of a ps.

With a collimator opening of 0.25 mm the decay curve of the fission gamma radiation was that shown in fig. 4. The setting of the collimator was performed in steps of 0.05 mm. Assuming a simple exponential decay of the gamma radiation gives a calculated curve best fitting the measured points and yielding a half-life of 7.5 ps.

A collimator slit width of 0.5 mm gives the calculated response curve presented in fig. 2. The decay curve of the fission gamma radiation is plotted in the same figure. There is a remarkable structure on top of the curve, caused by the reduced intensity sensed by the gamma detector due to scattering in the frame of the fission target holder as it just "passes" the collimator. Measurements of half-lives depend only on one half of the decay curve; for instance, in the case presented in this figure the right hand part of the curve is the one of interest. After corrections for contributions from general background and fission gammas of longer half-lives that part of the decay curve is drawn in fig. 5. Assuming a simple exponential decay gives a half-life of 18 ps.

Finally, in fig. 6 is shown the interesting part of the decay curve yielding a half-life of 60 ps. The collimator slit width was here 1.0 mm and the settings were performed in steps of 0.2 mm. The points in fig. 6 are the net results, i.e. background from the components of longer half-lives plus the general background have been subtracted.

To illustrate the variation in background as a function of gamma-ray energy, fig. 7 has been included. As regards measurements of gamma-ray energy spectra, this collimator setting represents a bad case, as it is not optimized to enhance radiation of a specific half-life. The reason for presentation of the figure is, however, to demonstrate the background variation. The average background as estimated from the time-of-flight spectrum was 47 %. The time-of-flight spectra were run, however, in the two-parameter mode, with gamma-ray energy on the second axis. By summing up time-of-flight spectra in energy portions, the background in the respective portion was obtained and plotted in fig. 7. This figure clearly demonstrates the improvements in the signal/background ratio as the gamma-ray energy is increased. It is reasonable to assume that, if the counting rate can be increased to something like 10^4 fissions/second, it would be possible to perform a measurement of fission gamma-rays in an energy region around 3 MeV and obtain a statistically acceptable number of counts within a week. Compared to the present work this means an increase in the fission rate by about a factor of 30.

4. DISCUSSION

In a recently published paper Skarsvåg [14] obtained a half-life of 80 ps in a time interval where the present experiment has given 60 ps. In the present measurement when the longer-lived components had not been subtracted, the decay curve of the raw data gave $T_{1/2}$ = 80 ps. In an earlier experiment at this laboratory [8] a value of 150 ps was obtained.

As regards the component with a half-life of less than 10 ps the present experiment has yielded 7.5 ps, whereas 8.5 ps was obtained by Armbruster et al. [6]. A value of 18 ps was then obtained in the present study for a slower component. A similar value was also estimated from Johansson's study of ^{252}Cf fission.

As was reported elsewhere [15], the respective half-lives and their associated yields of the bulk of gamma-rays strongly indicate that a very great part of the prompt fission gamma radiation consists of collective quadrupole radiation. It should be noted, however, that further measurements are required in order to draw a final conclusion about the multipolarity of the radiation consisting in studies of X rays and conversion electrons as well as time distributions of the gamma-rays. As regards the fastest components of the prompt gamma radiation, they are not so easily converted as are the slower ones with half-lives of 50 ps and more. This is due to the larger energies associated with the faster components compared to the slower.

There are a few factors affecting the resolution of the gamma peak in the time-of-flight spectra, most of which have been discussed elsewhere [11] . One factor which was not discussed is the spread in the time resolution brought about by the geometry of the gamma collimator, the extensions of the solid state detectors and the fission foil, and, moreover, that the two latter components are located rather close to each other. Fig. 8 illustrates the problem. The uncertainty depending on this will introduce an error in the absolute intensity determination of less than 30 %. The half-life determination, however, is not much affected, since it depends on relative measurements of the intensities.

The error in absolute intensity can be reduced by placing the fragment detector further away from the fissile foil or by using a smaller detector. With the detector further away the time resolution of the gamma peak in the time-of-flight spectrum will be reduced, so a smaller detector is therefore the better choice. As regards problems related to the time resolution of the gamma peak in the time-of-flight spectrum they have been discussed earlier [11] .

The estimates of the absolute intensity of the different components of the prompt gamma radiation are important to know in the study of the energy release of the excitation energy of the fragments. As regards the prompt components of half-lives of 7.5 and 18 ps it is possible to obtain a fairly good estimate of that energy release since the photons of these half-lives have similar energies within each component. It should be noted, however, that the average energies of the photons of half-lives around 60 ps vary strongly from one mass region to another. Therefore it is not possible to obtain a very good estimate of that energy release by simply multiplying the average number of photons by their average energies, but in the absence of any detailed results of these particular gamma-rays, this may therefore be the only method to use.

The average intensities of the various time components given in per cent of the total fission gamma radiation within the first nanosecond after scission are as follows: 35, 25 and 10 % for the respective half-lives of 7.5, 18 and 60 ps.

Johansson [3] stated that 55 - 65 % of the prompt photons are emitted with a half-life of about 10^{-11} s in ^{252}Cf fission. That value may be an average of the 7.5 and 18 ps found in the present measurements, if a slightly different collimator was used. The sum of the relative intensities of these two components is in fair agreement with that obtained for the 10 ps component in ^{252}Cf fission.

5. CONCLUSIONS

Measurements of the time distribution of the prompt gamma radiation from fragments in the thermal fission of ^{235}U have given half-lives of 7.5, 18 and 60 ps, and the relative intensities of these components are 35, 25, and 10 % respectively. The collimator technique has proved to be effective for determination of half-lives down to less than 10 ps. The half-lives determined agree well with those obtained at other laboratories.

ACKNOWLEDGEMENTS

The author wishes to express his sincere gratitude to Professor S. Johansson for valuable discussions and Professor N. Ryde and Dr. T. Wiedling for their interest in this work. The assistance from Mr. L. Lindow throughout the work is gratefully acknowledged.

REFERENCES

1. MAIER-LEIBNITZ H., ARMBRUSTER P., and SPECHT H.J., Prompt and delayed gamma-rays from fission. Physics and chemistry of fission. Proc. of a symp. Salzburg, 22 - 26 March, 1965. IAEA, Vienna, 1965. Vol. 2, p. 113.

2. MAIENSCHEIN F.C. et al., Gamma-rays associated with fission. U.N. intern. conf. on peaceful uses of atomic energy. 2. Geneva 1958. Proc. Vol. 15, p. 366. U.N., Geneva, 1958.

3. JOHANSSON S.A.E., Gamma de-excitation of fission fragments. (I). Prompt radiation. Nucl. Phys. 60 (1964) p. 378.

4. SKARSVÅG K. and SINGSTAD I., Angular correlation of fission fragments and prompt γ-rays from spontaneous fission of Cf^{252}. Nucl. Phys. 62 (1965) p. 103.

5. SKARSVÅG K., Angular correlation of fission fragments and prompt γ-rays from slow neutron fission of ^{235}U. Nucl. Phys. A96 (1967) p. 385.

6. ARMBRUSTER P. et al., Mass dependence of anisotropy and yield of prompt γ-rays in ^{235}U thermal fission. Physics and chemistry of fission. Proc. of a symp. Vienna, 28 July - 1 August, 1969. IAEA, Vienna, 1969, p. 545.

7. VAL'SKII G.V. et al., Concerning the emission times of γ-quanta as a result of fission. Soviet At. Energy 18 (1965) p. 279.

8. HIGBIE J., Gamma radiation from fission fragments. 1969. (AE-374).

9. WATSON R.L. et al., A study of the low-energy transitions arising from the prompt de-excitation of fission fragments. Nucl. Phys. A141 (1970) p. 449.

10. JOHN W., GUY F.W., and WESOLOWSKI J.J., Four parameter measurements of isomeric transitions in ^{252}Cf fission fragments. Phys. Rev. C 2 (1970) p. 1451.

11. ALBINSSON H. and LINDOW L.,
Prompt gamma radiation from fragments in the thermal fission of ^{235}U. 1970.
(AE-398).

12. BOWMAN H.R. et al.,
Velocity and angular distributions of prompt neutrons from spontaneous fission of Cf^{252}.
Phys. Rev. 126 (1962) p. 2120.

13. HIGBIE J.,
Gamma radiation from fission fragments.
Experimental apparatus - mass spectrum resolution. 1969.
(AE-367).

14. SKARSVÅG K.,
Time distribution of γ-rays from spontaneous fission of ^{252}Cf.
Nucl. Phys. A153 (1970) p. 82.

15. ALBINSSON H.,
Energies and yields of prompt gamma-rays from fragments in slow-neutron induced fission of ^{235}U. 1971.
(AE-420).

TABLE I

For notations, see fig. 3

x (cm)	d (mm)	a (cm)	y (mm)	Ω (10^{-4} sr)
4	1.0	4	1	1.69
8	1.0	4	0.5	1.23
20	0.5	4	0.1	0.307
40	0.5	4	0.05	0.165
13.5	1.00	1.60	0.118	0.985
13.5	0.50	1.60	0.059	0.493
13.5	0.25	1.60	0.030	0.246
13.5	0.15	1.60	0.018	0.148

Ω = the largest solid angle in each case in which a fragment is visible through the collimator.

y = the minimum distance between the foil and the nearest edge of the detector at which only one fragment can emit radiation through the collimator.

FIGURE CAPTIONS

Fig. 1 Block schematic of the electronic equipment.

Fig. 2 (a) The response curve for the 0.5 mm collimator for a ^{60}Co source. The line is the calculated response. (b) The response function for fission fragments with the same collimator.

Fig. 3 The collimator geometry drawn to illustrate the figures given in table I and the factors affecting the time resolution.

Fig. 4 The decay curve of the fission gamma radiation obtained with the 0.25 mm collimator. The value from each setting has been corrected for background from components of longer half-lives and general background. Assuming a simple exponential decay yields a half-life of 7.5 ps.

Fig. 5 The decay curve of the fission gamma radiation obtained with the 0.50 mm collimator. $T_{1/2} = 18$ ps.

Fig. 6 The decay curve of the fission gamma radiation obtained with the 1.0 mm collimator. $T_{1/2} = 60$ ps.

Fig. 7 Background levels in different gamma-ray energy portions with a 1.0 mm collimator located with its nearest edge about 1 mm from the foil.

Fig. 8 An illustration of two extreme flight paths of the fragments and the corresponding distances they are visible in the collimator.

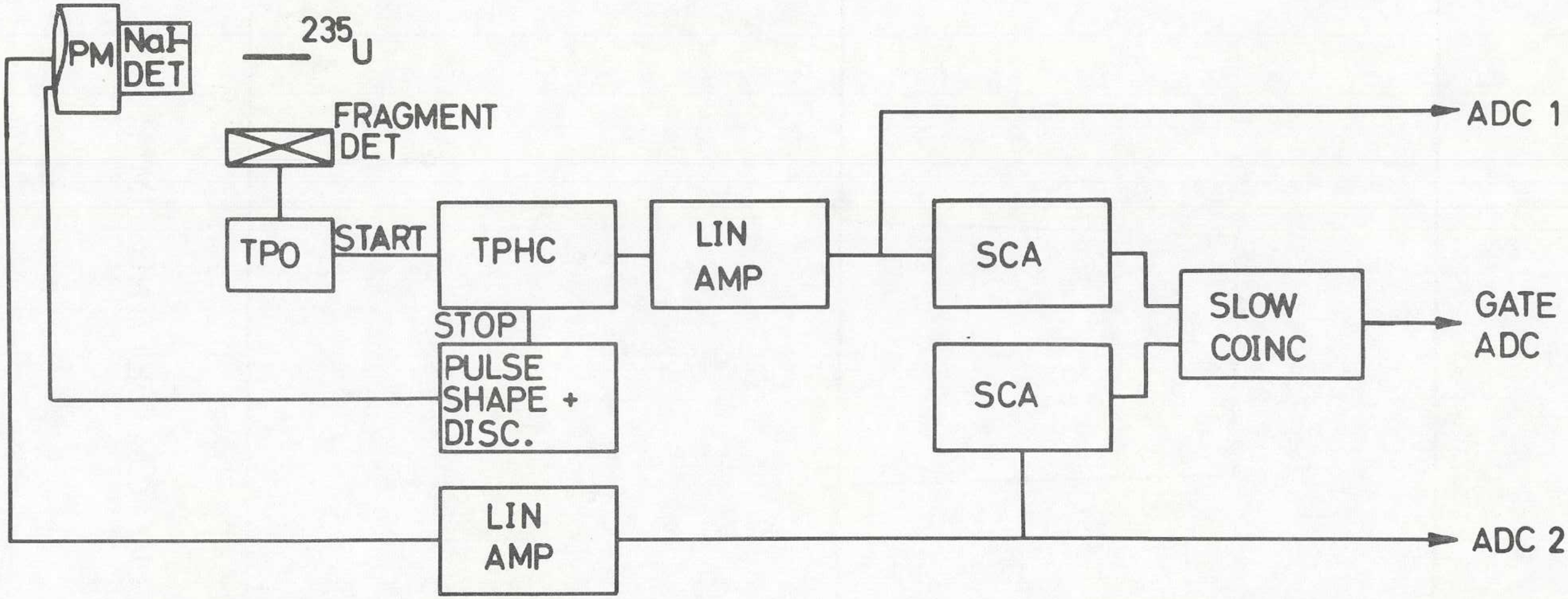
PM
NaI DET
235U
FRAGMENT DET
TPO
START
TPHC
STOP
PULSE SHAPE + DISC.
LIN AMP
SCA
SCA
SLOW COINC
LIN AMP
ADC 1
GATE ADC
ADC 2

Fig 1

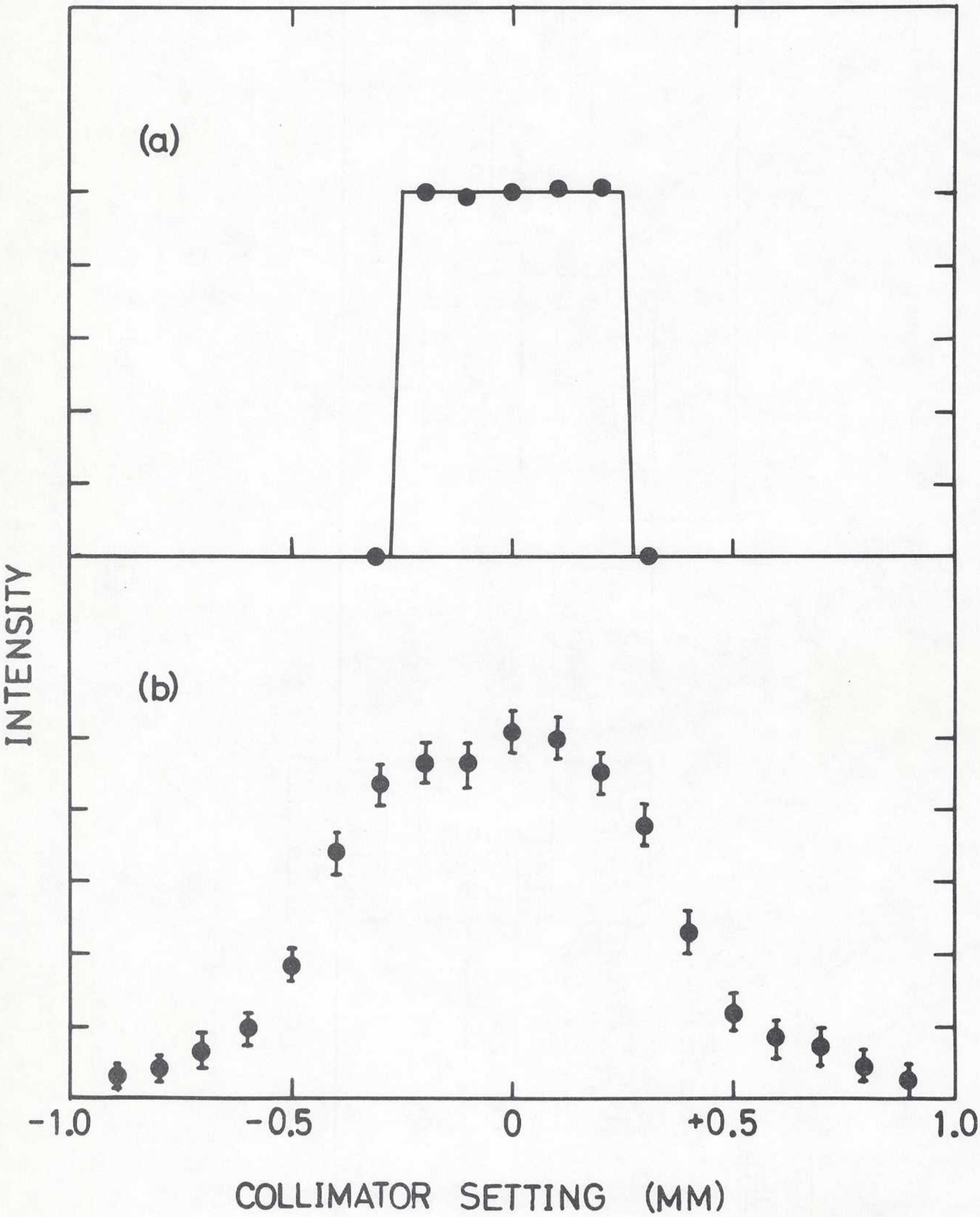

Fig 2

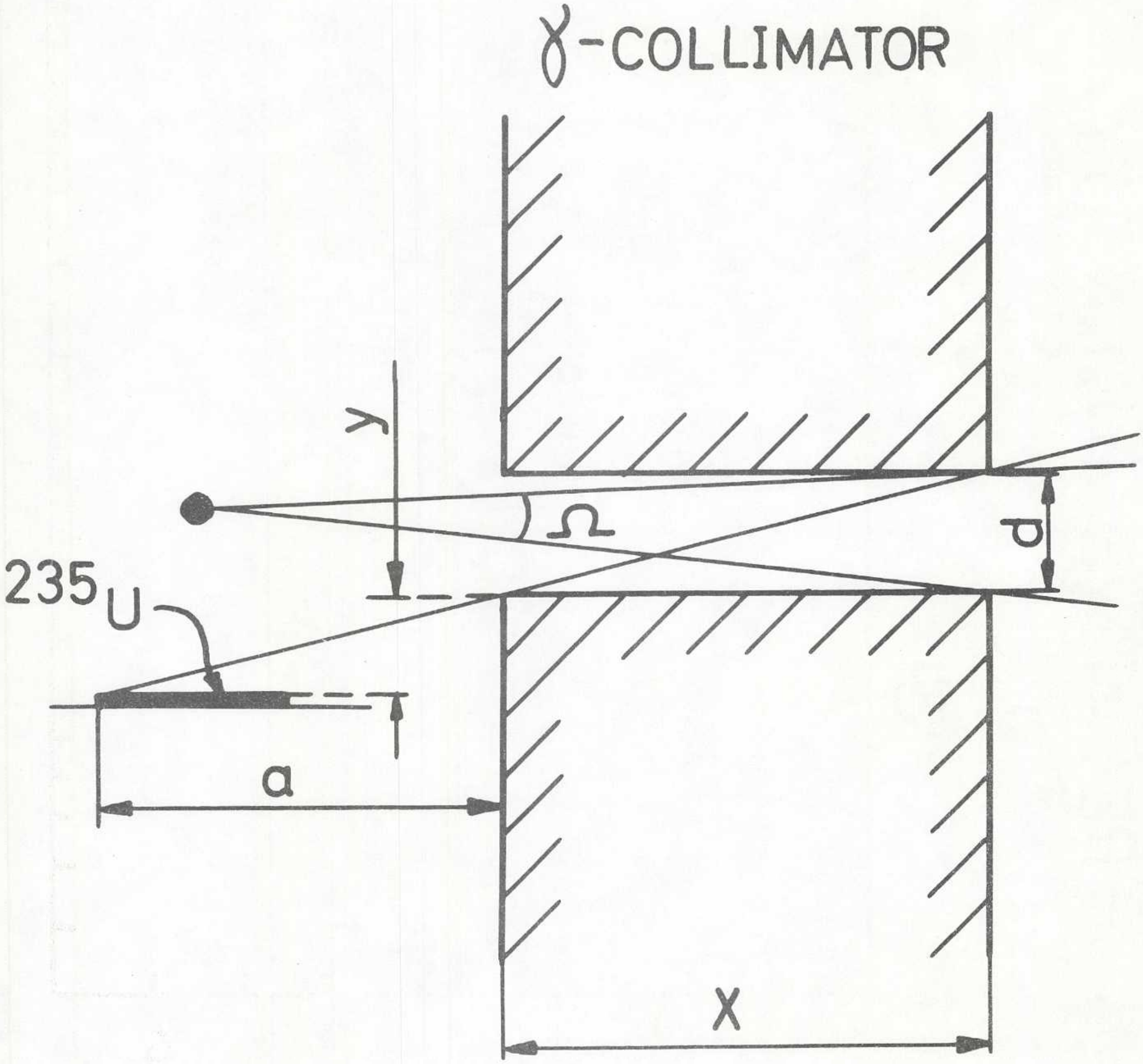

Fig 3

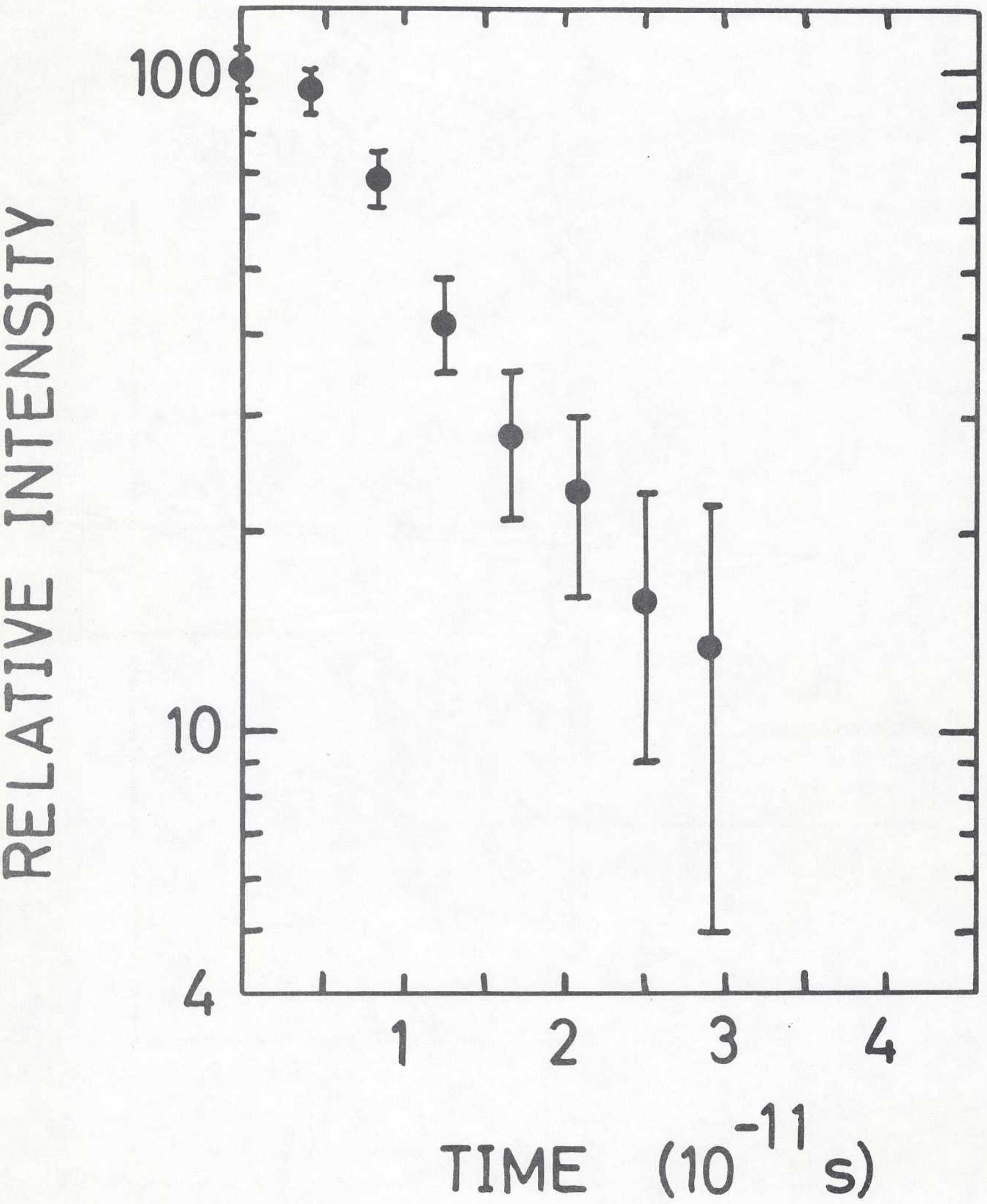

Fig 4

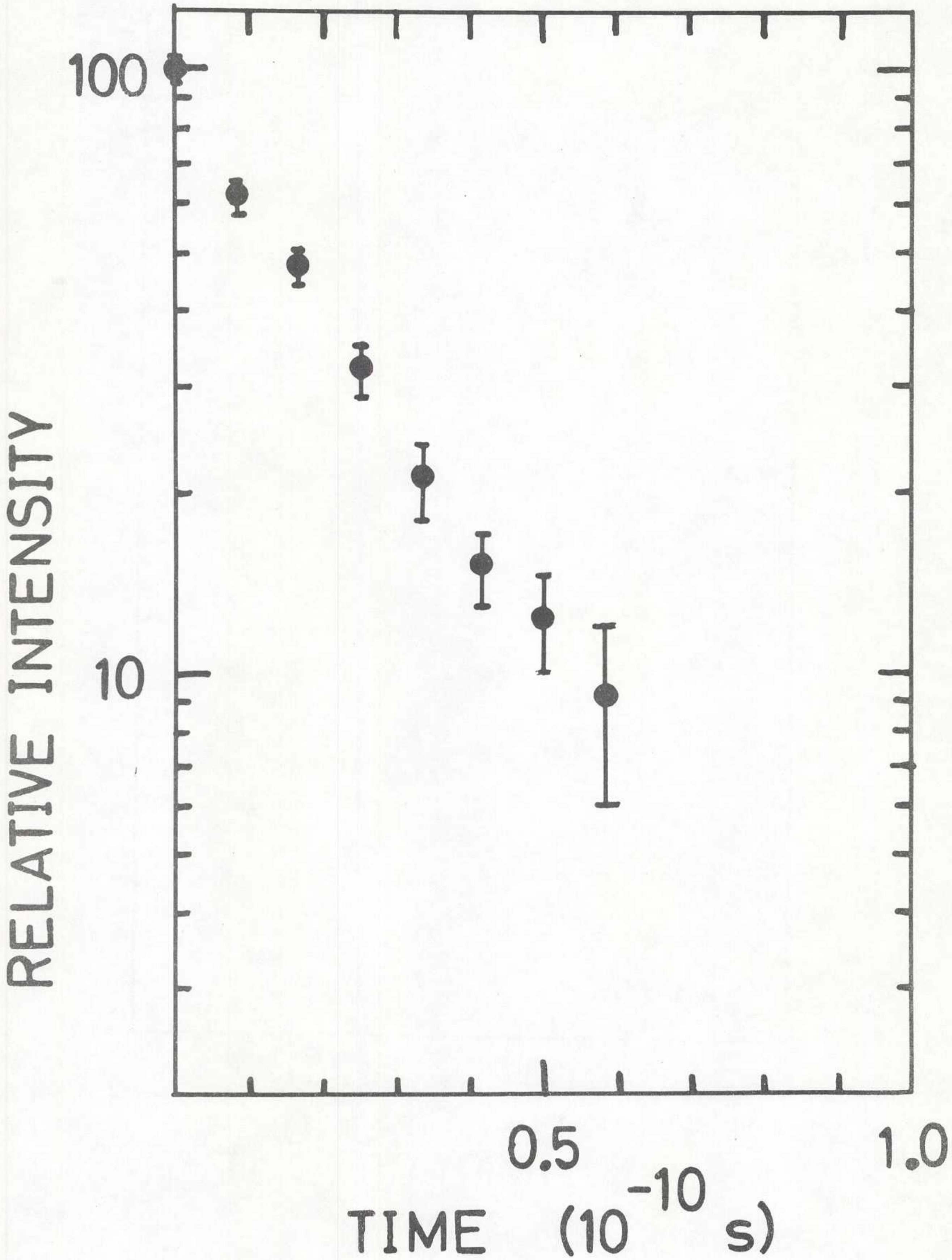

Fig 5

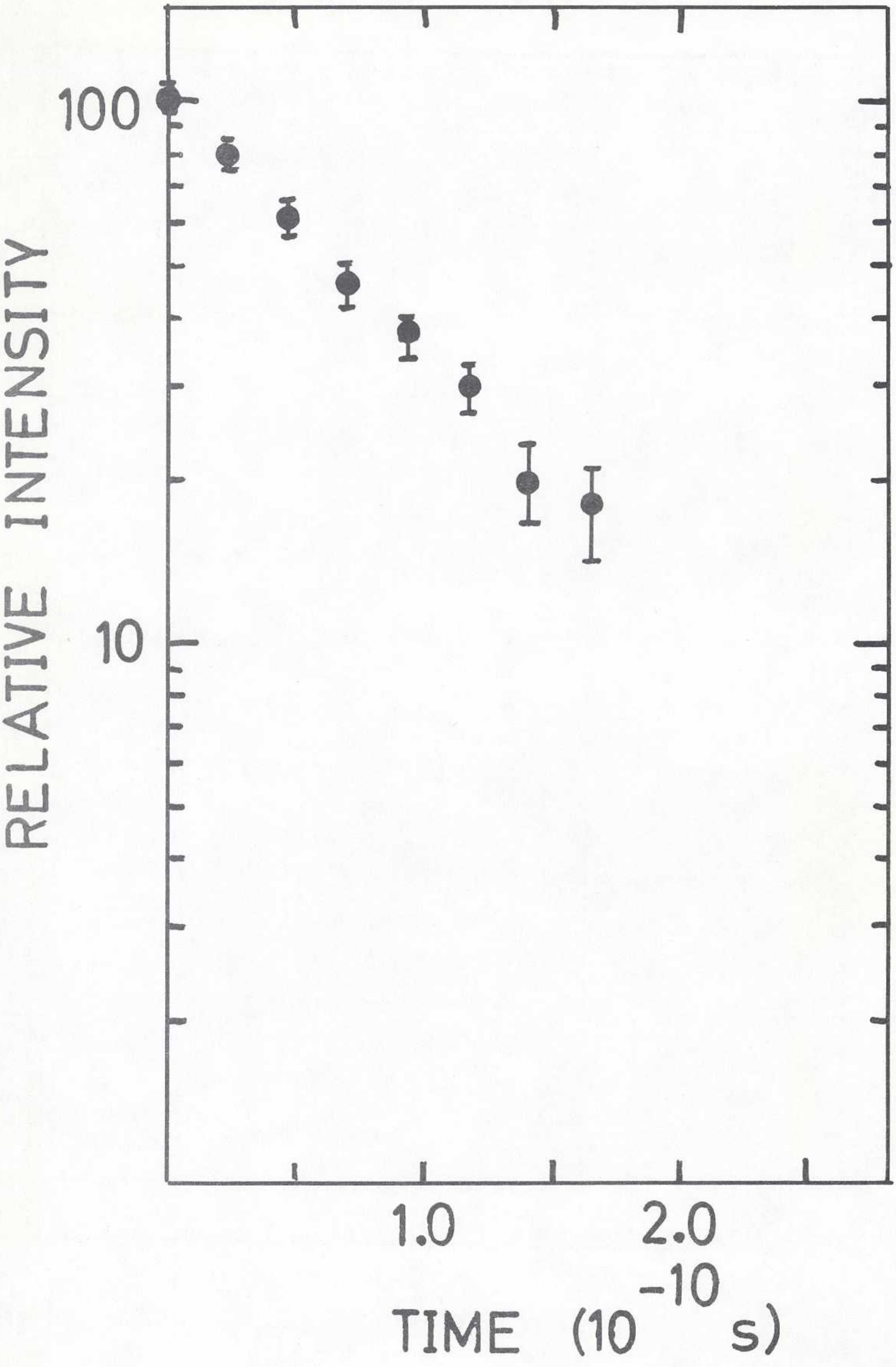

Fig 6

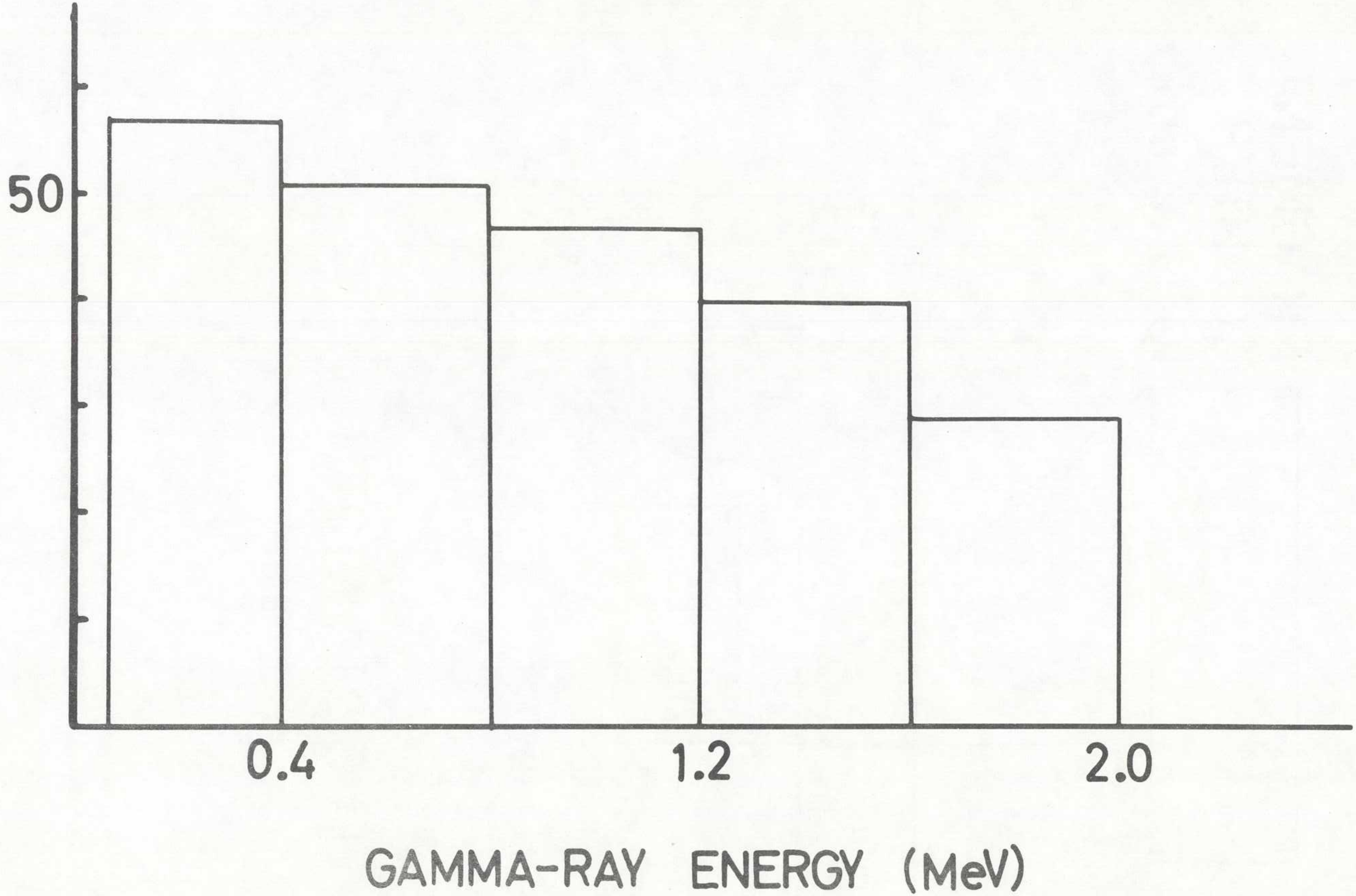

Fig 7

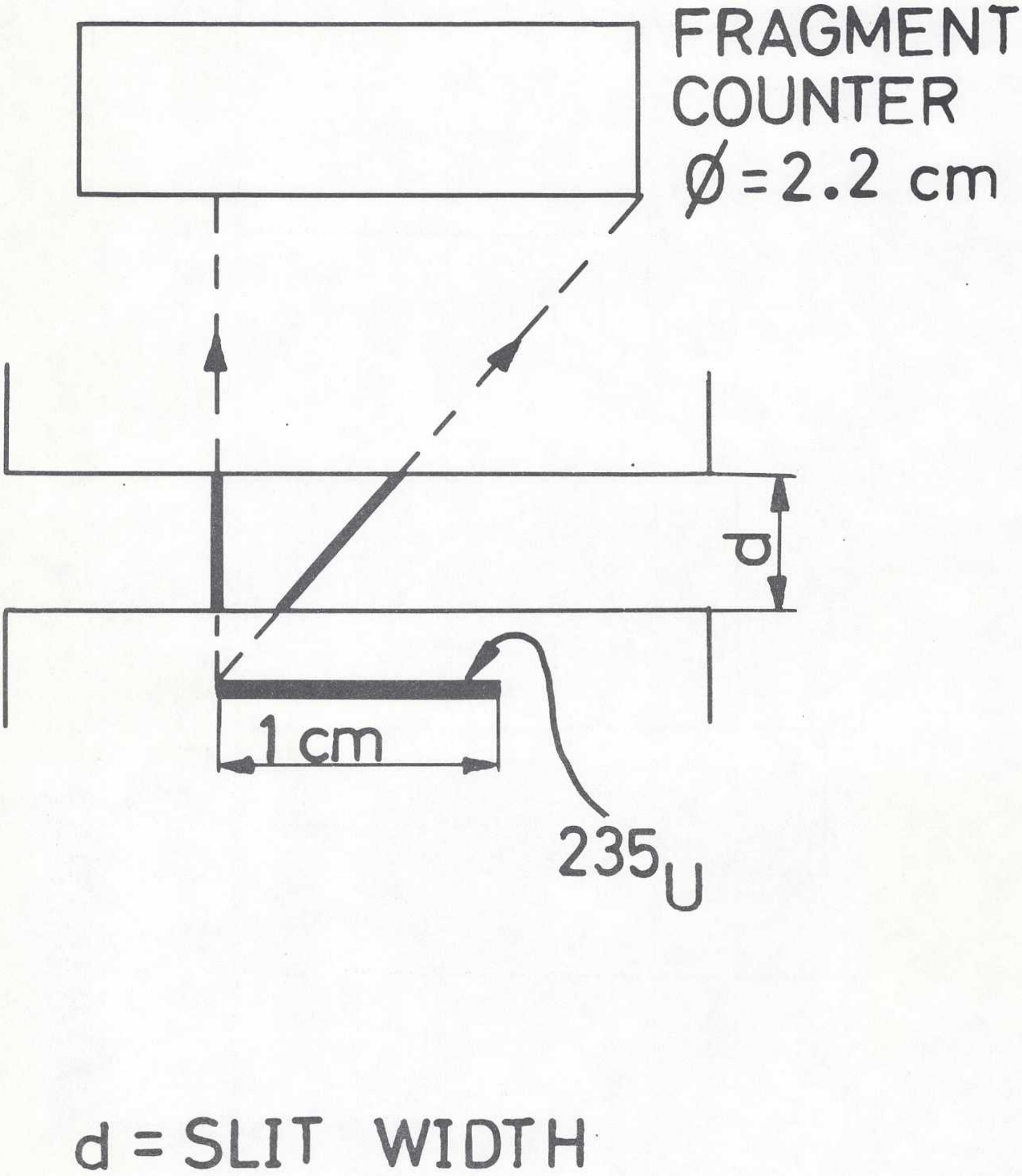

Fig 8

LIST OF PUBLISHED AE-REPORTS

1–350 (See back cover earlier repports.)

351. A determination of the 2 200 m/s absorption cross section and resonance integral of arsenic by pile oscillator technique. By E. K. Sokolowski and R. Bladh. 1969. 14 p. Sw. cr. 10:–.
352. The decay of ^{191}Os. By S. G. Malmskog and A. Bäcklin. 1969. 24 p. Sw. cr. 10:–.
353. Diffusion from a ground level point source experiment with thermoluminescence dosimeters and Kr 85 as tracer substance. By Ch. Gyllander, S. Hollman and U. Widemo. 1969. 23 p. Sw. cr. 10:–.
354. Progress report, FFN, October 1, – September 30, 1968. By T. Wiedling. 1969. 35 p. Sw. cr. 10:–.
355. Thermodynamic analysis of a supercritical mercury power cycle. By A. S. Roberts, Jr. 1969. 25 p. Sw. cr. 10:–.
356. On the theory of compensation in lithium drifted semiconductor detectors. By A. Lauber. 1969. 45 p. Sw. cr. 10:–.
357. Half-life measurements of levels in ^{75}As. By M. Höjeberg and S. G. Malmskog. 1969. 14 p. Sw. cr. 10:–.
358. A non-linear digital computer model requiring short computation time for studies concerning the hydrodynamics of the BWR. By F. Reisch and G. Vayssier. 1969. 38 p. Sw. cr. 10:–.
359. Vanadium beta emission detectors for reactor in-core neutron monitoring. By I. Ö. Andersson and B. Söderlund. 1969. 26 p. Sw. cr. 10:–
360. Progress report 1968. Nuclear chemistry. 1969. 38 p. Sw. cr. 10:–.
361. A half-life measurement of the 343.4 keV level in ^{175}Lu. By M. Höjeberg and S. G. Malmskog. 1969. 10 p. Sw. cr. 10:–.
362. The application of thermoluminescence dosimeters to studies of released activity distributions. By B-I. Rudén. 1969. 36 p. Sw. cr. 10:–.
363. Transition rates in ^{161}Dy. By V. Berg and S. G. Malmskog. 1969. 32 p. Sw. cr. 10:–.
364. Control rod reactivity measurements in the Ågesta reactor with the pulsed neutron method. By K. Björeus. 1969. 44 p. Sw. cr. 10:–.
365. On phonons in simple metals II. Calculated dispersion curves in aluminium. By R. Johnson and A. Westin. 1969. 124 p. Sw. cr. 10:–.
366. Neutron elastic scattering cross sections. Experimental data and optical model cross section calculations. A compilation of neutron data from the Studsvik neutron physics laboratory. By B. Holmqvist and T. Wiedling. 1969. 212 p. Sw. cr. 10:–.
367. Gamma radiation from fission fragments. Experimental apparatus – mass spectrum resolution. By J. Higbie. 1969. 50 p. Sw. cr. 10:–.
368. Scandinavian radiation chemistry meeting, Studsvik and Stockholm, September 17–19, 1969. By H. Christensen. 1969. 34.p. Sw. cr. 10:–.
369. Report on the personnel dosimetry at AB Atomenergi during 1968. By J. Carlsson and T. Wahlberg. 1969. 10 p. Sw. cr. 10:–.
370. Absolute transition rates in ^{188}Ir. By S. G. Malmskog and V. Berg. 1969. 16 p. Sw. cr. 10:–.
371. Transition probabilities in the 1/2+(631) Band in ^{235}U. By M. Höjeberg and S. G. Malmskog. 1969. 18 p. Sw. cr. 10:–.
372. E2 and M1 transition probabilities in odd mass Hg nuclei. By V. Berg, A. Bäcklin, B. Fogelberg and S. G. Malmskog. 1969. 19 p. Sw. cr. 10:–
373. An experimental study of the accuracy of compensation in lithium drifted germanium detectors. By A. Lauber and B. Malmsten. 1969. 25 p. Sw. cr. 10:–.
374. Gamma radiation from fission fragments. By J. Higbie. 1969. 22 p. Sw. cr. 10:–.
375. Fast neutron elastic and inelastic scattering of vanadium. By B. Holmqvist, S. G. Johansson, G. Lodin and T. Wiedling. 1969. 48 p. Sw. cr. 10:–
376. Experimental and theoretical dynamic study of the Ågesta nucler power station. By P. Å. Bliselius, H. Vollmer and F. Åkerhielm. 1969. 39 p. Sw. cr. 10:–.
377. Studies of Redox equilibria at elevated temperatures 1. The estimation of equilibrium constants and standard potentials for aqueous systems up to 374°C. By D. Lewis. 1969. 47 p. Sw. cr. 10:–.
378. The whole body monitor HUGO II at Studsvik. Design and operation. By L. Devell, I. Nilsson and L. Venner. 1970. 26 p. Sw. cr. 10:–
379. ATOMSPHERIC DIFFUSION. Investigations at Studsvik and Ågesta 1960–1963. By L-E. Hæggblom, Ch. Gyllander and U. Widemo. 1969. 91 p. Sw. cr. 10:–.
380. An expansion method to unfold proton recoil spectra. By J. Kockum. 1970. 20 p. Sw. cr. 10:–.
381. The 93.54 keV lever ^{91}Sr, and evidence for 3-neutron states above N=50. By S. G. Malmskog and J. McDonald. 1970. 24 p. Sw. cr. 10:–.
382. The low energy level structure of ^{191}Ir. By S. G. Malmskog, V. Berg, A. Bäcklin and G. Hedin. 1970. 24 p. Sw. cr. 10:–.
383. The drinking rate of fish in the Skagerack and the Baltic. By J. E. Larsson. 1970. 16 p. Sw. cr. 10:–.
384. Lattice dynamics of Nacl, KCl, RbCl and RbF. By G. Raunio and S. Rolandson. 1970. 26 p. Sw. cr. 10:–.
385. A neutron elastic scattering study of chromium, iron and nickel in the energy region 1.77 to 2.76 MeV. By B. Holmqvist, S. G. Johansson, G. Lodin, M. Salama and T. Wiedling. 1970. 26 p. Sw. cr. 10:–.
386. The decay of bound isobaric analogue states in ^{28}Si and ^{32}Si using (d. n-) reactions. By L. Nilsson, A. Nilsson and I. Bergqvist. 1970. 34 p. Sw. cr. 10:–
387. Transition probabilities in ^{189}Os. By S. G. Malmskog, V. Berg and A. Bäcklin. 1970. 40 p. Sw. cr. 10:–.
388. Cross sections for high-energy gamma transition from MeV neutron capture in ^{206}Pb. By I. Bergqvist, B. Lundberg and L. Nilsson. 1970. 16 p. Sw. cr. 10:–.
389. High-speed, automatic radiochemical separations for activation analysis in the biological and medical research laboratory. By K. Samsahl. 1970. 18 p. Sw. cr. 10:–.
390. Use of fission product Ru-106 gamma activity as a method for estimating the relative number of fission events in U-235 and Pu-239 in low-enriched fuel elements. By R. S. Forsyth and W. H. Blackadder. 1970. 26 p. Sw. cr. 10:–.
391. Half-life measurements in ^{134}I. By V. Berg and Å. Höglund. 1970. 16 p. Sw. cr. 10:–.
392. Measurement of the neutron spectra in FRO cores 5, 9 and PuB-5 using resonance sandwich detectors. By T. L. Andersson and M. N. Qazi. 1970. 30 p. Sw. cr. 10:–.
393. A gamma scanner using a Ge(Li) semi-conductor detector with the possibility of operation in anti-coincidence mode. By R. S. Forsyth and W. H. Blackadder. 1970. 22 p. Sw. cr. 10:–.
394. A study of the 190 keV transition in ^{141}La. By B. Berg, Å. Höglund and B. Fogelberg. 1970. 22 p. Sw. cr. 10:–.
395. Magnetoacoustic waves and instabilities in a Hall-effect-dominiated plasma. By S. Palmgren. 1970. 20 p. Sw. cr. 10:–.
396. A new boron analysis method. By J. Weitman, N. Dåverhög and S. Farvolden. 1970. 26 p. Sw. cr. 10:–.
397. Progress report 1969. Nuclear chemistry. 1970. 39 p. Sw. cr. 10:–.
398. Prompt gamma radiation from fragments in the thermal fission of ^{235}U. By H. Albinsson and L. Lindow. 1970. 48 p. Sw. cr. 10:–.
399. Analysis of pulsed source experiments performed in copper-reflected fast assemblies. By J. Kockum. 1970. 32 p. Sw. cr. 10:–.
400. Table of half-lives for excited nuclear levels. By S. G. Malmskog. 1970. 33 p. Sw. cr. 10:–.
401. Needle type solid state detectors for in vivo measurement of tracer activity. By A. Lauber, M. Wolgast. 1970. 43 p. Sw. cr. 10:–.
402. Application of pseudo-random signals to the Ågesta nuclear power station. By P-Å. Bliselius. 1970. 30 p. Sw. cr. 10:–.
403. Studies of redox equilibria at elevated temperatures 2. An automatic divided-function autoclave and cell with flowing liquid junction for electrochemical measurements on aqueous systems. By. K. Johnsson, D. Lewis and M. de Pourbaix. 1970. 38 p. Sw. cr. 10:–.
404. Reduction of noise in closed loop servo systems. By K. Nygaard. 1970. 23 p. Sw. cr. 10:–
405. Spectral parameters in water-moderated lattices. A survey of experimental data with the aid of two-group formulae. By E. K. Sokolowski. 1970. 22 p. Sw. cr. 10:–.
406. The decay of optically thick helium plasmas, taking into account ionizing collisions between metastable atoms or molecules. By J. Stevefelt. 1970. 18 p. Sw. cr. 10:–.
407. Zooplankton from Lake Magelungen, Central Sweden 1960-63. By E. Almquist. 1970. 62 p. Sw. cr. 10:–.
408. A method for calculating the washout of elemental iodine by water sprays. By E. Bachofner and R. Hesböl. 1970. 24 p. Sw. cr. 10:–.
409. X-ray powder diffraction with Guinier–Hägg focusing cameras. By A. Brown. 1970. 102 p. Sw. cr. 10:–.
410. General physic section. Progress report. Fiscal year 1969/70. By J. Braun. 1970. 92 p. Sw. cr. 10:–.
411. In-pile determination of the thermal conductivity of UO_2 in the range 500–2 500 degrees centigrade. By J-Å Gyllander. 1971. 70 p. Sw. cr. 10:–.
412. A study of the ring test for determination of transverse ductility of fuel element canning. By G. Anevi and G. Östberg. 1971. 17 p. Sw. cr. 15:–.
413. Pulse radiolysis of Aqueous Solutions of aniline and substituted anilines. By H. C. Christensen. 1971. 40 p. Sw. cr. 15:–.
414. Radiolysis of aqueous toluene solutions. By H. C. Christensen and R. Gustafson. 1971. 20 p. Sw. cr. 15:–.
415. The influence of powder characteristics on process and product parameters in UO_2 pelletization. By U. Runfors. 1971. 32 p. Sw. cr. 15:–.
416. Quantitative assay of Pu239 and Pu240 by neutron transmission measurements. By E. Johansson. 1971. 26 p. Sw. cr 15:–.
417. Yield of prompt gamma radiation in slow-neutron induced fission of ^{235}U as a function of the total fragment kinetic energy. By H. Albinsson. 1971. 38 p. Sw. cr. 15:–.
418. Measurements of the spectral light emission from decaying high pressure helium plasmas. By J. Stevefelt and J. Johansson. 1971. 48 p. Sw. cr. 15:–.
419. Progress report 1970. Nuclear chemistry. 1971. 32 p. Sw. cr. 15:–.
420. Energies and yields of prompt gamma rays from fragments in slow-neutron induced fission of ^{235}U. By H. Albinsson. 1971. 56 p. Sw. cr. 15:–.
421. Decay curves and half-lives of gamma-emitting states from a study of prompt fission gamma radiation. By H. Albinsson. 1971. 28 p. Sw. cr. 15:–.

List of published AES-reports (In Swedish)

1. Analysis by means of gamma spectrometry. By D. Brune. 1961. 10 p. Sw. cr. 6:–
2. Irradiation changes and neutron atmosphere in reactor pressure vessels-some points of view. By M. Grounes. 1962. 33 p. Sw. cr. 6:–.
3. Study of the elongation limit in mild steel. By G. Östberg and R. Attermo. 1963. 17 p. Sw. cr. 6:–.
4. Technical purchasing in the reactor field. By Erik Jonson. 1963. 64 p. Sw. cr. 8:–.
5. Ågesta nuclear power station. Summary of technical data, descriptions, etc. for the reactor. By B. Lilliehöök. 1964. 336 p. Sw. cr. 15:–
6. Atom Day 1965. Summary of lectures and discussions. By S. Sandström. 1966. 321 p. Sw. cr. 15:–.
7. Building materials containing radium considered from the radiation protection point of view. By Stig O. W. Bergström and Tor Wahlberg. 1967. 26 p. Sw. cr. 10:–.

Additional copies available from the Library of AB Atomenergi, Fack, S-611 01 Nyköping 1, Sweden.

EOS-tryckerierna, Stockholm 1971